JOHANNES GUTENBERG UNIVERSITÄT MAINZ

Paul-Ehrlich-Institut

Canonical and non-canonical autophagy modulation in human primary macrophages and its effect on the adaptive immune system

Dissertation

zur Erlangung des Grades
Doktor der Naturwissenschaften

am Fachbereich Biologie
der Johannes Gutenberg-Universität Mainz

Rebecca Bohn

geb. am 31.12.1988 in Karlsruhe

Mainz, 2017

Dekan

1. **Berichterstatter**

2. **Berichterstatter**

Tag der mündlichen Prüfung:

The obtained research data during this PhD project and collaborative studies led to the following publications:

Rebecca Bohn, Anne-Kathrin Knuth, Peter Crauwels, Stefan Schille, Ger van Zandbergen: LC3-associated phagocytosis as mechanism to secure *Leishmania* survival in human host macrophages. 2017, in preparation, abstract accepted for manuscript submission in *Frontiers in Immunology*

Rebecca Bohn, Peter Crauwels, Pascal Devant, Tim Haselwander, Jan W. Drijfhout, Stefan Tenzer, Ger van Zandbergen: Autophagy in human primary macrophages is independent of ULK-1 and Beclin-1. 2017, submitted

Peter Crauwels, **Rebecca Bohn** and Ger van Zandbergen: Autophagy during infection – friend or foe? 2017, submitted

Krämer S, Crauwels P, **Bohn R**, Radzimski C, Szaszák M, Klinger M, Rupp J, van Zandbergen G.: AP-1 transcription factor serves as a molecular switch between *Chlamydia pneumoniae* replication and persistence. *Infect Immun* 2015 83:2651–2660. PMID: 25895972

Peter Crauwels, **Rebecca Bohn**, Meike Thomas, Stefan Gottwalt, Florian Jäckel, Susi Krämer, Elena Bank, Stefan Tenzer, Paul Walther, Max Bastian & Ger van Zandbergen: Apoptotic-like *Leishmania* exploit the host´s autophagy machinery to reduce T-cell mediated parasite elimination. *Autophagy* 2015, 11:2, 285-297 PMID: 25801301

Summary

In this study we focused on the modulation of autophagy mechanisms in human monocyte derived macrophages (hMDM) focusing on (i) modulation of autophagy in pro- (hMDM-1) and anti-inflammatory (hMDM-2) macrophages as prototypic immunomodulatory cells, (ii) the role of autophagy in antigen processing and presentation, (iii) the impact of the *Leishmania* virulence factor GP63 on the host cells' autophagy machinery and adaptive immunity and (iv) LC3-associated phagocytosis (LAP) as immune evasion mechanism for *Leishmania*.

Autophagy in hMDM-1 and hMDM-2 was induced by the chemicals Rapamycin, AZD8055 and PI-103 as well as by the peptide Tat-Beclin. In general, hMDM-2 were more susceptible for autophagy induction. Autophagy inhibition was achieved by Spautin-1 and Wortmannin treatment in both phenotypes and with LY294002 only in hMDM-1. Using RNA interference to achieve autophagy inhibition, a time- and target-dependent efficiency of protein reduction was observed. Interestingly, autophagy could be induced independently of ULK-1 and Beclin-1 in hMDM-1. Autophagy modulation in hMDM had no impact on Tetanus Toxoid induced T cell proliferation. Surprisingly, we found hMDM-2 to be superior to hMDM-1 in activating lymphocytes. Proteome and surface marker analysis revealed higher expression of proteins being involved in antigen processing and presentation in hMDM-2.

Based on the hypothesis that apoptotic *Leishmania* (*Lm*) induce the non-canonical autophagy pathway LAP resulting in a reduced T cell proliferation, we aimed to modulate LAP and analyzed the effect on the adaptive immune response. Replacing apoptotic parasites by LAP inducing stimuli such as zymosan and phosphatidylserine coated beads suppressed the *Leishmania* induced T cell proliferation and consequently enhanced intracellular parasite survival. Analyzing the underlying mechanisms of LAP in hMDM, inhibition of the NADPH oxidase by DPI blocked LAP induction. In addition, infection of hMDM with Staurosporine-treated *Lm,* being ROS positive, increased LC3 conversion which suggests ROS-dependent LAP induction in hMDM. Infection with apoptotic *Lm* and zymosan leads to enhanced phagolysosomal acidification, which might be a potential mechanism for altered antigen processing resulting in a reduced T cell proliferation.

In conclusion, these data provide a better understanding of autophagy in hMDM being a potential immune evasion mechanism for *Leishmania*. The obtained results may contribute in the development of safe and efficient therapeutic interventions in humans for the treatment of autophagy-related diseases.

Zusammenfassung

In der vorliegenden Arbeit fokussierten wir uns auf die Modulation von Autophagie Mechanismen in humanen primären Makrophagen (hMDM) und untersuchten dabei folgende Punkte: (i) Modulation von Autophagie in pro- (hMDM-1) und anti-inflammatorischen (hMDM-2) Makrophagen als prototypische immunmodulierende Zellen, (ii) die Rolle von Autophagie für Antigen-Prozessierung und -Präsentation, (iii) den Einfluss des Leishmanien Virulenzfaktors GP63 auf den Autophagieprozess der Wirtszelle und die adaptive Immunantwort und (iv) LC3-assoziierte Phagozytose (LAP) als Ausweichmechanismus für Leishmanien vor dem Immunsystem.

Autophagie konnte mit den Chemikalien Rapamycin, AZD8055 und PI-103 als auch mit dem Peptid Tat-Beclin in hMDM-1 und hMDM-2 induziert werden. Generell zeigten hMDM-2 eine stärkere Autophagie Induktion. Inhibition wurde durch Behandlung mit Spautin-1 und Wortmannin in beiden Phenotypen und mit LY294002 nur in hMDM-1 erreicht. Mit Hilfe von RNA Interferenz zur Autophagie Inhibition wurde eine Zeit- und Target-abhängige Proteinreduktion beobachtet. Interessanterweise konnte Autophagie unabhängig von ULK-1 und Beclin-1 in hMDM-1 induziert werden. Die Modulation von Autophagie hatte keinen Einfluss auf die Tetanus Toxoid induzierte T Zell Proliferation. Überraschenderweise zeigten hMDM-2 eine bessere Aktivierung von Lymphozyten als hMDM-1. Proteom- und Oberflächenmarker-Analyse wiesen auf eine höhere Expression von Proteinen, die an der Antigen-Prozessierung und -Präsentation beteiligt sind, in hMDM-2 hin.

Basierend auf der Hypothese, dass apoptotische Leishmanien den nicht-kanonischen Autophagie-Mechanismus LAP induzieren was zu reduzierter T Zell Proliferation führt, modulierten wir LAP und analysierten den Effekt auf die adaptive Immunantwort. Das Ersetzen von apoptotischen Parasiten durch LAP-induzierende Stimuli wie Zymosan und phosphatidylserin-beschichtete Partikel unterdrückte die Leishmanien-induzierte T Zell Proliferation und erhöhte das intrazelluläre Überleben der Parasiten. Die Analyse der zugrundeliegenden Mechanismen zeigte, dass die Inhibition der NADPH Oxidase durch DPI die Induktion von LAP in hMDM blockierte. Weiterhin resultierte die Infektion von hMDM mit Staurosporin-behandelten Leishmanien, die ROS positiv sind, in einer erhöhten LC3 Konversion, die eine ROS-abhängige Induktion von LAP in hMDM suggeriert. Die Infektion mit apoptotischen Leishmanien und Zymosan führte zu einer verstärkten phagolysosomalen Ansäuerung, die ein potentieller Mechanismus für eine veränderte Antigen-Prozessierung, resultierend in verminderter T Zell Proliferation, sein könnte.

Abschließend liefern diese Daten ein besseres Verständnis von Autophagie in hMDM welche als möglicher Ausweichmechanismus für Leishmanien vor dem humanen Immunsystem dienen könnte. Die erhaltenen Ergebnisse liefern einen wertvollen Beitrag zur Entwicklung von sicheren und effizienten therapeutischen Ansätzen zur Behandlung von Autophagie-bedingten Krankheiten beim Menschen.

Table of content

1 Introduction

1.1 Autophagy

1.1.1 Historical background

Research on autophagy started more than 60 years ago by the discovery of the lysosome, a late organelle in the autophagic process (Duve et al., 1955). In the following years, Novikoff and Clark described “dense bodies” harboring organelles, which were later identified as autolysosomal compartments (Novikoff et al., 1956; Clark, 1957; Novikoff, 1959). In 1963, de Duve postulated the term “autophagy” as a sequestration process present in all cell types leading to the degradation of cytoplasmic content in autophagosomes (Duve and Wattiaux, 1966). Extensive research revealed that autophagy is induced in nutrient poor conditions and is inhibited by the addition of amino acids to the culture medium (Mortimore et al., 1983). A huge breakthrough in understanding the molecular pathway was achieved in the 1990s in Ohsumi’s lab by screening yeast deletion mutants, which led to the identification of autophagy-related (ATG) genes and proteins (Takeshige et al., 1992; Tsukada and Ohsumi, 1993; Baba et al., 1995). Almost twenty years ago, Mizushima postulated that autophagy is conserved from yeast to mammals (Mizushima et al., 1998a). Until then, autophagy was monitored by electron microscopy when Kabeya and colleagues discovered the microtubule-associated protein 1 light chain 3, short LC3, as a marker on autophagosomes enabling detection by immunofluorescence and Western Blot (Kabeya et al., 2000). Since then, the number of papers per year increased exponentially, highlighting important functions of autophagy for health and disease (Ohsumi, 2014). Ohsumi’s work on the autophagic process was awarded in 2016 with the Nobel Prize for medicine.

1.1.2 Autophagy in health and disease

Macroautophagy (greek: *auto* – self, *phagein* – eating; hereafter referred to as autophagy) is a self-eating process and a key mechanism to ensure survival during harsh conditions. The digestion of particles ranging in size from small molecules to whole organelles is unique and provides the cell with nutrients in times of starvation ensuring energy homeostasis (**Figure 1**) (Mizushima et al., 2008; Levine et al., 2011). Furthermore, the degradation of defect organelles or misfolded proteins prevents the outcome of neurodegenerative diseases like Parkinson or Alzheimer (Pan et al., 2008; Lynch-Day et al., 2012; Nixon, 2013). Consequently, mutations in autophagy related genes are associated with increased risk of developing diseases. Mono-allelic deletion of Beclin-1, a critical regulator protein of autophagy, has been observed in some

cancers (Choi, 2012; White, 2012). In addition, T300A mutation in ATG16L1 increases the incidence to develop inflammatory bowel diseases (Salem et al., 2015; Hooper et al., 2017).

In addition to unselective bulk degradation of endogenous components, autophagy can target material in a selective manner e.g. mitophagy, peroxyphagy, aggrephagy or ribophagy. The specific targeting of invading microbes by autophagy receptors such as p62 and NDP52, called xenophagy, provides an additional cellular defense mechanism (Samson, 1981; Kirkegaard et al., 2004). These examples highlight the crucial role of autophagy in cellular wellbeing, which makes it an important target for therapeutic interventions (Rubinsztein et al., 2012). So far, the lysosomal inhibitor Hydroxychloroquine has been used in phase 1 and 2 clinical trials for the treatment of cancer however the mechanism how autophagy contributes to tumor cell survival is not yet fully understood (Jiang and Mizushima, 2014; Poklepovic and Gewirtz, 2014).

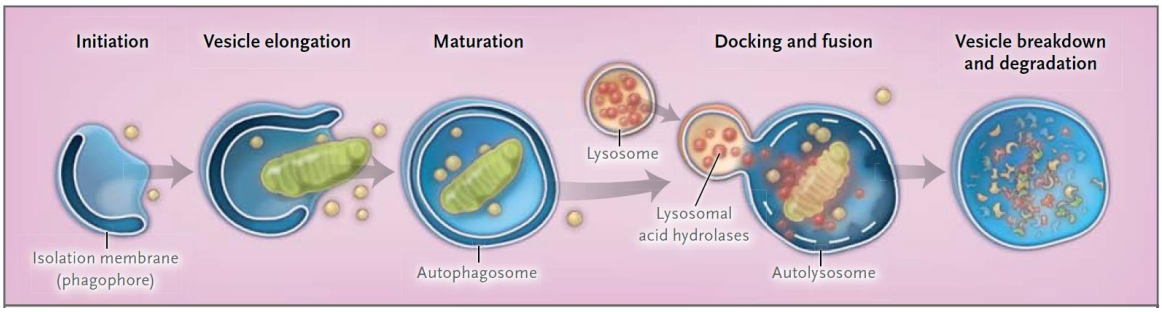

Figure 1: The autophagic sequestration process. Induction of autophagy leads to the formation of a double membrane, called phagophore, which encloses cytoplasmic cargo. Upon vesicle elongation forming an autophagosome, the fusion with lysosomes building an autolysosome enables the degradation of engulfed cargo by lysosomal hydrolases (Choi et al., 2013).

1.1.3 Molecular pathway

So far, more than 30 autophagy-related (ATG) genes and their corresponding proteins that participate in the process of autophagy have been identified (Mizushima et al., 2008; Ravikumar et al., 2010) (**Figure 2**). Nutrient starvation or growth factor signaling initiates the induction of autophagy by inhibition of mTOR leading to its dissociation of the ULK-1 complex. This complex consists of ULK-1/2, ATG13 and FIP200, which further activates the formation of a double membrane structure, called phagophore (Chan et al., 2007; Chang and Neufeld, 2009; Ganley et al., 2009). Thus far, the membrane dynamics and the membrane sources of the phagophore are not yet fully understood. Several membranes serving as nucleation sites of the phagophore have been proposed like the plasma membrane, mitochondria, Golgi and endoplasmatic reticulum (Hailey et al., 2010; Ravikumar et al., 2010; Lamb et al., 2013). The formation of the phagophore requires the class III phosphatidylinositol 3-kinase (PI3K) complex,

consisting of Vps34, Vps15 ATG14 and Beclin-1, which produces phosphatidylinositol-3-phosphate (PI3P) (Liang et al., 1999; Kihara et al., 2001; Axe et al., 2008; Itakura and Mizushima, 2014). Membrane-bound PI3P leads to the recruitment of two ubiquitin-like conjugating systems, which mediate the elongation of the membrane (Geng and Klionsky, 2008). First, ATG12 is covalently conjugated to ATG5 mediated by ATG7, an E1 ubiquitin-activating enzyme, and ATG10, an E2 ubiquitin-conjugating enzyme (Mizushima et al., 1998b). The complex of ATG12-ATG5 is further stabilized by ATG16L1 and then associates with phagophores but dissociates from completed autophagosomes (Mizushima, 2003). The formation of the second complex is initiated by cleavage of pro-LC3 in LC3 (or LC3-I) by ATG4 (Hemelaar et al., 2003; Tanida et al., 2004a). Subsequently, ATG7 and ATG3 (E2-like) catalyze the ligation of cytosolic LC3-I to phosphatidylethanolamine (PE), forming autophagosome-associated LC3-PE (or LC3-II) (Tanida et al., 2004b). Cross-talk between the two complexes has been suggested and the ATG16L1 complex is believed to facilitate the subcellular location of LC3-I to the site of its lipidation on the autophagosomal membrane (Fujita et al., 2008). At the autophagosome, LC3-II has been shown to possess a dual role, in selecting cargo for degradation through interaction with adaptor proteins such as p62 and by promoting membrane tethering and fusion (Nakatogawa et al., 2007; Pankiv et al., 2007). During maturation, the phagophore closes to an autophagosome, which fuses with lysosomes forming an autolysosome. The influx of hydrolases and the acidification of the autolysosomal lumen results in the complete degradation of the enclosed luminal content together with the inner autophagosomal membrane (Mizushima et al., 2002; Yang and Klionsky, 2010). So far, only LC3-II is known to be predominantly associated with autophagosomes until the formation of an autolysosome and therefore serves as a widely used marker to monitor autophagy (Kabeya et al., 2000; Mizushima et al., 2010; Klionsky et al., 2014; Klionsky et al., 2016).

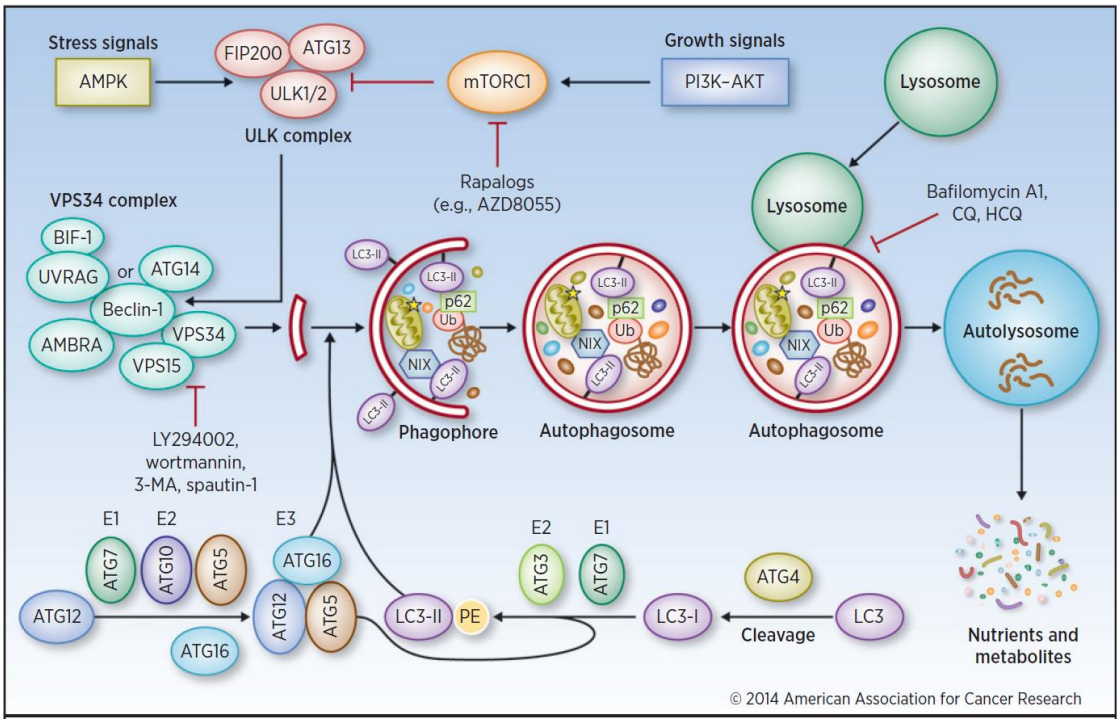

Figure 2: Molecular process of mammalian autophagy. Upon autophagy inducing signals, inhibition of mTOR leads to the activation of the ULK-1 complex which phosphorylates Beclin-1. Subsequently the class III PI3K complex is recruited and production of PI3P initiates the formation of the phagophore. The recruitment of two Ubiquitin-like protein complexes (ATG12-ATG5–ATG16L1 and ATG7–ATG3) promotes the closure of the phagophore to an autophagosome and the lipidation of LC3-I to membrane bound LC3-II. During maturation the autophagosome fuses with lysosomes resulting in the influx of hydrolases and acidification of the autophagosomal lumen, which results in the degradation of the engulfed cargo (Cicchini et al., 2015).

1.1.4 Modulation of autophagy

Building up the autophagosome is a multistep process allowing various possibilities for intervention and modulation (**Figure 2**). Under physiological conditions, the best stimulus for autophagy induction is nutrient starvation. Abundant nutrients and growth factors are detected by the mammalian target of Rapamycin (mTOR), a nutrient sensor kinase. Activated mTOR phosphorylates and thereby blocks ULK-1/2 and subsequently suppresses autophagy induction (Jung et al., 2009). The best known chemical mTOR inhibitor is Rapamycin, a lipophilic macrolide antibiotic, which binds to the cytosolic FKBP12 (immunophilin FK506-binding protein of 12 kDa), thereby inhibiting the kinase activity of mTOR (Heitman et al., 1991; Noda and Ohsumi, 1998; Kim et al., 2002). In addition to Rapamycin, AZD8055 is an ATP-competitive mTOR inhibitor which was already used in clinical trials for anti-tumor therapy and is used *in vitro* to induce autophagy (Chresta et al., 2010; Sini et al., 2010; Huang et al., 2011).

A more upstream target to induce autophagy is the inhibition of the class I PI3K complex, which can be achieved by treatment with the dual PI3K class I and mTOR inhibitor PI-103 (Fan et al., 2006; Park et al., 2008). Recently, specific autophagy

induction by an autophagy inducing peptide, Tat-Beclin, was shown. This peptide is based on the Beclin-interacting sequence with the HIV-1 virulence factor Nef (Shoji-Kawata et al., 2013).

On the other hand, current strategies to block autophagy predominantly target (i) the inhibition of the class III PI3K complex, (ii) the disruption of lysosomal functions or (iii) the blocking of ATG protein expression (Vinod et al., 2014). The most commonly used autophagy inhibitor is 3-Methyladenine (3-MA) targeting the class III PI3K complex (Seglen and Gordon, 1982; Miller et al., 2010; Workman and van Montfort, 2010). In addition to 3-MA, LY294002 and Wortmannin both inhibit the Vps34 kinase in the class III PI3K complex and subsequently prevent autophagic sequestration (Arcaro and Wymann, 1993; Blommaart et al., 1997). Furthermore, a novel chemical autophagy inhibitor, Spautin-1, was described. Spautin-1 was shown to increase the ubiquitination of Beclin-1 leading to its degradation through the proteasomal pathway. Treatment with Spautin-1 was shown to reduce the amount of GFP-LC3 puncta per cell (Liu et al., 2011; Mateo et al., 2013). Furthermore the degradation of autophagosomes (autophagic flux) can be blocked by Bafilomycin A1. Bafilomycin A1 blocks the lysosomal V-ATPase, thereby preventing the acidification of lysosomes (Yoshimori et al., 1991; Yamamoto et al., 1998).

1.1.5 LC3-associated phagocytosis

In addition to the canonical autophagy process described above, LC3 can be recruited to single membrane compartments in a process called LC3-associated phagocytosis (LAP) (**Figure 3**). In general, canonical autophagy and LAP require the same molecular machinery. In contrast to autophagy, LAP is triggered from outside the cell via receptor engagement leading to particle uptake in single membrane compartments. Autophagy is initiated via intracellular signals or the regulation by mTOR resulting in the formation of a double membrane structure (Florey et al., 2011).

LAP is triggered after receptor engagement and similar to canonical autophagy, the recruitment of LC3-II to the phagosome is dependent on Beclin-1 and class III PI3K activity whereas mTOR signaling and the ULK-complex are dispensable. Furthermore, both of the ubiquitin-like conjugating systems are required for LAP, as cells lacking either ATG5 or ATG7 fail to recruit LC3 to phagosomes (Sanjuan et al., 2007; Martinez et al., 2011; Henault et al., 2012). Thus far, there are several receptors known which are involved in the initiation of LAP. Activation of TLR1, TLR2 and TLR4 by particles like zymosan or LPS- and PAM3CSK4-coated beads was shown to result in LC3 recruitment to single membrane phagosomes (Sanjuan et al., 2007). The recognition of DNA-containing immune complexes (DNA-IC) by Fcγ receptor and subsequent TLR9 activation required LAP for the secretion of type I interferons such as IFN-α (Henault et

al., 2012). Besides TLR stimulation, also engagement of Dectin-1 by β-glucan from fungal cell walls was shown to trigger LAP resulting in rapid lysosomal maturation (Ma et al., 2012; Mansour et al., 2013). Furthermore, LAP in macrophages is induced upon uptake and clearance of apoptotic cells mediated by the phosphatidylserine (PS) receptor T cell immunoglobulin domain and mucin domain protein-4 (TIM4) resulting in the production of anti-inflammatory cytokines (Martinez et al., 2011).

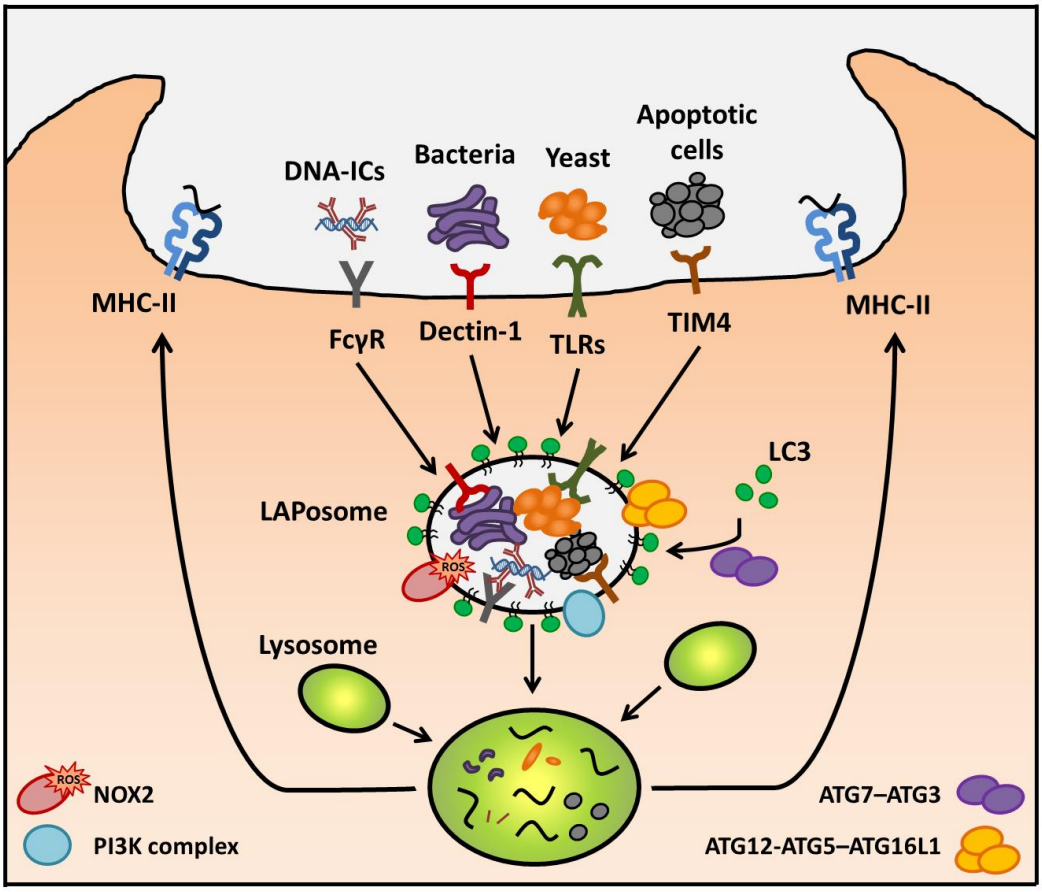

Figure 3: LC3-associated phagocytosis (LAP). LC3-associated phagocytosis is induced through receptor engagement by FcγR, Dectin-1, TLRs or TIM4. The internalization of receptor and bound particles results in the recruitment of the class III PI3K complex and NOX2, producing ROS, to the phagosomal membrane. Subsequently, the ATG12-ATG5–ATG16L1 and the ATG7–ATG3 complex mediate the formation of membrane bound LC3-II. Enhanced phagosomal maturation and fusion with lysosomes efficiently degrades the engulfed cargo and provides presentation of antigens on major histocompatibility complex II (MHC-II) molecules (adapted from Mehta et al., 2014).

Recently, Martinez and colleagues identified Rubicon as a molecular switch between the repression of macroautophagy and the activation of LAP. In the absence of Rubicon, the activation of a specific class III PI3K subcomplex containing UVRAG (UV radiation resistance-associated gene), and subsequently the recruitment of LC3, was impaired (Martinez et al., 2015). Rubicon was suggested to interact with proteins of the NADPH oxidase complex that were already demonstrated to be important for LAP induction (Yang et al., 2012). The activation of TLRs initiates the production of reactive

oxygen species (ROS) by NOX2, an isoform of the NADPH oxidase in macrophages (Huang et al., 2009). NOX2 is composed of the integral membrane-bound NOX2/gp91^{phox} and p22^{phox} and a complex of cytosolic components p67^{phox}, p47^{phox}, p40^{phox} and Rac2 (Nauseef, 2008). PI3P production of activated class III PI3K recruits the soluble oxidase component p40^{phox}. Furthermore, Rubicon binds p22^{phox} and thereby stabilizes the oxidase complex directly. The activated complex transfers electrons from the substrate (NADPH) through a flavin and heme group to oxygen inside the phagosome, building superoxides (Panday et al., 2015). The production of ROS is necessary for the recruitment of ubiquitin-like conjugating systems mediating the membrane attachment of LC3. LC3 on the LAPosome enhances maturation resulting in phagosomal fusion with lysosomes and a rapid and efficient degradation of the engulfed cargo.

The activity of NOX2 can be inhibited by Diphenyleneiodonium (DPI), an uncompetitive inhibitor of flavoproteins (Riganti et al., 2004). On the other hand, LAP induction via TLR2 engagement induced by zymosan, a glucan found in the cell wall of fungi like yeast, is commonly used. Stimulation of macrophages with zymosan results in a pro-inflammatory response and cytokine secretion (Sato et al., 2003; Du et al., 2006).

1.2 Macrophages

1.2.1 Macrophage subtypes and their activation

Macrophages (MFs), discovered in 1882 by the Russian zoologist Élie Metchnikoff, are found in all tissues and serve as a first line of defense against invading microbes (Nathan, 2008). They originate from hematopoietic stem cells in the bone marrow and are released into the circulation as macrophage precursor cells called monocytes (Murray and Wynn, 2011). In steady state, they enter the tissue to differentiate in either (anti-inflammatory) MFs or dendritic cells and replenish the long-lived, tissue resident populations (Gordon and Taylor, 2005). Furthermore, they can be specifically recruited to the side of infection by chemotaxis (Jones, 2000). Once in the tissue, MFs are exposed to a whole bunch of stimulatory and suppressive signals. Depending on the local stimuli, MFs adopt context-dependent phenotypes that either promote or inhibit immunity and inflammatory responses (Adams and Hamilton, 1984). The term “activated macrophage” was introduced by Mackaness in the 1960s, which can be further subdivided in classically activated MFs (M1) or alternatively activated MFs (M2a, M2b, M2c) promoting either Th1 or Th2 responses and resulting in different disease outcome (Mills et al., 2000; Mantovani et al., 2004).

Stimulation with pro-inflammatory molecules such as IFN-γ, secreted by activated Th1 cells or NK cells, in combination with TLR activation by e.g. LPS and production of

TNF-α by the macrophage itself, leads to M1 polarization (Mosser, 2003; Mantovani et al., 2004). Those classically activated MFs produce pro-inflammatory cytokines like IL-1β, IL-6, IL-12, TNF and IL-23 (Verreck et al., 2004; Mosser and Edwards, 2008). Furthermore, co-stimulatory molecules and proteins involved in antigen processing and presentation become upregulated favoring an inflammatory Th1 mediated immune response (Martinez and Gordon, 2014). M1 possess an antimicrobial arsenal like production of reactive oxygen species (ROS) that mediate host defence from a variety of bacteria, protozoa and viruses and have roles in anti-tumor immunity (Mackaness, 1962; Murray and Wynn, 2011). *In vitro* stimulation of monocytes with granulocyte macrophage colony-stimulating factor (GM-CSF) leads to the differentiation into MFs with a pro-inflammatory cytokine profile (Burgess and Metcalf, 1980; Verreck et al., 2004).

Besides classical activation, all other stimuli leading to macrophage polarization were termed as alternative activation. Stimulation with IL-4 and IL-13, secreted by Th2 cells, eosinophils or basophils, leads to M2a polarization which possesses tissue repair effector functions (Stein et al., 1992). These MFs are more susceptible to some intracellular infections such as *Mycobacterium tuberculosis* or *Leishmania* (Kropf et al., 2005; Harris et al., 2007). Furthermore, stimulation of monocytes with IgG immuncomplexes in combination with TLR ligands such as LPS, retains high expression of inflammatory cytokines (IL-1, IL-6, TNF) in combination with an IL-10^{high} and IL-12^{low} profile (Gerber and Mosser, 2001; Mantovani et al., 2004). Those MFs, also termed M2b or regulatory macrophages, are potent inhibitors of inflammation (Mosser and Edwards, 2008). Stimulation of monocytes with Glucocorticoids and IL-10 is referred to as M2c macrophage polarization. Glucocorticoids are released by adrenal cells in response to stress and inhibit inflammatory functions of MFs. Those MFs secrete IL-10 and TGF-β leading to immune suppression and induce the development of regulatory T cells (Mantovani et al., 2004; Mosser and Edwards, 2008). IL-10 producing macrophages possess a high capability for the clearance of apoptotic cells (Xu et al., 2006). In general, alternatively activated MFs counteract the pro-inflammatory functions of M1 MFs providing immune regulation as well as immune inhibition by promoting Th2 responses. Additionally, they are essential in helminth killing and tissue remodeling although interaction with mast cells, basophils, eosinophils, NKT cells and IgE promotes allergy and hypersensitivity (Gordon and Martinez, 2010; Locksley, 2010). *In vitro* stimulation of monocytes with macrophage colony-stimulating factor (M-CSF) leads to the differentiation into MFs with an anti-inflammatory cytokine profile and features of M2 macrophages (Verreck et al., 2004; Lacey et al., 2012).

1.2.2 MFs are professional phagocytes and mediators of adaptive immunity

A major factor that differentiates professional from non-professional phagocytes is the multitude of surface receptors pattern-recognition receptors such as the Toll-like receptors (TLRs), C-type lectin receptors (CLRs), NOD-like receptors (NLRs), DNA sensing receptors or retinoic acid inducible gene I (RIG-I) like receptors that detect signals that are not normally found in healthy tissue (Murray and Wynn, 2011). Receptor triggering by foreign material like pathogens results in their engulfment in phagosomes. During phagosome maturation, phagosomes fuse with lysosomes resulting in pH acidification (4 – 4.5) and the influx of proteases generically called cathepsins (Blum et al., 2013). These conditions mediate the denaturation of engulfed material by proteolytical cleavage producing peptides of >11 amino acids for presentation on MHC-II molecules (van Kasteren and Overkleeft, 2014; Rossjohn et al., 2015). MHC-II molecules are restricted to antigen presenting cells (APC), whereas MHC-I molecules are abundantly expressed on all cell types as they are loaded with cytosolic, proteasomal processed peptides of 8-10 amino acids containing a broad spectrum of self-peptides which are presented to $CD8^+$ T cells (van Kasteren and Overkleeft, 2014; Rossjohn et al., 2015). Prior of antigen loading to MHC-II molecules, the invariant chain (Ii) which occupies the binding groove needs to be removed. MHC-II, being assembled in the endoplasmatic reticulum of α- and β-chains associated with the Ii, is transported to MHC class II compartments (MIIC) (Neefjes et al., 1990). The Ii is processed by Cathepsin S, resulting in a 25 aa class-II associated invariant chain peptide (CLIP) that is exchanged by Cathepsin V and the chaperone HLA-DM for a high affinity peptide (Tolosa et al., 2003; van Kasteren and Overkleeft, 2014). Subsequently, the peptide-MHC complex is transported to the cell surface for immune surveillance by $CD4^+$ T cells (Neefjes et al., 2011). T cell activation requires at least two signals namely the complex of a peptide and a MHC molecule binding the T cell receptor (TCR) and a second co-stimulatory signal e.g. the binding of CD80 (B7-1)/CD86 (B7-2) or CD40 on APCs to CD28 or CD40L on T cells (Medzhitov and Janeway, JR, 2000) (**Figure 4**). The surface expression of co-stimulatory molecules on APCs is induced by TLRs upon recognition of their cognate pathogen-associated molecular pattern (PAMP) in the presence of infection leading to the activation of pathogen-specific T cells (Medzhitov and Janeway, JR, 2000).

In addition to the classical phagolysosomal pathway, also conventional autophagy and LC3-associated phagocytosis can be involved in antigen processing. In the case of autophagy processing of endogenous antigens for MHC-II presentation takes place, which is also known as cross-presentation (Munz, 2016a). Thereby, these pathways are directly associated with pathogen recognition, autolysosomal degradation and the induction of an adaptive immune response (Dengjel et al., 2005; Munz, 2016b) (**Figure**

4). Especially for professional phagocytes like macrophages, the autophagic sequestration process is of great importance. Autophagy ensures the macrophages' homeostasis as they are faced with changes in nutrient and oxygen availability when they enter inflamed or tumor tissues and mediates pathogen degradation (Martinez et al., 2013). Furthermore the pre- or absence of autophagy influences macrophage polarization as impaired autophagy promotes pro-inflammatory macrophage generation (Liu et al., 2015). Facing *Mycobacterium tuberculosis* infection, IFN-γ induced autophagy eliminates the bacterial infection whereas exposure of macrophages to Th2 cytokines like IL-4 or IL-13 abrogates autophagy leading to failure of pathogen control (Harris et al., 2007; Matsuzawa et al., 2012).

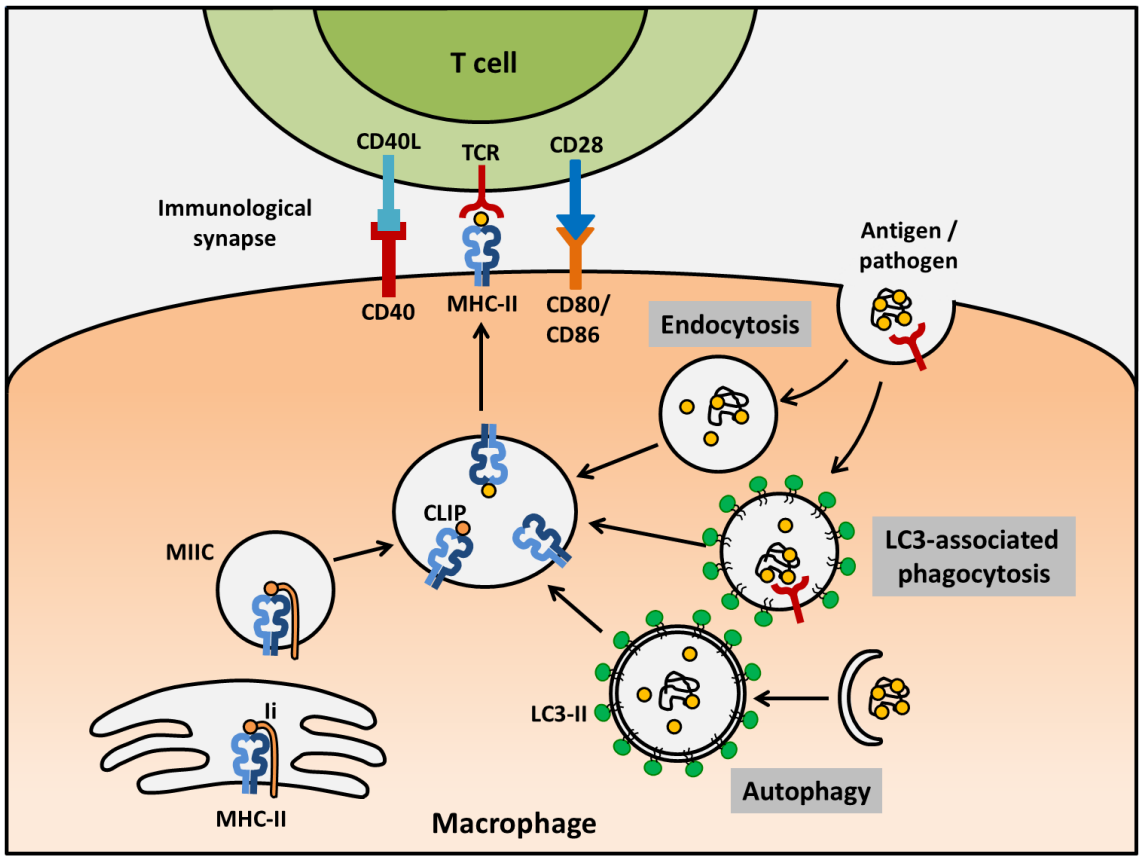

Figure 4: MHC-II antigen processing and presentation pathways. Antigens or pathogens from extracellular sources are taken up in a non-specific way in endosomes or by receptor engagement in phagosomes, whereas intracellular cargo is targeted by conventional autophagy. Endolysosomal, phagolysosomal or autophagolysosomal antigen processing provides peptides for MHC-II presentation. The class-II-associated invariant chain peptide (CLIP), which is derived from the MHC-II-associated invariant chain (Ii) is replaced by a high affinity peptide. The MHC-II-peptide complex presents antigens to $CD4^+$ T cells. In addition to MHC-II-TCR recognition, T cell activation requires co-stimulatory signals such as the binding of CD40 or CD80/CD86 on APCs to CD40L or CD28 on T cells (adapted from Greenwood et al., 2006; Kobayashi and van den Elsen, 2012).

1.3 Leishmaniasis

1.3.1 Epidemiology

Leishmaniasis is caused by the protozoan vector-born parasites of the genus *Leishmania*, which are transmitted by the bite of infected female sandflies (mainly of the subfamily *Phlebotominae* or *Lutzomyia*) (Goto and Lauletta Lindoso, 2012). According to the WHO it is classified as neglected tropical disease which is endemic in more than 90 countries in the tropics, subtropics and southern Europe (**Figure 5**). Leishmaniasis affects currently over 350 million, mainly economically disadvantaged people in many developing countries. Roughly, 12 million people suffer from the disease with about 1.3 million new infections and over 20.000 deaths annually (CDC, 02-2017, WHO, 02-2017). Leishmaniases rank among the top three most common travel-associated skin diseases. Although the disease prevails in tropical and subtropical areas, globalization and global warming allows the sandflies to spread also in non-endemic areas. Recently, a sandfly of the subfamily *Phlebotominae* was reported in the German state of Hesse (Stebut, 2015).

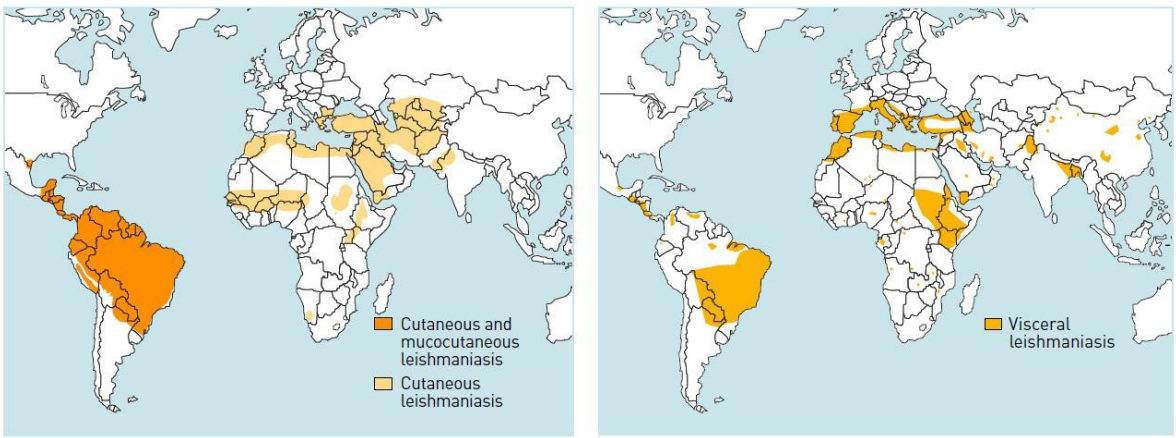

Figure 5: Geographical distribution of cutaneous and mucocutaneous (left) and visceral leishmaniasis (right) (DNDi – drugs for Neglected Diseases initiative, 02-2017).

1.3.2 Clinical manifestations

Leishmaniasis can be subdivided in three clinical manifestations of the disease caused by infection with different *Leishmania* (*L.*) subspecies. Furthermore, the immunological status of the affected patient influences the disease outcome.

The most common (ca. 90%) and least severe form is cutaneous leishmaniasis (CL), mainly caused by *Leishmania major* (*Lm*), *L. tropica, L. mexicana* or *L. aethiopica*. CL is characterized by skin lesions ranging from disseminated, non-ulcerative, nodular lesions to chronic, ulcerative lesions on exposed parts of the body. In immunocompetent individuals, CL is self-healing within 6-18 months leaving permanent scars (Goto and Lauletta Lindoso, 2012). The second form, mucocutaneous

leishmaniasis (MCL), is caused by *L. baziliensis* and occurs mainly in South America. MCL is leading to partial or total destructive lesions of the mucous membranes of the nose, mouth and throat cavities and surrounding tissue. It can occur months to years after the resolution of CL and is associated with inadequate treatment of the primary infection (Stebut, 2015); WHO, 2017). The third and most severe form is visceral leishmaniasis (VL), also known as kala-azar or black fever and is fatal if left untreated. VL is typically caused by *L. donovani* (India and Africa), *L. infantum* (Mediterranean) and *L. chagasi* (Latin America). Disease outcome is characterized by irregular bouts of fever, substantial weight loss, anemia and swelling of the spleen and liver due to parasitic infection. Several years after healing of VL, patients can develop post kala-azar dermal leishmaniasis (PKDL), which is characterized by a rush of papular, nodular or macular skin lesions. PKDL patients are considered to be a potential pathogen reservoir (WHO, 2017). Especially co-infection of *Leishmania* and HIV leads to increased incidence of developing a severe form of leishmaniasis (Lindoso et al., 2016).

1.3.3 Therapy

In the case of cutaneous ulcers, local treatment is sufficient whereas for invasive lesions, mucosal involvement or visceral leishmaniasis, a systemic therapy is required. The selection of therapy is dependent of the causative *Leishmania* subspecies as well as on the severity of the disease and the immune status of the patient. The most commonly used drugs are pentavalent antimonials, Amphotericin B, Paromomycin, Pentamidine, Miltefosine, Imiquimod or Azoles (McGwire and Satoskar, 2014). While, these interventions have severe toxic side effects, poor patient compliance and the emergence of drug-resistant strains is rapidly increasing, new therapies against leishmaniasis are needed (Kumar and Engwerda, 2014). Besides drugs, cryo-therapy with liquid nitrogen application directly to the cutaneous lesion or heat therapy (50°C for 30 sec) is used (McGwire and Satoskar, 2014). To date, there are no vaccines approved for general use but there are numerous attempts to develop a successful one. Those can be divided in three categories: (1) live attenuated *Leishmania* vaccines, including genetically modified strains, (2) killed parasite vaccines and (3) defined vaccines consisting of recombinant proteins, immunogenic surface antigens, DNA or a combination of them (Kumar and Engwerda, 2014; Srivastava et al., 2016).

1.4 *Leishmania*

1.4.1 Taxonomy

The protozoan parasites of the genus *Leishmania* belong to the class of Kinetoplastea and the family of Trypanosomatidae. In 1903, Ronald Ross classified the genus *Leishmania*, named after William Boog Leishman due to his method of staining blood for malaria and other parasites (Rioux et al., 1990; Akhoundi et al., 2016). *Leishmania* species are unicellular, obligate intracellular parasites with a well-defined nucleus, a large DNA-containing mitochondrium (kinetoplast) and a flagellum (promastigote form).

1.4.2 Life cycle

Leishmania are protozoan parasites which sustain their life cycle through transmission between the intestinal tract of a sandfly and phagocytes in a mammalian host (**Figure 6**). Among this life cycle, *Leishmania* pass in two different life stages, namely the promastigote and the amastigote form. In the midgut of the sandfly, *Leishmania* procyclic promastigotes proliferate and differentiate into infective, non-dividing metacyclic promastigotes in a process called metacyclogenesis (Giannini, 1974). Therefore typical environmental parameters of the sand fly midgut as alkaline pH and temperatures between 22°C and 28°C are necessary (Zilberstein and Shapira, 1994). During blood meal, the sandfly regurgitates about 100-3000 metacyclic promastigotes together with immunomodulatory parasite-derived proteophosphoglycans and various salivary components (Warburg and Schlein, 1986; Kaye and Scott, 2011).

Once in the skin, the majority of parasites is killed in the extracellular tissue by complement mediated lysis (Mosser and Edelson, 1984). Remaining parasites are phagocytosed by resident skin macrophages, dendritic cells or rapidly infiltrating polymorphonuclear neutrophil granulocytes (PMN) as a first line of immune defense towards invading pathogens (Laskay et al., 2003). Neutrophils are attracted to the side of infection by the release of a soluble *Leishmania* chemotactic factor (LCF) (van Zandbergen et al., 2002). The neutrophils engulf the virulent inoculum of *Leishmania* comprising a mixture of viable and apoptotic parasites, of which the latter ones are crucial for disease development (van Zandbergen et al., 2006). The uptake of apoptotic cells, characterized by phosphatidylserine (PS) on their surface, represents a “no danger” signal to immune cells. Hence, a silent phagocytosis of the parasite takes place thereby suppressing innate intracellular antimicrobial mechanisms. Furthermore, the release of cytokines such as TGF-β and IL-10 creates an anti-inflammatory environment (Voll et al., 1997; Huynh et al., 2002; van Zandbergen et al., 2007). Additionally, the rapid and spontaneous apoptosis of neutrophils is delayed up to two days, providing a transient shelter for *Leishmania* (Aga et al., 2002).

Subsequently, macrophages are recruited to the side of infection by the release of macrophage inflammatory protein-1 (MIP-1β) from infected neutrophils. Macrophages favor neutrophil apoptosis by membrane TNF and clear the tissue from apoptotic cell corpses (Menten et al., 2002; Allenbach et al., 2006). The uptake of infected and apoptotic neutrophils provides a silent entry mechanism ("Trojan horse strategy") for the parasites into their final host cells, the macrophages (Laskay et al., 2003). Another study revealed that *Leishmania*-containing neutrophils were not directly phagocytosed by macrophages. However, in neutrophil depleted mice, macrophages are able to directly take up parasites (Peters et al., 2008; Charmoy et al., 2010). Inside macrophages, promastigotes delay the phagolysosomal biogenesis by lipophosphoglycan (LPG), present on the membrane of the parasites, to allow the adaption to the acidic conditions (Desjardins and Descoteaux, 1997; Rodriguez et al., 2006). The parasitophorous vacuole is characterized by a pH of 4.7-5.2 (Antoine et al., 1990), lysosomal hydrolases (Prina et al., 1990), lysosomal-membrane markers LAMP-1 and LAMP-2 (Russell et al., 1992), a proton ATPase (Sturgill-Koszycki et al., 1994) and MHC class II molecules (Lang et al., 1994). This acidic and warmer (32-37°C subcutaneous-visceral) environment of phagolysosomal compartments initiates the transformation of metacyclic promastigotes into the aflagellate amastigote form (Zilberstein and Shapira, 1994). This differentiation process starts within the first 5-12 hours after phagocytosis and is completed on day 2-5, depending on the infecting strain (Courret et al., 2002). Amastigotes are adapted to survive the harsh lysosomal conditions and can even start replication. After cell burst, they can infect further macrophages and are responsible for disease development. During another blood meal, the sandfly takes up amastigote-infected phagocytes which can redifferentiate into infectious promastigotes in the sandfly's midgut completing the *Leishmania* life cycle (Kaye and Scott, 2011).

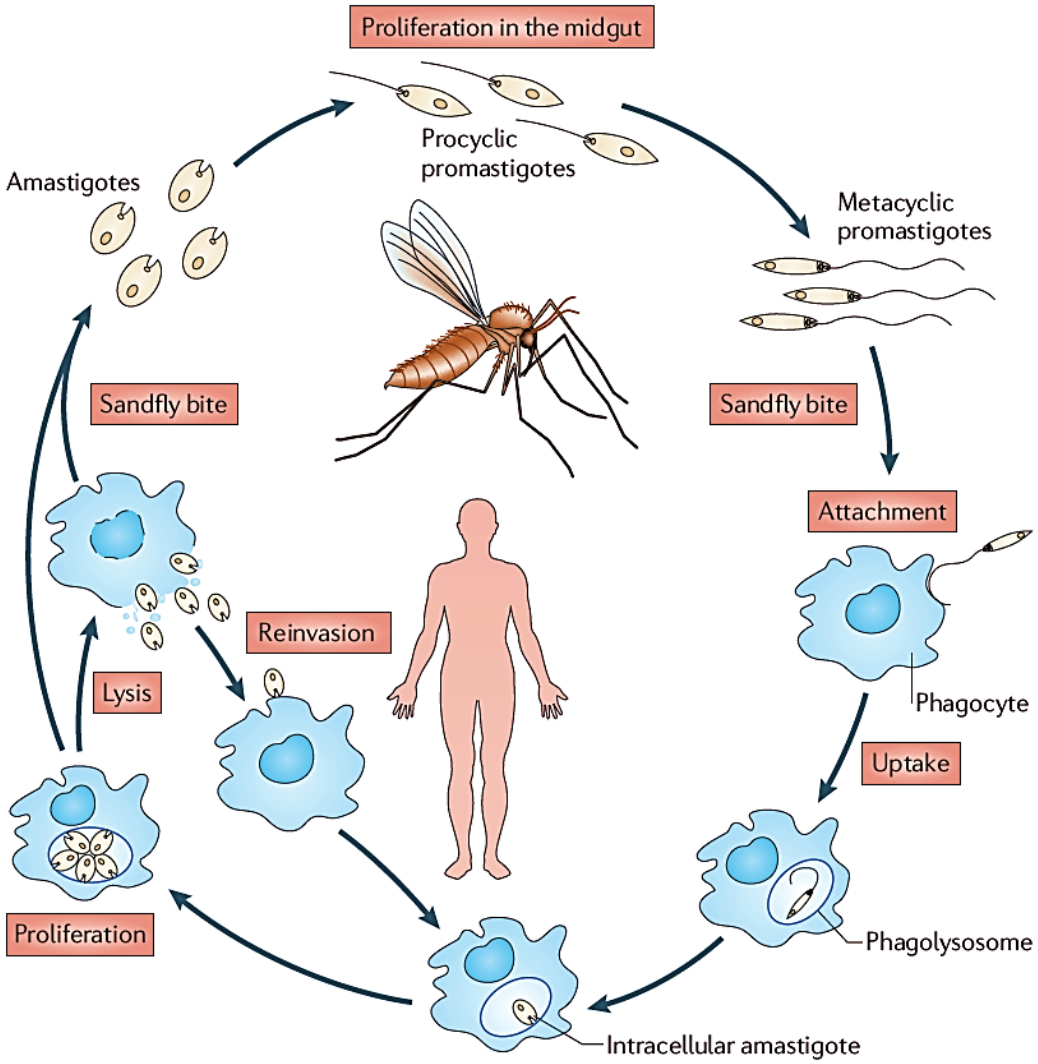

Figure 6: Life cycle of *Leishmania*. *Leishmania* procyclic promastigotes proliferate in the midgut of the sandfly into metacyclic promastigotes which are transmitted by bite of a sandfly to a mammalian host. Within the skin, *Leishmania* are taken up by phagocytes such as neutrophils, dendritic cells or macrophages into a phagolysosomal compartment. Due to the environmental changes, promastigotes transform into aflagellate, disease propagating amastigotes that undergo replication. Amastigotes can infect surrounding cells or can be taken up again by a second bite of a sandfly (Kaye and Scott, 2011).

In vitro, the growth of *Leishmania* promastigotes is characterized by two distinct growth stages, namely the logarithmic phase (log. phase, day 2-3, low virulence, mainly viable parasites) and the stationary phase (stat. phase, day 6-8, highly virulent, mixture of viable and apoptotic parasites) causing disease (Sacks and Perkins, 1984; da Silva and Sacks, 1987). The presence of about 50 % apoptotic promastigotes in the stat. phase enables survival of non-apoptotic *Leishmania* promastigotes in the virulent inoculum (van Zandbergen et al., 2006).

1.4.3 Macrophage receptors mediate *Leishmania* uptake

As *Leishmania* are obligate intracellular pathogens, their entry in macrophages as final host cell for parasite development and division is crucial for disease progression. *Leishmania* can enter macrophages either by the “Trojan Horse” strategy in apoptotic neutrophils or via direct binding to macrophage surface receptors (Ueno and Wilson, 2012). There are several receptors on macrophages reported to be responsible for *Leishmania* uptake such as complement receptors 1 and 3 (CR1 and CR3), mannose receptor (MR), fibronectin receptor (FnR) or Fcγ receptors (Mosser and Rosenthal, 1993; Kane and Mosser, 2000).

Opsonic serum complement enabling uptake via complement receptors is important for parasite adhesion to MFs and improves parasite survival (Mosser and Edelson, 1987; Mosser et al., 1992). *Leishmania* activate the complement component C3 to C3b and opsonization with the inactive form of this component (iC3b) mediates uptake via CR3 (Mosser and Edelson, 1985). CR3 (CD11b/CD18) contains two binding sites, one for particles opsonized with iC3b and second a complement independent lectin binding domain (Ehlers, 2000). In contrast, opsonization with C3b provides uptake via CR1 (CD35) (Da Silva et al., 1989; Rosenthal et al., 1996). Interaction with this receptor is only transiently because C3b is immediately cleaved to iC3b by either factor 1 of CR1 or by leishmanial GP63. Consequently, CR3-dependent recognition is predominant for parasite adhesion and uptake (Brittingham et al., 1995; Kane and Mosser, 2000). Triggering of CR1 or CR3 does not induce inflammatory responses such as respiratory burst (Wright and Silverstein, 1983; Da Silva et al., 1989), IL-12 secretion (Marth and Kelsall, 1997) and inhibits accumulation of phagosome maturation markers like LAMP-1 and Cathepsin D (Podinovskaia and Descoteaux, 2015).

In the absence of complement, the *Leishmania* surface molecules lipophosphoglycan (LPG) and GP63 are describes as attachment factors that mediate adhesion to MFs (Handman and Goding, 1985; Rizvi et al., 1988; Russell and Wright, 1988). The highly glycosylated LPG serves as a ligand for the mannose receptor but can also bind to the lectin site of CR1 and CR3 (Blackwell, 1985). In contrast to CR1 and CR3, the MR is not located in lipid microdomains containing cholesterol (Pucadyil and Chattopadhyay, 2007) and is mainly involved in the uptake of non-metacyclic promastigotes (Wilson and Pearson, 1988; Ueno and Wilson, 2012). The MR, FnR and Fcγ receptor are associated with an inflammatory response triggering a respiratory burst by activation of the NADPH oxidase (Linehan et al., 2000; Podinovskaia and Descoteaux, 2015).

1.4.4 The *Leishmania* virulence factor GP63

Leishmania express two predominant surface molecules, a zink metalloprotease, referred to as leishmanolysin or GP63 (Etges et al., 1986; Button and McMaster, 1988)

and a lipophosphoglycan, also known as LPG (King et al., 1987). Focusing on GP63, it is a glycophosphatidylinositol (GPI) anchored metalloprotease belonging to the metzincin class (Schlagenhauf et al., 1998), which is characterized by a sequence motif HExxHxxGxxH and an N-terminal pro-peptide (Yiallouros et al., 2002). To avoid self-destruction by active GP63, a cysteine residue in the pro-peptide binds the zinc atom at the active site thereby inhibiting enzyme activity (Macdonald et al., 1995). GP63 is abundantly expressed on promastigotes but gets downregulated during life stage transformation to amastigotes (Medina-Acosta et al., 1989; Frommel et al., 1990; Schneider et al., 1992). It was shown that each promastigote contains $5x10^5$ GP63 molecules on its surface (Bouvier et al., 1985). The proteolytical activity of GP63 ensures promastigote survival by cleavage of the complement component C3 to C3b and iC3b and thereby provides opsonization for uptake by CR1 and CR3 (Brittingham et al., 1995). In addition, GP63 mediates protection of amastigotes by inhibiting phagolysosomal degradation of proteins entrapped in GP63-coated liposomes (Chaudhuri et al., 1989). Furthermore, GP63 can cleave host cell proteins and consequently influences signaling pathways of the macrophage which affect downstream transcription factors (Gomez et al., 2009; Olivier et al., 2012). Already in the 1980s it was postulated that an increased GP63 expression correlates with higher infectivity (Kweider et al., 1987; Yao et al., 2003). The stated properties of GP63 make it an attractive target for further research; hence the group of McMaster used targeted gene deletion to generate a GP63 knockout strain (Joshi et al., 1998).

1.4.5 Adaptive immunity in response to *Leishmania* infection

The immunological response to *Leishmania* is mainly mediated by T cells (Sharma and Singh, 2009). From studies in phenotypically predisposed mice it is known, that a strong Th1 response (secretion of IFN-γ and IL-2) in C57BL/6 mice leads to parasite elimination whereas leishmaniasis susceptible Balb/c mice possess disease-mediating $CD4^+$ T cells that exhibit a Th2 cytokine profile (secretion of IL-4, IL-5 and IL-10) (Bogdan et al., 1990; Bogdan et al., 1996). However, the simplicity of the Th1/Th2 paradigm is questioned by the identification of more and more T cell subsets and cannot be adapted to humans (Alexander and Brombacher, 2012).

In MCL lesions and sera of VL patients, high levels of IL-4 were detected. However, there is no evidence that IL-4 is involved in the down regulation of the Th1 response in human leishmaniasis, as treatment with monoclonal antibodies against IL-4 did not restore the lymphoproliferative response or IFN-γ production (Pirmez et al., 1993; Ribeiro-de-Jesus et al., 1998; Wilson et al., 2005). In localized CL, a Th1 predominates over a Th2 response and IL-2 and IFN-γ secreting cells are found in the skin lesions (Pirmez et al., 1993; Gaafar et al., 1995). Comparable to the mouse model, IFN-γ

mediates killing of the parasites in human phagocytes and the lack of IFN-γ production by poorly proliferating PBMCs seems to predict the progression of developing VL (Haldar et al., 1983; Murray et al., 1983; Carvalho et al., 1985). Furthermore, IFN-γ was demonstrated to activate nitric oxide (NO) production by macrophages, which is secreted as free radicals in an immune response being toxic for bacteria and parasites (Nathan et al., 1983). In addition, the ligation of the FcεRII with CD23 induces NO production by human monocytes mediating *Leishmania* killing (Dugas et al., 1995; Vouldoukis et al., 1995). This mechanism has been used for treatment of cutaneous leishmaniasis with nitric oxide donors (Lopez-Jaramillo et al., 1998).

Next to IFN-γ, the inflammatory cytokine TNF-α was shown to exhibit important functions for parasite control (Laskay et al., 1991; Ribeiro-de-Jesus et al., 1998). Furthermore, recent studies emphasize the importance of two regulatory cytokines, IL-12 and IL-10, as critical for the regulation of the immune response (Sharma and Singh, 2009). IL-12 enhances Th1 responses and restores lymphocyte proliferation and IFN-γ production thereby counter-acting the effects of IL-10 (Ghalib et al., 1995). Immunosuppression of lymphocytes in *Leishmania*-infected individuals by IL-10 can be restored by applying anti-IL-10 antibodies (Ghalib et al., 1993; Hailu et al., 2005). Interestingly, characterization of lesion-isolated or *in vitro* stimulated proliferating T cells revealed a $CD45RO^{+}$ memory phenotype (Pirmez et al., 1990; KEMP et al., 1992). Cured patients possess a strong protective immunity and re-stimulation of lymphocytes with parasite antigens *in vitro* results in a vigorous proliferation and secretion of IFN-γ, IL-2 and IL-12 (Carvalho et al., 1994; Cillari et al., 1995).

Taken together, the disease outcome and progression is complicated to predict as the immune status of the host as well as the different *Leishmania* species can elicit very different immunological responses. Leishmaniasis affects a tremendous ecological and genetic diversity of the human population making it difficult to elucidate parameters of resistance and control.

1.4.6 Immune evasion strategies by *Leishmania*

To establish successful infection, *Leishmania* parasites have developed various strategies that provide evasion of the host's defense system during all stages of the immune response (Bogdan et al., 1990; Gupta et al., 2013). Once transmitted from the sandfly vector to the mammalian skin, infective metacyclic promastigotes are partially resistant to serum-mediated killing by complement components (Puentes et al., 1988). This resistance is linked to the expression of surface antigens such as LPG and GP63 (Da Silva et al., 1989). GP63 mediates the cleavage of the complement component C3 to C3b and iC3b which enables uptake via the complement receptors CR1 and CR3. Uptake in macrophages via those receptors leads to a "silent entry" that inhibits

triggering of oxidative burst (Murray, 1981; Pearson et al., 1982; Da Silva et al., 1989). Within macrophages LPG delays lysosomal acidification and protects the parasites from lysis until transformation into the acid-resistant amastigote form occurred (Spath et al., 2003; Winberg et al., 2009). A similar role was also reported for GP63 as it protects the parasites' membrane from cytolytic damages and subsequent phagolysosomal degradation in macrophages (Chaudhuri et al., 1989). Furthermore, an interaction of *Leishmania* and host cell signaling was shown which suppresses the secretion of pro-inflammatory cytokines (Privé and Descoteaux, 2000; Bhattacharyya et al., 2001). The dampening influence on the adaptive immune system is supported as infection with *L. donovani* was shown to reduce MHC-II expression and IL-1 secretion leading to the inhibition of T cell activation (Reiner et al., 1988). In addition, MHC-II molecules can be endocytosed by amastigotes followed by cysteine protease-mediated degradation and *Leishmania* impair CD40-CD40L signaling (Souza Leao et al., 1995; Awasthi et al., 2003). Patients suffering from leishmaniasis possess regulatory T cells at the lesion side that suppress anti-leishmanial immunity (Ganguly et al., 2010; Katara et al., 2011; Rai et al., 2012). Moreover, apoptotic parasites in the virulent inoculum have a crucial role in dampening innate and adaptive immune responses enabling disease progression (van Zandbergen et al., 2006; Crauwels et al., 2015).

1.5 Hypothesis and Aims

1.5.1 The role of autophagy in human primary macrophages

Macrophages are crucial for mediating innate and adaptive immune responses in health and disease. Autophagic degradation mechanisms in macrophages are versatile and can have cytoprotective as well as immunomodulatory functions. Therefore, autophagy proteins in macrophages are an interesting evasion target for intracellular pathogens and an interesting new class for therapeutic approaches in cancer and immune diseases. Most of our knowledge on autophagy in macrophages is based on cell line and mouse model research. Consequently, in this thesis we hypothesize that:

"The autophagic machinery in macrophages depends on the cells' origin, phenotype and applied stimulus. In addition, autophagy modulation in macrophages influences the adaptive immune response"

To investigate this hypothesis we have the following aims:

Aim 1:

a) Assessing autophagy modulation and autophagic flux in hMDM induced by chemicals and the peptide Tat-Beclin using Western Blot analysis for LC3-I to LC3-II conversion and LC3 immunofluorescence stainings.

b) Investigate chemical autophagy inhibition in hMDM.

c) Establish siRNA knockdowns for various autophagy related proteins and assess the knockdown efficiency on mRNA and on protein level. In addition, ULK-1 and Beclin-1 knockdown macrophages will be functionally characterized for their ability to induce autophagy.

Aim 2: Analyzing the impact of autophagy on antigen processing and presentation in hMDM using the recall antigen Tetanus Toxoid (TT). The adaptive immune response to TT will be characterized in hMDM-1 and hMDM-2. Furthermore, the impact of autophagy modulation, by induction with AZD8055 and inhibition using an ULK-1 siRNA knockdown, on T cell proliferation will be investigated.

Aim 3: Investigation of the *Leishmania* virulence factor GP63 for its potential to influence infection of hMDM, the *Leishmania* specific T cell proliferation and the host cells' autophagic process.

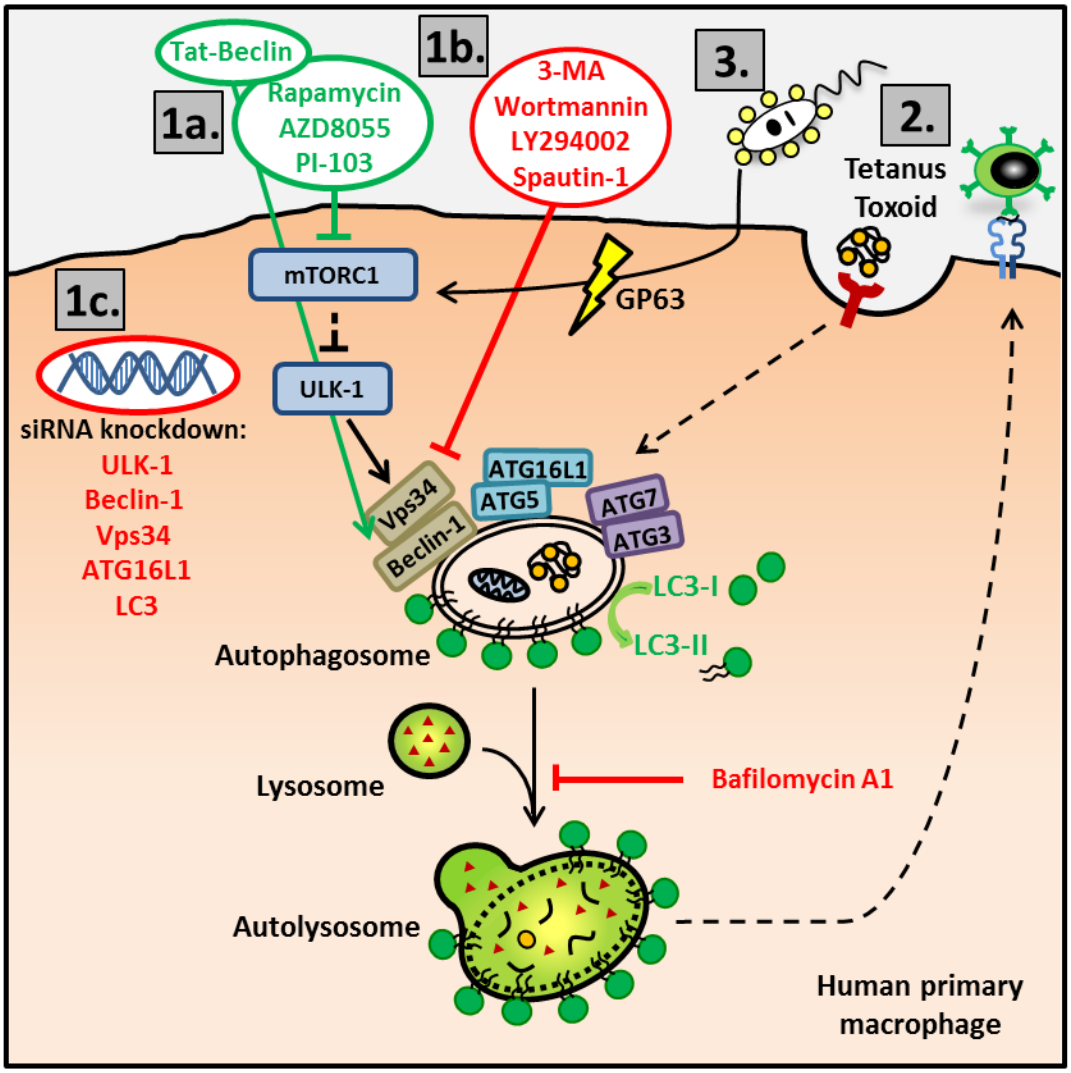

Figure 7: Schematic presentation of the autophagy related aims and hypothesis of this thesis. 1) Assessing autophagy modulation in hMDM using chemical inducers, an autophagy inducing peptide, chemical inhibitors and siRNA-mediated knockdown of autophagy related proteins. 2) Analyze the role of autophagy modulation on antigen processing and presentation using Tetanus Toxoid. 3) Investigation of the *Leishmania* virulence factor GP63 for its potential to modulate host-pathogen interactions and autophagy induction.

1.5.2 The role of LAP during *Leishmania* infection

In addition to conventional autophagy, extracellular particles can be taken up receptor-mediated by LAP. LC3 recruitment to phagosomes leads to enhanced maturation, lysosomal degradation of engulfed particles and peptide presentation on MHC-II molecules to $CD4^+$ T cells. We could already show that apoptotic *Leishmania* reside within a single-membrane, $LC3^+$ compartment indicating LAP. Furthermore, the presence of apoptotic parasites in the virulent inoculum leads to disease progression *in vivo* and a reduced T cell response *in vitro*. Consequently, we hypothesize:

"The induction of LAP by apoptotic *Leishmania* is an immune evasion mechanism enabling disease progression"

To investigate this hypothesis, we have the following aims:

Aim 1: Establish a suitable LAP-inducing particle to replace apoptotic parasites.

Aim 2: Investigate the ability of LAP-inducing particles to dampen the *Leishmania* specific T cell proliferation and analyze the effect on parasite survival.

Aim 3: Characterize the underlying mechanisms which lead to the induction of LAP upon infection of hMDM with *Leishmania* or stimulation with LAP-inducing particles and analyze the effect of LAP modulation on the adaptive immune response.

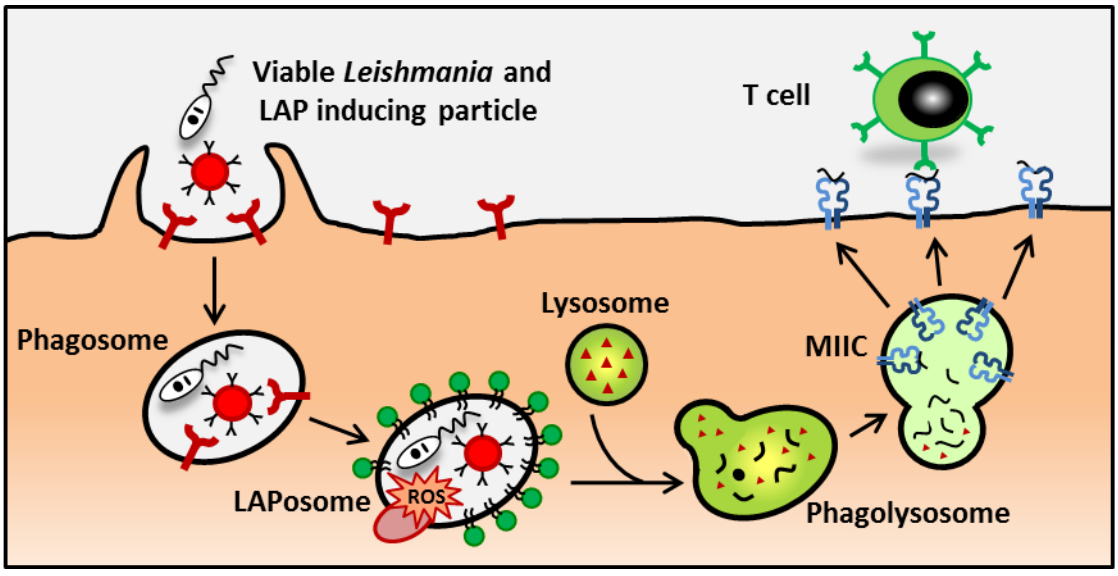

Figure 8: Schematic presentation of the LAP-related aims and hypothesis of this thesis. Apoptotic *Leishmania* will be replaced by an LAP-inducing particle and the effect of LAP modulation on the adaptive immune response will be analyzed.

2 Material and methods

2.1 Material

2.1.1 Chemicals

2- Propanol	VWR, Bruchsal, GER
3-Methyladenine	Selleckchem, Houston, USA
β-Mercaptoethanol	Sigma-Aldrich, Taufkirchen, GER
Acetic acid	Merck, Darmstadt, GER
Acrylamide-Bis solution 30%	SERVA, Heidelberg, GER
Adenine	Sigma-Aldrich, Taufkirchen, GER
Agarose LE	Biozym Scientific GmbH, Oldendorf, GER
Ammonium chloride	In-house facility PEI, Langen, GER
Ammoniumpersulfat (APS)	Serva, Heidelberg, GER
Aqua bidest.	In-house facility PEI, Langen, GER
AZD8055	Selleckchem, Houston, USA
Biotin	Sigma-Aldrich, Taufkirchen, GER
Bafilomycin-A1	Sigma-Aldrich, Taufkirchen, GER
Bovine Serum Albumin (BSA)	Applichem, Darmstadt, GER
CASYton	OLS-OMNI, Bremen, GER
Cytochalasin D	Calbiochem, Merck, Darmstadt, GER
Developer (G153 A) and Fixer (G354)	AGFA, Mortsel, BE
Difco™ Brain Heart Infusion Agar	Becton Dickenson, Sparks, USA
Dimethylsulfoxid (DMSO)	Sigma Aldrich, Taufkirchen, GER
Diphenyleneiodonium chloride (DPI)	Sigma-Aldrich, Taufkirchen, GER
Dithiothreitol (DTT)	Sigma-Aldrich, Taufkirchen, GER
dNTP-Mix (10 mM each)	NEB, Frankfurt am Main, GER
Ethanol (EtOH), absolut	Applichem, Darmstadt, GER
FACS Clean	In-house facility PEI, Langen, GER
FACS Flow (Sheath Solution)	In-house facility PEI, Langen, GER
FACS Rinse	In-house facility PEI, Langen, GER
Fetal Calf Serum (FCS)	Sigma-Aldrich, Taufkirchen, GER
Glutamine (L-Glutamine)	Biochrom AG, Berlin, GER
Glycerol (99 %)	Citifluor, London, UK
Glycine	In-house facility PEI, Langen, GER
HEPES (4-(2-hydroxyethyl)-1-piperazineethanesulfonic acid)	Biochrom AG, Berlin, GER
High purity water	In-house facility PEI, Langen, GER
Histopaque 1077	Sigma-Aldrich, Taufkirchen, GER

Human recombinant Granulocyte Macrophage Colony Stimulating Factor (GM-CSF)	Bayer Healthcare Pharmaceutical, Leverkusen, GER
Human recombinant Macrophage Colony Stimulating Factor (M-CSF)	R&D Systems, Minneapolis, USA
Human Serum Type AB	Sigma-Aldrich, Taufkirchen, GER
Hydrochloric acid (HCl), 37%	VWR, Bruchsal, GER
Hygromycin B, solution	Invitrogen, San Diego, USA
Immersion oil (Immersol™ 518F)	Carl Zeiss, Jena, GER
Luminata Forte Western HRP Substrate	Millipore, Billerica, USA
LY294002	Selleckchem, Houston, USA
Methanol	Merck, Darmstadt, GER
Milk powder Sucofin	TSI GmbH & Co. KG, Zeven, GER
Miltefosine	Merck-Millipore, Darmstadt, GER
Oligonucleotides	Eurofins MWG Operon, Ebersberg, GER
Paraformaldehyde (PFA)	Sigma-Aldrich, Taufkirchen, GER
Penicillin/Streptomycin	Biochrom AG, Berlin, GER
Phosphate buffered saline (1x PBS) w/o Ca^{2+}, Mg^{2+}; pH 7.1	In-house facility PEI, Langen, GER
Phosphatidylserine beads	Micromod, Rostock, GER
PI-103	Selleckchem, Houston, USA
Plain beads (sicastar®)	Micromod, Rostock, GER
ProLong® Gold antifade reagent	Invitrogen, Darmstadt, GER
Rabbit, Blood, defibrinated	Elocin-Lab GmbH, Gladbeck, GER
Rapamycin	Selleckchem, Houston, USA
Ringer-Solution	Braun Melsungen AG, Melsungen, GER
RNase AWAY	VWR, Darmstadt, GER
Roswell Park Memorial Institute (RPMI) 1640 Medium	Sigma-Aldrich, Deisenhof, GER Biowest (VWR), Darmstadt, GER
Saponin from Quillaja bark	Sigma-Aldrich, Taufkirchen, GER
siRNA	Qiagen, Hilden, GER
Sodium acetat	Sigma-Aldrich, Taufkirchen, GER
Sodium azide (NaN_3)	Sigma-Aldrich, Taufkirchen, GER
Sodium chloride (NaCl)	Merck, Darmstadt, GER
Sodium Dodecyl Sulfate (SDS)	Merck, Darmstadt, GER
Sodium hydroxide (NaOH) solution (10M)	Merck, Darmstadt, GER
Spautin-1	Sigma Aldrich, Taufkirchen, GER
Staurosporine	Sigma Aldrich, Taufkirchen, GER
TEMED (N, N, N´,N´-tetramethylethylenediamine)	Serva, Heidelberg, GER
Tetanus Toxoid	Aventis, Frankfurt a. M., GER

Tris(hydroxylmethyl)-aminomethan (Tris)	In-house facility PEI, Langen, GER
Tween 20	Sigma-Aldrich, Steinheim, GER
Western Blot Detection Substrate	GE Healthcare, Buckinghamshire, UK
Wortmannin	Sigma-Aldrich, Steinheim GER
Zymosan A *S. cerevisiae* BioParticles™	Invitrogen, Thermo Fisher, Dreieich, GER

2.1.2 Culture Medium

Leishmania promastigote Medium (Lm-medium)	500 ml	RPMI-1640 Medium
	5%	FCS (v/v)
	2 mM	L-Glutamine
	50 µM	β-Mercaptoethanol
	100 U/ml	Penicillin
	100 µg/ml	Streptomycin
	10 mM	HEPES
Macrophage Complete Medium (complete-medium)	500 ml	RPMI 1640 Medium
	10%	FCS (v/v)
	2 mM	L-Glutamine
	50 µM	β-Mercaptoethanol
	100 U/ml	Penicillin
	100 µg/ml	Streptomycin
	10 mM	HEPES
Novy-McNeal-Nicolle Blood Agar	50 ml	defibrinated rabbit blood
	20.8 g	Difco™ Brain Heart Infusion (BHI) agar
	400 ml	high-purity water
	100 ml	PBS w/o Ca^{2+} and Mg^{2+}, pH 7.1
	66.2 U/ml	Penicillin
	66.2 µg/ml	Streptomycin

2.1.3 Buffer and solutions

Antibody dilution buffer		TBST solution
	5%	BSA (1^{st} antibody) or skimmed milk powder (2^{nd} antibody)
	0.01%	NaN_3 (1^{st} antibody only)
Ammoniumchloride solution	0.15 M	Ammoniumchloride
		Aqua bidest.
Auto-MACS buffer pH 7.2		1x PBS
	2 mM	EDTA
	0.5%	BSA (w/v)
Blocking solution (WB)		TBST solution
	5%	skimmed milk powder (w/v)

Blotting buffer (WB)	50 mM	Tris
	40 mM	Glycin
	0.0375%	SDS (w/v)
	2.5%	Methanol (v/v)
		Aqua bidest.
DNA loading dye (10x)	3.3 ml	150 mM Tris-HCl pH 7.4
	6 ml	Glycerol
	0.7 ml	Aqua bidest.
	2.5 mg	Bromphenol blue
FACS / IF blocking buffer		PBS
	10%	FCS (w/v)
	10%	human serum (v/v)
		0.45 µm sterile filtrated
FACS staining buffer		PBS
	1%	FCS (w/v)
	1%	human serum (v/v)
		0.45 µm sterile filtrated
HEPES buffer (1M) pH 7.2		Biochrom AG, Berlin, GER
IF fixation solution		PBS
	4%	Paraformaldehyde (PFA)
IF staining buffer		PBS
(permeabilization)	1%	FCS (w/v)
	1%	human serum (v/V)
	0.5%	Saponin
		0.45 µM sterile filtrated
MACS-I buffer		Ringer solution
	0.5%	BSA (w/v)
MACS-II buffer		PBS
	0.5%	BSA (w/v)
Laemmli-Buffer (6x)	500 mM	Tris-HCl pH 6.8
	38%	Glycerol (v/v)
	10%	SDS (w/v)
	0.93 g	DTT
	0.01%	bromphenol blue (w/v)
		Aqua bidest.
PBS w/o Ca^{2+} and Mg^{2+}	136.9 mM	sodium chloride
pH 7.1	2.68 mM	potassium chloride
	1.47 mM	potassium dihydrogen orthophosphate
	8.1 mM	sodium dihydrogen phosphate
		Aqua bidest.

Ringer solution		B. Braun Melsungen AG, Melsungen, GER
Running buffer (5x) (WB)	125 mM 1.25 M 0.5%	Tris Glycine SDS (w/v) Aqua bidest.
Separating gel buffer pH 8.8	1.5 M 0.4%	Tris-HCl pH 8.8 SDS (w/v) Aqua bidest.
Stacking gel buffer pH 6.8	0.5 M 0.4%	Tris-HCl pH 6.8 SDS (w/v) Aqua bidest.
TAE buffer (20x)	0.8 M 20 mM 2.25%	Tris-HCl pH 8.0 EDTA acetic acid Aqua bidest.
TBS buffer (10x)	50 mM 150 mM	Tris-HCl pH 7.4 NaCl Aqua bidest.
TBS/T solution	 0.05%	1x TBS buffer Tween 20 (v/v)
Tris-HCl (0.5 M) pH 6.8	460 mM 40 mM	Tris(hydroxymethyl)-aminomethan hydrochlorid Tris(hydroxymethyl)-aminomethan Aqua bidest. pH 6.8 adjusted with 1 N HCl
Tris-HCl (1.5 M) pH 8.8	1.5 M	Tris(hydroxymethyl)-aminomethan Aqua bidest. pH 8.8 adjusted with 25% HCl
Washing buffer (PBMC isolation)	 5%	PBS complete-medium (v/v)

2.1.4 Human primary cells

Human peripheral blood mononuclear cells (PBMCs) were obtained from buffy coats of healthy german donors from the blood donation service in Frankfurt (DRK-Blutspendedienst). Subsequently, leukocytes were isolated and differentiated as described in 2.2.5.2.

2.1.5 *Leishmania* strains

Leishmania major isolate MHOM/IL/81/FEBNI:
Originally isolated from a skin biopsy of an Israeli patient and kindly provided by Dr. Frank Ebert (Bernhard Nocht Institute for Tropical Medicine, Hamburg, Germany)

Leishmania major dsRed:
MHOM/IL/81/FEBNI isolates genetically transfected with the red fluorescent dsRed gene (from Discosoma) together with a hygromycin phosphotransferase as selection marker (Mißlitz et al., 2000).

Leishmania major Seidmann (SD) isolate MHOM/SN/74/SD:
Leishmania major SD Wildtyp (WT; ATCC# PRA-348), ∆gp63 1-7 (KO; ATCC# PRA-385) and ∆gp63 1-7 + gp63-1 (KO+gp63; ATCC# PRA-386) were purchased from ATCC, Manassas, USA. The wildtype was initially isolated from a cutaneous Leishmaniasis patient in Senegal in 1973 and was genetically modified by Robert McMaster. Geneticin serves as a selection marker to maintain the genomic integration of gp63-1.

2.1.6 Oligonucleotides

Name	Sequence
ATG16L1 Fwd	TCTGGGACATTCGATCAGAGAG
ATG16L1 Rev	CCTTTCTGGGTTTAAGTCCAGG
Beclin-1 Fwd	GGTGTCTCTCGCAGATTCATC
Beclin-1 Rev	TCAGTCTTCGGCTGAGGTTCT
CYBB Fwd	AACGAATTGTACGTGGGCAGA
CYBB Rev	GAGGGTTTCCAGCAAACTGAG
GAPDH Fwd	GAGTCAACGGATTTGGTCGT
GAPDH Rev	TTGATTTTGGAGGGATCTCG
LC3 Fwd	AAGGCGCTTACAGCTCAATG
LC3 Rev	CTGGGAGGCATAGACCATGT
ULK-1 Fwd	AGCACGATTTGGAGGTCGC
ULK-1 Rev	GCCACGATGTTTTCATGTTTCA
Vps34 Fwd	TAGGAGGAACAACGGTTTCGC
Vps34 Rev	GCTTCTACATTAGGCCAGACTTT

2.1.7 siRNA

Allstars Negative Control siRNA	SI03650318	Qiagen, Hilden, GER
ATG16L1_1	SI04139121	Qiagen, Hilden, GER

Beclin-1_4	SI00055594	Qiagen, Hilden, GER
CYBB	SI03075709 SI03028424 SI00008729 SI00008722	Qiagen, Hilden, GER
LC3_9	SI04219614	Qiagen, Hilden, GER
ULK-1_5	SI02223270	Qiagen, Hilden, GER
Vps34	SI00605829 SI00605822 SI03649527 SI03649520	Qiagen, Hilden, GER

2.1.8 Peptides

Name	Sequence	Manufacturer
Tat-Beclin	YGRKKRRQRRR-GG- TNVFNATFEIWHDGEFGT	J. W. Drijfhout, Leiden, NL B. Levine, Dallas, USA
Tat-Scramble	YGRKKRRQRRR-GG- VGNDFFINHETTGFATEW	J. W. Drijfhout, Leiden, NL Beth Levine, Dallas, USA

2.1.9 Enzymes

Rec. RNasin® Ribonuclease Inhibitor (20-40 U/µl)	Promega, Mannheim, GER
ImPromII^{TM} Reverse Transcriptase	Promega, Mannheim, GER
Taq-polymerase (5 U/µl)	NEB, Frankfurt a.M., GER

2.1.10 Antibodies

Mouse, α-actin	Cell Signaling, Danvers, USA
Mouse, α-Beclin-1	BD Pharmingen, Heidelberg, GER
Mouse, α-GAPDH	GeneTex, Irvine, USA
Mouse, α-gp91 phox (NOX2)	Santa Cruz Biotechnology, Dallas, USA
Mouse, α-p62	Santa Cruz Biotechnology, Dallas, USA
Mouse, α-gp63 (α-*Lm*) (1-1.5 mg/ml)	AbD Serotec, Puchheim, GER
Rabbit, α-ATG16L1	Cell Signaling, Danvers, USA
Rabbit, α-LC3 (73.5 µg/ml)	Cell Signaling, Danvers, USA
Rabbit, α-ULK-1	Santa Cruz Biotechnology, Dallas, USA
Rabbit, α-Vps34	Cell Signaling, Danvers, USA

Isotype controls

Mouse, IgG2a kappa	BD Pharmingen, Heidelberg, GER
Mouse, IgG2a kappa, V450	BD Pharmingen, Heidelberg, GER
Mouse, IgG1 kappa, APC-Cy7	BioLegend, Aachen, GER

Mouse, IgG1 kappa, APC	BD Pharmingen, Heidelberg, GER
Mouse, IgG1 kappa, PE	BD Pharmingen, Heidelberg, GER
Mouse, IgG1 kappa, V450	BD Pharmingen, Heidelberg, GER
Mouse, IgG1 kappa, FITC	BD Pharmingen, Heidelberg, GER
Mouse, IgG2 kappa, Pacific blue	BD Pharmingen, Heidelberg, GER
Rabbit polyclonal serum (75.3 µg/ml)	Uwe Ritter, Regensburg, GER

HRP coupled antibodies

Goat, α-rabbit-HRP	Santa Cruz Biotechnology, Dallas, USA
Goat, α-mouse-HRP	Santa Cruz Biotechnology, Dallas, USA

Fluorescent labeled antibodies

Chicken, α-mouse-Alexa Fluor 488	Invitrogen, Thermo Fisher Scientific, GER
Goat, α-rabbit-Alexa Fluor 568	Invitrogen, Thermo Fisher Scientific, GER
Mouse, α-CD3, APC	BD Pharmingen, Heidelberg, GER
Mouse, α-CD4, APC-Cy7	BD Pharmingen, Heidelberg, GER
Mouse, α-CD8, Pacific blue	BD Pharmingen, Heidelberg, GER
Mouse, α-CD40, PE	BD Pharmingen, Heidelberg, GER
Mouse, α-CD80, V450	BD Pharmingen, Heidelberg, GER
Mouse, α-CD86, FITC	BD Pharmingen, Heidelberg, GER
Mouse, α-MHC-II, Pacific blue	BioLegend, Aachen, GER

2.1.11 Dyes and Marker

Bromphenol blue dye	Serva, Heidelberg, GER
CFSE (5(6)-Carboxyfluorescein diacetate N-succinimidyl ester)	Sigma Aldrich, Steinheim, GER
DAPI (5 µg/mL)	Molecular Probes, California, USA
Diff-QUIK®	Medion Diagnostics, Düdingen, CH
DNA ladder 1kb	NEB, Frankfurt a. M., GER
DNA ladder 100 bp	NEB, Frankfurt a. M., GER
Ethidium bromide solution (1% in water)	Merck, Darmstadt, GER
GelRed (10000x in H_2O)	Biotium Inc., Hayward, USA
LysoTracker® red	Molecular Probes Invitrogen, GER
PageRuler Prests. Protein Ladder	Thermo Fisher Scientific, Dreieich, GER

2.1.12 Ready to use Kits

Annexin V MicroBeads	Miltenyi Biotec, Bergisch Gladbach, GER
Amersham ™ ECL ™ Western Blotting Analysis System	GE Healthcare, Buckinghamshire, UK

CD14 MicroBeads, human	Miltenyi Biotec, Bergisch Gladbach, GER
Human IL-10 DuoSet ELISA	R&D systems, Minneapolis, USA
Human TNFα DuoSet ELISA	R&D systems, Minneapolis, USA
Im Prom-II Reverse Transkription System	Promega, Mannheim, GER
MESA Blue qPCR MasterMix Plus for SYBR Assay No Rox	Eurogentec, Köln, GER
RNeasy Plus Mini Kit	Qiagen, Hilden, GER
Stemfect™ RNA Transfection Kit	Stemgent, San Diego, USA

2.1.13 Laboratory supplies

Cell culture flasks with filter (25 cm2, 75 cm2 and 175 cm2)	Greiner Bio-One, Frickenhausen, GER
Cell culture petri dish (10 cm diameter)	Sarstedt, Nümbrecht, GER
Cell culture plates (96-well f-/v-/u-bottom)	Sarstedt, Nümbrecht, GER
Cell culture plates (6-well flat)	Sarstedt, Nümbrecht, GER
Cellfunnel (single, double)	Tharmac GmbH, Waldsolms, GER
Cellspin filter cards (one/two hole/s)	Tharmac GmbH, Waldsolms, GER
Cell Scraper, 16 cm	Sarstedt, Nümbrecht, GER
Centrifuge tubes (0.2 mL)	Sarstedt, Nümbrecht, GER
Centrifuge tubes (1.5 mL, 2.0 mL)	Eppendorf, Hamburg, GER
Centrifuge tubes PCR Tube Multiply® Pro (0.5 mL)	Sarstedt, Nümbrecht, GER
Chamberslide, 12-well, ibidi-treat	ibidi GmbH, Planegg / Martinsried, GER
Cover Slide (24x50 mm)	VWR, Darmstadt, GER
Cryogenic vial, internal thread (2 mL)	Greiner Bio-One, Frickenhausen, GER
Cytocentrifuge Slides one circle, uncoated	Tharmac GmbH, Waldsolms, GER
FACS microtubes (2 mL)	Micronic, Lelystad, NL
FACS tubes (5 mL) with snap-cap	Greiner Bio-One, Frickenhausen, GER
Falcons (15 mL, 50 mL)	Greiner Bio-One, Frickenhausen, GER
Hyperfilm™ ECL	GE Healthcare, Buckinghamshire, UK
Light Cycler 96-well plates with foil, white	Roche Applied Science, Darmstadt, GER
MACS LD column or LS column	Miltenyi Biotec, Bergisch Gladbach, GER
Manufix sensitive gloves	Braun Melsungen AG, Melsungen, GER
Microplate (96-well flat, transparent)	Greiner Bio-One, Frickenhausen, GER
MidiMACS separator	Miltenyi Biotec, Bergisch Gladbach, GER
Millipore Express® PLUS Membrane Filters, polyethersulfone, 0.22 µm; 0.45 µm	Merck Millipore, Billerica, USA
Multichannel pipette (Research® Plus)	Eppendorf, Hamburg, GER
Nalgene™ Mr. Frosty Freezing Container	Thermo Scientific, Dreieich, GER

Nitril gloves	Ansell Healthcare, Brussels, BE
Nitrocellulose membrane (Hybond ECL blot membrane)	GE Healthcare, Buchinghamshire, UK
Neubauer improved cell counting chamber (depth 0.1 mm, 0.02 mm)	VWR, Darmstadt, GER
Petri dish (3 cm diameter)	Greiner Bio-One, Kremsmünster, AT
Pipette controller (accu-jet® pro)	BRAND, Wertheim, GER
Pipette filter tips (1-10 µL; 10-200 µL, 100-1000 µL)	Nerbe plus, Winsen/Luhe, GER
Pipettes (Research® plus: 0.5-10 µL; 10-100 µL, 20-200 µL, 100-1000 µL)	Eppendorf, Hamburg, GER
Pipette tips (0.5-10 µL; 2-200 µL; 50-1000 µL)	Eppendorf, Hamburg, GER
Polyallomer Centrifuge Tubes	Beckmann Coulter GmbH, Krefeld, GER
Polystyrene Lids, PS, High profile	Greiner Bio-One, Frickenhausen, GER
Serological pipettes, sterile (2.5 mL; 5 mL; 10 mL; 25 mL)	Greiner Bio-One, Kremsmünster, AT
Sterile filter (0.22 µm, 0.45 µm)	Sarstedt, Nümbrecht, GER
Transfer pipette (3.5 mL)	Sarstedt, Nümbrecht, GER
Whatman paper gel blotting	VWR, Darmstadt, GER

2.1.14 Instruments

Centrifuges

BIOLiner Buckets (75003670; 7500368)	Thermo Scientific, Dreieich, GER
Bioshield 1000 A swing-out rotor	Thermo Scientific, Dreieich, GER
Bench top centrifuges 5430 and 5430R	Eppendorf, Hamburg, GER
Cytocentrifuge Cellspin II Universal 320R	Tharmac GmbH, Waldsolms, GER
Heraeus Megafuge 40R	Thermo Scientific, Dreieich, GER
Sprout Mini-Centrifuge	Biozym, Hamburg, GER

Electrophoresis and Blotting

Curix 60 tabletop processor	AGFA, Mortsel, BE
Horizontal electrophoresis equipment	Biotec-Fischer, Reiskirchen, GER
Mini-PROTEAN® Tetra Cell	Bio-Rad, München, GER
Power Supply “PowerPac™ 200/2.0”	Bio-Rad, München, GER
Semi-Dry Transfer Unit TE 77 PWR	Amersham Biosciences, Freiburg, GER
UV-Transilluminator GenoView	VWR International, Darmstadt, GER

Flow Cytometer	
Flow Cytometer LSR II SORP	Becton Dickinson, Heidelberg, GER

Imaging	
Microscope AxioPhot	Carl Zeiss, Jena, GER
Microscope Axio Vert.A1	Carl Zeiss, Jena, GER
Microscope LSM 7 *Live*	Carl Zeiss, Jena, GER
Microscope Primo Star	Carl Zeiss, Jena, GER

Incubators	
CO_2-Incubator Forma Series II Water Jacket	Thermo Scientific, Marietta, USA
CO_2 incubator, Heraeus Auto Zero	Thermo Fisher Scientific, Dreieich, GER
Recirculating cooler	Julabo, Seebach, GER

Lamina air flow	
Workbench MSC-Advantage	Thermo Fisher Scientific, Dreieich, GER
Steril Gard III Advance	The Baker Company, Sanford, USA
Steril Gard Hood	The Baker Company, Sanford, USA

PCR Thermo Cycler	
LightCycler® 480 System	Roche Applied Science, Mannheim, GER
Personal Cycler	Biometra, Göttingen, GER

Others	
Analytical balance KB BA 100	Sartorius, Göttingen, GER
AutoMACS Pro separator	Miltenyi Biotec, Bergisch Gladbach, GER
Autoclave Systec vx-150	Systec, Wettenberg, GER
CASY Modell TT	Roche Innovatis AG, Reutlingen, GER
ELISA Reader Infinite® F50	Tecan Group Ltd, Männedorf, CH
Ice machine AF 1000	Scotsman, Pogliano Milanese, IT
Freezer (-20°C)	Bosch, Stuttgart, GER
Freezer U725-G (-80°C)	New Brunswick, Eppendorf, Hamburg, GER
Magnetic stirrer IKA® C-MaG HS7	IKA®-Werke, Staufen, GER
Microwave	Bosch, Gerlingen, GER
NanoDrop 2000c	PeqLab, Erlangen, GER
Nitrogen container “Chronos”	Messer, Bad Soden, GER

pH Meter PB-11	Sartorius, Göttingen, GER
Thermomixer 5437 (1.5 mL)	Eppendorf, Hamburg, GER
Thermomixer comfort (1.5 mL)	Eppendorf, Hamburg, GER
Ultrasonic bath Sonorex Super RK103H	Bandelin, Berlin, GER
Vortex mixer VV3	VWR International, Darmstadt, GER
Water bath	Köttermann VWR International, Darmstadt, GER

2.1.15 Software

Axio Vision Rel. 4.8	Carl Zeiss, Jena, GER
BD Diva Software (V6.1.3)	Becton Dickinson, Heidelberg, GER
Citavi 5	Swiss Academic Software GmbH
FlowJo Vx	Miltenyi Biotec, Bergisch Gladbach, GER
GraphPad Prism 6	GraphPad Software, Inc., La Jolla, USA
ImageJ and FiJi	Open Source
Light Cycler software LC480 (v1.5.0 SP4)	Roche Applied Science, Mannheim, GER
Mendeley Desktop	Mendeley Ltd., London, UK
Microsoft® Office 2010	Microsoft, Redmont, US
NCBI Nucleotide Blast® (blastn)	National Library of Medicine, Bethesda, USA
Zen 2012 (blue edition, black edition)	Carl Zeiss, Jena, GER

2.2 Methods

All cell culture work was carried out using a laminar air flow workbench providing sterile and endotoxin free conditions. Cells were cultivated in humidified incubators with 5% CO_2 at 37°C (human cells) or 27°C (*Leishmania* promastigotes).

2.2.1 Cell culture of *Leishmania major* (*Lm*) promastigotes

2.2.1.1. Preparation of blood agar plates

For cultivation of *Lm* promastigotes on NNN biphasic blood agar medium, the blood agar was prepared in a 96-well plate. First, 20.8 g Brain Heart Infusion (BHI) agar was dissolved in 400 ml water and autoclaved for 15 min at 121°C. 100 ml PBS was prewarmed to 42°C in a petri dish with a diameter of 25 cm and the cooled BHI agar (~55°C) was added. Subsequently, 4 ml penicillin/streptomycin and finally 50 ml aseptically collected defibrinated rabbit blood were added. Flat-bottom 96-well plates were put in a 45° angle and 60 µl blood agar was distributed in each well with a multi-channel pipette to achieve sloped blood agar. As soon as the blood agar became solid, plates were sealed and stored at 4°C for up to 4 months.

2.2.1.2. Counting L. major promastigotes

Leishmania parasites were counted using a hemocytometer (Neubauer chamber with a depth of 0.02 mm). 5 µl of the cell suspension was added to the chamber and at least 8 small squares were counted at a 40x magnification. When counting promastigotes, both viable and apoptotic parasites were counted. For calculation of cell concentrations per ml, the amount of counted parasites was divided through the amount of counted squares, multiplied by 16 and multiplied with the chamber factor ($5x10^4$).

2.2.1.3. Cultivation of L. major promastigotes

Leishmania promastigotes were cultured in biphasic NNN blood agar medium. For passaging, 3 wells out of a 6-8 day old *Leishmania* culture were collected in 3 ml Lm-Medium for counting. The parasites were adjusted to a final concentration of $1x10^6$/ml, then $1x10^5$ cells in 100 µl were distributed in each well of a new blood agar plate using a multi-channel pipette. The plate was incubated at 27°C and 5% CO_2.The first days after passage, the parasites are in a logarithmic growth phase and from day 5 on they reach the stationary growth phase with equal amounts of viable and apoptotic parasites. The parasites were cultured up to 8 serial passages until new *Leishmania* were thawed from liquid nitrogen.

For the passage of *L. major* (FEBNI) dsRed, 20 ng/ml hygromycin and for *L. major* SD KO+GP63 50 µg/ml geneticin was added to maintain selection pressure for keeping the genomic integration.

2.2.1.4. Long-time storage of L. major promastigotes

For long-time storage of *L. major* promastigotes, the cells were pelleted at 2400 g for 8 min and resuspended in cold Lm-medium supplemented with 20% FCS. 100-200x10^6 parasites in 1 ml were transferred into cryo tubes and 10% DMSO was added. The cells were cooled down overnight in a Mr. Frosty freezing container at -80°C prior to storage in liquid nitrogen.

For thawing, the parasites were warmed at 37°C and added drop wise to 7 ml Lm-medium. After centrifugation (2400 g, 8 min, RT), promastigotes were resuspended in 12 ml Lm-medium and 100 µl of the suspension were transferred per well to a new blood agar plate. The culture was not used until parasites were passaged the first time.

2.2.2 MACS separation of viable and apoptotic *L. major* promastigotes

During early events of apoptosis phosphatidylserine (PS) is translocated from the inner side to the outer side of the plasma membrane and can be bound by Annexin V under physiological concentrations of calcium (Ca^{2+}). Separation of viable from apoptotic *L. major* promastigotes was achieved by magnetic activated cell sorting (MACS) using Annexin V MicroBeads. MicroBeads are 50 nm large super paramagnetic particles that do not activate cells due to their small size. First of all, stationary phase promastigotes were counted (2.2.1.2). 500x10^6 parasites were pelleted (2400 g, 8 min, 4°C) and washed twice with 20 ml and 10 ml MACS-I buffer. Next, the pellets were resuspended in 800 µl MACS-I buffer. 200 µl Annexin V MicroBeads were added gently mixed and incubated for 15 min at 4°C. In the meantime a MACS LS column, designed for positive selection and containing ferromagnetic spheres, was calibrated three times with 3 ml MACS-I buffer. After incubation 10 ml MACS-I buffer was added to the parasites, cells were centrifuged, the pellet was resuspended in 1 ml MACS-I buffer and the cell suspension was applied onto the column. The flow-through containing unlabeled PS-negative parasites was collected in a 15 ml tube. The column was washed three times with 3 ml MACS-I buffer to collect PS^- promastigotes which are mainly viable. For the elution of PS-positive (PS^+) promastigotes, mainly apoptotic parasites, the column was washed three times with 3 ml MACS-II buffer. Purity of both fractions was checked in a counting chamber (2.2.1.2). To improve the purity of the PS^- fraction, viable promastigotes were separated via a second, LD column. Therefore 100x10^6 pre-separated viable promastigotes were resuspended in 160 µl MACS-I buffer and 20 µl

Annexin V MicroBeads. Basically, the separation procedure was the same as described above. The purity of the obtained fractions was checked microscopically.

2.2.3 Chemical treatment of *Leishmania* promastigotes

To induce apoptosis in *Leishmania*, the parasites were treated with 25 µM staurosporine or 25 µM miltefosine for 48 h at 27°C and 5% CO_2. DNA fragmentation was analyzed by a TUNEL assay (data not shown). Subsequently, the parasites were used for an infection experiment of hMDM followed by the generation of Western Blot samples.

2.2.4 Cell culture of human primary cells

2.2.4.1. Counting PBMCs, monocytes, hMDMs and PBLs

PBMCs after gradient isolation, monocytes after CD14 separation and differentiated hMDMs were counted using an automatic CASY Cell Counter and a 150 µm capillary. Therefore, 10 µl of the cell suspension were added to 10 ml CASY ton in a CASY tube. The cell counter determines the cell concentration, cell viability, cell size, cell debris as well as cell aggregation. The aggregation factor (AF) indicates clumping of the cells, so the cell concentration was divided by the AF, if it was > 1.00. For counting peripheral blood lymphocytes (PBLs) after thawing, a hemocytometer (Neubauer chamber with a 0.1 mm depth) was used. For calculation of cell concentrations per ml, the amount of counted cells was divided through the amount of counted squares, multiplied by 16 and by the chamber factor ($1x10^4$).

2.2.4.2. Isolation of Peripheral Blood Mononuclear Cells (PBMCs)

PBMCs were isolated from buffy coats of healthy donors (obtained from the DRK Blutspendedienst, Frankfurt) containing 30-50 ml blood. First the buffy coat was diluted with prewarmed PBS to a final volume of 100 ml and 25 ml of this solution was layered carefully on top of 15 ml prewarmed leukocyte separation medium (Histopaque 1077) in a 50 ml tube. The tubes were centrifuged at 573 g for 30 min and 20°C with acceleration and deceleration at minimum level to separate the different blood cells and to split off the plasma. The PBMCs were collected from the interphase and distributed into 6 new tubes for the following washing steps. Wash-Buffer (PBS + 5% Complete-Medium) was added till a final volume of 50 ml. To remove cell debris and thrombocytes several washing steps at different rotation speeds (1084 g, 573 g, 143 g, 8 min, 20°C) were performed until the supernatant was clear. If the pellet was still red, erythrocytes were lysed by incubation with 10 ml cold ammonium chloride (0.15 M in H_2O) for 10-15 min (20°C). Subsequently, the cells were washed with Wash-Buffer (143 g, 8 min), pooled in one tube and counted using a CASY Cell Counter as

described in 2.2.4.1.. Isolation of monocytes ($CD14^+$ cells) was achieved by plastic adherence or $CD14^+$ MACS selection.

2.2.4.3. Generation of hMDM by plastic adherence

For the generation of hMDMs by plastic adherence, $40x10^6$ freshly isolated PBMCs were seeded in 5 ml Complete-Medium supplemented with 1% human serum in a 25 cm^2 culture flask. The cells were incubated for 1 h at 37°C and 5% CO_2 to let the monocytes adhere to the plastic. Subsequently, the supernatant with the non-adherent cells, mainly lymphocytes, was removed by gently washing the flasks with prewarmed washing buffer. The lymphocytes (PBLs) were collected in a 50 ml tube for freezing and a later use in proliferation assays. To differentiate the monocytes in macrophages, Complete-Medium supplemented with 10 ng/ml GM-CSF (generation of hMDM-1) or 30 ng/ml M-CSF (generation of hMDM-2) was added. The cells were incubated 5-7 days at 37°C and 5% CO_2.

2.2.4.4. Generation of hMDM by AutoMACS separation

For $CD14^+$ separation of monocytes, $100x10^6$ freshly isolated PBMCs per preparation were put in a 15 ml tube and were washed with 10 ml Auto-MACS buffer (322 g, 8 min, 20°C). The pellet was resuspended in 960 µl Auto-MACS buffer and 40 µl CD14 MicroBeads were added. PBMCs and beads were incubated 15 min at 4°C. Subsequently the cells were washed with Auto-MACS buffer (322 g, 8 min, 20°C) and the pellet was resuspended in 500 µl Auto-MACS buffer. The labeled cells were put in an AutoMACS separator and separation was achieved with the program “posseld” (positive selection double column). After separation, the isolated monocytes were pooled and counted by a CASY Cell Counter. $4x10^6$ cells (in 2.5 ml) were seeded per well in a 6 well plate. To differentiate the monocytes into hMDM-1 or hMDM-2, the Complete-Medium was supplemented with GM-CSF (10 ng/ml) or M-CSF (30 ng/ml). The $CD14^-$ cells were pooled for freezing and a later use in proliferation assays. The cells were incubated for 3 days at 37°C and 5% CO_2. To provide better growth and differentiation, growth factors were refreshed. Therefore, 1.5 ml medium per well were removed, same conditions were pooled, centrifuged (322 g, 8 min, 20°C) and resuspended in Complete-Medium containing growth factors.

2.2.4.5. Thawing of peripheral blood lymphocytes (PBLs)

The cryo-tube was thawed in the water bath at 37°C. The thawed PBLs were carefully transferred to 7 ml prewarmed Complete-Medium. Residual DMSO was removed by centrifugation (143 g, 8 min, 20°C) and the pellet was resuspended in Complete-

Medium. The cells were counted using a hemocytometer (Neubauer chamber 0.1 mm depth) as described in 2.2.4.1.

2.2.4.6. Harvesting of differentiated hMDMs

Prior to harvesting the differentiated 5-7 day old hMDM, morphological features like shape and adherence as well as cell count were checked microscopically. Subsequently, the flasks or plates were put on ice for 30 min to enable detachment. Macrophages were harvested using a cell scraper and pooled in a 50 ml tube. To increase the yield, the flaks were washed with cold PBS. The tubes were centrifuged (143 g, 8 min, 20°C) and the pellet was resuspended in an appropriate amount of Complete-Medium and counted using a CASY cell counter as described in 2.2.4.1.

2.2.5 Autophagy / LAP modulation in hMDM

Prior to assessing autophagy and LAP modulation by Western Blot or Immunofluorescence, hMDM were cultured in 1.5 ml cytocentrifuge tubes or chamberslides, respectively.

For chemical autophagy induction, hMDM were stimulated with PI-103, AZD8055 or Rapamycin (all 10 µM) for 2 h at 37°C and 5% CO_2. For stimulation with Tat-Beclin or Tat-Scramble (5-30 µM), hMDM were incubated 4.5 h at 37°C and 5% CO_2. Chemical autophagy inhibition was performed by pretreatment of hMDM with Spautin-1 (10 µM, overnight), 3-Methyladenine (1 mM, overnight), LY294002 (20 µM, 2 h) or Wortmannin (100 nM, 1 h) at 37°C and 5% CO_2 and subsequently, autophagy inducers were added to check the hMDMs ability to induce autophagy. For the induction of LAP, hMDM were treated with plain beads, PS-beads, zymosan or *Leishmania* parasites (Multiplicity of Infection (MOI) 10 or 20) for different periods of time. For the inhibition of LAP, the macrophages' NADPH oxidase, NOX2, was inhibited with 10 µM Diphenyliodonium (DPI) for 30 min at 37°C and 5% CO_2. Subsequently, the cells were washed three times with complete medium (208 g, 8 min, RT) and used for infection experiments.

2.2.6 CFSE based proliferation assay

2.2.6.1. Labeling of PBLs with Carboxyfluorescein succinimidyl ester (CFSE)

For labeling PBLs with CFSE, $10x10^6$ PBLs were put in 2 ml prewarmed Complete-Medium and 500 µl Complete-Medium with 4 µM CFSE was added. The cells were incubated for 10 min at 37°C and 5% CO_2. To remove excessive CFSE, 5 ml Complete-Medium was added and the tube was centrifuged (143 g, 8 min, 20°C). The pellet was resuspended in 10 ml Complete-Medium to obtain a concentration of $1x10^6$ PBLs/ml. In the same way, the harvested macrophages were labeled.

2.2.6.2. Co-culture of infected hMDM and PBLs

The desired amount of macrophages was adjusted to a cell concentration of $0.4x10^6$ /ml. In 1.5 ml centrifuge tubes, $2x10^5$ cells per sample (in 500 µl) were infected with different Multiplicities of Infection (MOI) of *Leishmania* parasites, zymosan, plain beads, phosphatidylserine beads in 50 µl or were stimulated with Tetanus Toxoid (TT) in different concentrations. The cells were incubated for 18 hours at 37°C and 5% CO_2.

The next day, the samples were centrifuged (68 g, 8 min) to wash away remaining *Leishmania* parasites or beads. Subsequently, the cells were resuspended in 500 µl Complete-Medium and transferred in a round-bottom 96 well plate (4x50 µl per sample, $2x10^4$ hMDM). Autologous, CFSE-labeled PBLs were added to the wells ($1x10^5$ cells/well in 100 µl) and the plates were incubated for 6 days at 37°C and 5% CO_2. To assess lymphocyte proliferation as $CFSE^{low}$ cells, the samples were analyzed by flow cytometry.

2.2.6.3. Assessing hMDM infection rate

Macrophages were harvested and counted as described in 2.2.4.6. and 2.2.4.1. $0.4x10^6$ macrophages per sample were put in 1 ml Complete-Medium and infected with *Leishmania* dsRed and/or beads for 18 h at 37°C and 5% CO_2. The next day, remaining *Leishmania* parasites or beads were washed away two times (68 g, 8 min) and the pellet was resuspended in Complete-Medium. Each sample was split into four tubes ($0.1x10^6$ cells in 250 µl). Autologous PBLs were thawed, counted in a Neubauer Chamber (0.1 mm depth) and $0.5x10^6$ PBLs in 500 µl were added to the hMDM. After incubation at 37°C and 5% CO_2 for 6 days, same samples were pooled and centrifuged (322 g, 8 min, RT). The pellets were resuspended in 100 µl FACS buffer, transferred in FACS tubes and infection rate as dsRed positive cells was analyzed by flow cytometry.

2.2.7 Flow Cytometry

Flow cytometry is used to assess cell characteristics such as size, granularity and fluorescence. All samples were suspended to a single cell solution and were analyzed by a BD™ LSR II SORP flow cytometer and FACSDiva™ software. Further data analysis and representative dot plots were obtained with FlowJo™ software.

2.2.7.1. Surface expression of GP63 on Lm SD promastigotes

Leishmania major SD promastigotes were analyzed for their surface expression of GP63. Therefore, $10x10^6$ logarithmic *Lm* promastigotes were incubated in a V-shaped 96 well plate for 15 min on ice in 100 µl FACS blocking buffer. Subsequently, the plate was centrifuged (439 g, 8 min, 4°C), the supernatant removed and the pellets were washed once in FACS buffer. Staining of GP63 was done by incubation of *Lm*

promastigotes with primary antibody (mouse α-GP63, approximately 1 µg/ml) or isotype control (mouse IgG2a kappa, 10 µg/ml) in FACS buffer for 30 min on ice. Excessive primary antibody was washed away by centrifugation (439 g, 8 min, 4°C) followed by one washing step with FACS buffer. Subsequently, the cells were incubated in secondary antibody (chicken α-mouse, Alexa Fluor 488) for 30 min on ice in the dark. Incubation was followed by two washing steps with FACS buffer. The expression of GP63 was analyzed with a threshold of 200 and logarithmic scaled axes for FSC, SSC and FITC by flow cytometry.

2.2.7.2. Proliferation of PBLs

After 6 days of co-culture of hMDM and PBLs, the plate was taken out of the incubator and 4 wells containing the same sample were pooled in a V-shaped 96 well plate. The plate was centrifuged (439 g, 8 min, 4°C) and the pellets were resuspended in 100 µl FACS buffer.

2.2.7.3. Phenotyping of proliferating PBLs

After 6 days of co-culture of Tetanus stimulated hMDMs and PBLs, the proliferating subset was characterized for surface markers. Therefore, the cells, obtained from the proliferation assay, were washed in FACS buffer (439 g, 4 min, 4°C). Next, the cells were resuspended in FACS blocking buffer and incubated for 15 min on ice. Subsequently, the cells were washed again and incubated with anti-CD3, anti-CD4, anti-CD8 or the respective isotype controls for 30 min at 4°C in the dark. After incubation, the cells were washed with FACS buffer and the pellet was resuspended in 100 µl FACS buffer. Analysis of surface expression was performed by flow cytometry.

2.2.7.4. Characterization of surface marker on hMDM

Macrophages, harvested and counted as described in 2.2.4.6. and 2.2.4.1., were put in centrifuge tubes and were stimulated with 10 µg/ml Tetanus Toxoid for 24 h at 37°C and 5% CO_2 or left untreated. After incubation, the cells were centrifuged (439 g, 8 min, RT) and transferred to a V-shaped 96 well plate ($0.3x10^6$/well). Subsequently, the cells were incubated in 100 µl FACS blocking buffer for 15 min at 4°C to prevent unspecific binding of the antibodies. After a washing step with FACS buffer, the cells were incubated with the desired antibody/isotype for 30 min at 4°C in the dark. Subsequently, the cells were washed twice with FACS buffer and after resuspension in 100 µl FACS buffer, the cells were transferred in FACS tubes to assess surface marker expression by flow cytometry.

2.2.7.6. Infection rate of hMDM with CFSE-labeled Lm SD promastigotes

For assessing the infection rate of hMDM with *Lm* promastigotes, *Leishmania* were labeled with CFSE. Therefore, $5x10^6$ parasites were incubated in 2.5 ml complete-medium containing 1 µM CFSE for 10 min at 27°C and 5% CO_2. Excessive CFSE was removed by two washing steps (2400 g, 8 min, 20°C). Subsequently, $0.5x10^6$ hMDM were incubated with a MOI 10 of *Leishmania* in cytocentrifuge tubes for 2 h at 37°C and 5% CO_2 followed by one washing step (68 g, 8 min, 20°C) to remove extracellular *Leishmania*. The pellet was resuspended in 100 µl PBS and analyzed by flow cytometry as CFSE positive cells being infected.

2.2.7.6. Assessing lysosomal acidification

To assess lysosomal acidification, hMDM were treated in centrifuge tubes with an MOI 10 of MACS-separated *Leishmania* or zymosan particles for 1, 3 and 5 h at 37°C and 5% CO_2. After incubation, extracellular *Leishmania* or zymosan were washed away (68 g, 8 min, RT) and subsequently, Lysotracker® Red DND-99 (final conc. 1 µM) was added, staining acidic organelles like lysosomes. The cells were incubated for 10 at 37°C and 5% CO_2 followed by two washing steps with cold wash buffer. Acidification of hMDM as mean fluorescence intensity (MFI) in the PE channel was immediately assessed by flow cytometry. MFI values were normalized to the respective medium control.

2.2.8 Molecular biology methods

2.2.8.1. Assessing nucleic acid concentrations

Nucleic acid concentrations were determined using a NanoDrop 2000c UV-Vis spectrometer. Therefore, 2 µl of the sample were pipetted on the quartz cell and concentration was measured at a wavelength of 260 nm in duplicates. For blanking, corresponding buffers in which samples were dissolved, were used.

2.2.8.2. Transfection of hMDM with siRNA

For siRNA transfection, hMDM (isolated as described in 2.2.4.4.) were washed with 1 ml RPMI-Medium without supplements and 1 ml RPMI-Medium without supplements was added per well. For the transfection, two solutions (A and B) were prepared at RT and mixed within 5 min. For each well, 4.6 µl Stemfect RNA transfection reagent and 20 µl transfection buffer (solution A) were mixed with 2 µl specific siRNA or Non-Target siRNA (10 µM) and 20 µl transfection buffer (solution B). The transfection mixture was incubated for 20 min at RT and then added dropwise to the wells. The final concentration of siRNA was approximately 20 nM. The cells were incubated at 37°C and 5% CO_2 for 7 h and subsequently a medium change was performed. Therefore,

the cells were washed once with complete-medium and 2.5 ml complete-medium was added per well. 2 days post transfection, hMDM were harvested, counted by a CASY cell counter and used for RNA isolation (2.2.8.3.), Western Blot samples (2.2.9.1.) or proliferation assays (2.2.6.2.).

2.2.8.3. RNA isolation

RNA was isolated using the RNeasy Plus Mini Kit according to the manufacturer's instructions. Therefore, at least $0.3x10^6$ hMDM were washed with cold PBS (1024 g, 8 min, 20°C). Subsequently, the pellet was lysed in 350 µl RLT-Plus-Buffer by resuspending and the homogenized lysate was transferred to a gDNA Eliminator spin column and centrifuged (15300 g, 30 sec, 20°C) to get rid of genomic DNA. 350 µl 70% ethanol was added to the flow-through and this mixture was transferred to a RNeasy spin column. After the following centrifugation step (15300 g, 30 sec, 20°C) the flow-through was discarded and the column was washed with 700 µl RW1 Buffer (15300 g, 30 sec, 20°C). The washing was repeated twice with 500 µl RPE Buffer (15300 g, 30 sec and 2 min, 20°C) and the column was dried by centrifugation in a fresh collection tube (18000 g, 1 min, 20°C). RNA was eluted from the column with 30 µl RNase-free water in a fresh 1.5 mL centrifuge tube by centrifugation (15300 xg, 30 s, RT).The isolated RNA was either placed on ice for a further use or was frozen at -80°C.

2.2.8.4. Test PCR of isolated RNA

To confirm that the isolated RNA is free of DNA contaminations, a Test-PCR was performed using human GAPDH primer. In addition, a negative control without template (H_2O) and a positive control with cDNA as template were prepared. A Master-Mix without template was prepared and distributed to the 0.2 µl PCR tubes.

Volume [µl]	**Reagent**	**Final conc.**
1-2 (50-100 ng)	RNA (or 2 µl cDNA/H_2O)	
1	Forward Primer (10 µM)	0.2 µM
1	Reverse Primer (10 µM)	0.2 µM
5	dNTP-Mix (2mM each)	0.2 mM
5	NEB Taq-Buffer (10x)	1x
0.25	NEB-Taq-Polymerase (5 U/µl)	1.25 U
ad 50	ddH_2O	

Subsequently, the template was added and the PCR with the following program was run.

Step	Temp. [°C]	time [s]
Initial denaturation	95	30
Amplification (30 cycles)		
Denaturation	95	30
Annealing	60	30
Elongation	68	30
Final Elongation	68	10 min
Cooling	4	∞

The PCR products were separated electrophoretically with a 1% Agarose gel containing GelRed® and analyzed under UV light. Only the positive control with cDNA as template should show a product.

2.2.8.5. Reverse transcription – cDNA synthesis

For cDNA synthesis the ImProm-II Reverse Transcription System Kit™ was used according the manufacturer's instructions. The Reverse Transcriptase (RT) is a RNA-dependent polymerase which catalyzes the generation of cDNA from a RNA template. For one reaction:

Volume [µl]	Reagent
1	ImPromII™ Random Primer Mix
50 ng	Template RNA
ad 5 µl	Nuclease-free H_2O

The primer-template RNA mixture was incubated 5 min at 70°C for thermally denaturation and subsequently chilled on ice. A reverse transcription reaction mix was prepared on ice and added to each sample. For one reaction:

Volume [µl]	Reagent	Final conc.
6.5	Nuclease-free H_2O	
4	ImPromII™ Reaction Buffer (5x)	1x
2	$MgCl_2$ (25 mM)	2.5 mM
1	dNTP Mix (10 mM each)	0.5 mM
0.5	Recombinant RNasin® Ribonuclease Inhibitor (20-40 U/µl)	10-20 U
1	ImPromII™ Reverse Transcriptase	

After addition of the Master Mix, the tubes were shortly spinned down and placed in the PCR cycler performing the following program:

Step	Temp. [°C]	Time [min]
Annealing	25	5
Reverse transcription	42	60
Inactivation	70	15
Cooling	4	∞

The synthesized cDNA samples were stored at -20°C.

2.2.8.6. Quantitative Real-Time PCR (qRT-PCR)

Quantitative real-time PCR was used to amplify DNA and quantify the arising DNA amounts during analysis. Therefore a MESA Blue qPCR MasterMix Plus for SYBR Assay No Rox Kit was used according to the manufacturer's instructions. A master mix for each primer pair was prepared.

Volume [µl]	Reagent	Final conc.
10	MESA Blue qPCR MasterMix (2x)	1x
6	Aqua bidest.	
1	Forward Primer (10 µM)	0.5 µM
1	Reverse Primer (10 µM	0.5 µM
2	cDNA (undiluted)	

The fluorescent dye SYBR Green intercalates into double-stranded DNA, which is present after amplification. Based on the fluorescence intensity, which is proportional to the DNA amount, the amplification of the target genes can be measured. The used primers were proven to be specific (melting curve and agarose gel separation of amplified products) and efficient (primer efficiency test) and are listed in 2.1.6. All samples were measured in duplicates and a sample containing the Master-Mix with H_2O instead of cDNA was used as negative control. Amplification was done using a Light Cycler LC480 from Roche running the following program:

Step	Temp. [°C]	time [s]	°C/s
Taq activation	95	10 min	4.4
Amplification (45 cycles)			
Denaturation	95	10	4.4
Annealing	60	10	2.2
Elongation	72	15	4.4
Final Elongation	85	10	4.4
Melting curve	60-99		0.11
Cooling	40	20 min	2.2

Evaluation of generated data was performed with the applied software LC480 (version 1.5.0 SP4) analyzing the so-called CT-value (cycle threshold), which indicates the cycle in which the fluorescence signal significantly exceeds the background signal for the first time. Relative gene expression was evaluated by the $2^{-\Delta\Delta CT}$ method according to Livak and Schmittgen (Livak and Schmittgen, 2001).

2.2.9 Western Blot analysis

2.2.9.1. Sample preparation

For Western Blot analysis, 0.3-0.5x10^6 hMDM or 3-5x10^6 *L. major* parasites were pelleted (345 g, 8 min, 20°C for hMDM and 2400 g, 8 min, 20°C for *L. major*) and lysed in 20 µl 1x Laemmli-Buffer by heating at 95°C for 10 min. Samples were vortexed, spinned down and stored at -20°C. The modulation of autophagy and LAP was analyzed by LC3-I to LC3-II conversion by Western Blot and by p62 degradation (just autophagy).

2.2.9.2. SDS-Polyacrylamide Gel Electrophoresis (SDS-PAGE)

SDS-PAGE is used to separate a denatured protein mixture according to their electrophoretic mobility which correlates with the molecular weight (Laemmli, 1970). 10% or 15% SDS-polyacrylamide gels were prepared according to a standard protocol. The samples as well as a prestained protein marker were loaded onto the gel. Electrophoresis was performed in a Mini-PROTEAN® Tetra cell with 1x running buffer at constant 70 V for protein passage through the stacking gel and with constant 100 V through the separation gel.

Chemicals	**Separation gel (15%)**	**Separation gel (10%)**	**Stacking gel (4%)**
ddH_2O	4.5 ml	5 ml	2.5 ml
Separation gel buffer	4.5 ml	3 ml	-
Stacking gel buffer	-	-	1 ml
Acrylamide/bis solution 30%	9 ml	4 ml	0.5 ml
TEMED	40 µl	25 µl	5 µl
APS 10%	180 µl	120 µl	20 µl

2.2.9.3. Western Blot and protein band detection

Western Blot was used to transfer electrophoretically separated proteins from a polyacrylamide gel onto a nitrocellulose membrane. Therefore, a semi-dry blotting system was used and transfer was performed for 1 h at constant 1.5 mA/cm^2. Subsequently, the immobilized proteins can be detected with specific antibodies and be visualized by chemi-luminescence. To avoid unspecific antibody binding, the

membrane was blocked with TBST + 5% skimmed milk for 1 h at RT. Subsequently, the membrane was washed with TBST to remove residual milk and the primary antibody was added over night at 4°C by gently agitation on a shaker. The next day, the membrane was washed 3 times for 10 min with TBST and a secondary HRP-coupled antibody was added in TBST + 5% milk for 1 h at RT. After another 3 washing steps for 10 min at RT, protein bands were detected using Amersham ECL™ or Luminata forte substrate according to the manufacturer´s protocol. High performance ECL films were exposed to the membrane for distinct durations in the dark followed by development in an AGFA processor or a LICOR C-Digit Blot scanner. Densitometry analysis of Western Blot bands was done by ImageJ. Glyderaldehyde 3-phosphate dehydrogenase (GAPDH) or β-actin were used as loading control and for calculation of normalized protein amounts.

2.2.10 Enzyme-linked immunosorbent assay (ELISA)

To measure the secreted IL-10 and TNF-α concentration, $0.1x10^6$ macrophages per ml were infected with a MOI 10 of *Leishmania* parasites or zymosan. After 18 hours, the supernatants were collected and frozen at -80°C. Subsequently, 100 µl of the supernatants were used diluted for TNF-α (1:10 or 1:20) or undiluted for IL-10 in duplicates. The ELISA was performed according to the manufactures instructions and the plates were read in by a Tecan infinite F50 ELISA reader.

2.2.11 Microscopy

2.2.11.1. Cytocentrifugation of Leishmania and hMDM

For the generation of cytospins, $2x10^6$ *Leishmania* parasites or $1x10^5$ hMDMs were resuspended in 100 µl medium or buffer. Cells were centrifuged on glass slides in a cytocentrifuge at 500 g for 10 min (*Leishmania*) or at 75 g for 5 min (hMDM). Subsequently, slides were air-dried and stained using DiffQuick® solutions.

2.2.11.2. DiffQuick® staining

DiffQuick® staining is a histological staining and the kit is consisting out of three different solutions. Fist, air-dried cytospin slides were incubated for 2 min in fixation solution containing methanol. Subsequently, they were incubated in Staining Solution 1 for 2 min, an eosinophilic staining of the cytoplasm. Next, the cells were incubated for 2 min in Staining Solution 2, a basophilic staining of the nucleus or the kinetoplast. The slides were rinsed in tap water and air-dried for microscopical analysis using an AxioPhot microscope.

2.2.11.3. LC3 staining in chamberslides

To assess LC3 recruitment to autophagosomes or phagosomes by immunofluorescence, $0.1x10^6$ hMDM in 100 µl complete-medium were added per well in a 12-well chamberslide. The adherence of hMDM was checked microscopically after 30 min at 37°C and 5% CO_2. Autophagy was induced by incubation with PI-103, AZD8055 or Rapamycin (all 10 µM) for 30-40 min at 37°C and 5% CO_2. LC3-associated phagocytosis was induced by incubation with zymosan, plain beads or PS-Beads for 2 h. After incubation all wells were washed twice with 100 µl prewarmed wash buffer. Subsequently, the cells were fixated through incubation with 100 µl PBS containing 4% paraformaldehyde (PFA) for 2 min at 4°C in the dark. After removing the PFA all wells were washed with 100 µl of Buffer-1 followed by 100 µl of Buffer-2 containing saponin. To each well 100 µl complete-medium containing 183.75 ng/ml primary antibody (polyclonal rabbit α-LC3) and 2 µl DAPI or 100 µl complete-medium containing 183.75 ng/ml isotype control (polyclonal rabbit serum) and 2 µl DAPI was added and incubated for 30 min at 4°C in the dark. Subsequently, the supernatant was removed and the wells were washed with 100 µl Buffer-2. To each well 100 µl complete-medium containing 0.5 µl secondary antibody (goat α-rabbit Alexa-Fluor-568) was added and incubated for 30 min at 4°C in the dark. Subsequently, the wells were washed with 100 µl Buffer-2 followed by 100 µl of Buffer-1. All liquid was removed completely. To preserve the sample for microscopically analysis, a cover slip was applied with 3 drops of ProLong® Gold Antifade Reagent. Surplus ProLong® Gold Antifade Reagent was removed with cellulose papers. The Chamber Slide was stored in the dark at 4°C. Analysis of Chamber Slides was performed by a LSM7 Live microscope with a 630x magnification and by ZEN blue software.

2.2.12 Transduction of hMDM with eGFP-LC3 lentiviral particles

For transduction with lentiviral particles, $2x10^5$ $CD14^+$ separated monocytes (2.2.4.4) were seeded in chamberslides for microscopic analysis. Adherent macrophages were transduced with an MOI 0.1 of eGFP-LC3 lentiviral vector particles and incubated for 4 h at 37°C and 5% CO_2. Subsequently, a medium change was performed and the cells were further incubated for 4-5 days at 37°C and 5% CO_2 before being used for stimulation with zymosan particles. The formation of LC3 positive compartments was analyzed by live cell imaging using a LSM7 Live microscope with a 630x magnification and by ZEN blue software.

2.2.13 Statistical analysis

All data were shown as mean ± SD (standard deviation). To determine whether differences were statistically significant, the results were analyzed with a Wilcoxon matched-pairs signed-rank test and GraphPad Prism software. Values of $p < 0.05$ (*), $p < 0.01$ (**) and $p < 0.001$ (***) were considered as significant.

3 Results

3.1 Autophagy modulation in human primary macrophages

In the first part of this thesis, we focused on the modulation of autophagy in human primary macrophages using GM-CSF and M-CSF differentiated monocytes as model phenotypes representing a pro- and an anti-inflammatory macrophage, respectively.

3.1.1 PI-103, AZD8055 and Rapamycin induce autophagy in hMDM

The best known stimulus to induce autophagy is the inhibition of the nutrient sensor kinase mTOR. Therefore, pro-inflammatory macrophages were stimulated with the mTOR inhibitors Rapamycin and AZD8055 and with the dual class I PI3K/mTOR inhibitor PI-103. Subsequently, we assessed the protein expression levels of the autophagy marker LC3 by immunofluorescence. All chemical autophagy inducers were shown to induce LC3 protein expression compared to the respective control (**Figure 9A**). Analyzing the corrected total cell fluorescence (CTCF), significantly augmented LC3 levels upon PI-103 (1.35 ± 0.8 fold) and AZD8055 (1.39 ± 0.47 fold) treatment were confirmed indicating no superior effect of dual class I PI3K/mTOR compared to single mTOR inhibition. Concerning stimulation with Rapamycin, elevated LC3 expression levels were observed (1.13 ± 0.37 fold) (**Figure 9B**).

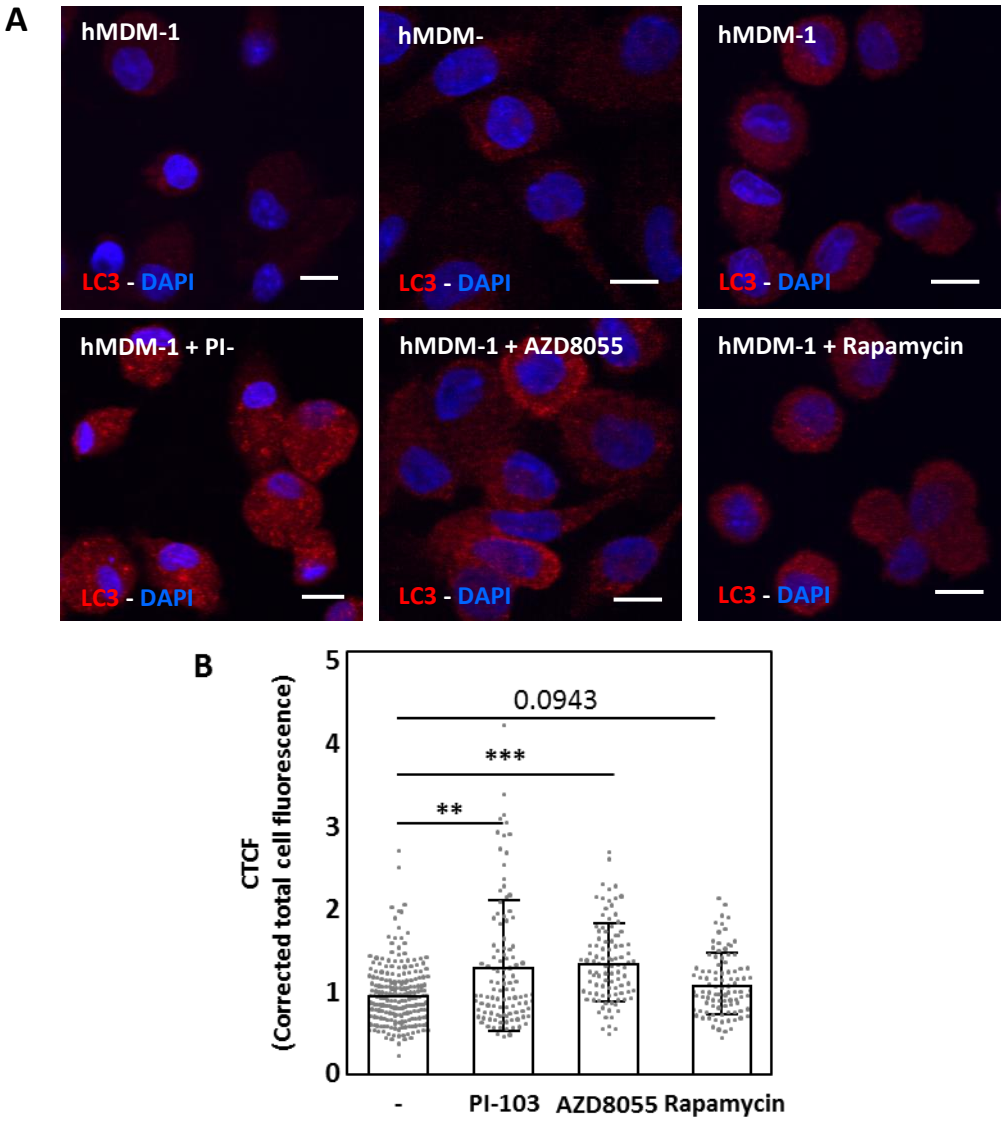

Figure 9: PI-103, AZD8055 and Rapamycin increase the expression of LC3 in hMDM-1. hMDM-1 were treated with PI-103, AZD8055 or Rapamycin (all 10 µM) for 40 min. Subsequently the cells were fixed and stained with an anti-LC3 antibody (red) and nuclei were counterstained with DAPI (blue). (**A**) Representative images were taken with a Zeiss LSM-Live 7 microscope and a 630x magnification. (**B**) The corrected total cell fluorescence (CTCF) was calculated by ImageJ. Data are representative for at least three independent experiments and are shown as mean ± SD (each dot represents the CTCF of one cell, n = 95-222; scale bar is 10 µm).

As only the total amount of LC3, meaning LC3-I and LC3-II, can be analyzed by immunofluorescence, we performed Western Blots to analyze if LC3-I is lipidated to its membrane bound form LC3-II which is located on autophagosomes. Pro- and anti-inflammatory macrophages were stimulated with PI-103, AZD8055 or Rapamycin and LC3 conversion was assessed. All chemical inducers could be demonstrated to significantly increase LC3-I to LC3-II conversion shown by Western Blot (**Figure 10A**). The potential of the analyzed modulators to induce LC3 conversion is in line with the expression levels shown by immunofluorescence. PI-103 (4.4 ± 3 fold; 6 ± 2.8 fold) was

shown to induce autophagy the highest, followed by AZD8055 (3.5 ± 2.4 fold; 5 ± 3.1 fold) and Rapamycin (3 ± 2.3 fold; 4.1 ± 2.8 fold) in hMDM-1 and hMDM-2 respectively. Furthermore, we observed that anti-inflammatory macrophages were more susceptible to chemical autophagy induction.

Another marker to investigate autophagy induction is the intracellular autophagy adaptor protein p62 (SQSTM-1) which targets cytosolic proteins for their degradation in autophagosomes. For this, p62 binds to ubiquitinylated proteins and with its LIR motif (LC3-interacting region) to LC3 on phagophores. Consequently, along with increased autophagy induction and LC3 lipidation, p62-protein complexes are degraded in autolysosomes. Indeed, we could show that upon chemical induction of autophagy a reduced level of p62 was detected for treatment with PI-103 (0.68 ± 0.31 fold, 0.77 ± 0.27 fold), AZD8055 (0.75 ± 0.39 fold, 0.79 ± 0.27 fold) and Rapamycin (0.97 ± 0.36 fold, 0.89 ± 0.41 fold), in hMDM-1 and hMDM-2 respectively (**Figure 10B**).

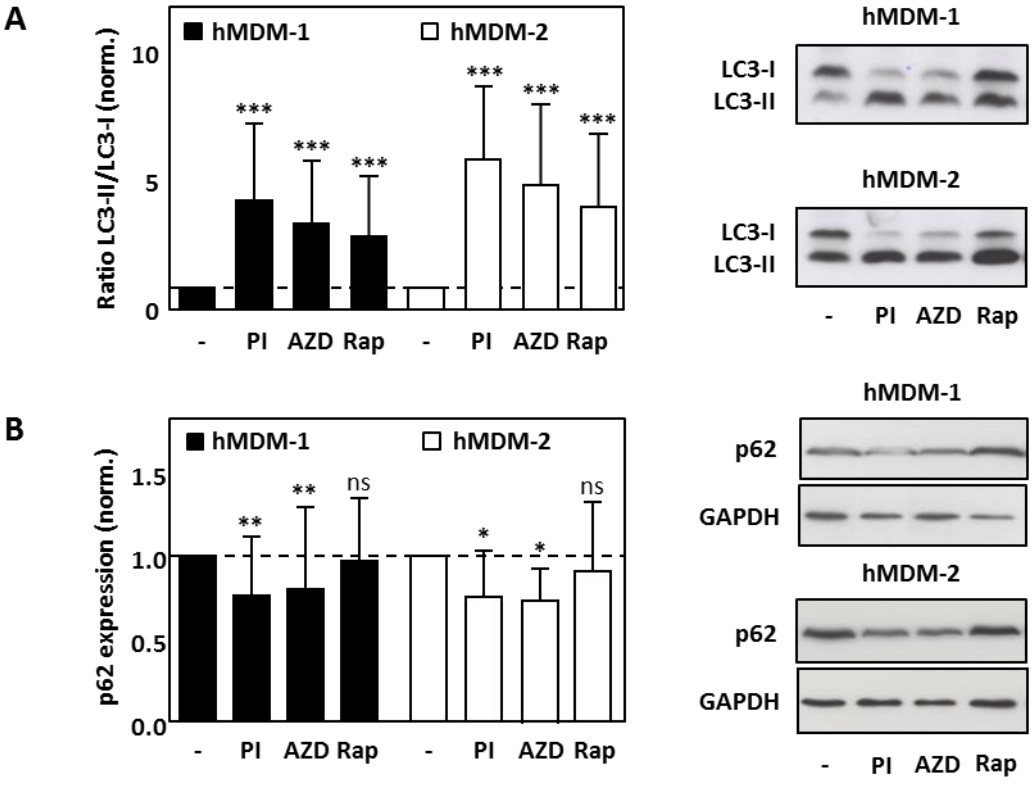

Figure 10: PI-103, AZD8055 and Rapamycin increase LC3 conversion and p62 degradation in hMDM. hMDM were treated with PI-103, AZD8055 or Rapamycin (all 10 µM) for 2 h. Autophagy induction was analyzed by (**A**) conversion of LC3-I to LC3-II and (**B**) p62 expression using Western Blot and densitometry analysis. GAPDH or β-actin was used as loading control. Data are representative for at least three independent experiments and are shown as mean ± SD (A: n = 11-20, B: n = 10-15).

As increased LC3-II levels indicate either enhanced autophagosome formation or reduced autophagosome turnover, the autophagic flux was assessed by inhibiting

lysosomal acidification using Bafilomycin A1 (**Figure 11**). As expected, pretreatment with Bafilomycin A1 led to an accumulation of LC3-II, indicating a basal autophagy level in macrophages, which was further increased through treatment with autophagy inducers in hMDM-1 and hMDM-2 respectively (**Figure 11A**). Moreover, also the p62 levels were increased upon blocking of autophagic flux with Bafilomycin A1 demonstrating inhibition of p62 degradation by autolysosomes (**Figure 11B**).

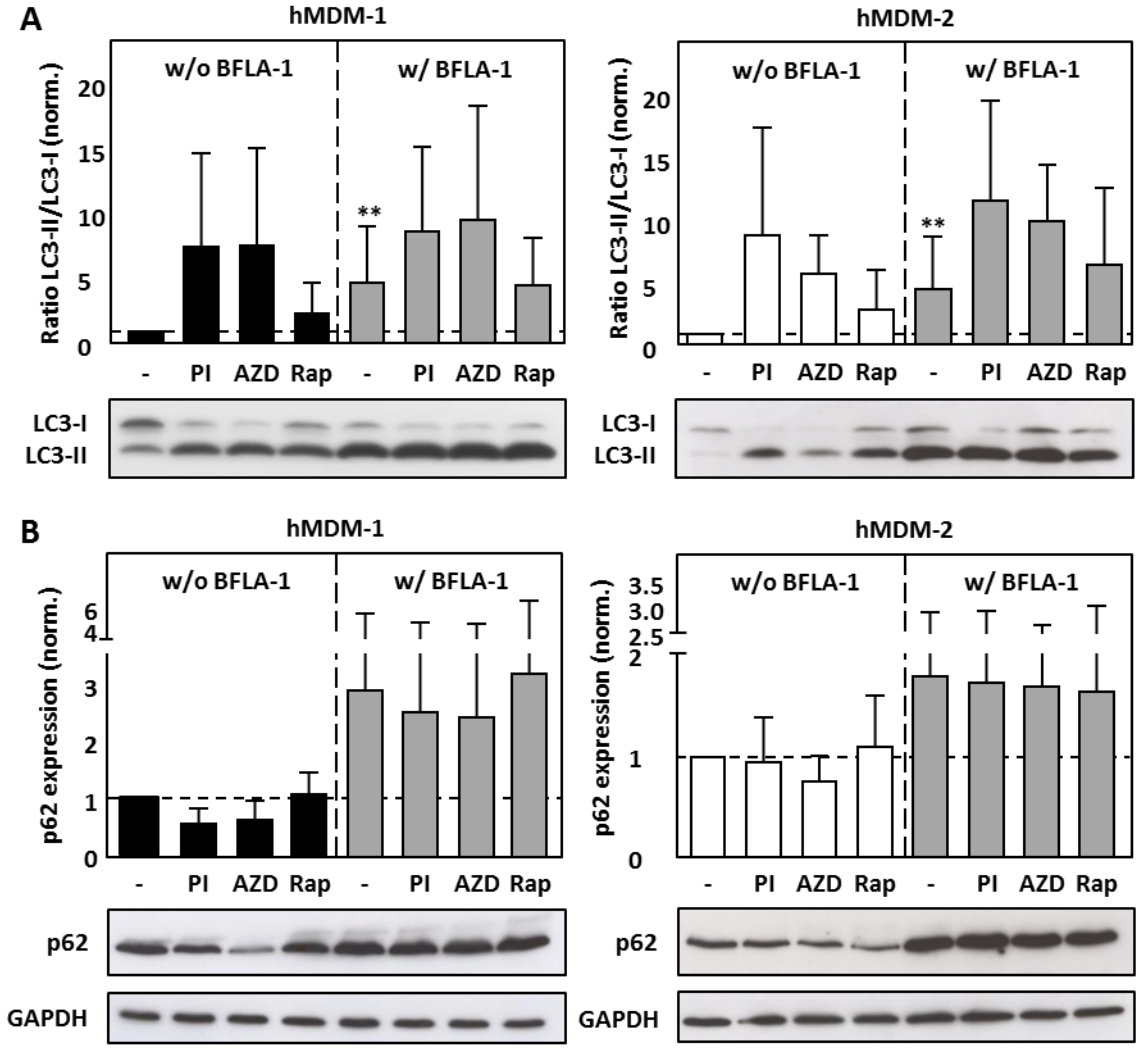

Figure 11: Blocking of autophagic flux in hMDM with Bafilomycin A1. hMDM were pretreated with Bafilomycin A1 (30 nM, 1 h) and subsequently treated with PI-103, AZD8055 or Rapamycin (all 10 µM) for 2 h. Blocking of autophagic flux was analyzed by (**A**) conversion of LC3-I to LC3-II and (**B**) p62 expression using Western Blot and densitometry analysis in hMDM-1 and hMDM-2 respectively. GAPDH was used as loading control. Significances were calculated against the untreated control. Data are representative for at least three independent experiments and are shown as mean ± SD (n = 12 for LC3, n = 5 for p62).

3.1.2 Autophagy induction with the peptide Tat-Beclin

To induce autophagy more specifically, the autophagy inducing peptide, Tat-Beclin, was used. This peptide could be shown to induce LC3 conversion at concentrations of 30 µM (8.6 ± 11.5 fold; 9.5 ± 13.7 fold) in hMDM-1 and hMDM-2 respectively, in contrast to the corresponding Tat-Scramble control peptide (1.7 ± 0.6 fold; 1.9 ± 0.8

fold) (**Figure 12A**). At lower concentrations of Tat-Beclin, no significant changes in LC3 conversion were detectable. Concerning p62 levels, no degradation upon autophagy induction with Tat-Beclin could be detected in hMDM-1 and a minor, not significant reduction in hMDM-2 (**Figure 12 B**).

Similar to the chemical autophagy induction by PI3K/mTOR inhibitors, hMDM-2 induced a stronger LC3-I to LC3-II conversion and p62 degradation compared to hMDM-1.

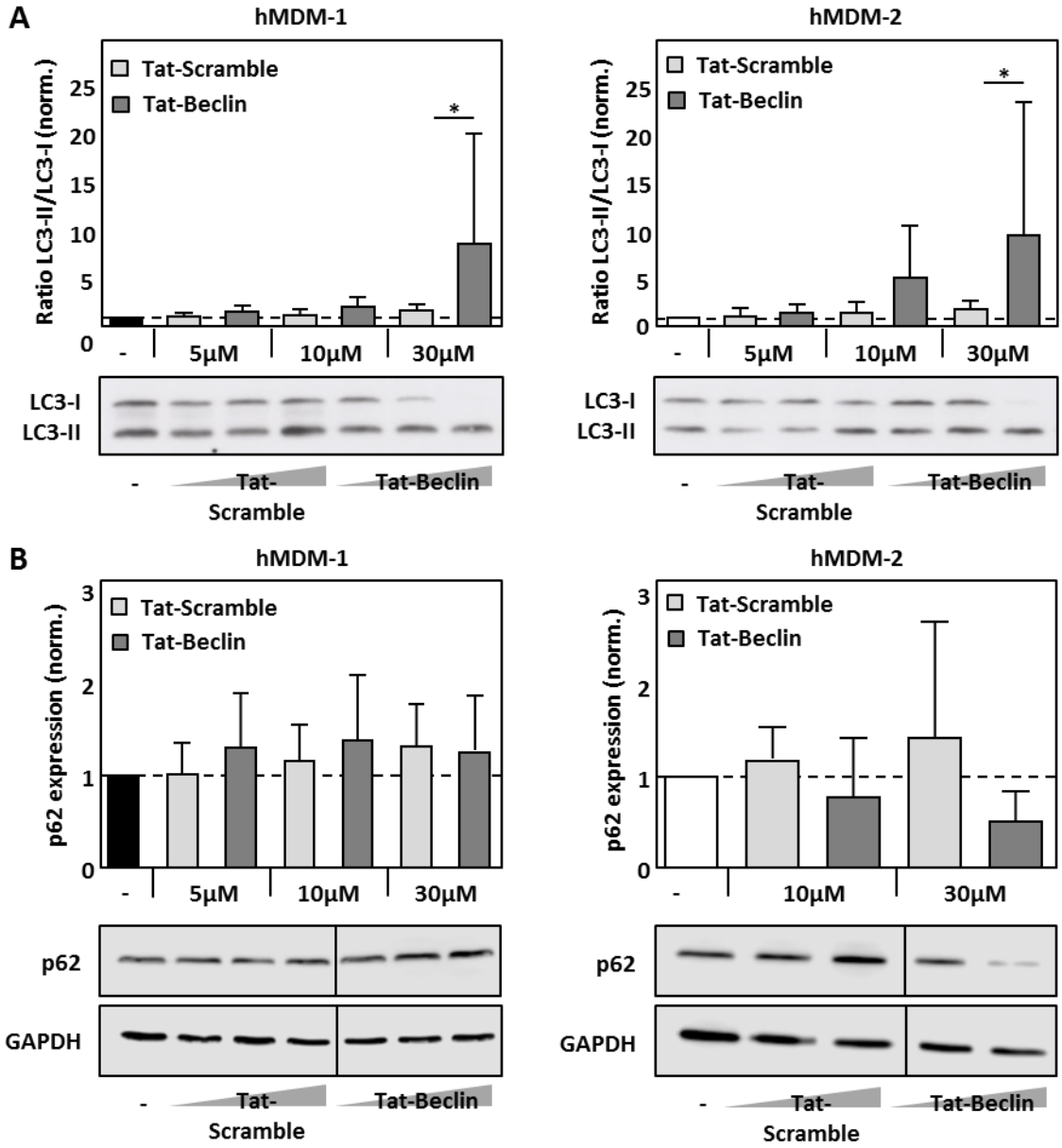

Figure 12: Tat-Beclin induces LC3 conversion in hMDM. hMDM were treated with Tat-Scramble or Tat-Beclin (5-30 µM) for 4.5 h. Autophagy induction was analyzed by (**A**) conversion of LC3-I to LC3-II and (**B**) p62 degradation using Western Blot and densitometry analysis in hMDM-1 and hMDM-2. Data are representative for at least three independent experiments and are shown as mean ± SD (n = 5-9 for LC3; n = 2-4 for p62).

3.1.3 Inhibition of class III PI3 kinase pathway by Wortmannin and Spautin-1 blocks autophagy induction in hMDM

Next, we aimed to modulate autophagy negatively using the class III PI3-kinase inhibitors 3-Methyladenine, Wortmannin and LY294002. Furthermore, Spautin-1, which targets Beclin-1 for proteasomal degradation, is used.

To identify the potential of 3-Methyladenine, Wortmannin, LY294002 and Spautin-1 to inhibit autophagy, macrophages were pretreated with the inhibitors and subsequently autophagy was induced using PI-103, AZD8055 or Rapamycin in hMDM-1 (**Figure 13A**) and hMDM-2 (**Figure 13B**). By assessing LC3 conversion in PI-103 treated hMDM (5.5 ± 4 fold; 7 ± 5.1 fold), pretreatment with Spautin-1 (1.6 ± 0.9 fold; 2.0 ± 1.4 fold) and Wortmannin (1.8 ± 1.3 fold and 3 ± 2.8 fold) could be demonstrated to decrease the cellular LC3 conversion levels significantly in both hMDM-1 and hMDM-2, respectively. Remarkably, pretreatment with 3-Methyladenine even led to an increased autophagy induction in hMDM-1 (11.3 ± 8.6 fold) and just a minor decrease in hMDM-2 (6.2 ± 2.6 fold). Interestingly, the preincubation of macrophages with LY294002 followed by autophagy induction was able to block LC3 conversion in hMDM-1 (2.8 ± 1.8 fold) but induced the conversion in hMDM-2 (8.7 ± 5.9 fold).

Comparable results were obtained by the application of Rapamycin or AZD8055 as inducing stimuli. Taken together, autophagy induction was successfully inhibited by the pretreatment with Spautin-1, Wortmannin and LY294002 in hMDM-1 and with Spautin-1 and Wortmannin in hMDM-2.

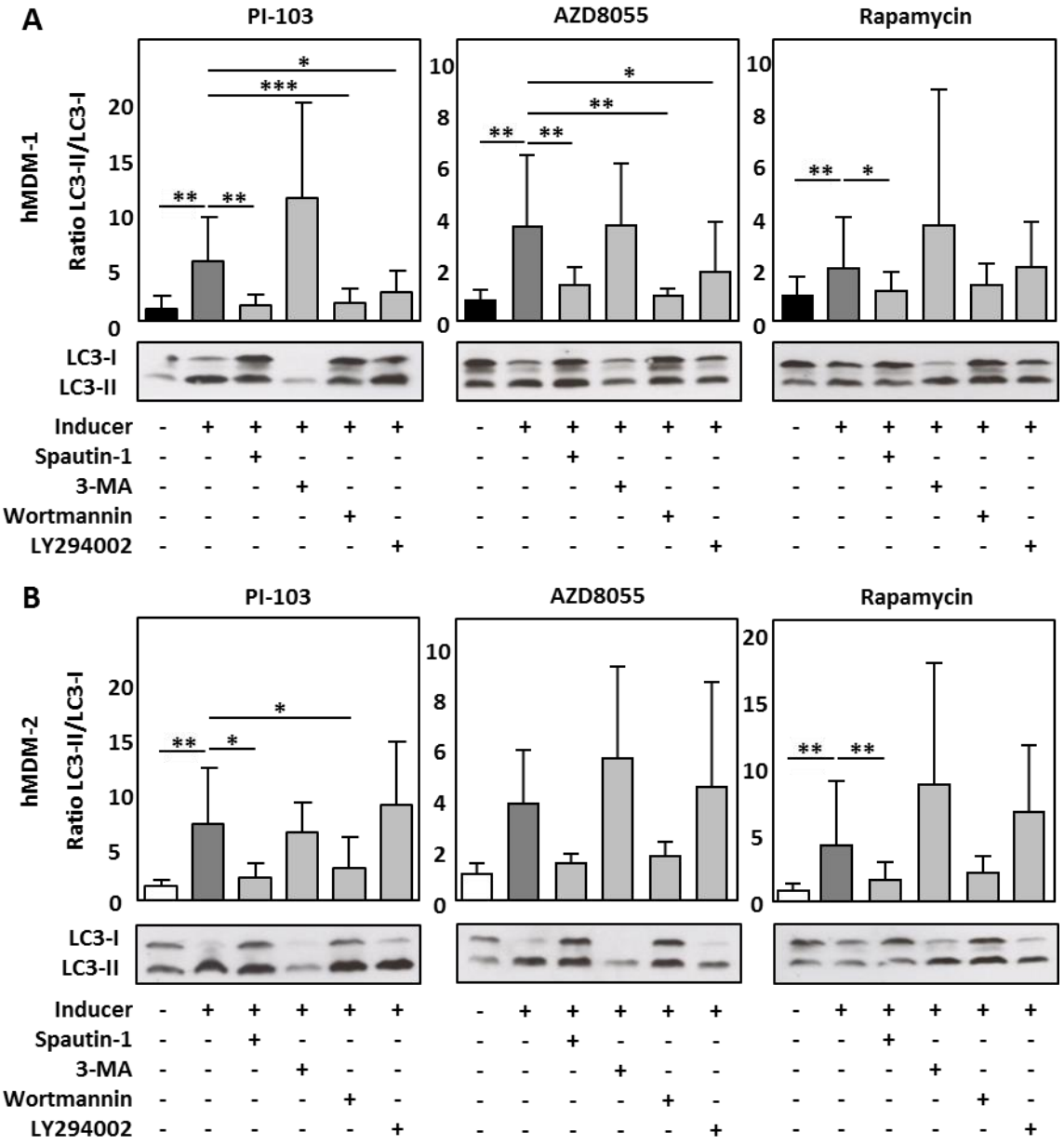

Figure 13: Spautin-1 and Wortmannin inhibit the induction of autophagy in hMDM. (**A**) hMDM-1 and (**B**) hMDM-2 were treated with the autophagy inhibitors Spautin-1 (10 µM, overnight), 3-Methyladenine (1 mM, overnight), Wortmannin (100 nM, 2 h) or LY294002 (20 µM, 1h) and subsequently autophagy was induced using PI-103, AZD8055 or Rapamycin (all 10 µM) for 2 h. Autophagy induction was analyzed by conversion of LC3-I to LC3-II by Western Blot and densitometry analysis. Data are representative for at least three independent experiments and are shown as mean ± SD (n = 5-12).

3.1.4 Autophagy inhibition by siRNA knockdown

After successful inhibition of autophagy by different chemicals targeting class III PI3K or Beclin-1, we asked the question whether we could confirm those data by specific siRNA-mediated knockdown of autophagy related proteins.

Therefore, we targeted ULK-1, Vps34, Beclin-1, ATG16L1 and LC3 for siRNA knockdown in human primary macrophages. At given time points after siRNA

treatment, mRNA and protein levels were assessed using qRT-PCR (**Figure 14**) and Western Blot analysis (**Figure 15**).

Regarding mRNA levels, the treatment of hMDM-1 with ULK-1 siRNA revealed the mRNA levels to be constantly reduced for up to one week (45% ± 19% on day 2-3; 26% ± 7.4% on day 4-5; 30% on day 6-7) (**Figure 14A**). Focusing on Vps34, the mRNA level was reduced to 44% ± 30% on day 2-3 and 60% ± 34% on day 4-5 (**Figure 14B**). Targeting Beclin-1 revealed the mRNA levels to be reduced for up to one week (11% ± 7% on day 2-3; 21% ± 3% on day 4-5 and 23% ± 0.07% on day 6-7) (**Figure 14C**). Analyzing ATG16L1, the lowest mRNA level was demonstrated on day 2-3 post transfection (30% ± 0.5% on day 2-3; 53% ± 48% on day 4-5; 71% ± 57% on day 6-7) (**Figure 14D**). Concerning LC3, the mRNA level was reduced early after knockdown (34% ± 11% on day 2-3) and increased again over time (68% ± 48% on day 4-5) (**Figure 14E**).

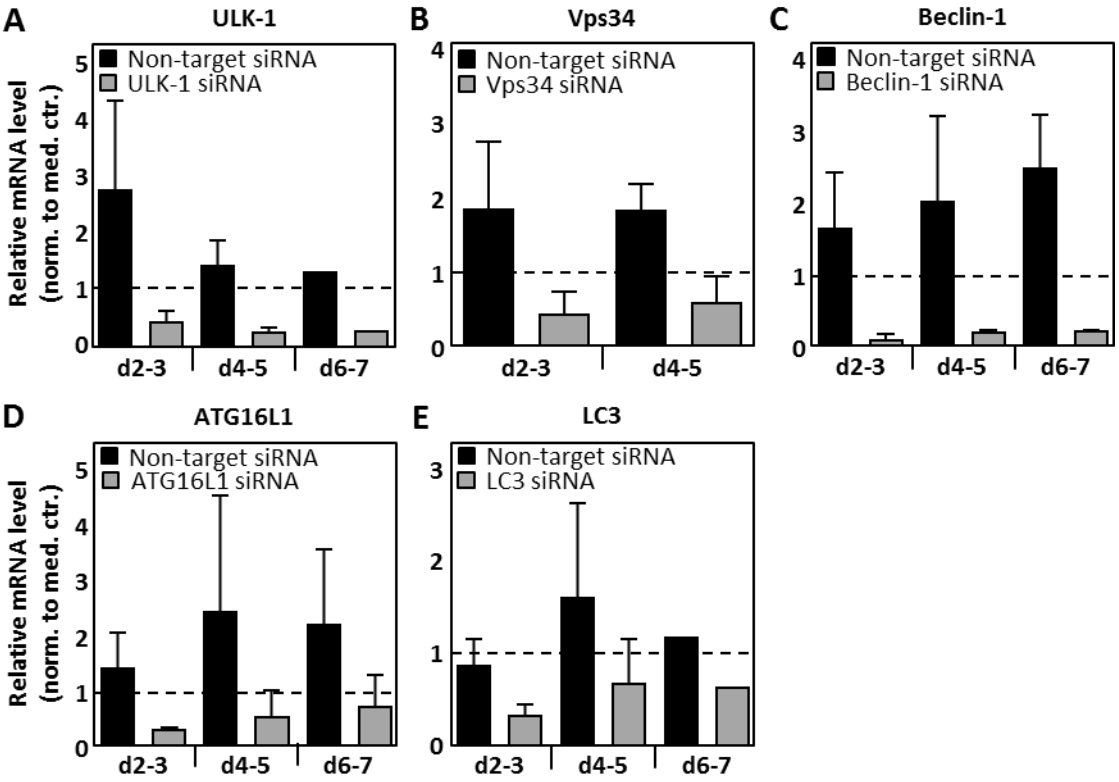

Figure 14: mRNA level of ULK-1, Vps34, Beclin-1, ATG16L1 and LC3 in hMDM-1 treated with siRNA. hMDM were treated with non-target siRNA or specific siRNA (ULK-1 (**A**), Vps34 (**B**), Beclin-1 (**C**), ATG16L1 (**D**) or LC3 (**E**)) and subsequently the mRNA level was assessed over time by qRT-PCR. The mRNA expression of GAPDH was used as housekeeping gene. Data are shown as mean ± SD.

Next, we analyzed if reduced mRNA levels result in protein reduction. By targeting ULK-1, the protein amount was reduced to 19% ± 12% on day 4-5 but getting re-expressed after 7 days (**Figure 15A**). Concerning Vps34, the reduced mRNA levels did not affect the protein levels over time, indicating strong protein stability (**Figure 15B**).

By targeting Beclin-1 it took up to 7 days until the protein amount is reduced to 39% ± 32% compared to the medium control (**Figure 15C**). The same was observed for ATG16L1, the protein levels did not decrease at early time points after knockdown (90% ± 35% on day 2-3) but dropped strongly after 7 days to 35% ± 12% (**Figure 15D**). Focusing on LC3, the protein level was reduced early after knockdown (25% ± 10% on day 2-3 and increased again over time (68% ± 56 % on day 4-5) (**Figure 15E**).

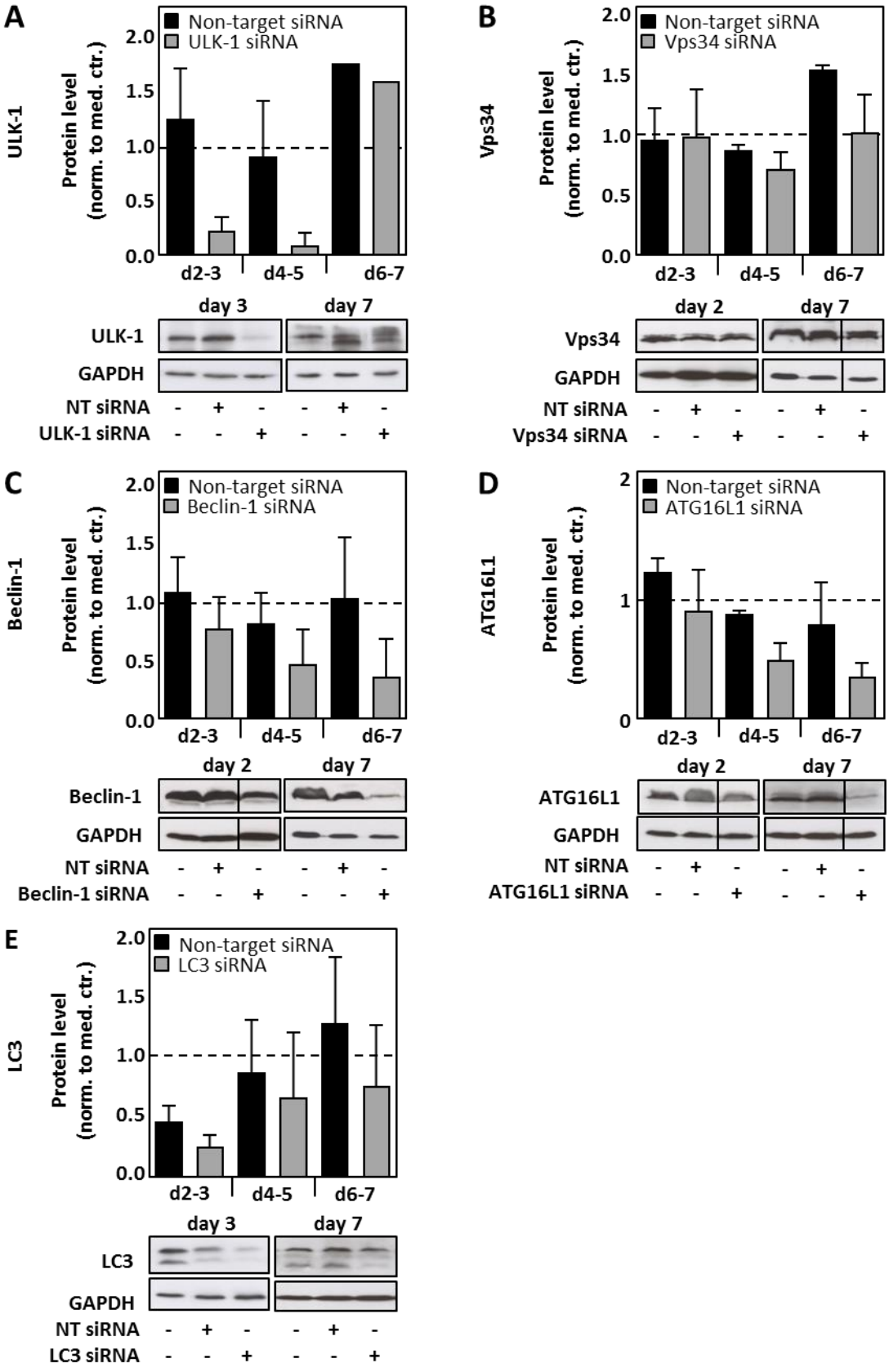

Figure 15: Protein level of ULK-1, Vps34, Beclin-1, ATG16L1 and LC3 in hMDM-1 treated with siRNA. hMDM were treated with non-target siRNA or specific siRNA (ULK-1 (**A**), Vps34 (**B**), Beclin-1 (**C**), ATG16L1 (**D**) or LC3 (**E**)) and subsequently the protein level was assessed over time by Western Blot and densitometry analysis. GAPDH was used as loading control. Data are shown as mean ± SD.

To investigate the efficiency of the knockdown, we selected ULK-1, Beclin-1 and LC3 knockdown macrophages for the application of autophagy inducers and analyzed LC3 conversion (**Figure 16, 17 and 18**). Therefore, the cells were treated with the prototypic autophagy inducers PI-103, AZD8055 or Rapamycin and the effect on LC3-I to LC3-II conversion and p62 degradation was analyzed by Western Blot.

First we investigated ULK-1 knockdown macrophages three days after siRNA application and subsequent treatment with the respective autophagy inducer. All inducers resulted in increased LC3 conversion (Medium 8.0 ± 5.6 fold, NT 17.3 ± 3.3 fold, ULK-1 siRNA 9.9 ± 3.5 fold for PI-103, Medium 4.5 ± 1.6 fold, NT 13.1 ± 5.8 fold, ULK-1 siRNA 5.1 ± 2.3 fold for AZD8055 and Medium 3.1 ± 1.5 fold, NT 3.5 ± 1.6 fold, ULK-1 siRNA 3.1 ± 1.8 fold for Rapamycin) (**Figure 16A**). Vice versa, the intracellular adaptor protein p62 is targeted for degradation in autolysosomes. Stimulation of siRNA treated hMDM and controls with PI-103 or AZD8055 resulted in reduced p62 levels whereas stimulation with Rapamycin was not effective (Medium 0.7 ± 0.22 fold, NT 0.56 ± 0.38 fold, ULK-1 siRNA 0.85 ± 0.06 fold for PI-103, Medium 0.08 ± 0.06 fold, NT 0.43 ± 0.52 fold, ULK-1 siRNA 0.32 ± 0.28 fold for AZD8055 and Medium 0.53 ± 0.37 fold, NT 1.08 ± 0.33 fold, ULK-1 siRNA 1.39 ± 0.78 fold for Rapamycin) (**Figure 16B**).

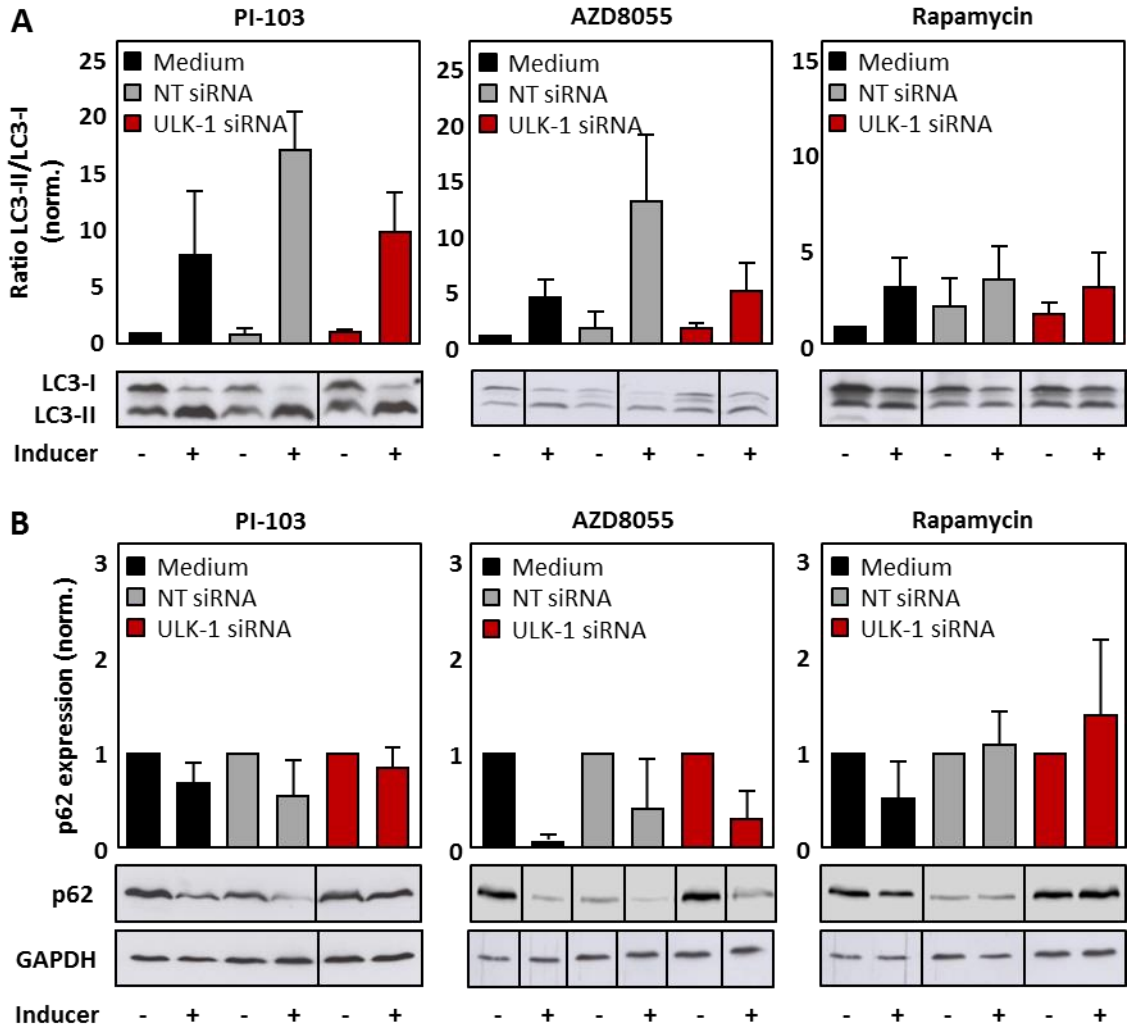

Figure 16: Autophagy induction in ULK-1 knockdown cells. hMDM were treated with non-target siRNA or specific siRNA for ULK-1. On day 3 after KD autophagy was induced with PI-103, AZD8055 or Rapamycin (10 µM, 2 h). (**A**) LC3-I to LC3-II conversion and (**B**) p62 levels were assessed by Western Blot and densitometry analysis. GAPDH was used as loading control. Data are shown as mean ± SD (n = 3 for PI-103 and AZD8055 and n = 4 for Rapamycin).

Similar results regarding increasing LC3-II to LC3-I ratios were obtained for treating Beclin-1 knockdown cells with PI-103 (Medium 1.8 ± 0.1 fold, NT 4.4 ± 0.7 fold, Beclin-1 siRNA 3.4 ± 1.9 fold), AZD8055 (Medium 3.9 ± 5.5 fold, NT 3.8 ± 3.6 fold, Beclin-1 siRNA 5.6 ± 6.4 fold) or Rapamycin (Medium 3.7 ± 3.0 fold, NT 2.0 ± 0.7 fold, Beclin-1 siRNA 1.8 ± 0.4 fold) (**Figure 17A**). Focusing on the p62 levels, treatment with AZD8055 or Rapamycin led to reduced p62 levels (Medium 1.08 ± 0.47 fold, NT 0.51 ± 0.26 fold, Beclin-1 siRNA 0.61 ± 0.29 fold for AZD8055 and Medium 0.77 ± 0.45 fold, NT 0.75 ± 0.52 fold, Beclin-1 siRNA 0.82 ± 0.41 fold for Rapamycin) (**Figure 17B**).

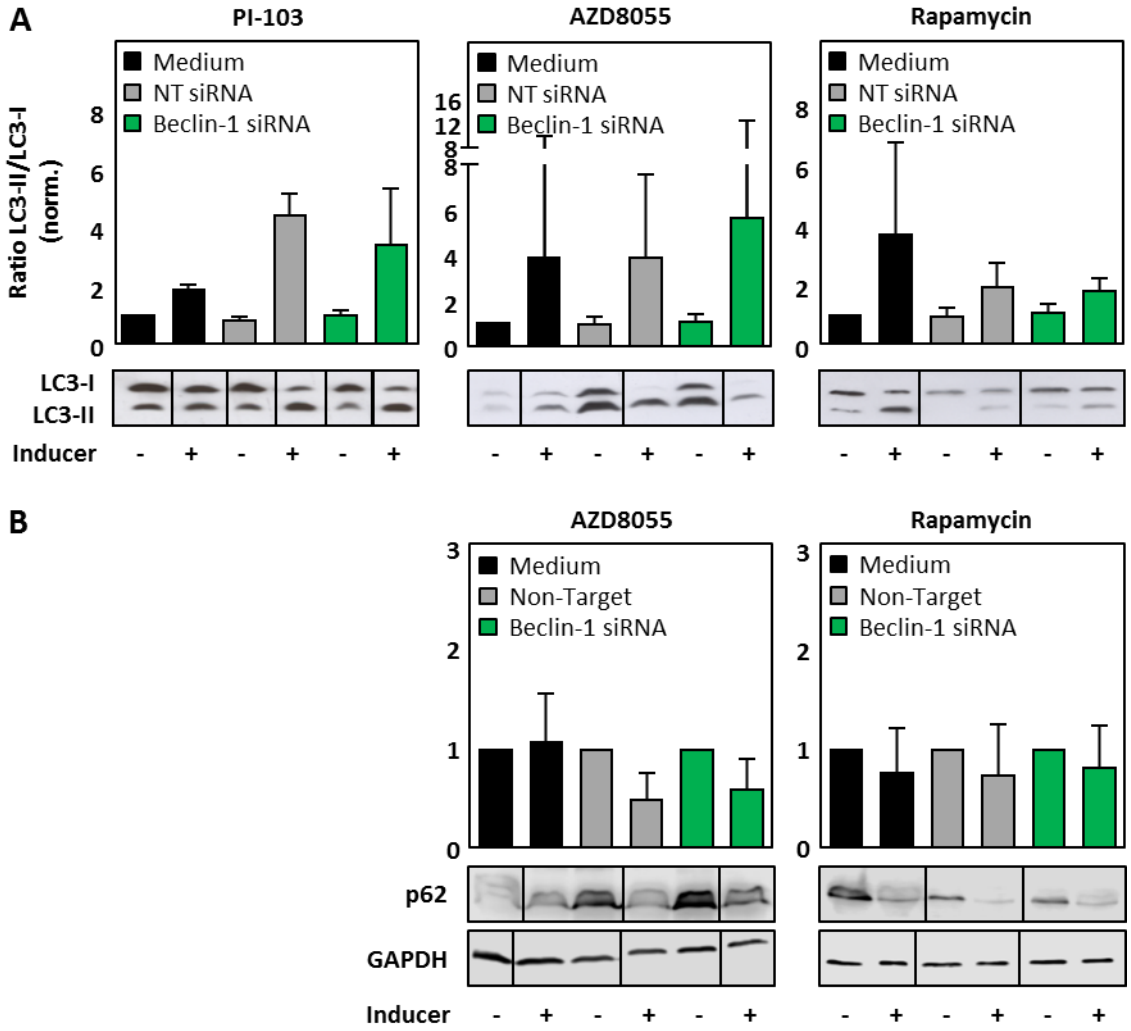

Figure 17: Autophagy induction in Beclin-1 knockdown cells. hMDM were treated with non-target siRNA or specific siRNA for Beclin-1. On day 7 after KD autophagy was induced with PI-103, AZD8055 or Rapamycin (10 µM, 2 h). (**A**) LC3-I to LC3-II conversion and (**B**) p62 levels were assessed by Western Blot and densitometry analysis. GAPDH was used as loading control. Data are shown as mean ± SD (n = 2 for PI-103; n = 5 (LC3) and n = 3 (p62) for AZD8055 and Rapamycin).

Furthermore, the autophagy marker LC3 was targeted for siRNA knockdown as well. Stimulation of siRNA treated hMDM and controls with PI-103 resulted in reduced p62 levels in Medium and NT-treated cells but not in LC3 knockdown cells (Medium 0.7 ± 0.22 fold, NT 0.55 ± 0.38 fold, LC3 siRNA 1.11 ± 0.41 fold) (**Figure 18**).

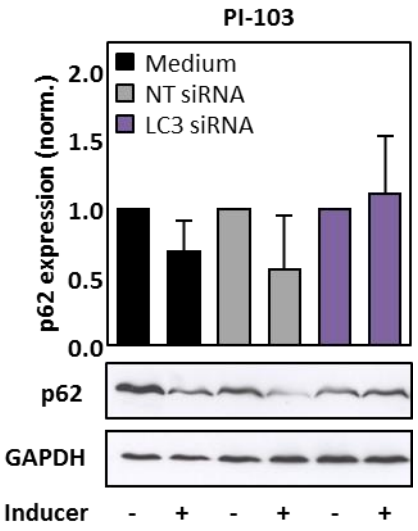

Figure 18: Autophagy induction in LC3 knockdown cells. hMDM were treated with non-target siRNA or specific siRNA for LC3 and on day 3 after KD autophagy was induced with PI-103 (10 µM, 2h). The protein level of p62 was assessed by Western Blot and densitometry analysis. GAPDH was used as loading control. Data are shown as mean ± SD (n = 3).

3.2 Effect of autophagy modulation on antigen processing using the recall antigen Tetanus Toxoid

Macrophages are immunomodulatory cells which are involved in antigen processing and presentation to the adaptive immune system. In addition, various studies demonstrated the involvement of autophagic degradation in antigen processing for MHC class II presentation (Schmid and Munz, 2007; Munz, 2016a). Therefore, we aimed to analyze the effect of autophagy modulation on antigen processing using the recall antigen Tetanus Toxoid (TT) as a model antigen. Hence, autophagy in human primary macrophages was induced by AZD8055 or inhibited by siRNA knockdown of ULK-1 and the effect on lymphocyte proliferation in response to Tetanus Toxoid stimulation was analyzed.

3.2.1 Characterization of the Tetanus Toxoid specific T cell proliferation

First of all, the immune response against stimulation of hMDM with Tetanus Toxoid was characterized to ensure that antigens undergo processing and are presented via MHC-II to $CD4^+$ T cells. Hence, a proliferation kinetic in response to different TT concentrations was assessed by a CFSE-based proliferation assay (**Figure 19**). Therefore, macrophages were stimulated with TT overnight and subsequently co-cultured with autologous, CFSE-labeled peripheral blood lymphocytes (PBLs) for 6 days. Upon T cell activation, half of the initial CFSE molecules are transferred to the daughter cell with each cell division. Accordingly, lymphocyte proliferation can be analyzed by measuring the percentage of $CFSE^{low}$ proliferating cells.

After three days of co-cultivation, lymphocyte proliferation arises and is steadily increasing until day 6, reaching 15-20%. Analyzing longer periods of co-cultivation revealed unspecific proliferation in the unstimulated controls (data not shown). There were no significant changes observed regarding the applied concentrations. For the following experiments a concentration of 10 µg/ml was used and proliferation was assessed on day 6 post co-cultivation.

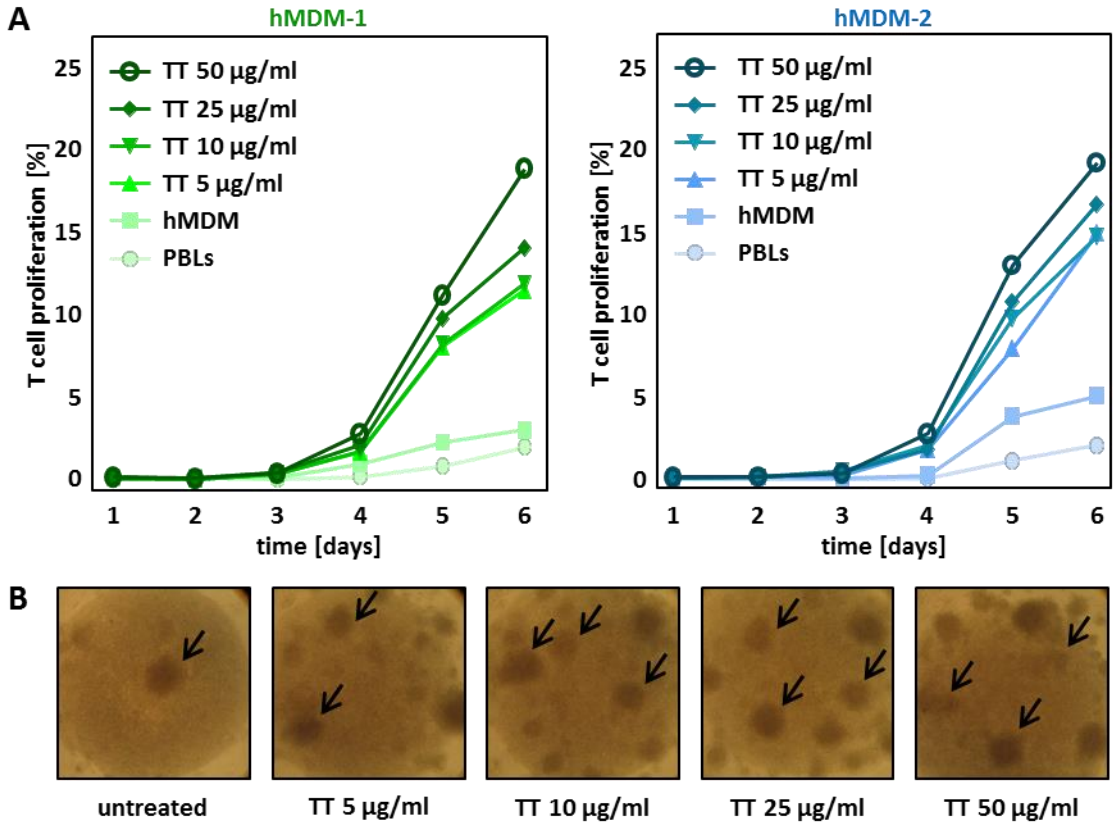

Figure 19: Proliferation kinetic in response to hMDM stimulated with different concentrations of Tetanus Toxoid. hMDM were treated with Tetanus Toxoid (5-50 µg/ml) overnight and autologous, CFSE-labeled lymphocytes were added. (**A**) T cell proliferation as $CFSE^{low}$ cells was measured over time by flow cytometry in hMDM-1 and hMDM-2. (**B**) Representative pictures of the co-culture were depicted (arrows indicate cluster formation of proliferated T cells). Data are representative for at least three independent experiments and are shown as mean ± SD (n = 2-13 for hMDM-1 and n = 2-8 for hMDM-2).

In the next step, the proliferating PBLs in response to TT were further characterized in terms of phenotyping the proliferating T cell subset. By flow cytometry, the FSC/SSC gate was used to gate on the lymphocyte population and subsequently the $CFSE^{low}$ cells within the lymphocyte gate were gated. From this gate, the amount of $CD3^+$ cells followed by the characterization of $CD4^+$ and $CD8^+$ cells was analyzed (**Figure 20**). We found the proliferating cells to be mainly positive for CD3 (72.3 ± 11.3%, 81.7 ± 3.9%) and CD4 (75.8 ± 13.9%, 82.5 ± 13.5%) but not for CD8 (7.4 ± 5.7%, 6.8 ± 7.9%) for co-culture with hMDM-1 and hMDM-2 respectively. Interestingly, there was a small amount of $CD3^+$ cells being double negative for CD4 and CD8 detectable (16.6 ± 11.7% for hMDM-1, 10.3 ± 8.6% for hMDM-2).

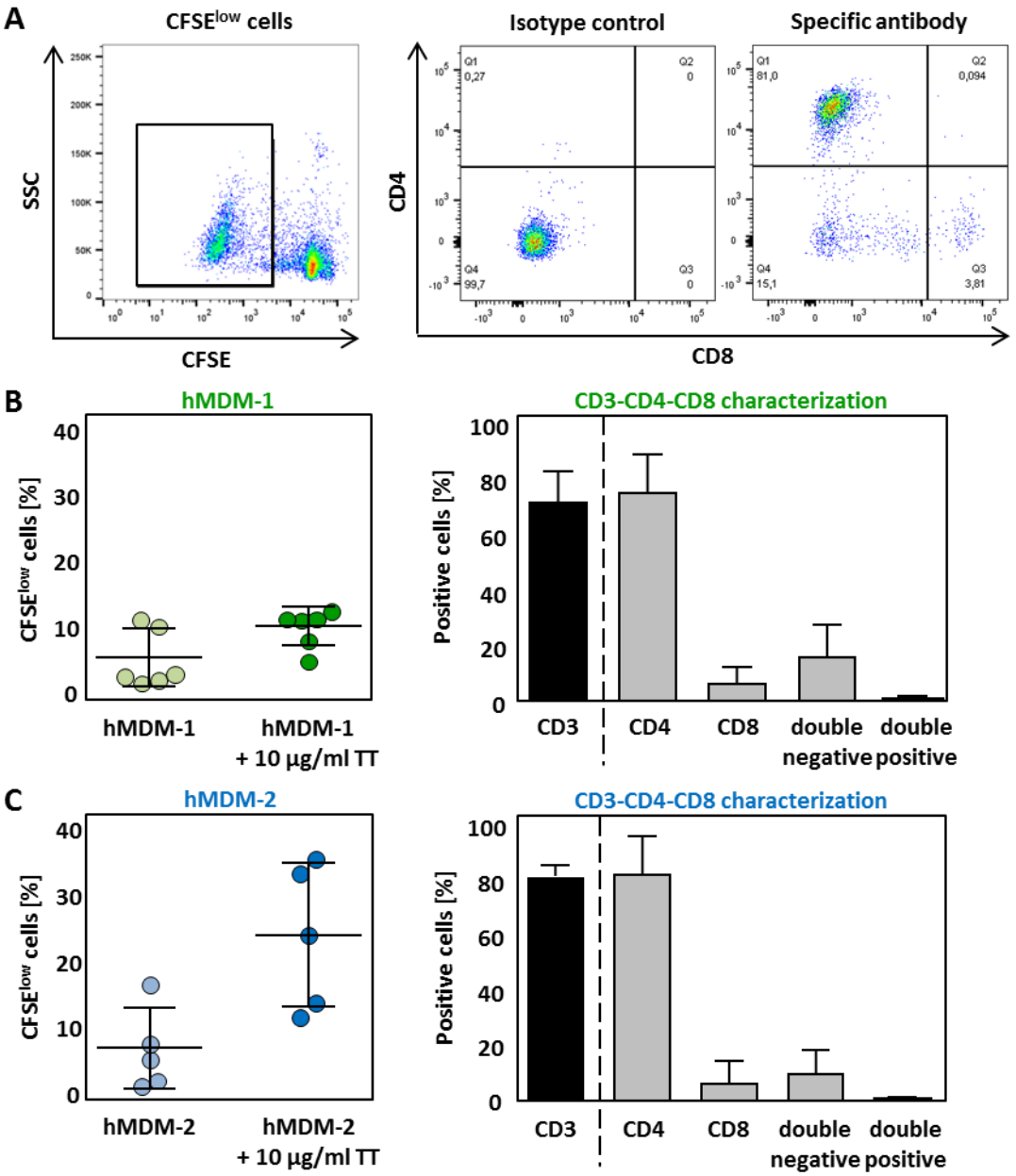

Figure 20: Phenotyping of proliferating T cells in response to Tetanus Toxoid. hMDM were treated with Tetanus Toxoid (10 µg/ml) overnight and autologous, CFSE-labeled lymphocytes were added. After 6 days of co-culture, T cell proliferation as $CFSE^{low}$ cells as well as T cell marker expression (CD3, CD4 and CD8) was analyzed by flow cytometry (**A**) Representative pictures of the gating strategy were depicted. For TT treated samples, it was gated on lymphocytes, $CFSE^{low}$ cells, $CD3^+$ cells and $CD4^+$ versus $CD8^+$ cells. Lymphocyte proliferation and CD3-CD4-CD8 characterization for (**B**) hMDM-1 and (**C**) hMDM-2 was analyzed. Data are representative for at least three independent experiments and are shown as mean ± SD (n = 6 for hMDM-1 and n = 5 for hMDM-2).

3.2.2 Impact of autophagy modulation on the TT specific T cell proliferation

Autophagy is shown to be involved in antigen processing for presentation on MHC-II molecules (Munz, 2016a). To analyze if autophagy is involved in the processing of Tetanus Toxoid, we induced autophagy with AZD8055 and inhibited autophagy by siRNA knockdown of ULK-1 and subsequently analyzed the effect on T cell

proliferation. The stimulation of macrophages with TT induced a T cell proliferation of 11.1 ± 6.2% for hMDM-1 and 12.1 ± 3% for hMDM-2. The prestimulation with AZD8055 had no influence on the adaptive immune response (13.7 ± 9.5% in hMDM-1, 12.7 ± 3.5% in hMDM-2) (**Figure 21**).

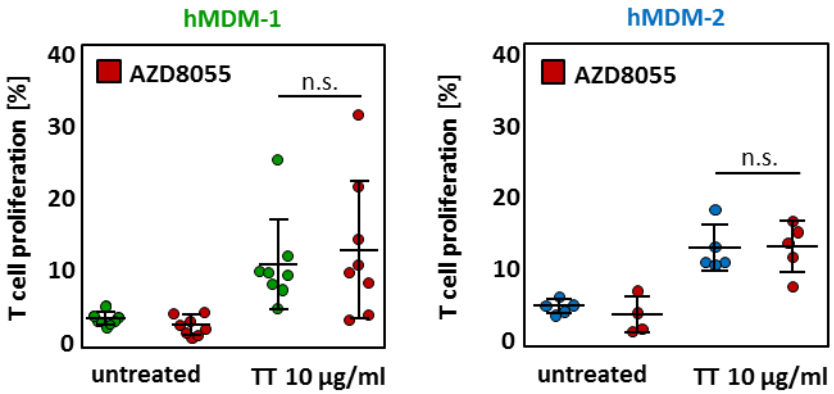

Figure 21: Autophagy induction by AZD8055 did not influence the Tetanus Toxoid induced T cell proliferation. hMDM-1 (left panel) and hMDM-2 (right panel) were prestimulated with AZD8055 (10 µM, 45 min) and subsequently stimulated with Tetanus Toxoid (10 µg/ml) overnight. Autologous, CFSE-labeled lymphocytes were added and co-cultivated for 6 days. T cell proliferation as $CFSE^{low}$ cells was assessed by flow cytometry. Data are representative for at least three independent experiments and are shown as mean ± SD (n = 8 for hMDM-1 and n = 5 for hMDM-2).

On the other hand, the impact of autophagy inhibition on T cell proliferation was analyzed by an ULK-1 siRNA knockdown (**Figure 22**). In general, it could be observed that the proliferation is approximately twice as high as for the last experiments, which is probably due to the generation method of hMDM. In the previous experiments, hMDM were generated by plastic adherence whereas for knockdown experiments CD14 positive MACS was used. Presumably, the binding of CD14-beads to the CD14 receptor, which is also a LPS receptor, leads to a preactivation of hMDM resulting in a higher T cell proliferation. Autophagy inhibition by ULK-1 knockdown had no impact on the Tetanus Toxoid induced lymphocyte proliferation (Medium 25.7 ± 9.2%, NT 26.9 ± 13.1%, ULK-1 siRNA 26.2 ± 9.9% for hMDM-1; Medium 25.3 ± 10%, NT 26.8 ± 12.3%, ULK-1 siRNA 25.7 ± 9.4%).

Taken together, autophagy was suggested to be not involved in TT induced T cell proliferation which might indicate that autophagy does not affect antigen processing of this model antigen.

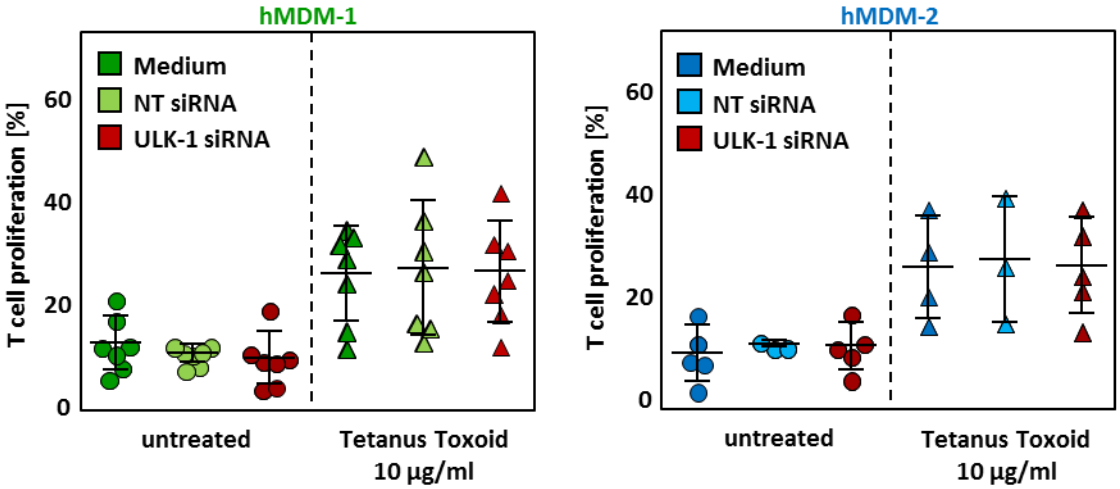

Figure 22: Autophagy inhibition by ULK-1 knockdown did not influence the Tetanus Toxoid induced T cell proliferation. hMDM-1 (left panel) and hMDM-2 (right panel) were treated with non-target siRNA or specific siRNA for ULK-1. On day 2 post KD, hMDM were stimulated with Tetanus Toxoid (10 µg/ml) overnight. Autologous, CFSE-labeled lymphocytes were added and co-cultivated for 6 days. T cell proliferation as $CFSE^{low}$ cells was assessed by flow cytometry. Data are representative for at least three independent experiments and are shown as mean ± SD (n = 7 for hMDM-1 and n = 3-5 for hMDM-2).

3.2.3 Macrophage phenotypes and their ability to activate T cells

Surprisingly, by comparing the ability of hMDM-1 and hMDM-2 to activate the adaptive immune system, the anti-inflammatory hMDM-2 were shown to be more potent (**Figure 23**). Stimulation of hMDM-1 with Tetanus Toxoid resulted in a lymphocyte proliferation of 12 ± 6.4%, whereas stimulation of hMDM-2 induced a significantly higher T cell proliferation of 16.6 ± 6.8%. Already by comparing the background proliferation induced by unstimulated macrophages, hMDM-2 were shown to promote a significantly higher immune activation.

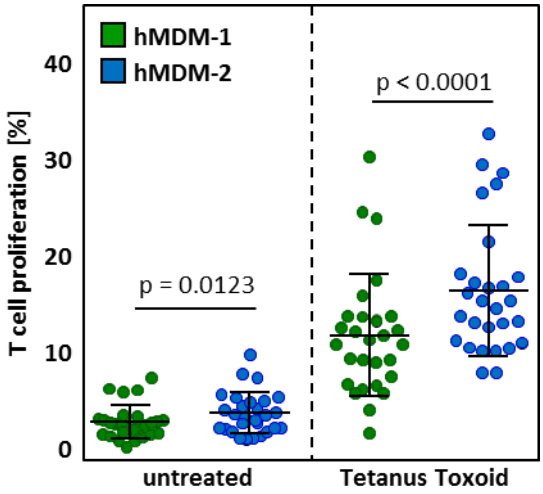

Figure 23: Proliferation of T cells in response to Tetanus Toxoid treated hMDM-1 vs. hMDM-2. hMDM-1 (green) and hMDM-2 (blue) were treated with Tetanus Toxoid (10 µg/ml) overnight and autologous, CFSE-labeled lymphocytes were added. After 6 days of co-culture, T cell proliferation as $CFSE^{low}$ cells was analyzed by flow cytometry. Data are representative for at least three independent experiments and are shown as mean ± SD (n = 28).

In vivo, anti-inflammatory type 2 macrophages are supposed to dampen the immune system. To further analyze the ability of hMDM-2 to induce a stronger immune response *in vitro*, we characterized both phenotypes for their expression of co-stimulatory surface markers being important for T cell activation (**Figure 24**). We investigated the expression of CD40, MHC-II, CD80 and CD86. In general, we could not observe an upregulation of activation markers upon the stimulation with Tetanus Toxoid for 24 h.

Regarding CD40, which mediates the activation of antigen presenting cells upon binding of CD40L on T_H cells, a third of the macrophage population was found to be positive (32.7 ± 18.2% for hMDM-1, 26.0 ± 11.5% for hMDM-2) (**Figure 24A**). Furthermore, we analyzed the expression of MHC class II being important for the presentation of peptides derived from extracellular proteins to $CD4^+$ T cells. As expected for macrophages being professional antigen presenting cells, a high positivity was observed for the MHC-II expression (84.8 ± 9.3% for hMDM-1, 93.3 ± 3.9% for hMDM-2) (**Figure 24B**). Remarkably, for hMDM-2 a 10% higher MHC-II positivity compared to hMDM-1 was observed. The marker CD80, also named B7-1, is a costimulatory molecule necessary for the activation and survival of T cells. It is higher expressed on hMDM-1 compared to hMDM-2 (38.5 ± 16.4%, 10.6 ± 6.1%) (**Figure 24C**). Concerning CD86, also named B7-2, which is a co-stimulatory molecule working in tandem with CD80, equal expression levels for both phenotypes were obtained (29.9 ± 14.5% for hMDM-1, 24.3 ± 13.1 % for hMDM-2) (**Figure 24D**).

In conclusion, an equal expression level was demonstrated for CD40 and CD86 on hMDM-1 and hMDM-2. Regarding CD80, it is barely expressed on hMDM-2 and around 40% positivity was shown for hMDM-1. The antigen presenting molecule, MHC-II, is abundantly expressed on macrophages but predominantly on hMDM-2.

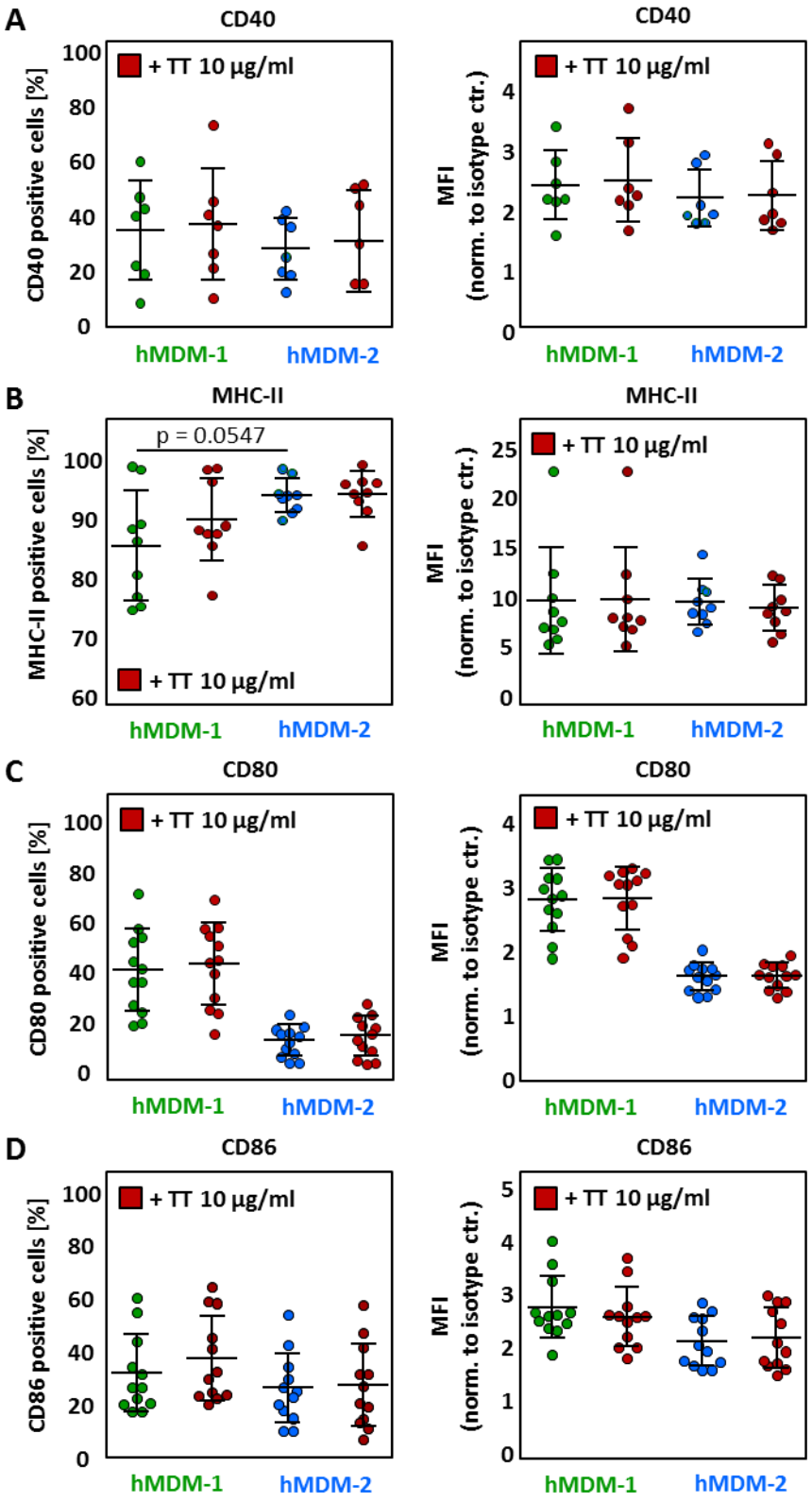

Figure 24: Analysis of maturation marker on hMDM-1 and hMDM-2 upon Tetanus Toxoid treatment. hMDM were treated with Tetanus Toxoid (10 µg/ml) overnight and were stained for surface marker expression analyzed by flow cytometry: (**A**) CD40, (**B**) MHC-II, (**C**) CD80 and (**D**) CD86. Data are representative for at least three independent experiments and are shown as mean ± SD (n = 7 for CD40; n = 9 for MHC-II; n = 12 for CD80 and CD86).

In parallel to the assessment of surface activation marker expression, macrophages were used for proteome analysis to identify intracellular proteins being involved in antigen processing and presentation (in cooperation with Stefan Tenzer, University of Mainz). In general, a different proteome profile of hMDM-1 and hMDM-2 was detected, indicative for the fact that we generated two different phenotypes of macrophages. Stimulation with Tetanus Toxoid had only a minor effect on altering the protein expression profiles (3-6 proteins being up- or downregulated in hMDM-1 and hMDM-2 upon stimulation with TT; data not shown).

By comparing hMDM-1 vs. hMDM-2, the proteins being at least 2 fold upregulated (**Table 1**) were used for a string analysis (**Figure 25**). Within those proteins, 3 were identified to be involved in antigen processing and mediating adaptive immunity, namely vesicle associated membrane protein 8 (VAMP8), V-type proton ATPase subunit B and the Calcineurin binding protein cabin-1.

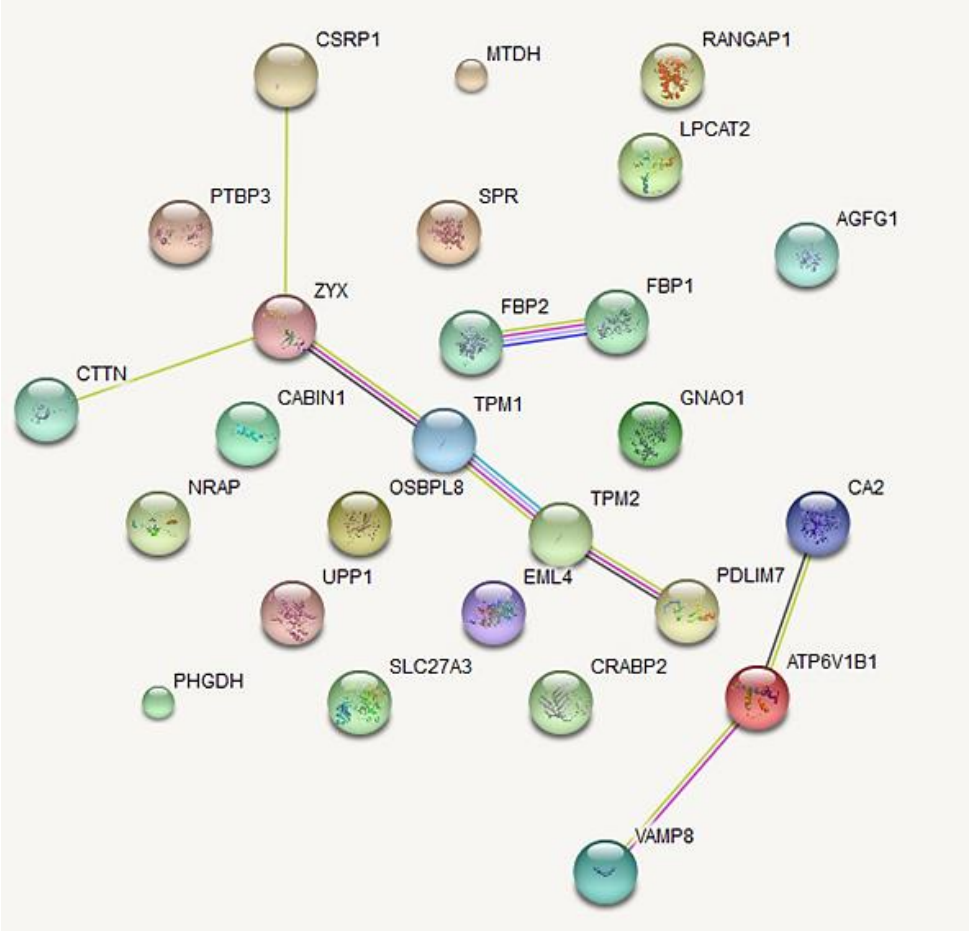

Figure 25: STRING analysis of upregulated proteins in hMDM-1 vs hMDM-2. Proteome analysis of hMDM-1 and hMDM-2 using mass spectrometry. Depicted are proteins that are at least 2 fold upregulated in hMDM-1 compared to hMDM-2. Data are representative for at least three independent experiments (n = 6).

Table 1: Proteome analysis of hMDM-1 vs. hMDM-2. Depicted are proteins that are at least 2 fold upregulated in hMDM-1 compared to hMDM-2. Proteins were sorted by highest upregulation on top to lowest upregulation on bottom and proteins being involved in antigen processing and presentation are illustrated in bold.

String name	Entry name	Full name
NRAP	NRAP_HUMAN	Nebulin-related anchoring protein
RANGAP1	RAGP1_HUMAN	Ran GTPase-activating protein 1
PTBP3	PTBP3_HUMAN	Polypyrimidine tract-binding protein 3
ATP6V1B1	**VATB1_HUMAN**	**V-type proton ATPase subunit B, kidney isoform**
GNAO1	GNAO_HUMAN	Guanine nucleotide-binding protein G(o) subunit alpha
TPM1	TPM1_HUMAN	Tropomyosin alpha-1 chain
TPM2	TPM2_HUMAN	Tropomyosin beta chain
FBP2	F16P2_HUMAN	Fructose-1,6-bisphosphatase isozyme 2
PHGDH	SERA_HUMAN	D-3-phosphoglycerate dehydrogenase
UPP1	UPP1_HUMAN	Uridine phosphorylase 1
SLC27A3	S27A3_HUMAN	Long-chain fatty acid transport protein 3
PDLIM7	PDLI7_HUMAN	PDZ and LIM domain protein 7
EML4	EMAL4_HUMAN	Echinoderm microtubule-associated protein-like 4
CSRP1	CSRP1_HUMAN	Cysteine and glycine-rich protein 1
CABIN1	**CABIN_HUMAN**	**Calcineurin-binding protein cabin-1**
CA2	CAH2_HUMAN	Carbonic anhydrase 2
CRABP2	RABP2_HUMAN	Cellular retinoic acid-binding protein 2
MTDH	LYRIC_HUMAN	Protein LYRIC
EIF4H	IF4H_HUMAN	Eukaryotic translation initiation factor 4H
OSBPL8	OSBL8_HUMAN	Oxysterol-binding protein-related protein 8
VAMP8	**VAMP8_HUMAN**	**Vesicle-associated membrane protein 8**
SPR	SPRE_HUMAN	Sepiapterin reductase
FBP1	F16P1_HUMAN	Fructose-1,6-bisphosphatase 1
AGFG1	AGFG1_HUMAN	Arf-GAP domain and FG repeat-containing protein 1
CTTN	SRC8_HUMAN	Src substrate cortactin
ZYX	ZYX_HUMAN	Zyxin
LPCAT2	PCAT2_HUMAN	Lysophosphatidylcholine acyltransferase 2

Vice versa, we analyzed the proteins that are at least two fold upregulated in hMDM-2 compared to hMDM-1 (**Table 2**) and illustrated them by string analysis (**Figure 26**). A number of proteins were identified that are involved in antigen processing (Legumain, L-amino-acid oxidase and the probable serine carboxypeptidase CPVL), phagocytosis (Sialoadhesin) and priming of an immune response (Galectin 10, CD163).

In conclusion, by comparing the two macrophage phenotypes, hMDM-2 were shown to have a higher expression profile of proteins being involved in antigen processing. The

identified proteins will be modulated in following experiments aiming to explain why hMDM-2 are superior to hMDM-1 in priming an adaptive immune response.

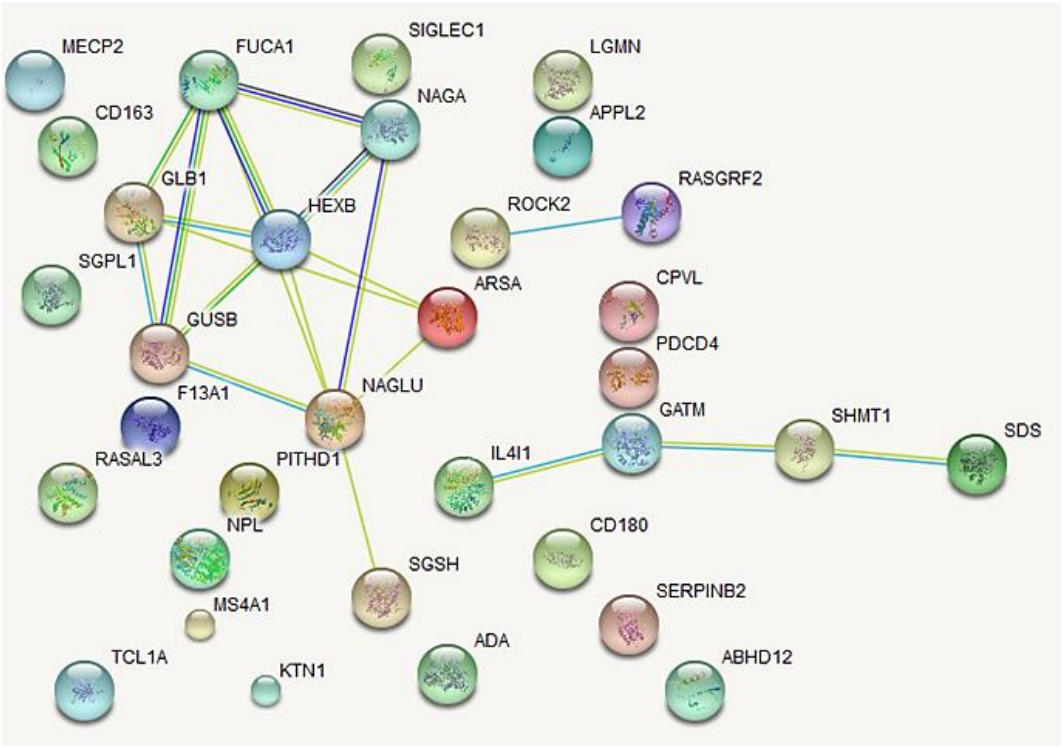

Figure 26: STRING analysis of upregulated proteins on hMDM-2 vs hMDM-1. Proteome analysis of hMDM-2 and hMDM-1 using mass spectrometry. Depicted are proteins that are at least 2 fold upregulated in hMDM-2 compared to hMDM-1. Data are representative for at least three independent experiments (n = 6).

Table 2: Proteome analysis of hMDM-2 vs. hMDM-1. Depicted are proteins that are at least 2 fold upregulated in hMDM-2 compared to hMDM-1. Proteins were sorted by highest upregulation on top to lowest upregulation on bottom and proteins being involved in antigen processing and presentation are illustrated in bold.

String name	Entry name	Full name
not found	IGHM_HUMAN	Ig mu chain C region
RASGRF2	RGRF2_HUMAN	Ras-specific guanine nucleotide-releasing factor 2
TCL1A	TCL1A_HUMAN	T-cell leukemia/lymphoma protein 1A
F13A1	F13A_HUMAN	Coagulation factor XIII A chain
LGMN	**LGMN_HUMAN**	**Legumain**
SERPINB2	PAI2_HUMAN	Plasminogen activator inhibitor 2
FUCA1	FUCO_HUMAN	Tissue alpha-L-fucosidase
MS4A1	CD20_HUMAN	B-lymphocyte antigen CD20
ADA	ADA_HUMAN	Adenosine deaminase
ROCK2	ROCK2_HUMAN	Rho-associated protein kinase 2
not found	**LEG10_HUMAN**	**Galectin-10**
IL4I1	**OXLA_HUMAN**	**L-amino-acid oxidase**
CPVL	**CPVL_HUMAN**	**Probable serine carboxypeptidase CPVL**
CD180	CD180_HUMAN	CD180 antigen

NAGA	NAGAB_HUMAN	Alpha-N-acetylgalactosaminidase
PITHD1	PITH1_HUMAN	PITH domain-containing protein 1
SHM1	SPHM_HUMAN	N-sulphoglucosamine sulphohydrolase
CD163	**C163A_HUMAN**	**Scavenger receptor cysteine-rich type 1 protein M130**
GLB1	BGAL_HUMAN	Beta-galactosidase
HEXB	HEXB_HUMAN	Beta-hexosaminidase subunit beta
SDS	SDHL_HUMAN	L-serine dehydratase/L-threonine deaminase
ARSA	ARSA_HUMAN	Arylsulfatase A
NAGLU	ANAG_HUMAN	Alpha-N-acetylglucosaminidase
GATM	GATM_HUMAN	Glycine amidinotransferase, mitochondrial
APPL2	DP13B_HUMAN	DCC-interacting protein 13-beta
GUSB	BGLR_HUMAN	Beta-glucuronidase
SGPL1	SGPL1_HUMAN	Sphingosine-1-phosphate lyase 1
NPL	NPL_HUMAN	N-acetylneuraminate lyase
SIGLEC1	**SN_HUMAN**	**Sialoadhesin**
PDCD4	PDCD4_HUMAN	Programmed cell death protein 4
ABHD12	ABD12_HUMAN	Monoacylglycerol lipase ABHD12
KTN1	KTN1_HUMAN	Kinectin
MECP2	MECP2_HUMAN	Methyl-CpG-binding protein 2
RASAL3	RASL3_HUMAN	RAS protein activator like-3
SHMT2	GLYC_HUMAN	Serine hydroxymethyltransferase, cytosolic

3.3 Investigation of the *Leishmania* virulence factor GP63

In addition to nutrient and chemical modulation of autophagy, also pathogens have been shown to modulate the host cells' autophagy machinery for their own benefit (Lee et al., 2008; Wang et al., 2009). Concerning *Leishmania* parasites a potential autophagy modulating factor is the metalloprotease GP63, which influences various host cell signaling pathways amongst others, mTOR (Gomez et al., 2009; Jaramillo et al., 2011). Therefore, we aimed to investigate if the *Leishmania* virulence factor GP63 is involved in autophagy modulation in hMDM. First of all, the growth behavior of the GP63 knockout (KO) parasites compared to the two controls, wildtype (WT) and KO+GP63 (KO parasites with addback of a *gp63*-containing plasmid), was investigated. Subsequently, the impact of GP63 as virulence factor concerning infection of hMDM and adaptive immune response was determined. And finally, the effect on autophagy modulation was analyzed.

3.3.1 Growth characteristics of *Leishmania* GP63 knockout parasites

Leishmania major Seidmann (SD) promastigotes were cultured *in vitro* in a biphasic Novy Nicolle McNeal blood agar culture system and the growth characteristics, by counting viable and apoptotic promastigotes, were analyzed over one week (**Figure 27**). During the first few days after passage, the parasites are in a logarithmic growth phase (log. ph. *Lm*) containing mainly viable and exponentially dividing parasites. From day 4-5 on, the parasites reach the stationary growth phase (stat. ph. *Lm*) comprising a mixture of apoptotic and viable parasites (**Figure 27A**). This mixture of elongated, viable as well as round shaped, apoptotic parasites is comparable to the infectious mixture in the midgut of the sandfly namely the virulent inoculum. Comparing the growth of *Lm* SD WT, *Lm* GP63 KO and *Lm* KO+GP63, a similar growth behavior was observed and day 5 old cultures as infectious mixture were chosen for the following infection experiments. The presence of GP63 was confirmed for WT and KO+GP63 parasites and the absence was proven for the KO parasites by genomic DNA isolation followed by PCR amplifying GP63 (data not shown) as well as by antibody staining analyzed by flow cytometry (**Figure 27B**).

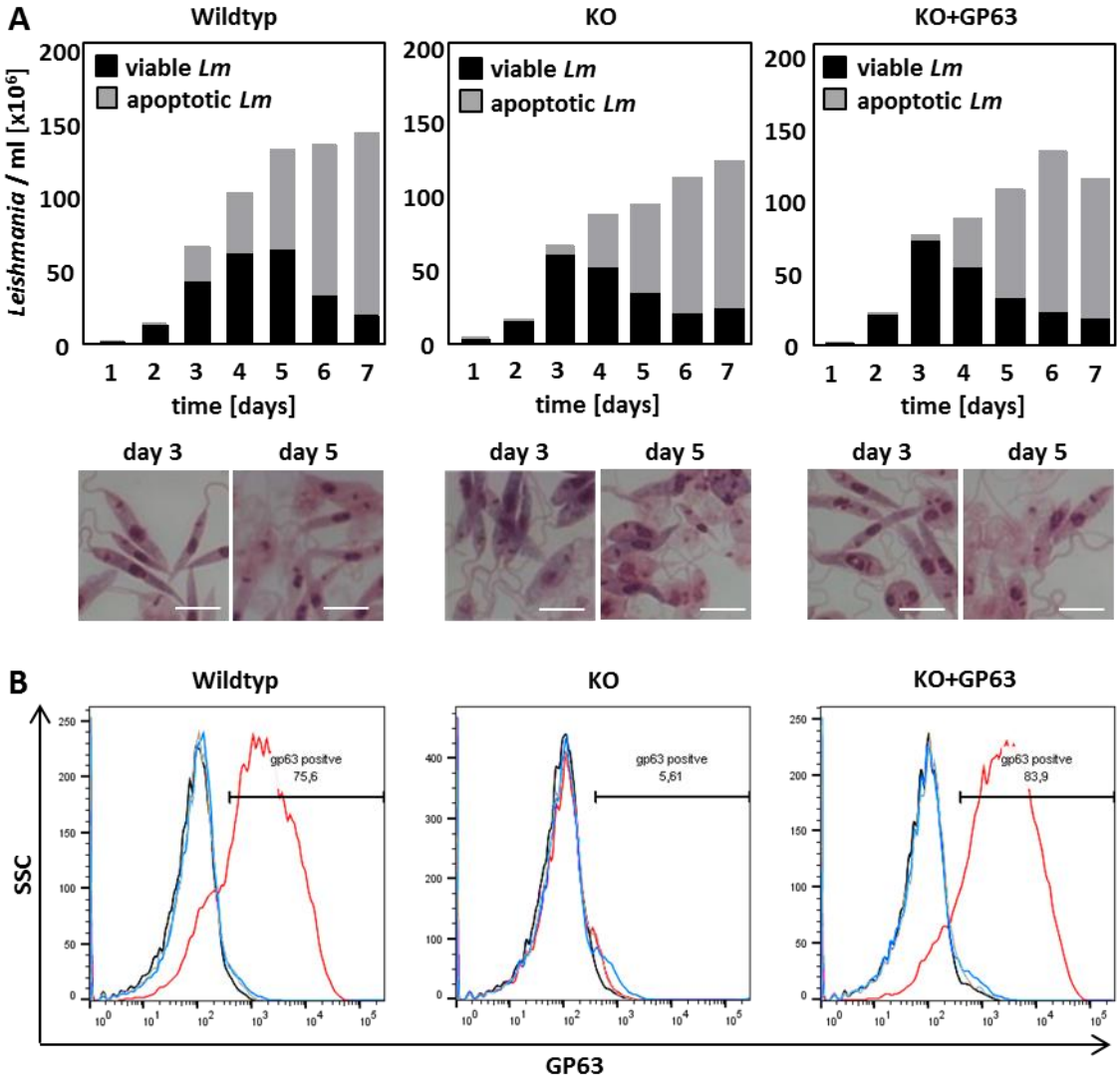

Figure 27: Growth characteristics of *Leishmania major* Seidmann. The amount of viable and apoptotic parasites in a blood agar culture of *Lm* SD was counted daily over one week and (**A**) representative DiffQuick® pictures are depicted (n = 2-6; scale bar 10 µm). (**B**) Surface expression of GP63 was assessed by an antibody staining using flow cytometry (black line: unstained, blue line: isotype control, red line: GP63 staining).

3.3.2 GP63 has no impact on the infection rate of hMDM

To analyze if GP63 is involved in the uptake by hMDM, we co-incubated macrophages with CFSE-labeled *Leishmania* promastigotes for 3 h and analyzed the infection rate using flow cytometry (**Figure 28**). All three *Leishmania* types were able to infect macrophages with the same efficiency (WT 60.2 ± 15.2%, 43 ± 18%; KO 60.1 ± 14.6, 46.8 ± 17%; KO+GP63 57.1 ± 15.4%, 43.6 ±16.1% for hMDM-1 and hMDM-2 respectively). Surprisingly, hMDM-2, comprising a higher phagocytic capacity, showed a lower infection rate compared to hMDM-1.

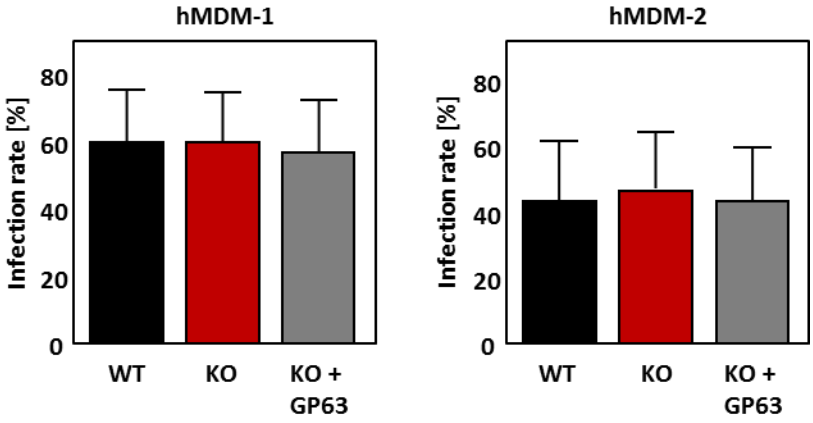

Figure 28: Infection rate of hMDM with *Lm* SD WT, *Lm* SD KO and *Lm* SD KO+GP63. hMDM-1 and hMDM-2 were infected with a MOI 10 of CFSE-labeled *Leishmania* promastigotes for 3 h. Infection rate was analyzed by flow cytometry. Data are representative for at least three independent experiments and are shown as mean ± SD (n = 8).

3.3.3 GP63 has no impact on T cell proliferation

Although, no impact of GP63 on the infection rate of macrophages was detectable, we asked whether GP63 expression on *Lm* has an effect on the adaptive immune response (**Figure 29**). Therefore, hMDM were infected overnight with *Leishmania* promastigotes and subsequently co-cultured with autologous, CFSE-labeled peripheral blood lymphocytes (PBLs) for 6 days.

Remarkably, we could detect a *Leishmania* specific T cell proliferation in previously unexposed german blood donors (discussed in Crauwels et al., 2015). This is probably due to a cross reaction with antigens the donors have been previously exposed with e.g. through immunization. Though, this proliferation did not differ between the different *Leishmania* types. T cell proliferation as percentage of $CFSE^{low}$ cells were in both types of macrophages around 25-30% (WT 26.9 ± 11.7%, KO 28.5 ±13.9%, KO+GP63 26.3 ± 10.5% for hMDM-1 and WT 21.9 ± 11.6%, KO 26.8 ± 12.5%, KO+GP63 22.4 ± 10.4% for hMDM-2).

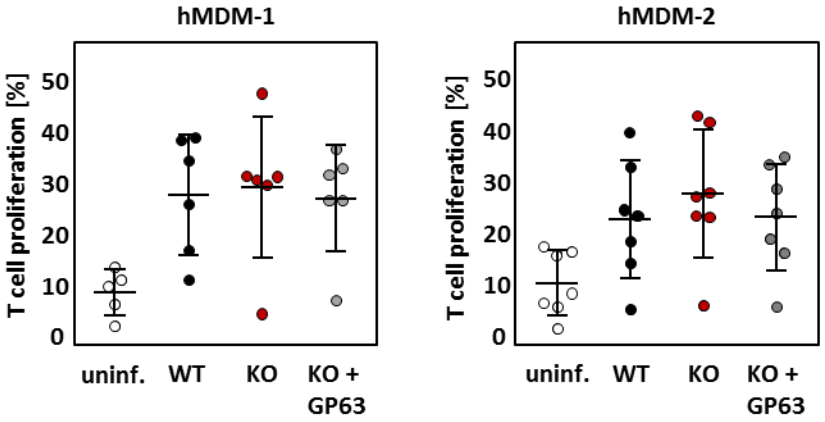

Figure 29: T cell proliferation in response to hMDM infected with *Lm* SD WT, *Lm* SD KO and *Lm* SD KO+GP63. hMDM were infected overnight with a MOI 10 of *Lm* promastigotes and were co-cultured with autologous, CFSE-labeled lymphocytes for 6 days. T cell proliferation was

assessed as $CFSE^{low}$ cells by flow cytometry. Data are representative for at least three independent experiments and are shown as mean ± SD (n = 6-7).

3.3.4 Infection of hMDM with *Leishmania* induces autophagy independently of GP63

Although no impact of GP63 on infection rate and adaptive immunity was shown, we asked the question if the metalloprotease activity of GP63 influences intracellular host cell signaling pathways such as the induction of autophagy. Therefore, we assessed the ability of *Leishmania* SD parasites to modulate the host cells autophagy machinery and whether this is dependent on GP63 expression. LC3 conversion in infected macrophages was analyzed by Western Blot (**Figure 30**). Infection of hMDM with different *Leishmania* types led to the conversion of LC3-I to LC3-II but this was independent on the presence of GP63. There was just a minor reduced LC3 conversion detectable upon infection with GP63-depleted parasites (WT 2.0 ± 1.2 fold, KO 1.7 ± 0.7 fold, KO+GP63 2.3 ± 0.8 fold).

Taken together, GP63 has no impact on the infection rate of hMDM, on immune cell activation and on the induction of autophagy. In accordance with previous results in our group, the infection of macrophages with *Leishmania* promastigotes (in this case *Lm* FEBNI) induces autophagy (Crauwels et al., 2015).

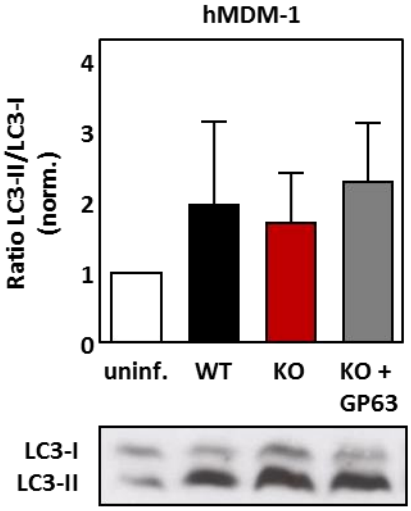

Figure 30: *Leishmania* SD promastigotes induce LC3 conversion in hMDM independently of GP63. hMDM-1 were infected with a MOI 10 of *Lm* SD WT, *Lm* SD KO or *Lm* SD KO+GP63 for 3 h. Subsequently, LC3-I to LC3-II conversion was analyzed by Western Blot and densitometry analysis. Data are representative for at least three independent experiments and are shown as mean ± SD (n = 4).

3.4 Modulation of LC3-associated phagocytosis

Previous studies in our group demonstrated that *Leishmania* promastigotes are taken up in a single membrane phagosome. The uptake of apoptotic promastigotes initiates the recruitment of the autophagy marker LC3 to the phagosomal membrane (Crauwels et al., 2015). As LC3 recruitment is independent of ULK-1, we suggested that apoptotic *Leishmania* are taken up by an autophagy related process, termed LC3-associated phagocytosis LAP (PhD thesis of Meike Thomas). Furthermore, the presence of apoptotic parasites in the virulent inoculum was shown to reduce the *Leishmania* specific adaptive immune response (Crauwels et al., 2015). Thus, we hypothesize, that the presence of LAP inducing agents like apoptotic *Leishmania* parasites, phosphatidylserine (PS) coated beads or zymosan leads to a reduced immune response. Hence, in the last part of this thesis, we focused on the modulation of the autophagy related pathway LAP in human primary macrophages. Subsequently, the impact of LAP modulation on the adaptive immune system was analyzed.

3.4.1 LAP induction by phosphatidylserine beads

It is well known, that LAP is induced by the activation of specific cell surface receptors like TLRs, Dectin-1, Fcγ- or PS-receptors (Mehta et al., 2014). Apoptotic *Leishmania* express phosphatidylserine on their surface, which might cause LAP induction via the PS-receptor, although the responsible receptor for the uptake of apoptotic *Leishmania* is still unknown. We could already show that apoptotic promastigotes are taken up in LC3 positive compartments upon phagocytosis by hMDM (Crauwels et al., 2015). In the following part, we aim to induce LAP by particles which can replace the apoptotic *Lm* in the virulent inoculum. First, we chose phosphatidylserine-coupled beads and their respective uncoated control, named plain beads.

LC3 immunofluorescence stainings were used to assess the formation of $LC3^+$ compartments (**Figure 31**). In untreated macrophages, a uniformly LC3 distribution in the cytoplasm was observed (**Figure 31A**). Surprisingly, stimulation of hMDM with uncoated plain beads resulted in the formation of LC3 positive compartments (**Figure 31B**). As expected, PS beads were taken up in LC3 positive compartments within hMDM (**Figure 31C**).

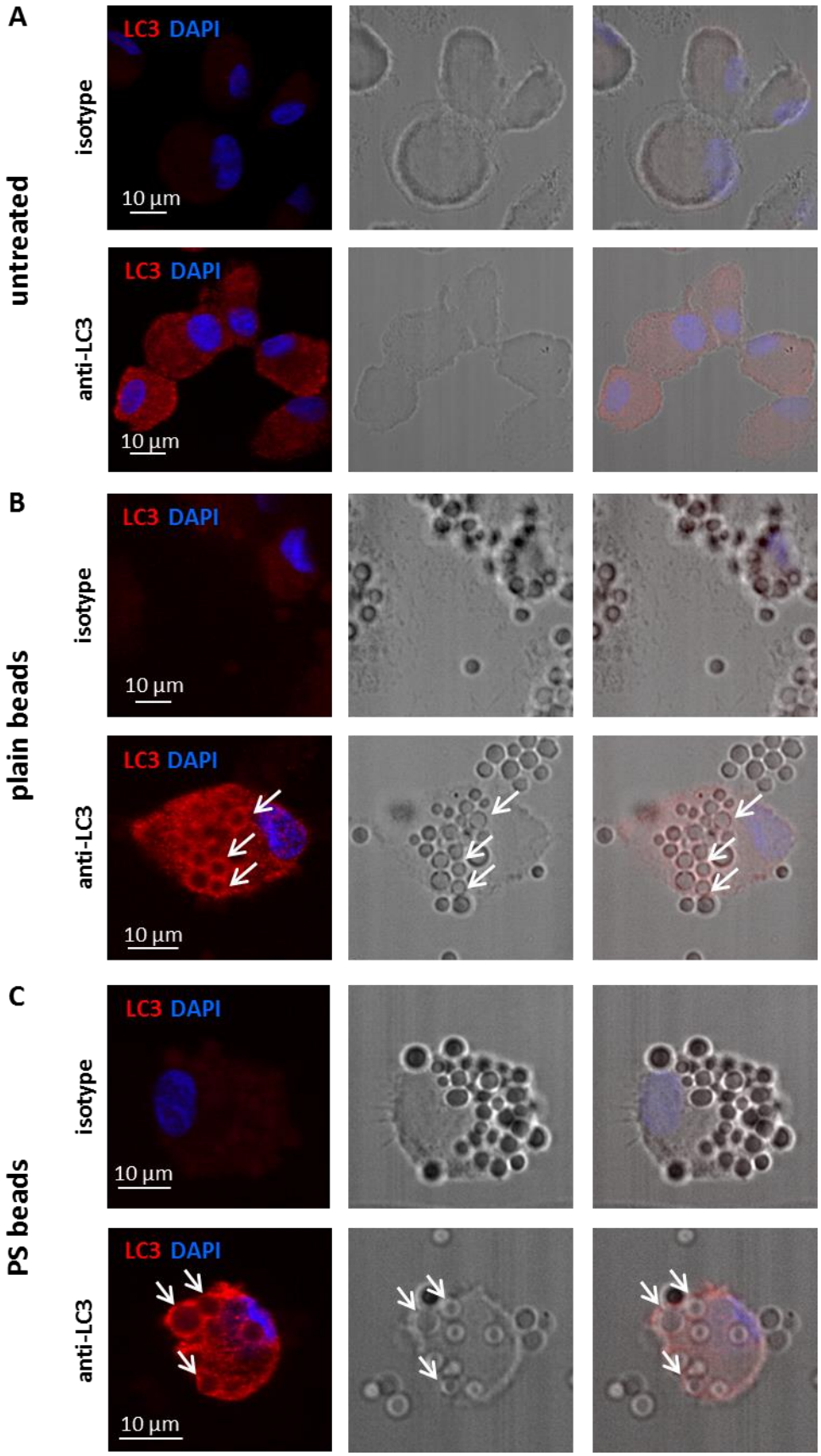

Figure 31: Plain beads and PS beads reside in LC3-positive compartments in hMDM. hMDM were left (**A**) untreated or were treated with a MOI 20 of (**B**) plain beads or (**C**) PS beads for 3 h. Subsequently, the cells were fixed and stained with an anti-LC3 antibody (red) and nuclei were counterstained with DAPI (blue) (arrows indicate engulfed beads in $LC3^{+}$

compartments). Representative images were taken with a Zeiss LSM-Live 7 microscope and a 630x magnification.

As LC3 immunostainings are not able to distinguish between the cytosolic form LC3-I and the membrane bound form LC3-II, we performed Western Blots to confirm the induction of LAP (**Figure 32**). The stimulation of macrophages with PS beads induced the conversion of LC3-I to LC3-II, being detectable from 2 to 4 h post stimulation in hMDM-1 and hMDM-2 respectively (4.7 ± 4.7 fold, 5.5 ± 3.8 fold, 2.6 ± 3.1 fold in hMDM-1 and 3.2 ± 2.4 fold, 3.1 ± 2.5 fold, 2.8 ± 1.7 fold in hMDM-2). As already indicated by immunofluorescence, also the stimulation with plain beads led to the conversion of LC3 (1.7 ± 1.2 fold, 4.1 ± 4.4 fold, 1.2 ± 0.6 fold in hMDM-1 and 2.6 ± 0.8 fold, 3.2 ± 1.6 fold, 1.4 ± 0.6 fold in hMDM-2). Lacking an appropriate control bead which does not induce LAP, we incubated plain beads overnight in a BSA solution to obtain BSA-coupled beads. Stimulation of hMDM with either BSA-coupled beads or latex beads resulted in increased LC3 conversion as well, making them not suitable as control beads (data not shown).

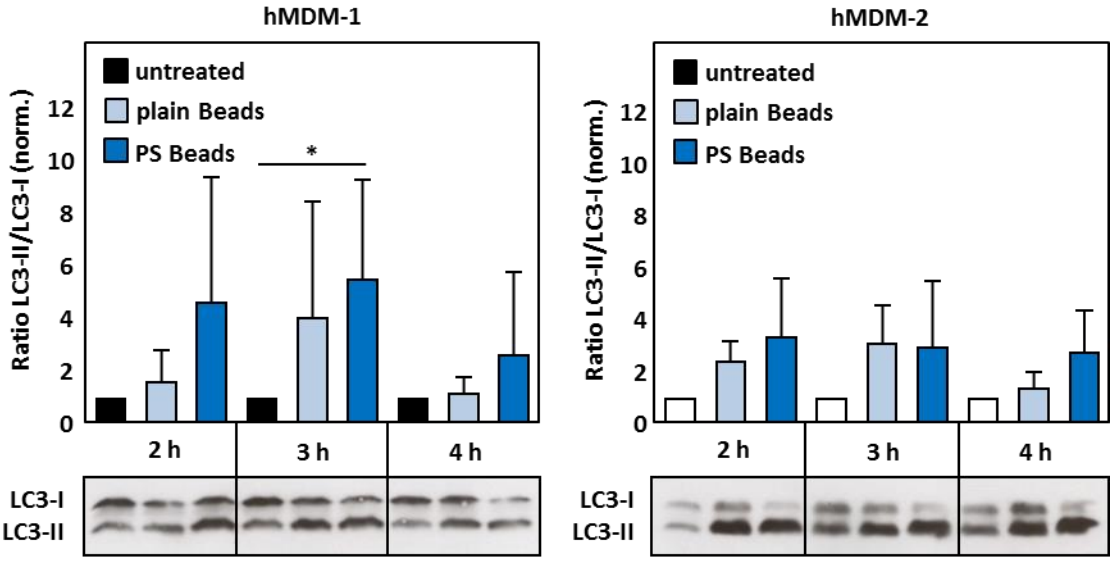

Figure 32: Stimulation of hMDM with plain beads and PS beads induces LC3 conversion. hMDM-1 (left panel) and hMDM-2 (right panel) were stimulated with a MOI 10 of plain beads or PS beads for 2, 3 and 4 h. Subsequently, LC3 conversion was assessed by Western Blot followed by densitometry analysis. Data are shown as mean ± SD (n = 6-8 for hMDM-1; n = 5 for hMDM-2).

Next, we intended to analyze if the replacement of apoptotic *Leishmania* by LAP inducing beads leads to a reduced T cell proliferation. Therefore, hMDM were infected with viable *Leishmania* alone or in combination with plain beads, PS beads or apoptotic parasites. The T cell proliferation was analyzed in a CFSE-based proliferation assay by flow cytometry (**Figure 33**).

Remarkably, already the stimulation of hMDM with plain beads results in a slightly increased T cell proliferation whereas stimulation with PS beads is comparable to the untreated control (20.5 ± 14.6%, 10.3 ± 11.2% in hMDM-1 and 16.4 ± 12.6%, 8.1 ± 9.3% in hMDM-2 respectively). The infection of hMDM with log. phase *Lm* (MOI 10), mainly viable parasites, leads to a higher T cell proliferation compared to infection with stat. phase *Lm* (MOI 10 viable parasites, MOI 10 apoptotic parasites) (33.7 ± 14.5%, 30.5 ± 14.4% in hMDM-1 and 27.9 ± 7.4%, 23.9 ± 10.1% in hMDM-2). Infection with viable parasites and plain beads results in an elevated T cell proliferation compared to viable parasites alone (42.6 ± 16.2% in hMDM-1 and 32.6 ± 18.2% in hMDM-2). Concerning the combination of viable *Leishmania* and PS beads a comparable proliferation as for stat. phase *Lm* was observed (29.3 ± 17.7% in hMDM-1 and 23.2 ± 13.2% in hMDM-2). Although due to the high donor variability, this was not significant.

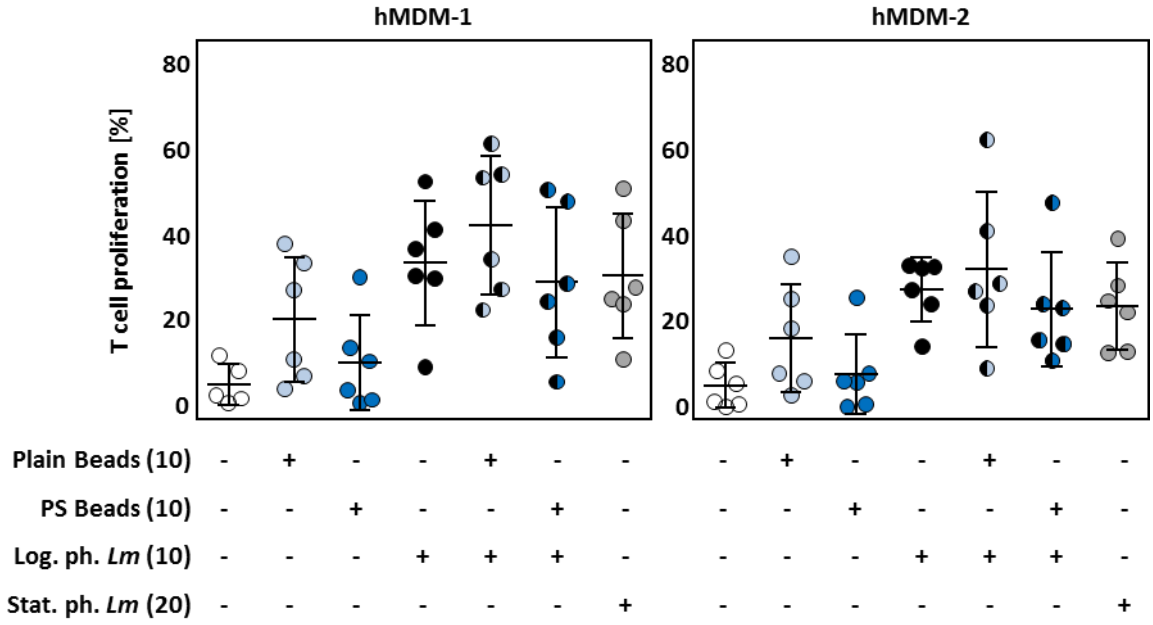

Figure 33: T cell proliferation in response to hMDM infected with *Leishmania* and/or plain or PS beads. hMDM-1 (left panel) and hMDM-2 (right panel) were infected overnight with a MOI 10 of plain beads, PS beads, viable *Lm*, a combination of viable *Lm* and beads or with a MOI 20 of stat. phase parasites. Subsequently, the infected hMDM were co-cultured with autologous, CFSE-labeled lymphocytes for 6 days. T cell proliferation was assessed as $CFSE^{low}$ cells by flow cytometry. Data are representative for at least three independent experiments and are shown as mean ± SD (n = 6).

Taken together, these data demonstrate that the specific PS-receptor stimulation with PS beads as well as the unspecific uptake of uncoated, plain beads leads to the formation of $LC3^{+}$ phagosomes and the conversion of LC3-I to LC3-II. By assessing the impact of LAP induction on T cell proliferation, we could observe, that the presence of plain beads increased the *Leishmania* induced T cell proliferation. On the other hand, the presence of PS beads or apoptotic parasites led to a reduced immune response.

3.4.2 LAP induction by zymosan particles

In addition to the replacement of apoptotic parasites by PS beads, we used zymosan particles as additional tool for LAP induction. Zymosan induces LAP by triggering TLR2 and is the most commonly used trigger to induce LAP (Sanjuan et al., 2007). Therefore, we analyzed the potential of zymosan for LAP induction in hMDM and to analyze if replacement of apoptotic parasites by zymosan is able to suppress the immune response.

First of all, immunofluorescence images were taken to confirm the uptake of zymosan particles in a $LC3^+$ compartment (**Figure 34**). Indeed, the stimulation of hMDM with zymosan results in the uptake of particles in LC3 positive compartments, shown by an antibody staining (**Figure 34A**) as well as by eGFP-LC3 lentiviral transduced hMDM and live cell imaging (**Figure 34B**).

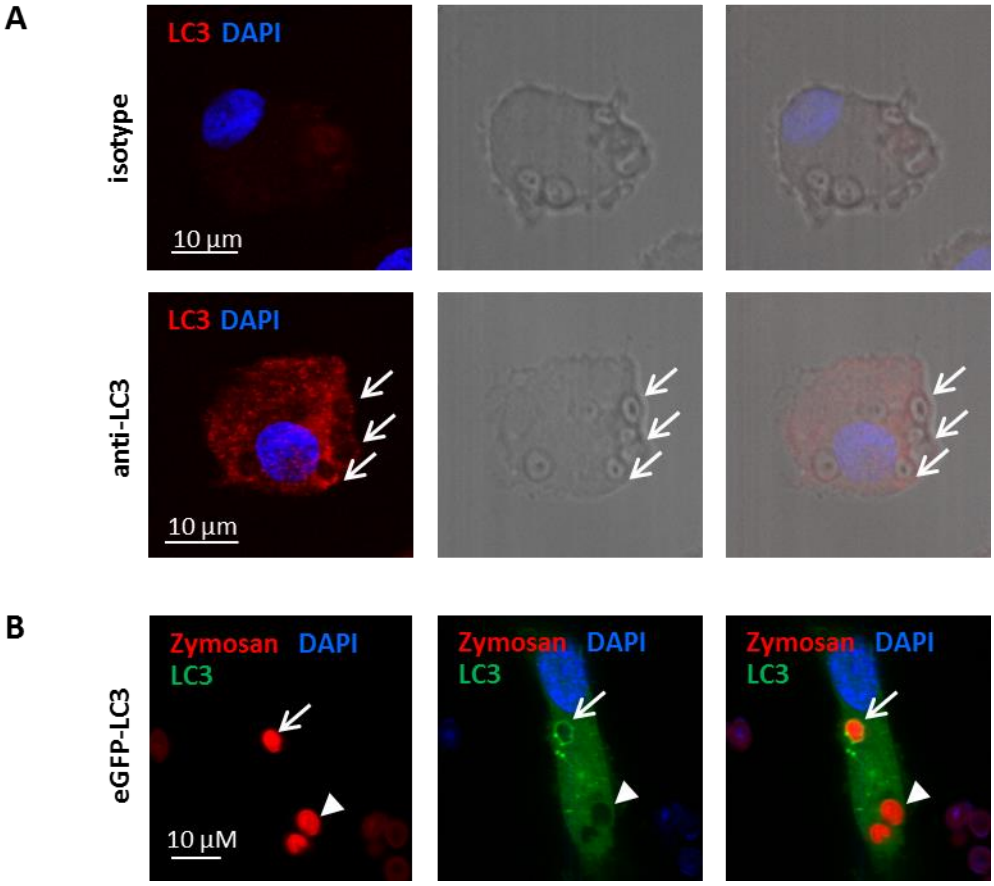

Figure 34: Zymosan particles reside in LC3 positive compartments in hMDM. (**A**) hMDM-1 were treated with a MOI 10 of zymosan particles for 2 h. Subsequently, the cells were fixed and stained with an anti-LC3 antibody (red) and nuclei were counterstained with DAPI (blue) (arrows indicate engulfed zymosan particles in $LC3^+$ compartments). (**B**) eGFP-LC3 transduced hMDM-1 were treated with a MOI 10 of red fluorescent zymosan particles and by live cell imaging the formation of LC3 positive phagosomes was observed (arrow indicates a zymosan particle in an $LC3^+$ compartment, arrow head indicates a zymosan particle in a $LC3^-$ compartment). Representative images were taken with a Zeiss LSM-Live 7 microscope and a 630x magnification.

To confirm LC3 lipidation, the LC3-I to LC3-II conversion in hMDM upon treatment with zymosan was analyzed by Western Blot (**Figure 35**). Stimulation with different MOIs of zymosan led to increasing LC3 conversion over time, peaking at 3 h in hMDM-1 (5.3 ± 3.6 fold for MOI 10 and 6.3 ± 4.9 fold for MOI 20) (**Figure 35A**). Concerning hMDM-2, significantly increased LC3 ratios were observed at 1, 1.5 and 2 h after stimulation, being the highest at 1 h (3.6 ± 4.3 fold for MOI 10 and 4.5 ± 3 fold for MOI 20) (**Figure 35B**). The efficiency of LAP induction was independent of the amount of particles that were used (MOI 10 or MOI 20).

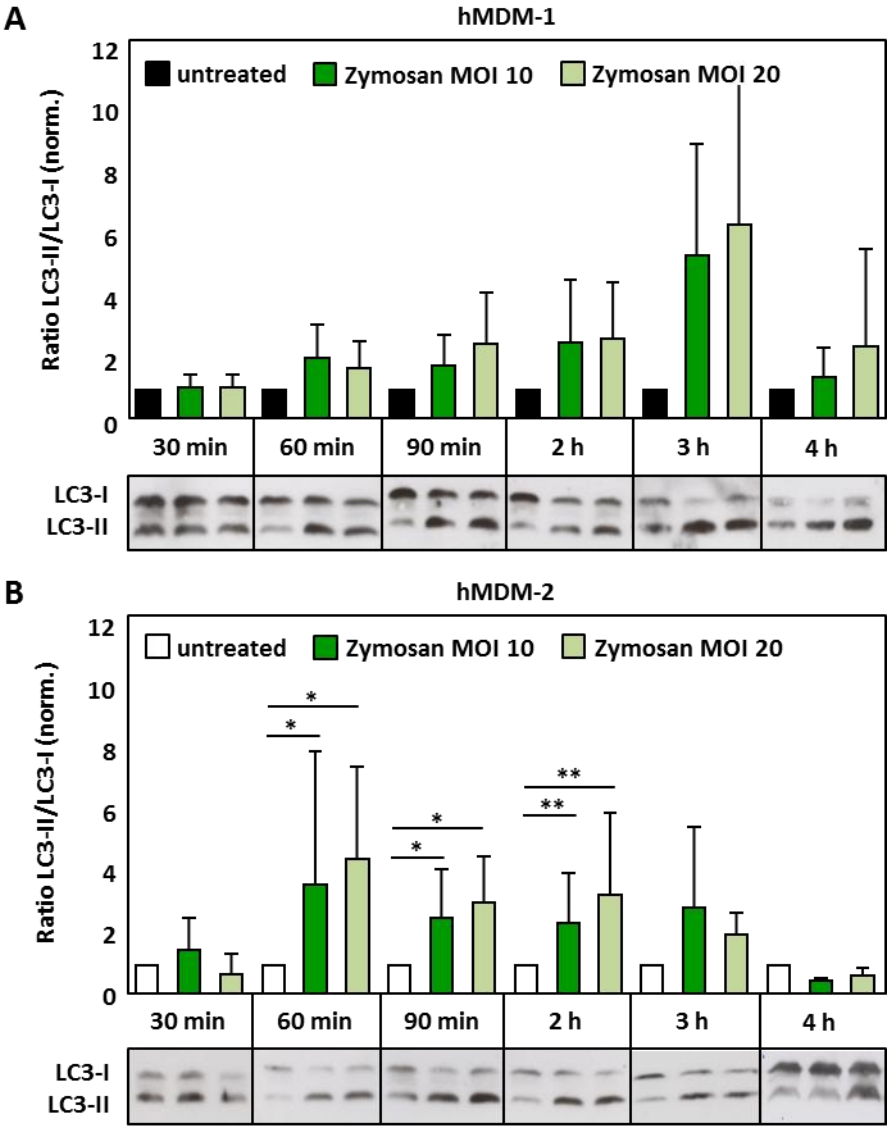

Figure 35: Stimulation of hMDM with zymosan particles induces LC3 conversion. (**A**) hMDM-1 and (**B**) hMDM-2 were stimulated with a MOI 10 or 20 of zymosan particles for 30 min to 4 h. Subsequently, LC3 conversion was assessed by Western Blot and densitometry analysis. Data are shown as mean ± SD (n = 5-7 for hMDM-1; n = 5-8 for hMDM-2).

3.4.3 The presence of zymosan or apoptotic *Lm* reduces the *Lm* specific T cell proliferation and enhances parasite survival

In the following step, the ability of zymosan particles to reduce the *Leishmania* induced T cell proliferation was analyzed (**Figure 36**). Stimulation of hMDM with zymosan induces a T cell proliferation of about 10-20%. High T cell responses in response to viable *Leishmania* of 43.4 ± 16.7% for hMDM-1 and 38.6 ± 11.1% for hMDM-2 could be significantly reduced by the addition of either zymosan particles (30.1 ± 18.8% for hMDM-1, 25 ± 12% for hMDM-2) or apoptotic parasites, present in the stat. phase (28.2 ± 17.3% in hMDM-1, 26.1 ± 10% in hMDM-2).

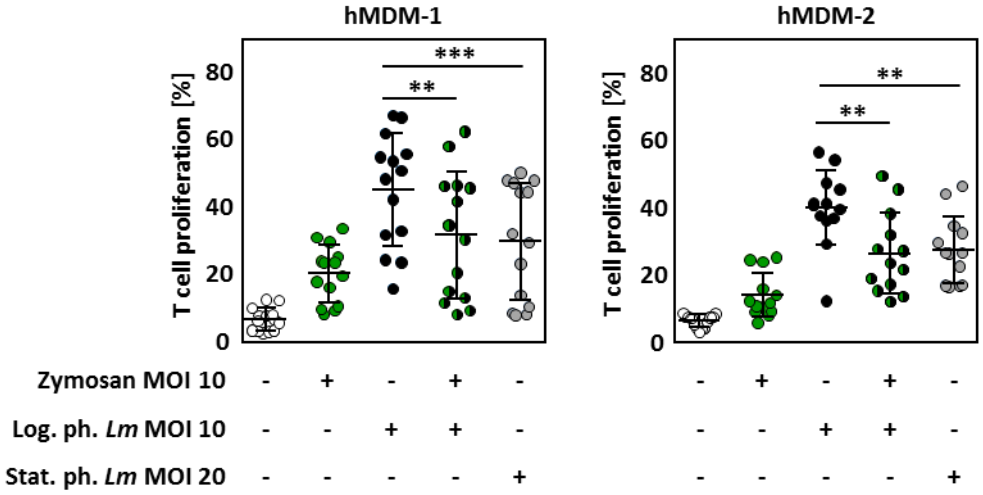

Figure 36: The presence of apoptotic *Leishmania* or zymosan leads to a reduced T cell response. hMDM-1 (left panel) and hMDM-2 (right panel) were infected with a MOI 10 of zymosan, viable *Lm*, a combination of both or with a MOI 20 of stat. phase parasites overnight. Subsequently, the infected hMDM were co-cultured with autologous, CFSE-labeled lymphocytes for 6 days. T cell proliferation was assessed as $CFSE^{low}$ cells by flow cytometry. Data are representative for at least three independent experiments and are shown as mean ± SD (n = 13-14).

During infection and immunity, a high T cell response leads to pathogen killing and infection control *in vivo*. To investigate if the *in vitro* proliferation of lymphocytes has an impact on intracellular parasite survival, we determined the infection rate (% *Lm* dsRed positive cells) and parasite load (mean fluorescence intensity (MFI) of dsRed) of hMDM (**Figure 37**).

Upon infection with viable *Leishmania* 8.4 ± 3.3% (hMDM-1) and 9 ± 4% (hMDM-2) of hMDM were still infected after 6 days. Concerning the infection of hMDM with a combination of viable parasites and zymosan or stat. phase *Lm*, a significantly higher infection rates were observed (19 ± 12.7%, 20.4 ± 11.8% for hMDM-1 and 18.7 ± 7.9%, 19 ± 7.3% for hMDM-2 respectively) (**Figure 37A**). A similar result was obtained concerning the parasite load (**Figure 37B**). The presence of either zymosan particles or apoptotic *Lm* leads to a significantly increased parasite load, measured as MFI of

dsRed, compared to viable parasites. The representative histograms show a dsRed^{high} subpopulation for hMDM infected with log. phase *Lm* and zymosan as well as in the stat. phase *Lm* treated hMDM. This subpopulation is absent in the uninfected (black line) or zymosan stimulated hMDM (green line) as well as in the log. phase *Lm* infected hMDM. Of note, a histological analysis was performed visualizing the changes in infection rate, which indicated that the presence of zymosan particles is beneficial for *Leishmania* survival (black arrows) (**Figure 37C**).

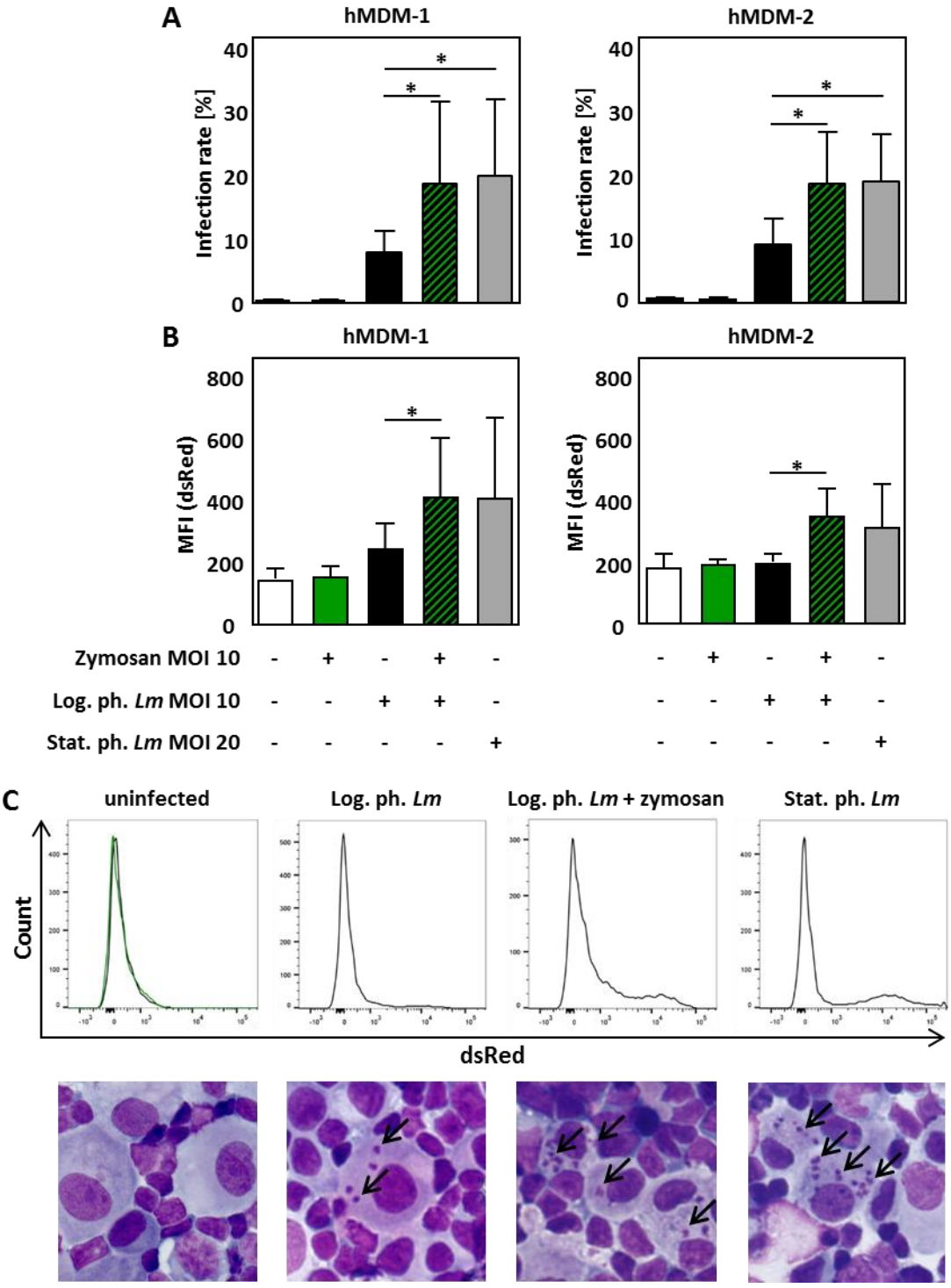

Figure 37: The presence of apoptotic *Leishmania* or zymosan leads to an enhanced infection rate and parasite load in hMDM. hMDM were infected overnight with a MOI 10 of

zymosan, viable *Lm* dsRed or a combination of both or with a MOI 20 of stat. phase *Lm* dsRed parasites. Subsequently, the infected hMDM were co-cultured with autologous lymphocytes for 6 days. (**A**) The infection rate (% $dsRed^+$ cells) and (**B**) parasite load (MFI) were assessed by flow cytometry. (**C**) Representative histograms and DiffQuick® pictures (black arrows indicating *Leishmania*) are depicted. Data are representative for at least three independent experiments and are shown as mean ± SD (n = 6).

Taken together, the high T cell response induced by hMDM infected with viable *Leishmania* led to a reduced infection rate indicating an effective, host protective immune response. The reduced lymphocyte proliferation in the presence of apoptotic *Lm* or zymosan particles is beneficial for the pathogen and enables a better intracellular survival of viable *Leishmania*.

The induction of an immune response is essentially dependent on cytokines, secreted by innate immune cells, such as macrophages. Therefore, we investigated if TNF-α or IL-10 secretion is altered upon infection resulting in more or less T cell proliferation (**Figure 38**). Remarkably, the addition of zymosan induces high cytokine release of IL-10 and TNF-α, which was independent on the presence of viable *Leishmania*. Concerning the cytokine secretion in response to only *Leishmania*, there was no *Leishmania*-induced IL-10 secretion detectable (**Figure 38A**) and just a moderate secretion of TNF-α, which was higher in hMDM-2 compared to hMDM-1 (**Figure 38B**).
In conclusion, the T cell proliferation data do not correlate with the measured cytokine secretion as we expected zymosan and apoptotic *Leishmania* to stimulate anti-inflammatory cytokine secretion and viable *Leishmania* to induce pro-inflammatory cytokine secretion.

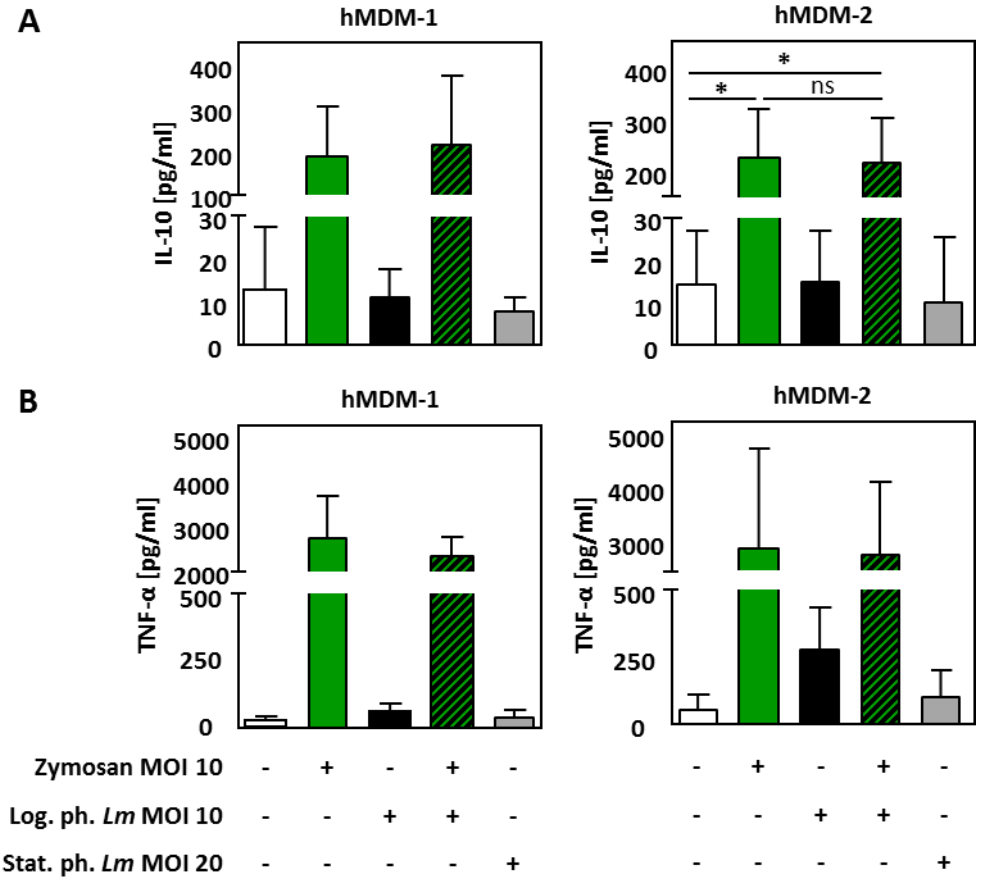

Figure 38: Stimulation of hMDM with zymosan particles increases the secretion of IL-10 and TNF-α. hMDM-1 (left panel) and hMDM-2 (right panel) were treated with a MOI 10 of log. phase *Leishmania*, zymosan, a combination of both or stat. phase *Lm* for 18 h. Subsequently, the supernatants of hMDM-1 and hMDM-2 were analyzed by ELISA to assess the secretion of (**A**) IL-10 and (**B**) TNF-α. Data are representative for at least three independent experiments and are shown as mean ± SD (n = 6 for IL-10 and n = 4 for TNF-α).

3.4.4 Impact of ROS for LAP induction

In the next part, we aimed to analyze the underlying mechanisms leading to LAP induction in hMDM. The production of reactive oxygen species (ROS) was shown to lead to the recruitment of LC3 to phagosomes (Huang et al., 2009). There exist two possibilities for ROS to occur within the phagosome. The molecules can be brought inside the cell by the parasite or can be produced by the macrophages' NADPH oxidase (NOX2) which is located on the phagosomal membrane.

First, we analyzed the importance of parasitic ROS for LAP induction. Therefore, we treated viable *Leishmania* parasites with two apoptosis inducing drugs, Staurosporine and Miltefosine. By analyzing the ROS positivity with 2′,7′-Dichlorodihydrofluorescein diacetate (H2DCFDA), dihydroethidium (DHE) and Dihydrorhodamine 123 (DHR123), Staurosporine treated *Leishmania* were shown to be ROS-positive whereas Miltefosine treated *Leishmania* were ROS-negative (MD thesis Jochen Steinacker). To assess if parasitic ROS is important for LAP induction, we used Staurosporine and Miltefosine

treated *Leishmania* for the infection of hMDM and subsequently analyzed LC3 conversion by Western Blot (**Figure 39**).

As expected, infection of hMDM with untreated *Lm* resulted in an increased LC3 conversion (log. ph. 1.1 ± 0.4 fold, stat. ph. 2.5 ± 1.1 fold in hMDM-1 and log. ph. 1.7 ± 1.2 fold, stat. ph. 1.1 ± 0.3 fold in hMDM-2). Infection of hMDM with Staurosporine treated *Leishmania* led to further increased LC3-II levels (log. ph. 7.1 ± 6.7 fold, stat. ph. 5.7 ± 3.3 fold in hMDM-1 and log. ph. 4.1 ± 1.7 fold, stat. ph. 2.9 ± 2.2 fold in hMDM-2) whereas Miltefosine treatment could not increase LC3 conversion as predominant as Staurosporine (log. ph. 3.2 ± 1.9 fold, stat. ph. 2.3 ± 2.2 fold in hMDM-1 and log. ph. 1.7 ± 0.7 fold, stat. ph. 1.6 ± 0.4 fold in hMDM-2).

Taken together, we could observe that apoptosis induction with Staurosporine (ROS positive) in *Leishmania* leads to an elevated LC3 conversion. Treatment of the parasites with Miltefosine (ROS negative) shows a LC3 conversion which is comparable to untreated *Leishmania*.

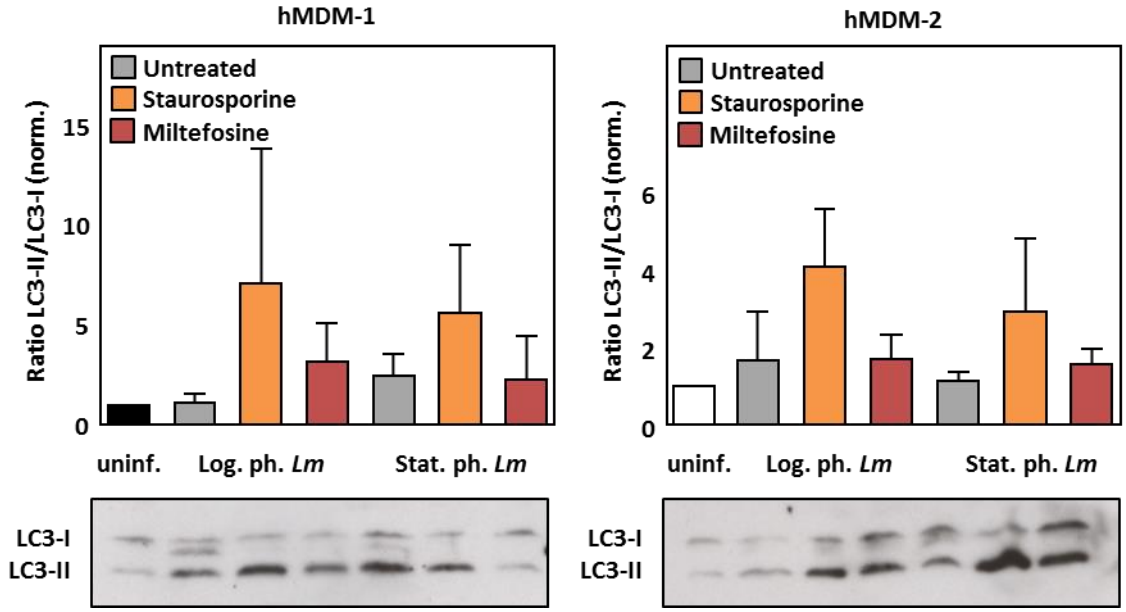

Figure 39: Staurosporine treated *Leishmania* lead to increased LAP induction in hMDM. hMDM-1 (left panel) and hMDM-2 (right panel) were infected with Staurosporine or Miltefosine treated *Leishmania* (25 µM, 48 h) for 3 h. LC3-I to LC3-II conversion was assessed by Western Blot and densitometry analysis. Data are representative for at least three independent experiments and are shown as mean ± SD (n = 3 for hMDM-1, n = 4 for hMDM-2).

3.4.5 Inhibition of LAP by NOX2 knockdown and NOX2 inhibition by DPI

Next, we investigated the impact of ROS produced by the macrophages' NADPH oxidase, NOX2. A crucial role for NOX2 in LAP induction using zymosan was demonstrated in bone marrow-derived macrophages (Martinez et al., 2015). Therefore, we aimed to inhibit NOX2 activity using a siRNA knockdown of CYBB mRNA (**Figure 40**). CYBB is the genomic name of the NOX2 protein, which is an isoform of the NADPH oxidase present in macrophages. By targeting NOX2 with CYBB specific

siRNA, the mRNA level was reduced to 5.4 ± 2% in hMDM-1. Assessing the protein level by Western Blot revealed the NOX2 levels to be reduced as well (NT 88.8 ± 75.2%, NOX2 siRNA 39.9 ± 50%).

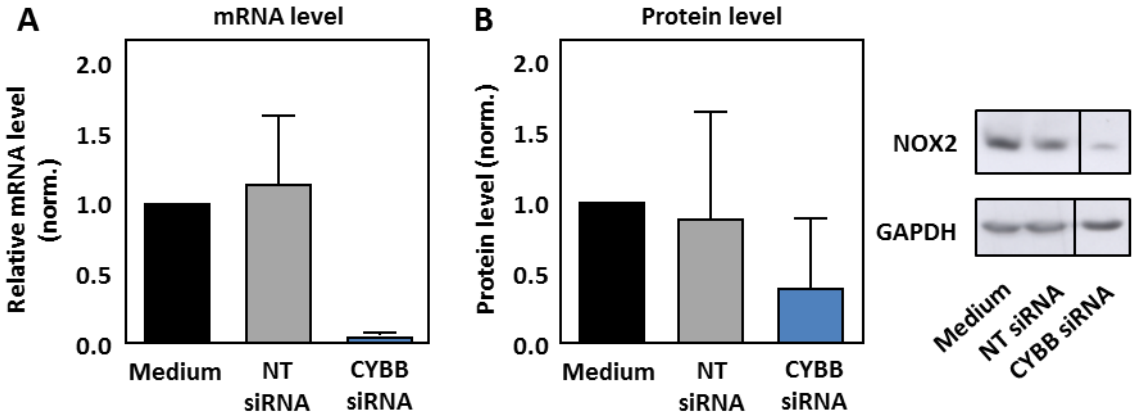

Figure 40: NOX2 knockdown efficiency in hMDM-1. hMDM were treated with non-target siRNA or specific siRNA for CYBB and subsequently (**A**) mRNA and (**B**) protein levels were assessed. GAPDH was used as loading control and a representative Western Blot was depicted. Data are representative for at least three independent experiments and are shown as mean ± SD (n = 4 for RNA level, n = 8 for protein level).

In the next step, we analyzed if the NOX2 knockdown influences the induction of LAP by zymosan or stat. phase *Lm*, assessed by Western Blot (**Figure 41**). Stimulation of hMDM-1 with zymosan or stat. phase *Lm* leads to the conversion of LC3-I to LC3-II (Medium 2.2 ± 0.7 fold and 2.7 ± 2.5 fold; NT 3.1 ± 2.5 fold and 3 ± 1.9 fold, respectively). In CYBB siRNA treated macrophages the LC3 conversion upon stimulation is not as pronounced as in non-treated or NT siRNA treated hMDM (1.9 ± 0.8 fold for Zymosan and 1.7 ± 1 fold for stat. ph. *Lm*). Taken together, NOX2 knockdown showed the tendency to suppress LC3 conversion upon infection or stimulation of hMDM-1 with *Leishmania* promastigotes or zymosan. The less pronounced effects might be due to the remaining NOX2 protein amount which could still produce ROS on the phagosomal membrane.

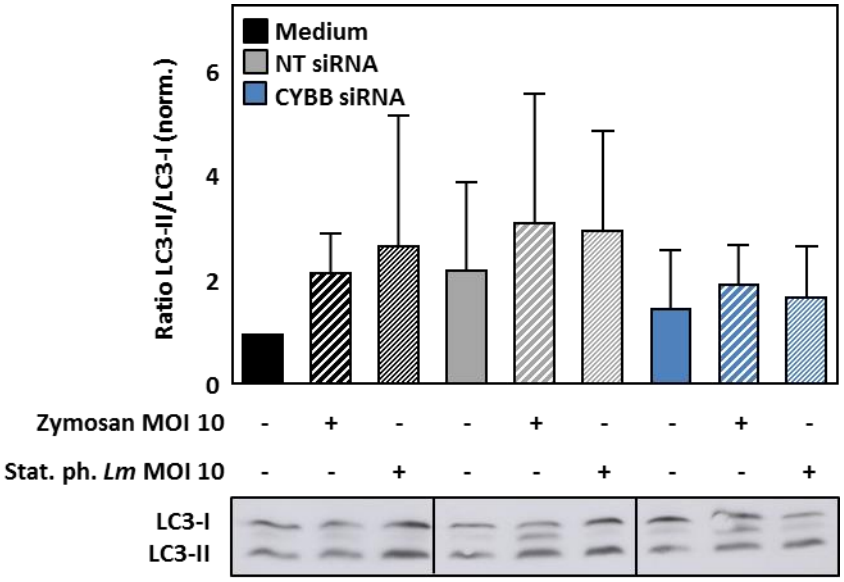

Figure 41: LAP induction in NOX2 knockdown hMDM with zymosan and stat. phase *Leishmania*. hMDM were treated with non-target siRNA or specific siRNA for CYBB and on day 3 after KD hMDM were stimulated with a MOI 10 of zymosan or stat. phase *Lm* for 3 h. LC3-I to LC3-II conversion was assessed by Western Blot and densitometry analysis. Data are representative for at least three independent experiments and are shown as mean ± SD (n = 5).

Although we could not detect significant changes for LAP induction in NOX2 knockdown hMDM by assessing LC3 conversion, we asked the question if NOX2 knockdown has an effect on T cell proliferation (**Figure 42**). If zymosan or apoptotic *Leishmania* are able to suppress T cell proliferation by LAP induction, we would consequently expect a higher T cell proliferation in the NOX2 knockdown cells. We observed that the *Leishmania* induced lymphocyte proliferation did not differ between control and knockdown macrophages (Medium 41.6 ± 3.8%, NT 43.6 ± 5.2%, CYBB siRNA 43.9 ± 4.8%).

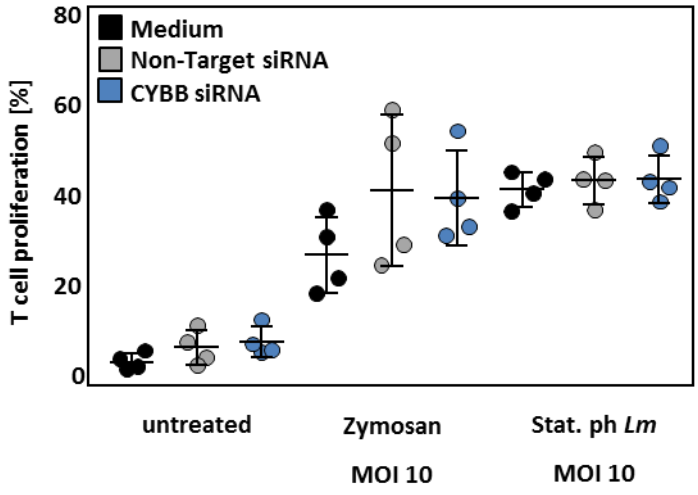

Figure 42: T cell proliferation in response to hMDM treated with zymosan or stat. phase *Leishmania*. hMDM-1 were stimulated with a MOI 10 of zymosan or stat. phase *Lm* overnight. Subsequently, the infected hMDM were co-cultured with autologous, CFSE-labeled lymphocytes for 6 days. T cell proliferation was assessed as $CFSE^{low}$ cells by flow cytometry.

Data are representative for at least three independent experiments and are shown as mean ± SD (n = 4).

As the remaining protein level in NOX2 knockdown macrophages (40%) might be sufficient to produce ROS for LAP induction, we targeted NOX2 by the chemical inhibitor Diphenyleneiodonium (DPI). By Western Blot analysis of LC3 conversion, a significantly increased lipidation was observed for treating hMDM with zymosan or stat. phase *Lm* (2.4 ± 1.3 fold, 2 ± 0.8 fold in hMDM-1 and 3.4 ± 1.6 fold, 3.3 ± 2 fold in hMDM-2). Pretreatment with DPI led to significantly reduced LC3-II levels for the stimulation with zymosan (1.4 ± 0.8 fold in hMDM-1 and 1.9 ± 1.3 fold in hMDM-2) and strongly reduced levels upon infection with stat. phase *Leishmania* (1.5 ± 0.9 fold in hMDM-1 and 1.8 ± 1 fold in hMDM-2) (**Figure 43**).

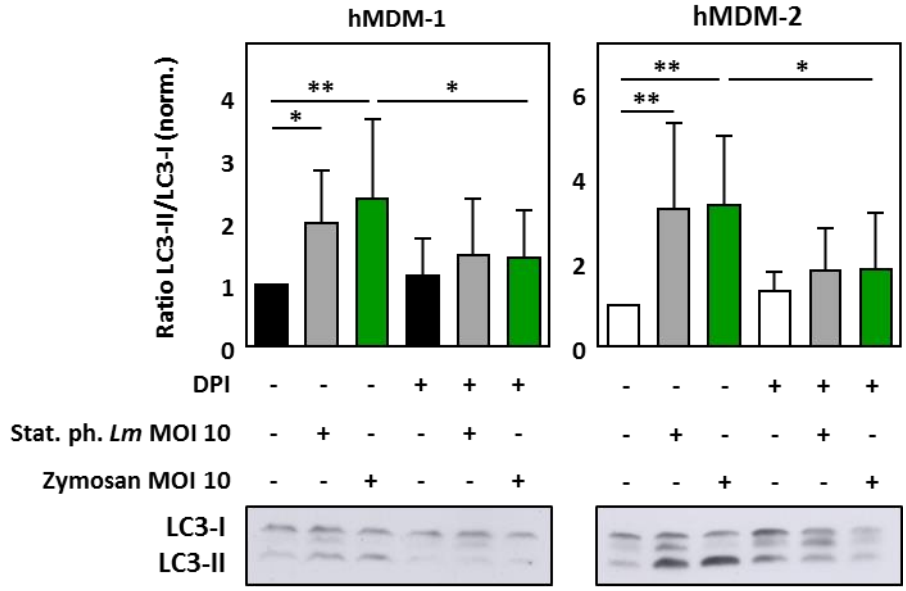

Figure 43: Pretreatment with DPI inhibits the LC3 conversion by zymosan or stat. phase *Lm* in hMDM. hMDM-1 (left panel) and hMDM-2 (right panel) were pretreated with 10 µM DPI for 30 min and subsequently stimulated with a MOI 10 of zymosan or stat. phase *Lm* for 3 h. LC3-I to LC3-II conversion was assessed by Western Blot and densitometry analysis. Data are representative for at least three independent experiments and are shown as mean ± SD (n = 9).

To analyze whether the inhibited induction of LAP has an impact on T cell proliferation, a CFSE-based lymphocyte proliferation assay was performed (**Figure 44**). The infection of hMDM with viable *Leishmania* resulted in a high T cell proliferation (31.2 ± 14.4% in hMDM-1 and 33.8 ± 9.5% in hMDM-2) which was reduced by the presence of apoptotic parasites in the stat. phase (21.6 ± 14.6% in hMDM-1 and 20.4 ± 11.5% in hMDM-2). The pretreatment with DPI was not able to modulate the T cell response.

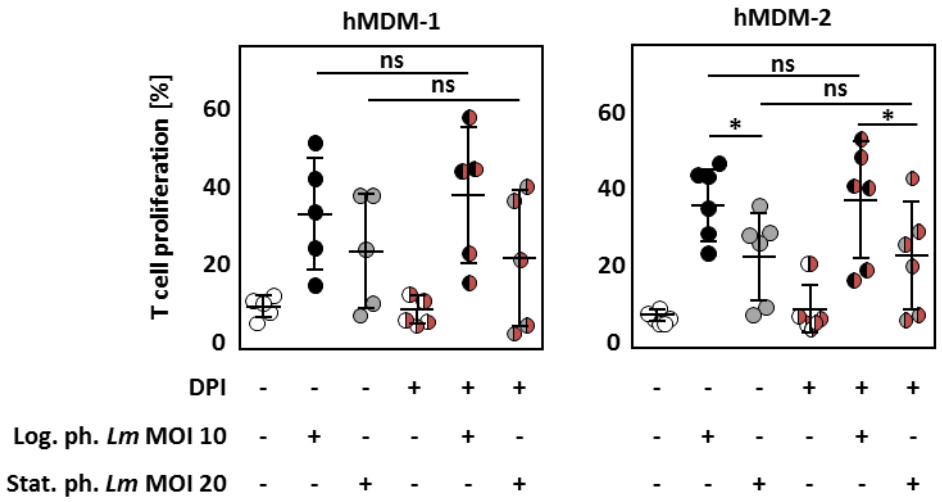

Figure 44: Pretreatment with DPI has no effect on *Leishmania* induced T cell proliferation. hMDM-1 (left panel) and hMDM-2 (right panel) were pretreated with 10 µM DPI for 30 min followed by infection with a MOI 10 of log. phase or stat. phase *Lm* overnight. Subsequently, the infected hMDM were co-cultured with autologous, CFSE-labeled lymphocytes for 6 days. T cell proliferation was assessed as $CFSE^{low}$ cells by flow cytometry. Data are representative for at least three independent experiments and are shown as mean ± SD (n = 5 for hMDM-1 and n = 6 for hMDM-2).

As the inhibition of LAP by DPI had no impact on T cell proliferation, we raised the question what else can lead to a less efficient T cell activation in the presence of zymosan and apoptotic *Leishmania*. As lysosomal degradation is a crucial step in the antigen processing pathway, we analyzed the intracellular fate of *Leishmania* parasites and zymosan in terms of the induction of lysosomal acidification in hMDM (**Figure 45**). First, apoptotic and viable promastigotes residing in a stat. phase culture were separated using AnnexinV labeled magnetic beads by MACS (magnetic activated cell sorting). Apoptotic parasites exposing phosphatidylserine on the surface are bound by AnnexinV beads and thereby magnetically separated from unbound viable parasites. Subsequently, macrophages were infected with viable *Lm*, apoptotic *Lm*, the mixture of both (stat. phase) or zymosan particles and lysosomal acidification was followed over time by the dye Lysotracker® which is selective for acid organelles. After 1 h, only apoptotic parasites were able to slightly increase the Lysotracker® positivity (1.1 ± 0.2 fold). Increasing values for lysosomal acidification were observed 3 h post infection or stimulation, being the highest for zymosan and apoptotic *Lm* and the lowest for viable *Lm* (viable *Lm* 1.1 ± 0.4 fold, apoptotic *Lm* 1.4 ± 0.5 fold, stat. ph. *Lm* 1.3 ± 0.5 fold, zymosan 1.6 ± 0.8 fold). This lysosomal acidification pattern was not further elevated after 5 h of stimulation (viable *Lm* 1.1 ± 0.4 fold, apoptotic *Lm* 1.4 ± 0.6 fold, stat. ph. *Lm* 1.2 ± 0.5 fold, zymosan 1.6 ± 0.9 fold).

Taken together, we conclude that both, the uptake of apoptotic *Lm* and zymosan, leads to an enhanced acidification in hMDM. Whereas, uptake of viable promastigotes did not increase the Lysotracker® positivity at early time points after phagocytosis.

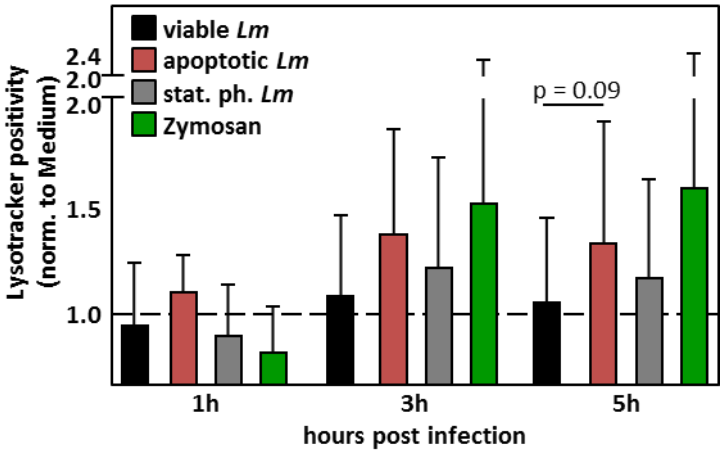

Figure 45: Uptake of apoptotic *Leishmania* or zymosan increases lysosomal acidification in hMDM. hMDM-1 were infected with viable, apoptotic or stat. phase *Lm* or were stimulated with zymosan for 1, 3 and 5 h. Subsequently, hMDM were stained with Lysotracker® (1 µM) for 10 min. Lysosomal acidification as MFI of PE was assessed by flow cytometry. Data are representative for at least three independent experiments and are shown as mean ± SD (n = 4).

3.4.6 Proteome analysis to identify additional factors leading to immune suppression upon *Leishmania* infection

One possible hint for the reduced T cell proliferation upon infection of hMDM with apoptotic parasites or zymosan is the enhanced lysosomal acidification. To identify influences of Leishmania on the host cells' immune activation machinery, we performed proteome analysis of uninfected hMDM and compared it to hMDM infected with stat. phase *Leishmania* (in cooperation with Stefan Tenzer, University of Mainz). Again, the proteins being at least 2-fold up- or downregulated were used for a string analysis.

Regarding hMDM-1, the infection with *Leishmania* led to the upregulation of the indoleamine 2,3-dioxygenase 1 (IDO) and MHC-I whereas the expression of MHC-II molecules was downregulated (**Figure 32 and Table 3**).

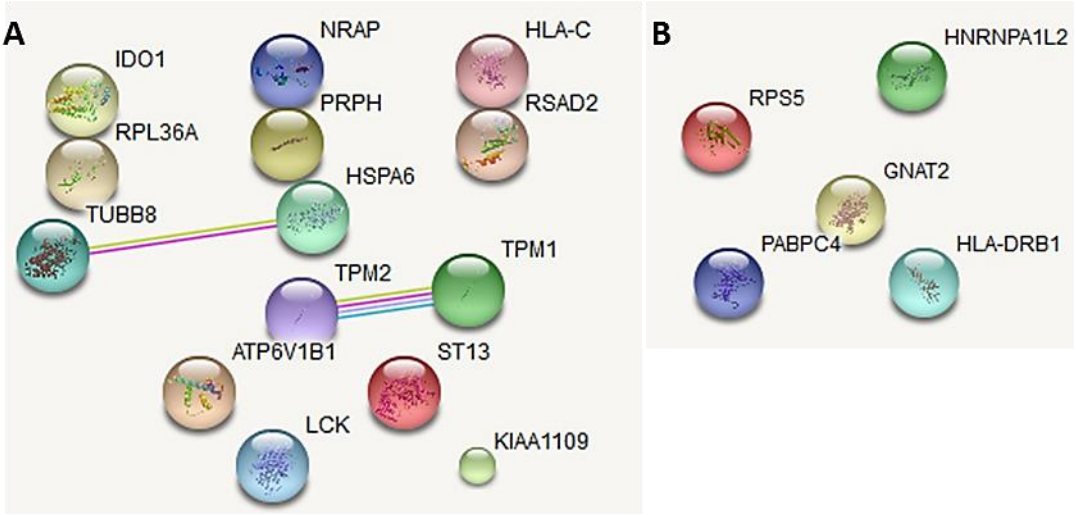

Figure 46: String analysis of upregulated (A) and downregulated (B) proteins in *Leishmania* infected hMDM-1. Proteome analysis by mass spectrometry of hMDM-1 and hMDM-1 infected with *Leishmania*. Depicted are proteins that are at least 2-fold up- or downregulated in infected compared to uninfected hMDM-1. Data are representative for at least three independent experiments (n = 6).

Table 3: Up- and downregulated proteins in *Leishmania* infected hMDM-1. Depicted are proteins that are at least 2-fold up- or downregulated in infected compared to uninfected hMDM-1. Proteins were sorted by highest up- or downregulation on top to lowest up- or downregulation on bottom and proteins being involved in immune activation are illustrated in bold.

String name	Entry name	Full name
Upregulated		
NRAP	NRAP_HUMAN	Nebulin-related-anchoring protein
ATP6V1B1	VATB1_HUMAN	V-type proton ATPase subunit B, kidney isoform
IDO1	**I23O1_HUMAN**	**Indoleamine 2,3-dioxygenase 1**
RSAD2	RSAD2_HUMAN	Radical S-adenosyl methionine domain-containing protein 2
TUBB8	TBB8_HUMAN	Tubulin beta-8 chain
RPL36A	RL36A_HUMAN	60S ribosomal protein L36a
LCK	LCK_HUMAN	Tyrosine-protein kinase Lck
TPM1	TPM1_HUMAN	Tropomyosin alpha-1 chain
TPM2	TPM2_HUMAN	Tropomyosin beta chain
ST13	F10A5_HUMAN	Putative protein FAM10A5
HSPA6	HSP76_HUMAN	Heat shock 70 kDa protein 6
HLA-C	**1C12_HUMAN**	**HLA class I histocompatibility antigen, Cw-12 alpha chain**
PRPH	PERI_HUMAN	Peripherin
KIAA1109	K1109_HUMAN	Uncharacterized protein KIAA1109
Downregulated		
HLA-DRB1	**2B1A_HUMAN**	**HLA class II histocompatibility antigen, DRB1-10 beta chain**
HNRNPA1L2	RA1L2_HUMAN	Heterogeneous nuclear ribonucleoprotein A1-like 2
GNAT2	GNAT2_HUMAN	Guanine nucleotide-binding protein G(t) subunit alpha-2

RPS5	RS5_HUMAN	40S ribosomal protein S5
PABPC4	PABP4_HUMAN	Polyadenylate-binding protein 4

Regarding hMDM-2, *Leishmania* infection resulted in a similar protein expression alteration profile as observed for infected hMDM-1. Among others, infection of hMDM-2 with *Leishmania* leads to the upregulation of IDO1 and MHC-I and downregulation of MHC-II (**Figure 33 and Table 4**).

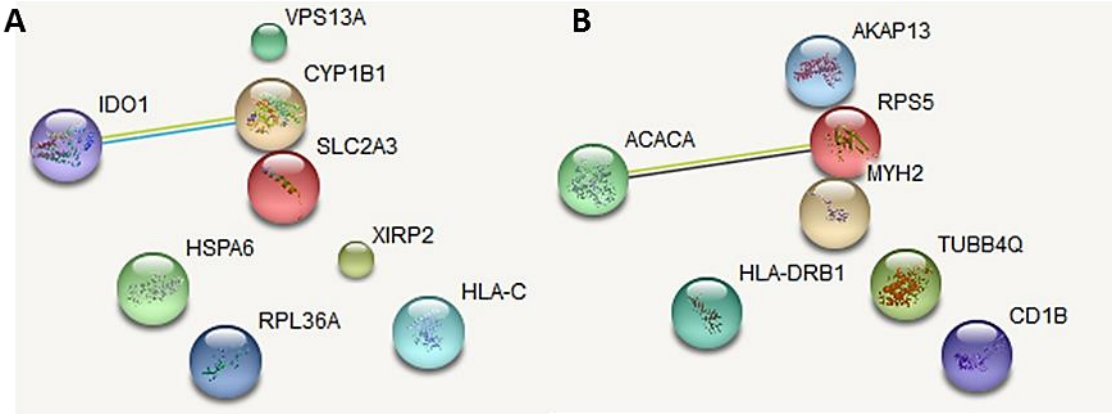

Figure 47: String analysis of upregulated (A) and downregulated (B) proteins in *Leishmania* infected hMDM-2. Proteome analysis by mass spectrometry of hMDM-2 infected with *Leishmania* and hMDM-2. Depicted are proteins that are at least 2-fold up- or downregulated in infected compared to uninfected hMDM-2. Data are representative for at least three independent experiments (n = 6).

Table 4: Up- and downregulated proteins in *Leishmania* infected hMDM-2. Depicted are proteins that are at least 2-fold up- or downregulated in infected compared to uninfected hMDM-2. Proteins were sorted by highest up- or downregulation on top to lowest up- or downregulation on bottom and proteins being involved in immune activation are illustrated in bold.

String name	Entry name	Full name
Upregulated		
RPL36A	RL36A_HUMAN	60S ribosomal protein L36a
HSPA6	HSP76_HUMAN	Heat shock 70 kDa protein 6
IDO1	**I23O1_HUMAN**	**Indoleamine 2,3-dioxygenase 1**
CYP1B1	CP1B1_HUMAN	Cytochrome P450 1B1
not found	NFL_HUMAN	Neurofilament light polypeptide
SLC2A3	GTR3_HUMAN	Solute carrier family 2, facilitated glucose transporter member 3
VPS13A	VP13A_HUMAN	Vacuolar protein sorting-associated protein 13A
HLA-C	**1C12_HUMAN**	**HLA class I histocompatibility antigen, Cw-12 alpha chain**
XIRP2	XIRP2_HUMAN	Xin actin-binding repeat-containing protein 2
Downregulated		
ACACA	ACACA_HUMAN	Acetyl-CoA carboxylase 1
HLA-DRB1	**2B1A_HUMAN**	**HLA class II histocompatibility antigen, DRB1-10 beta chain**

CD1B	CD1B_HUMAN	T-cell surface glycoprotein CD1b
MYH2	MYH2_HUMAN	Myosin-2
TIBB4Q	YI016_HUMAN	Putative tubulin beta chain-like protein
RPS5	RS5_HUMAN	40S ribosomal protein S5
AKAP13	AKP13_HUMAN	A-kinase anchor protein 13

The immunomodulatory proteins that were influenced upon *Leishmania* infection in hMDM are interesting new targets that might provide further inside in *Leishmania* immune evasion mechanisms and will be investigated in following experiments.

4 Discussion

4.1 Summary of the data

In the first part of this thesis we focused on the modulation of autophagy, a highly conserved cellular response mechanism to organismic stress. We aimed to investigate autophagy in two different phenotypes of immunomodulatory cells, namely pro- and anti-inflammatory human macrophages. By applying chemical class I PI3K/mTOR inhibitors or the peptide Tat-Beclin autophagy in hMDM was induced. In contrast, targeting the class III PI3K complex by Spautin-1 and Wortmannin blocked autophagy induction. Interestingly, hMDM-2 were in general more susceptible for autophagy induction. To inhibit autophagy more specifically, a siRNA approach was established and the knockdown efficiency could be shown to be time- and target-dependent. By functional characterization of ULK-1 and Beclin-1 knockdown cells, chemical autophagy induction could still take place, indicating an ULK-1- and Beclin-1-independent autophagy mechanism in hMDM. Regarding the role of autophagy modulation on antigen processing using the model antigen Tetanus Toxoid, no impact could be observed. Surprisingly, hMDM-2 were shown to be superior to hMDM-1 for priming an adaptive immune response which might be due to higher expression of MHC-II and proteins being involved in antigen processing.

Also pathogens such as *Leishmania* were shown to interact with the host cells' autophagy machinery. We demonstrated *Leishmania* to induce autophagy in hMDM however this occurred independent of the *Leishmania* virulence factor GP63. Furthermore, GP63 deficiency did not influence the infection of hMDM and the adaptive immune response.

In the second part we focused on the modulation of LC3-associated phagocytosis. In a previous study we could show that apoptotic *Lm* in the virulent inoculum induce LAP and suppress the adaptive immune response. Replacing apoptotic *Lm* by LAP-inducing PS beads or zymosan, we demonstrated the formation of $LC3^+$ phagosomes around those particles. Stimulation of hMDM with PS coated beads or zymosan and co-infection with viable *Lm* resulted in a reduction of T cell proliferation. Suppression of the adaptive immune response enabled an enhanced parasite survival. Analyzing the underlying mechanisms of LAP in hMDM, inhibition of the NADPH oxidase by DPI blocked LAP induction. In addition, infection of hMDM with Staurosporine-treated *Lm,* being ROS positive, increased LC3 conversion which suggests ROS-dependent LAP induction in hMDM. Furthermore, uptake of apoptotic *Lm* or zymosan led to enhanced acidification of hMDM indicating a role for improved antigen processing and presentation.

4.2 Autophagy modulation in human primary macrophages

Extensive research using cell lines or mouse model systems contributed strongly to the understanding of the autophagy process. Though still little is known of the autophagy pathway in human primary macrophages, playing a central role as immune modulating cells. In the first part of this study we focused on autophagy modulation in human primary macrophages, in which autophagy has the dual role of ensuring homeostasis and degrading invading pathogens for antigen presentation. Therefore, we took a closer look on autophagy modulation in two different phenotypes of macrophages, the pro-inflammatory type-I and the anti-inflammatory type-II macrophages.

Inhibition of the class I PI3K/mTOR pathway resulted in an induction of autophagy. Specifically, PI-103 and AZD8055 were shown to induce autophagy more potent than Rapamycin. This finding is in accordance with previous studies which revealed Rapamycin to be less potent for autophagy induction indicated by just modest LC3 conversion (Andersson et al., 2016). Furthermore, we could successfully prove the autophagy inducing peptide Tat-Beclin to induce autophagy in hMDM-1 and hMDM-2. This specific activation of Beclin-1 is in accordance with previous data in HeLa and cancer stem cells (Shoji-Kawata et al., 2013; Sharif et al., 2017).

Using pre-treatment of macrophages with Bafilomycin A1 which blocks lysosomal acidification and hence degradation of autophagosomal cargo, we demonstrated that the whole sequestration process was induced and not just the initial steps of autophagy. Our data are in line with previous studies showing LC3-II and p62 accumulation due to blocked degradation with Bafilomycin A1 (Bjorkoy et al., 2005; Watanabe and Tanaka, 2011; Klionsky et al., 2016).

Furthermore, we aimed to regulate autophagy negatively by chemical inhibition of the class III PI3K complex downstream of mTOR. In line with previous studies, Spautin-1 and Wortmannin were demonstrated to inhibit autophagy induction in human primary macrophages (Mateo et al., 2013). Our data indicate that LY294002 is capable of inhibiting autophagy in hMDM-1 but interestingly not in hMDM-2. Controversy results for LY294002 as autophagy inhibitor or inducer were already demonstrated. Blommaart et al. could demonstrate LY294002 to inhibit autophagy in rat hepatocytes, a finding in agreement with Petiot's data showing LY294002 to dampen autophagy activity in HT-29 cells (Blommaart et al., 1997; Petiot et al., 2000). Whereas Xing and colleagues could show LY294002 to induce autophagy in gastric cancer cells by activating p53 and caspase-3 which led to increased expression of LC3 (Xing et al., 2008). Our results and the given examples highlight the cell type specific function of LY294002 which seems to differ even between different macrophage phenotypes. Concerning the most commonly described autophagy inhibitor, 3-MA, pre-treatment of macrophages

with 1 mM even led to an increased LC3-I to LC3-II conversion. Previously, 3-MA was described to inhibit autophagy at high concentrations (e.g. 10 mM) in various cell types and even in low concentrations in the presence of active vitamin D3 in hMDM (Seglen and Gordon, 1982; Blommaart et al., 1997; Petiot et al., 2000; Yuk et al., 2009). In human prostate cancer cells, 5 mM 3-MA treatment could inhibit the autophagy inducing effects of PI-103 (Degtyarev et al., 2008). However there is rising evidence that 3-MA can also induce autophagy, shown by Lin and colleagues in RAW 264.7 macrophages or under nutrient rich conditions in mouse embryonic fibroblasts and L929 cells (Wu et al., 2010; Lin et al., 2012). Considering these results and based on our findings, we suggest that 3-MA induces autophagy in hMDM at low concentrations and possesses inhibitory capacities at higher concentrations.

Most strategies to gain information about the autophagic process focus on the inhibition of autophagy by genome editing, RNA interference or chemical modulation of class III PI3-kinase using pharmacological inhibitors. Chemical targeting of class III PI3K is associated with various side effects as Vps34 regulates cellular membrane trafficking processes and transport across the nuclear membrane (Roggo et al., 2002; Johnson et al., 2006). Indeed, we could observe reduced phagocytic capacity of hMDM upon stimulation with Wortmannin (data not shown). As chemical modulators are often not entirely specific, genetic intervention is preferred (Vinod et al., 2014). Therefore, we targeted several autophagy related proteins by siRNA knockdown. In general, we observed protein knockdowns in hMDM to be time and target dependent. We could show a long protein half-life for Vps34 suggested by protein stability for up to one week. In contrast, an effective protein knockdown by siRNA was reported in HeLa cells, demonstrating significantly reduced protein levels 2-5 days post knockdown (Nobukuni et al., 2005; Sagona et al., 2010). Moreover, RNAi knockdown of Beclin-1 was efficient 1-2 days post transfection in RAW 264.7 macrophages whereas we observed a longer protein half-life in hMDM indicated by reduced Beclin-1 levels on day 6-7 post siRNA application (Li et al., 2013; Martyniszyn et al., 2013). Our data demonstrate comparable protein stability of ATG16L1 to Beclin-1 in hMDM although in contrast, other studies could show efficient protein reduction 48 h post RNAi treatment in HeLa and HCT116 cell lines (Rioux et al., 2007; Homer et al., 2010) Hence, our data elucidate that findings on protein stability in cell lines can not be extrapolated to human primary cells.

Interestingly, although we demonstrated ULK-1 protein levels to be strongly reduced, the autophagy machinery in human macrophages was still functional. In contrast to our results, an essential role for ULK-1 as modulator of autophagy was shown by a kinase-specific siRNA screening in HEK293 cells (Young et al., 2006; Chan et al., 2007). In addition, the group of D. Green could show reduced LC3 levels and LC3 punctae in ULK-1 knockdown murine bone marrow-derived macrophages upon autophagy

induction with Rapamycin (Martinez et al., 2011). On the other hand and in line with our data, Alers et al. reported ULK-1/ULK-2-independent starvation-induced autophagy in DT40 cells assuming mTOR independent regulation of Atg13 and FIP200 by other kinases (Alers et al., 2014). In line with their results, an mTOR independent, but not yet identified pathway was proposed in COS7 cells by autophagy induction with Glucosamine (Shintani et al., 2010). Furthermore, controversy results for ULK-1/2 requirement for autophagy induction were obtained depending on the applied stimuli. ULK-1/2 are required for amino acid induced autophagy but dispensable for glucose deprivation induced autophagy in mouse embryonic fibroblasts (Cheong et al., 2011). It might be possible that also in human primary macrophages autophagy induction can precede via an mTOR- and accordingly ULK-1-independent mechanism. Moreover, ULK-1-independent autophagy in hMDM might be explained by the functional compensation by the structural related protein ULK-2. ULK-1 and ULK-2 redundancy is cell type specific, as ULK-2 can not compensate for ULK-1 in HEK293 cells and cerebellar granule neurons but is sufficient for autophagy induction in mouse embryonic fibroblasts (Chan et al., 2007; Kundu et al., 2008; Lee and Tournier, 2014). Comprehensively, further experiments need to be performed to rule out if the kinase activity of ULK-1 is compensated by ULK-2 in hMDM or if an ULK-independent mechanism for autophagy induction exists. A simultaneous knockdown of ULK-1 and ULK-2 will clarify if protein compensation occurs. Furthermore, if autophagy can proceed in ULK-1/2 knockdown cells, analyzing Beclin-1 phosphorylation will provide a hint for other kinases than ULK being involved in autophagy induction.

Assessing the role of Beclin-1 knockdown for autophagy induction, we could show that, similar to ULK-1 knockdown, LC3 conversion could still take place. In contrast to these data, Beclin-1-dependent autophagy induction with Rapamycin was shown in primary cortical neurons and murine bone marrow-derived macrophages (Grishchuk et al., 2011; Martinez et al., 2011). On the other hand and in line with our data are the results by Li et al., demonstrating that Beclin-1 is critical for starvation induced but not for Rapamycin induced autophagy in murine macrophages (RAW 264.7) (Li et al., 2013). Furthermore, other autophagy inducers could also be shown to induce LC3 conversion in a Beclin-1 independent manner in various cell types (Gao et al., 2010; Smith et al., 2010; Tian et al., 2010). Interestingly, Gossypol induces autophagy in a Beclin-1 dependent way in HeLa cells and in a Beclin-1 independent way in MCF-7 cells (Gao et al., 2010). Hence we suggest that autophagy induction in human primary macrophages is independent of Beclin-1.

By comparing two different macrophage phenotypes we observed that hMDM-2 were more susceptible for autophagy induction compared to hMDM-1. The physiological function of alternatively activated macrophages is the uptake of apoptotic or necrotic

cells and tissue repair functions and thus, possessing a higher phagocytic capacity, hMDM-2 might be of greater importance for maintaining homeostasis (Mosser and Edwards, 2008). In line with our data, a recently published study also indicates the autophagic sequestration pathway to be highly dependent on the investigated cell type and can even vary by applying different stimuli (Gomez-Sanchez et al., 2015).

Taken together, our data as well as the mentioned observations by other groups highlight the distinct regulation of autophagy in dependence of the used model systems and applied stimuli. Specifically, several autophagy-related proteins were demonstrated to be more stable in human primary cells compared to cell lines. Additionally, autophagic sequestration is ULK-1-dependent in HEK293 cells but ULK-1 is dispensable for autophagy induction in hMDM. Our results suggest that even in different phenotypes of macrophages, autophagy is differentially regulated as hMDM-2 possess higher autophagy inducibility and are not sensitive to LY294002 treatment.

4.3 Impact of autophagy on antigen presentation using the model antigen Tetanus Toxoid

The adaptive immune response is orchestrated by the processing and presentation of peptides on MHC molecules for the recognition by specific T cells (Munz, 2016a). For a long time, the endocytotic uptake and lysosomal degradation pathway was suspected to be responsible for the processing and presentation of exogenous antigens on MHC-II molecules (Roche and Furuta, 2015). The presentation of cytosolic antigens on MHC-II revealed the participation of the autophagic sequestration process to be involved in the priming of a $CD4^+$ T cell response (Nimmerjahn et al., 2003; Dengjel et al., 2005). Jagannath and colleagues could nicely demonstrate that starvation or Rapamycin induced autophagy enhances the efficacy of BCG vaccine by increasing peptide processing and presentation of cytosolic secreted Ag85B (Jagannath et al., 2009).

To analyze if autophagy in hMDM is involved in antigen processing, we used the recall antigen Tetanus Toxoid to initiate an adaptive immune response as German blood donors are commonly vaccinated against Tetanus. As expected from literature, we demonstrated the onset of a detectable T cell proliferation upon antigen processing and presentation by macrophages to T cells (Nielsen et al., 2010). In line with other studies, the proliferating T cells were shown to exhibit a $CD4^+$ phenotype, indicating peptide presentation via MHC-II molecules (Barbey et al., 2007; Cellerai et al., 2007). To investigate the role of autophagy in this MHC-II mediated antigen presentation, we induced autophagy by AZD8055 or inhibited it by siRNA knockdown of ULK-1. Neither the induction of autophagy nor the inhibition could be shown to influence the Tetanus

Toxoid specific T cell proliferation. The inactivation process of Tetanus Toxin by formaldehyde to generate the toxoid vaccine prevents the binding to gangliosides on motoneurons leading to the loss of its toxic effects. Hence, TT might be taken up by antigen presenting cells by endocytosis or pinocytosis without specific receptor engagement or by receptor-mediated phagocytosis (Kamphorst et al., 2010; Roche and Furuta, 2015). Consequently, the expendability of autophagy is probably due to the uptake process and intracellular localization of Tetanus Toxoid in an endosome making it inaccessible for autophagic targeting. Focusing on the latter uptake mechanism, specific receptor triggering initiating LC3-associated phagocytosis can modify endocytosis and degradation of extracellular material for MHC-II presentation (Munz, 2016a). The requirement of the LAP degradation process was shown in murine dendritic cells lacking ATG5 as $CD4^+$ T cell priming was strongly impaired, especially the processing and presentation of phagocytosed antigens containing Toll-like receptor stimuli (Blander and Medzhitov, 2006; Lee et al., 2010). According to these studies, the modulation of the conventional autophagy process by AZD8055 and ULK-1 might be “too upstream” as only the autophagy proteins downstream of mTOR and ULK-1 are required for LAP. As we did not further rule out the intracellular localization of Tetanus Toxoid, we can only assume that it is taken up in a compartment resulting in antigen processing independent on conventional autophagy. To clarify the participation of receptor-mediated LAP, a modulation downstream of mTOR such as an ATG5 knockdown, needs to be done.

Interestingly, T cell proliferation in response to co-cultivation of $CD14^+$ isolated monocytes (used for knockdown experiments) with PBLs was in general elevated compared to macrophages generated by plastic adherence. As CD14 is a surface pattern recognition receptor for LPS and a co-receptor for TLR2, the applied isolation method leads to macrophage activation prior to co-cultivation with autologous PBLs (Dobrovolskaia and Vogel, 2002). In line with this, CD14-dependent isolation of human monocytes results in enhanced phagocytic activity of *Listeria monocytogenes* (Neu et al., 2013).

4.4 Priming of an adaptive immune response by hMDM-1 vs. hMDM-2

Interestingly, direct comparison of the T cell response induced by hMDM-1 and hMDM-2 revealed anti-inflammatory macrophages to be superior in priming lymphocyte proliferation. Controversially, it is known from literature that monocytes differentiated by GM-CSF, inducing a pro-inflammatory phenotype, have a higher T cell stimulatory capacity (Xu et al., 2013). Looking for a possible explanation, we examined the expression of T cell activation marker on the surface of both phenotypes.

Oversimplified, neglecting environmental signs such as cytokines, activation of naïve CD4 T cells requires two distinct signals. On the one hand the ligation of a specific T cell receptor with a peptide bound to MHC class II and on the other hand a co-stimulatory signal which is not antigen specific (Janeway and Bottomly, 1994). In addition to antigen presentation, co-stimulation by CD80/CD86 or CD40 on antigen presenting cells binding to CD28 or CD40L respectively on T cells is essential for the induction of an adaptive immune response (Fujii et al., 2004; Murphy et al., 2012). Concerning the co-stimulatory molecules CD40 and CD86, we were not able to detect different expression patterns between hMDM-1 and hMDM-2. In accordance with previous studies, CD80 was proven to be a specific marker for GM-CSF generated macrophages (Ambarus et al., 2012). Although being indispensable for T cell activation, co-stimulatory molecules themselves could not induce any responses in T cells (Janeway and Bottomly, 1994). Consequently, the antigen-specific MHC signal accompanied by any co-stimulatory molecule might be limiting to induce more or less T cell activation (Germain, 1994). Indeed, we found MHC-II to be higher expressed on M-CSF generated macrophages (hMDM-2), which is in line with phenotyping by Verreck and colleagues (Verreck et al., 2006).

In addition to surface staining of MHC and co-stimulatory molecules using flow cytometry, we analyzed hMDM-1 and hMDM-2 by proteome analysis using Mass Spectrometry to identify additional immunomodulatory molecules. Focusing on upregulated proteins in hMDM-1 compared to hMDM-2, we found the Calcineurin-binding protein cabin-1 to be higher expressed. The Calcineurin-binding protein cabin-1 was shown to serve as a negative regulator of T cell receptor signaling via the inhibition of calcineurin (Sun et al., 1998). Furthermore, being in line with the increased microbicidal capacity of pro-inflammatory macrophages, the V-type proton ATPase subunit B and the SNARE protein VAMP8 are upregulated.

Concerning hMDM-2, more immunomodulatory involved proteins were shown to be upregulated compared to hMDM-1, namely CD163, Legumain, L-amino-acid oxidase, CPVL, Sialoadhesin and Galectin-10. As expected, the scavenger receptor cysteine-rich type 1 protein M130, also named CD163, was found to be higher expressed in hMDM-2. After shedding, the soluble form (sCD163) may play an important role in anti-inflammatory responses (Verreck et al., 2006; Moestrup and Møller, 2009). Focusing on proteins supporting antigen processing, Legumain was shown to be higher expressed in hMDM-2. It is found in lysosomes where its cysteine endopeptidase activity contributes to antigen processing for MHC-II presentation (Dall and Brandstetter, 2016). In addition, the L-amino-acid oxidase was shown by similarity to have a potential role in lysosomal antigen processing and presentation (Mason et al., 2004). CPVL, a probable serine carboxypeptidase, might be involved in the digestion of

phagocytosed particles in the lysosome, trimming of peptides for antigen presentation and the participation in an inflammatory protease cascade (Mahoney et al., 2001). Being in line with the higher phagocytic capacity of hMDM-2, Sialoadhesin was upregulated acting as endocytic receptor mediating clathrin-dependent endocytosis and providing sialic-acid dependent binding to lymphocytes (van den Berg et al., 1992; Vanderheijden et al., 2003; O'Neill et al., 2013). On the other hand, Galectin-10 regulates immune responses through the recognition of cell-surface glycans and is essential for the anergy and suppressive function of CD25 positive regulatory T cells (Kubach et al., 2007).

In conclusion, by comparing the two macrophage phenotypes, hMDM-2 were shown to have a higher expression profile of proteins being involved in antigen processing and presentation such as peptidases and MHC-II. Most likely, this makes them superior to hMDM-1 in priming an adaptive immune response. This assumption will be verified in following experiments by specific modulation of the identified targets such as MHC-II blocking experiments or inhibition (e.g. by specific protein down regulation) of the identified peptidases.

4.5 Influence of GP63 on infectivity, adaptive immunity and host cell autophagy

GP63 is a main surface protein of *Leishmania* parasites and described as virulence factor mediating attraction of and adhesion to macrophages, avoiding innate immune killing mechanisms and providing an enhanced intracellular parasite survival. Previously published data indicate a clear link between GP63 expression and infectivity or binding to macrophages (Kweider et al., 1987; Liu and Chang, 1992; Ahmed et al., 1998; Brittingham et al., 1999; Thiakaki et al., 2006). Kweider et al. used monoclonal IgM antibodies against *L. braziliensis* to block surface proteins leading to reduced percentage of infected MFs of about 25% and reduced intracellular survival (Kweider et al., 1987). In the studies of Liu et al., *L. amazonensis* was passaged for more than 3 years resulting in the loss of GP63 and hence reduced infectivity whereas overexpression of GP63 in those parasites could restore the binding to a murine macrophage cell line (Liu and Chang, 1992). In contrast to these data, we could not observe an altered infection rate of GP63-deficient parasites by infection of hMDM with *Lm* SD WT, *Lm* SD KO and *Lm* SD KO+GP63. In line with our data are results obtained by Joshi et al. using for the first time GP63 knockout parasites by targeted gene deletion of GP63 in *Lm* Seidmann. GP63 knockout and wildtype parasites showed similar early (1 h) and late (96 h) infection rates in mouse peritoneal MFs and comparable differentiation in amastigotes. Furthermore, the KO parasites were able to

induce lesion formation with an initial delay but unaltered disease progression in Balb/c mice. Similar to our results, Joshi et al. concluded that the GP63 gene products 1-6 do not play a role for the survival of *Leishmania* within macrophages (Joshi et al., 1998).

Since more than 25 years it is known, that the stimulation of PBMCs with crude *Leishmania* sonicates induces a memory T cell response in previously unexposed individuals (Kemp et al., 1991; Kemp et al., 1992). In accordance with these data, we also observed a lymphocyte proliferative response using a slightly different setting by prior incubation of hMDM with *Leishmania* and subsequent co-cultivation with PBLs allowing antigen processing, presentation and recognition. By comparing *Lm* SD WT and *Lm* SD GP63 KO parasites, no significant changes in the lymphocyte proliferative response were observed. Opposing results were obtained by Matheoud et al., demonstrating immune evasion of *Leishmania* by the inhibition of cross-presentation using direct cleavage of VAMP8 in a GP63-dependent manner (Matheoud et al., 2013). Analogical immune suppressing effects were demonstrated by the direct binding of GP63 to human primary NK cells leading to the inhibition of proliferation (Lieke et al., 2008). In addition it was shown that GP63 of *Lm* and *L. donovani* was able to cleave CD4 molecules on human T cells. However, in this study an artificial *in vitro* system was used and the biological significance was critically discussed (Hey et al., 1994). In line with our results, it was shown by various studies that GP63 seems to be no immunodominant antigen as stimulation of PBMCs with purified GP63 was not able to induce T cell proliferation in neither unexposed individuals nor any CL patient or cured patient (Mendonca et al., 1991; KEMP et al., 1994; Gaafar et al., 1995). On the other hand, immunization of mice with GP63 induces a significant level of protection highlighting again the T cell dichotomy between mice and human (Handman and Mitchell, 1985; Russell and Alexander, 1988). The unaltered infection rate and the inability of the GP63 protein itself to induce T cell proliferation gives an explanation of our results that GP63 seems to be neglectable for the induction of an adaptive immune response in hMDM. To further analyze GP63 and its role as virulence factor, the occurrence of an oxidative burst and hence impaired survival of GP63 KO parasites need to be investigated.

GP63 is known to mediate a silent uptake in macrophages via CR3 and additionally ensures survival by cleavage of macrophage signaling proteins (Gomez et al., 2009; Isnard et al., 2012). Host signaling is altered as GP63 gets access to the macrophages' cytoplasm through a process mediated in part by host lipid rafts enabling cleavage of the autophagy modulator mTOR (Gomez et al., 2009; Jaramillo et al., 2011). To investigate if mTOR cleavage has an impact on the macrophages' autophagy machinery, we analyzed autophagy modulation by LC3 conversion during infection with GP63-deficient *Lm* and the respective controls. Infection of hMDM with *Leishmania*

resulted in the induction of autophagy. The induction of autophagy in host macrophages by *Lm* is in agreement with results of Cyrino et al. demonstrating *L. amazonensis* to induce autophagy in Balb/c and C57BL/6 BMDM as well as in RAW macrophages (Cyrino et al., 2012). Also the visceral leishmaniasis causing strain *L. donovani* was recently shown to induce LC3-I to LC3-II conversion in THP-1 cells and to modulate host cell autophagy in a Beclin-1-dependent manner (Singh et al., 2016). We could not detect a GP63-mediated modulation of autophagy by analyzing LC3 lipidation. These results are in line with a recently published study in mice also indicating LC3 levels by Western Blot to be unaffected upon infection with *Lm* SD WT and *Lm* SD GP63 KO although by immunofluorescence they could show that the presence of GP63 on promastigotes impaired the recruitment of LC3 to phagosomes (Matte et al., 2016).

Taken together, these studies and our data indicate that the relevance of GP63 as *Leishmania* virulence factor is strongly dependent on the experimental setup and differs between mice and human. A role of GP63 on the hosts' autophagy machinery can not be completely ruled out. Overall levels of LC3 did not change, however the intracellular distribution might be altered. Further research has to be performed focusing on LC3 recruitment to parasite containing compartments assessed by immunofluorescence, which might be improved using GP63 KO parasites.

4.6 LAP as immune evasion mechanism during *Leishmania* infection

Host-pathogen-interactions are a well-studied key dogma in infectious diseases but far away from being fully understood. According to the "catch me if you can" principle, the pathogen tries to inhibit host defense mechanisms or even subverts them for its own benefit (Lennemann and Coyne, 2015). An evolutionary highly conserved cellular response mechanism is the non-canonical autophagic process "LC3-associated phagocytosis" (LAP), mediating rapid phagosomal acidification and enhanced killing of engulfed microbes (Sanjuan et al., 2007). For several pathogens like *Mycobacterium tuberculosis*, the autophagic sequestration process was shown to control infection (Gutierrez et al., 2004). Whereas other microbes such as the bacteria *Listeria monocytogenes* and *Burkholderia pseudomallei* evade LAP compartments and mutants lacking proteins for phagosomal escape were trapped in phagosomes for enhanced killing (Gong et al., 2011; Birmingham et al., 2014). For *Lm* we could already demonstrate that the apoptotic parasites reside in single membrane, $LC3^+$ compartments in host macrophages and the presence of apoptotic promastigotes in the virulent inoculum causes the suppression of an adaptive immune response allowing disease progression (van Zandbergen et al., 2006; Crauwels et al., 2015).

Replacing apoptotic parasites by phosphatidylserine (PS) beads and zymosan led to the formation of $LC3^+$ phagosomes and LC3 lipidation which is in line with previous studies in RAW 264.7 and murine bone marrow-derived macrophages (Sanjuan et al., 2007; Martinez et al., 2011). Co-incubation of hMDM with PS-beads and viable *Leishmania* dampened the T cell response to the same degree as apoptotic *Leishmania* did. In accordance with these results, Martinez et al. demonstrated that in the absence of LAP the uptake of dead cells results in the secretion of pro-inflammatory cytokines suggesting immune dampening effects for LAP-mediated phagocytosis (Martinez et al., 2011). We demonstrated zymosan to significantly suppress *Leishmania* induced T cell proliferation and hence resulting in enhanced parasite survival as observed for co-infection of hMDM with viable and apoptotic *Leishmania*. Treatment of hMDM with zymosan triggered a strong release of the pro-inflammatory cytokine TNF-α and the anti-inflammatory cytokine IL-10. In agreement with our results, Du and colleagues reported high secretion levels of TNF-α after 3 h and high levels of IL-10 6 h post stimulation of macrophages with zymosan (Du et al., 2006). The production of TNF-α leads to the recruitment of adaptive immune cells and subsequent secretion of IL-10 suppresses macrophage activation and dampens the immune response preventing autoimmunity (Arango Duque and Descoteaux, 2014). Additionally, the immune dampening effects of zymosan stimulation have been shown in autoimmune disease models for diabetes and multiple sclerosis. Injection of zymosan was able to delay diabetes onset by the expansion of $PD\text{-}L1^+$, $TGF\text{-}\beta^+$ macrophages and $Foxp3^+$ regulatory T cells in NOD mice (Burton et al., 2010). Furthermore, zymosan regulates the cytokine secretion in dendritic cells and macrophages resulting in immunological tolerance as the co-injection of zymosan and OVA plus LPS suppresses the OVA-specific T cell response by APCs secreting IL-10 and TGF-β but lacking IL-6 (Dillon et al., 2006). Another mechanism indicating the immune dampening effects of zymosan was reported by Yem demonstrating zymosan treatment of macrophages to result in surface Ia antigen loss from many macrophages leading to reduced T cell proliferation (Yem and Parmely, 1981).

Taken together, our data indicate, that the immune dampening effects of apoptotic *Leishmania* in the virulent inoculum or their replacement by PS beads and zymosan are probably due to anti-inflammatory cytokine secretion. Although zymosan induced strong TNF-α secretion, it is likely that anti-inflammatory cytokines halt adaptive immune activation as only a moderate T cell response was observed. To verify this mechanism, further experiments such as analyzing TGF-β secretion, need to be performed. The reduced T cell proliferation can be considered as immune evasion mechanism used by *Leishmania* as it enables improved intracellular parasite survival and differentiation in amastigotes.

Focusing on intracellular mechanisms leading to LAP induction, Huang and colleagues reported that activation and subsequent production of ROS by NOX2, a NADPH oxidase expressed in macrophages, is TLR- or FcγR-dependent and triggers the recruitment of LC3 to phagosomes (Huang et al., 2009; Scherz-Shouval and Elazar, 2011). Furthermore, the requirement of NOX2 for the induction of LAP but not for conventional autophagy was demonstrated by Martinez et al. in murine bone marrow-derived macrophages (Martinez et al., 2015). In agreement with the mentioned studies, our data give a hint for ROS dependent LAP induction in hMDM. *Leishmania* promastigotes that underwent an ROS-dependent death by treatment with Staurosporine (Jochen Steinacker, data not shown; (Shimizu et al., 2004)) induced enhanced LC3 lipidation compared to untreated parasites. Additionally, we inhibited the macrophages' NADPH oxidase which produces ROS at the phagosomal membrane. We could only show a moderate reduction of LAP induction being probably due to poor knockdown efficiency and residual activity of NOX2. Thus, we treated hMDM with Diphenyleneiodonium (DPI), a chemical NOX2 inhibitor. Treatment with DPI significantly inhibited LC3 lipidation upon stimulation of macrophages with zymosan and strongly inhibited LC3 lipidation upon infection with *Leishmania*. These data are in line with previously published results demonstrating the requirement of ROS for LC3 conversion during infection of BMDM with *Leishmania* (Matte et al., 2016). So far, our data suggest that *Leishmania* specific T cell proliferation is independent on the presence or production of ROS although further experiments blocking ROS production in *Leishmania* are necessary to draw a clear statement. In following analyzes *Leishmania* parasites will be treated with ROS scavengers such as N-acetylcysteine, Tempol, Trolox, ebselen or α-tocopherol and upon infection of hMDM, LC3 conversion and T cell proliferation will be assessed.

Looking for other mechanisms causing a reduced T cell proliferation we analyzed lysosomal acidification which provides antigen degradation for presentation on MHC-II molecules. We revealed apoptotic *Leishmania* and zymosan to enhance acidification in hMDM whereas infection with viable *Leishmania* did not. In accordance with our data, other reports show that viable *Leishmania* promastigotes are able to inhibit phagosome maturation such as the fusion with endosomes and lysosomes (Desjardins and Descoteaux, 1997). More recently, it was demonstrated that LPG of *L. donovani* impairs the recruitment of Synaptotagmin V to phagosomes thereby leading to the exclusion of the vesicular proton ATPase preventing phagosome acidification (Vinet et al., 2009). Furthermore our data are supported by studies presenting, LAP-inducing stimuli such as apoptotic cells or zymosan particles to accelerate phagosomal fusion with lysosomes leading to the degradation of the engulfed particles (Sanjuan et al., 2007; Florey et al., 2011; Martin et al., 2014). The influence of particle degradation by

LAP on the onset of an immune response was demonstrated by Ma et al. in murine macrophages and dendritic cells. In this study, $LC3^+$ phagosomes containing β-glucan particles co-localize with MHC-II molecules leading to increasing T cell activation (Ma et al., 2012). This finding is line with our data, that less immunogenic antigens of apoptotic *Leishmania* and zymosan get faster degraded and presented to T cells thereby suppressing the adaptive immune response. In contrast to the hypothesis of better T cell priming by LAP, there are several studies indicating that exacerbated antigen degradation is detrimental to antigen presentation to T cells and impairs cross presentation (Accapezzato et al., 2005; Delamarre et al., 2005; Savina et al., 2006). These studies suggest that limited lysosomal proteolysis favors antigen presentation by keeping the balance between “some” degradation to generate antigenic peptides and “not too much” degradation which would probably destroy potential T cell epitopes (Delamarre et al., 2005; Savina et al., 2006). By a follow up study, Delamarre and colleagues could show that the susceptibility of protein antigens to lysosomal proteolysis is important for their immunogenicity *in vivo*. Less digestible antigen forms were higher immunogenic inducing efficient T cell priming and antibody responses (Delamarre et al., 2006). As we did not further investigate the effects of differential lysosomal acidification upon infection with viable or apoptotic parasites or zymosan, also the latter studies could be in line with our data. The exacerbated antigen degradation upon infection with apoptotic *Leishmania* or zymosan might lead to less efficient antigen presentation and T cell priming. Whereas upon infection with viable parasites, impaired phagosomal acidification might provide longer antigen maintenance for continuous presentation on MHC-II molecules resulting in a higher T cell proliferation (Romao et al., 2013).

Using a more general approach to determine host factors involved in the regulation of an immune response which are modulated by pathogen infection, proteome analysis of hMDM compared to hMDM infected with *Leishmania* was done. *Leishmania* infection resulted in the upregulation of indoleamine 2,3-dioxygenase 1 (IDO1) which is an L-tryptophan-degrading enzyme catalyzing the first and rate-limiting step in the kynureine pathway (Murakami et al., 2013). It is induced by IFN-γ-dependent inflammatory responses and serves as mechanism for antimicrobial resistance restricting growth of intracellular pathogens such as Toxoplasma gondii (Pfefferkorn, 1984; Murray et al., 1989). On the other hand, IDO1 was demonstrated to attenuate immune responses by locally depleting tryptophan and hence preventing T cell proliferation (Munn et al., 1999). Also in *Leishmania* infection, a role for IDO1 was shown. *Leishmania*-induced IDO expression suppressed T cell stimulation by dendritic cells whereas IDO inhibition enhanced local expression of pro-inflammatory cytokines and improved host immunity (Makala et al., 2011; Donovan et al., 2012). Furthermore, *Leishmania* infection induced

upregulation of MHC-I and downregulation of MHC-II. Our finding is in line with other studies demonstrating that infection of macrophages with *L. donovani* leads to transcriptional inhibition of MHC-II molecule genes (Kwan et al., 1992). Additionally, *L. amazonensis* and *L. mexicana* amastigotes have been demonstrated to internalize and proteolytically degrade MHC-II molecules which are associated with the parasitophorous vacuole (Souza Leao et al., 1995; Antoine et al., 1999).

Taken together, the impact of *Leishmania* infection on immunomodulatory host cell proteins is suggested to provide further insight in immune evasion mechanisms exploited by the parasites. In following experiments the proteomic regulation will be verified. Furthermore, by inhibition or down regulation of IDO and overexpression of MHC-II their potential role as immune evasion target will be proven. We suggest that knockdown of IDO1 or the addition of L-tryptophan to the culture medium of macrophages will enhance pro-inflammatory cytokine secretion leading to increased T cell proliferation and consequently impaired *Leishmania* survival.

4.7 Concluding remarks

Taken together, our data provide a deeper insight in the autophagic process in human primary macrophages being different from previously published data in other model systems. We found autophagy modulation to be highly dependent on the applied stimuli and detected differences between cell phenotypes. In contrast to other studies, analyzing macrophage cell lines or mouse models, autophagy induction in human primary macrophages was not dependent on ULK-1 and Beclin-1, indicating ULK-1 and Beclin-1 independent pathways for autophagy induction or protein compensation by ULK-2 in hMDM. These findings should be considered before extrapolating cell line data for drug development in human applications.

These data highlight the importance of autophagy as immunomodulatory mechanism requiring profounder investigation in human primary cells. Given the therapeutic implications of autophagy in cancer, neurodegenerative as well as infectious diseases, a better understanding will contribute in the development of safe and efficient therapeutic interventions in humans.

Furthermore, we assume that the autophagy related process LAP, induced by apoptotic *Leishmania*, might be an immune evasion mechanism by dampening the adaptive immune response and promoting parasite survival. Additionally, by proteome analysis of hMDM infected with *Leishmania* we identified the upregulation of IDO1 and the downregulation of MHC-II as additional immune evasion strategies which will provide further insight in the interaction of *Leishmania* and their host cell promoting disease progression.

5 References

Accapezzato, D., Visco, V., Francavilla, V., Molette, C., Donato, T., Paroli, M., Mondelli, M.U., Doria, M., Torrisi, M.R., and Barnaba, V. (2005). Chloroquine enhances human CD8+ T cell responses against soluble antigens in vivo. The Journal of experimental medicine *202*, 817-828.

Adams, D.O., and Hamilton, T.A. (1984). The cell biology of macrophage activation. Annual review of immunology *2*, 283-318.

Aga, E., Katschinski, D.M., van Zandbergen, G., Laufs, H., Hansen, B., Muller, K., Solbach, W., and Laskay, T. (2002). Inhibition of the Spontaneous Apoptosis of Neutrophil Granulocytes by the Intracellular Parasite Leishmania major. The Journal of Immunology *169*, 898-905.

Ahmed, Wahbi, Nordlind, Kharazmi, Sundqvist, Mutt, and Liden (1998). In Vitro Leishmania major Promastigote-Induced Macrophage Migration is Modulated by Sensory and Autonomic Neuropeptides. Scand J Immunol *48*, 79-85.

Akhoundi, M., Kuhls, K., Cannet, A., Votypka, J., Marty, P., Delaunay, P., and Sereno, D. (2016). A Historical Overview of the Classification, Evolution, and Dispersion of Leishmania Parasites and Sandflies. PLoS neglected tropical diseases *10*, e0004349.

Alers, S., Löffler, A.S., Paasch, F., Dieterle, A.M., Keppeler, H., Lauber, K., Campbell, D.G., Fehrenbacher, B., Schaller, M., and Wesselborg, S., et al. (2014). Atg13 and FIP200 act independently of Ulk1 and Ulk2 in autophagy induction. Autophagy *7*, 1424-1433.

Alexander, J., and Brombacher, F. (2012). T helper1/t helper2 cells and resistance/susceptibility to leishmania infection. Is this paradigm still relevant? Frontiers in immunology *3*, 80.

Allenbach, C., Zufferey, C., Perez, C., Launois, P., Mueller, C., and Tacchini-Cottier, F. (2006). Macrophages Induce Neutrophil Apoptosis through Membrane TNF, a Process Amplified by Leishmania major. The Journal of Immunology *176*, 6656-6664.

Ambarus, C.A., Krausz, S., van Eijk, M., Hamann, J., Radstake, T.R.D.J., Reedquist, K.A., Tak, P.P., and Baeten, D.L.P. (2012). Systematic validation of specific phenotypic markers for in vitro polarized human macrophages. Journal of immunological methods *375*, 196-206.

Andersson, A.-M., Andersson, B., Lorell, C., Raffetseder, J., Larsson, M., and Blomgran, R. (2016). Autophagy induction targeting mTORC1 enhances Mycobacterium tuberculosis replication in HIV co-infected human macrophages. Scientific reports *6*, 28171.

Antoine, J.C., Lang, T., Prina, E., Courret, N., and Hellio, R. (1999). H-2M molecules, like MHC class II molecules, are targeted to parasitophorous vacuoles of Leishmania-infected macrophages and internalized by amastigotes of L. amazonensis and L. mexicana. Journal of cell science *112 (Pt 15)*, 2559-2570.

Antoine, J.C., Prina, E., Jouanne, C., and Bongrand, P. (1990). Parasitophorous vacuoles of Leishmania amazonensis-infected macrophages maintain an acidic pH. Infection and immunity *58*, 779-787.

Arango Duque, G., and Descoteaux, A. (2014). Macrophage cytokines. Involvement in immunity and infectious diseases. Frontiers in immunology *5*, 491.

Arcaro, A., and Wymann, M.P. (1993). Wortmannin is a potent phosphatidylinositol 3-kinase inhibitor. The role of phosphatidylinositol 3,4,5-trisphosphate in neutrophil responses. The Biochemical journal *296 (Pt 2)*, 297-301.

Awasthi, A., Mathur, R., Khan, A., Joshi, B.N., Jain, N., Sawant, S., Boppana, R., Mitra, D., and Saha, B. (2003). CD40 signaling is impaired in L. major-infected macrophages and is rescued by a p38MAPK activator establishing a host-protective memory T cell response. The Journal of experimental medicine *197*, 1037-1043.

Axe, E.L., Walker, S.A., Manifava, M., Chandra, P., Roderick, H.L., Habermann, A., Griffiths, G., and Ktistakis, N.T. (2008). Autophagosome formation from membrane compartments enriched in phosphatidylinositol 3-phosphate and dynamically connected to the endoplasmic reticulum. J Cell Biol *182*, 685-701.

Baba, M., Osumi, M., and Ohsumi, Y. (1995). Analysis of the Membrane Structures Involved in Autophagy in Yeast by Freeze-Replica Method. Cell Struct. Funct. *20*, 465-471.

Barbey, C., Pradervand, E., Barbier, N., and Spertini, F. (2007). Ex vivo monitoring of antigen-specific CD4+ T cells after recall immunization with tetanus toxoid. Clinical and vaccine immunology : CVI *14*, 1108-1116.

Bhattacharyya, S., Ghosh, S., Jhonson, P.L., Bhattacharya, S.K., and Majumdar, S. (2001). Immunomodulatory role of interleukin-10 in visceral leishmaniasis. Defective activation of protein kinase C-mediated signal transduction events. Infection and immunity *69*, 1499-1507.

Birmingham, C.L., Canadien, V., Gouin, E., Troy, E.B., Yoshimori, T., Cossart, P., Higgins, D.E., and Brumell, J.H. (2014). Listeria monocytogenes Evades Killing by Autophagy During Colonization of Host Cells. Autophagy *3*, 442-451.

Bjorkoy, G., Lamark, T., Brech, A., Outzen, H., Perander, M., Overvatn, A., Stenmark, H., and Johansen, T. (2005). p62/SQSTM1 forms protein aggregates degraded by autophagy and has a protective effect on huntingtin-induced cell death. The Journal of cell biology *171*, 603-614.

Blackwell, J.M. (1985). Role of macrophage complement and lectin-like receptors in binding Leishmania parasites to host macrophages. Immunology letters *11*, 227-232.

Blander, J.M., and Medzhitov, R. (2006). Toll-dependent selection of microbial antigens for presentation by dendritic cells. Nature *440*, 808-812.

Blommaart, E.F.C., Krause, U., Schellens, J.P.M., Vreeling-Sindelarova, H., and Meijer, A.J. (1997). The Phosphatidylinositol 3-Kinase Inhibitors Wortmannin and LY294002 Inhibit Autophagy in Isolated Rat Hepatocytes. Eur J Biochem *243*, 240-246.

Blum, J.S., Wearsch, P.A., and Cresswell, P. (2013). Pathways of antigen processing. Annual review of immunology *31*, 443-473.

Bogdan, C., Gessner, A., Werner, S., and Martin, R. (1996). Invasion, control and persistence of Leishmania parasites. Current opinion in immunology *8*, 517-525.

Bogdan, C., Röllinghoff, M., and Solbach, W. (1990). Evasion strategies of Leishmania parasites. Parasitology Today *6*, 183-187.

Bouvier, J., Etges, R.J., and Bordier, C. (1985). Identification and purification of membrane and soluble forms of the major surface protein of Leishmania promastigotes. The Journal of biological chemistry *260*, 15504-15509.

Brittingham, A., Chen, G., McGwire, B.S., Chang, K.P., and Mosser, D.M. (1999). Interaction of Leishmania gp63 with cellular receptors for fibronectin. Infection and immunity *67*, 4477-4484.

Brittingham, A., Morrison, C.J., McMaster, W.R., McGwire, B.S., Chang, K.P., and Mosser, D.M. (1995). Role of the Leishmania surface protease gp63 in complement fixation, cell adhesion, and resistance to complement-mediated lysis. Journal of immunology (Baltimore, Md. : 1950) *155*, 3102-3111.

Burgess, A.W., and Metcalf, D. (1980). The nature and action of granulocyte-macrophage colony stimulating factors. Blood *56*, 947-958.

Burton, O.T., Zaccone, P., Phillips, J.M., La Pena, H. de, Fehervari, Z., Azuma, M., Gibbs, S., Stockinger, B., and Cooke, A. (2010). Roles for TGF-beta and programmed cell death 1 ligand 1 in regulatory T cell expansion and diabetes suppression by zymosan in nonobese diabetic mice. Journal of immunology (Baltimore, Md. : 1950) *185*, 2754-2762.

Button, L.L., and McMaster, W.R. (1988). Molecular cloning of the major surface antigen of leishmania. The Journal of experimental medicine *167*, 724-729.

Carvalho, E.M., Bacellar, O., Brownell, C., Regis, T., Coffman, R.L., and Reed, S.G. (1994). Restoration of IFN-gamma production and lymphocyte proliferation in visceral leishmaniasis. Journal of immunology (Baltimore, Md. : 1950) *152*, 5949-5956.

Carvalho, E.M., Badaro, R., Reed, S.G., Jones, T.C., and Johnson, W.D., JR (1985). Absence of gamma interferon and interleukin 2 production during active visceral leishmaniasis. The Journal of clinical investigation *76*, 2066-2069.

Cellerai, C., Harari, A., Vallelian, F., Boyman, O., and Pantaleo, G. (2007). Functional and phenotypic characterization of tetanus toxoid-specific human CD4+ T cells following re-immunization. European journal of immunology *37*, 1129-1138.

Chan, E.Y.W., Kir, S., and Tooze, S.A. (2007). siRNA screening of the kinome identifies ULK1 as a multidomain modulator of autophagy. The Journal of biological chemistry *282*, 25464-25474.

Chang, Y.-Y., and Neufeld, T.P. (2009). An Atg1/Atg13 complex with multiple roles in TOR-mediated autophagy regulation. Molecular biology of the cell *20*, 2004-2014.

Charmoy, M., Auderset, F., Allenbach, C., and Tacchini-Cottier, F. (2010). The prominent role of neutrophils during the initial phase of infection by Leishmania parasites. Journal of biomedicine & biotechnology *2010*, 719361.

Chaudhuri, G., Chaudhuri, M., Pan, A., and Chang, K.P. (1989). Surface acid proteinase (gp63) of Leishmania mexicana. A metalloenzyme capable of protecting liposome-encapsulated proteins from phagolysosomal degradation by macrophages. The Journal of biological chemistry *264*, 7483-7489.

Cheong, H., Lindsten, T., Wu, J., Lu, C., and Thompson, C.B. (2011). Ammonia-induced autophagy is independent of ULK1/ULK2 kinases. Proceedings of the National Academy of Sciences of the United States of America *108*, 11121-11126.

Choi, A.M.K., Ryter, S.W., and Levine, B. (2013). Autophagy in human health and disease. The New England journal of medicine *368*, 651-662.

Choi, K.S. (2012). Autophagy and cancer. Experimental & molecular medicine *44*, 109-120.

Chresta, C.M., Davies, B.R., Hickson, I., Harding, T., Cosulich, S., Critchlow, S.E., Vincent, J.P., Ellston, R., Jones, D., and Sini, P., et al. (2010). AZD8055 is a potent, selective, and orally bioavailable ATP-competitive mammalian target of rapamycin kinase inhibitor with in vitro and in vivo antitumor activity. Cancer research *70*, 288-298.

Cicchini, M., Karantza, V., and Xia, B. (2015). Molecular pathways. Autophagy in cancer--a matter of timing and context. Clinical cancer research : an official journal of the American Association for Cancer Research *21*, 498-504.

Cillari, E., Vitale, G., Arcoleo, F., D 'Agostino, P., Mocciaro, C., Gambino, G., Malta, R., Stassi, G., Giordano, C., and Milano, S., et al. (1995). In vivo and in vitro cytokine profiles and mononuclear cell subsets in sicilian patients with active visceral leishmaniasis. Cytokine *7*, 740-745.

Clark, S.L. (1957). Cellular differentiation in the kidneys of newborn mice studies with the electron microscope. The Journal of biophysical and biochemical cytology *3*, 349-362.

Courret, N., Frehel, C., Gouhier, N., Pouchelet, M., Prina, E., Roux, P., and Antoine, J.-C. (2002). Biogenesis of Leishmania-harbouring parasitophorous vacuoles following phagocytosis of the metacyclic promastigote or amastigote stages of the parasites. Journal of cell science *115*, 2303-2316.

Crauwels, P., Bohn, R., Thomas, M., Gottwalt, S., Jackel, F., Kramer, S., Bank, E., Tenzer, S., Walther, P., and Bastian, M., et al. (2015). Apoptotic-like Leishmania exploit the host's autophagy machinery to reduce T-cell-mediated parasite elimination. Autophagy *11*, 285-297.

Cyrino, L.T., Araujo, A.P., Joazeiro, P.P., Vicente, C.P., and Giorgio, S. (2012). In vivo and in vitro Leishmania amazonensis infection induces autophagy in macrophages. Tissue & cell *44*, 401-408.

da Silva, R., and Sacks, D.L. (1987). Metacyclogenesis is a major determinant of Leishmania promastigote virulence and attenuation. Infection and immunity *55*, 2802-2806.

Da Silva, R.P., Hall, B.F., Joiner, K.A., and Sacks, D.L. (1989). CR1, the C3b receptor, mediates binding of infective Leishmania major metacyclic promastigotes to human macrophages. Journal of immunology (Baltimore, Md. : 1950) *143*, 617-622.

Dall, E., and Brandstetter, H. (2016). Structure and function of legumain in health and disease. Biochimie *122*, 126-150.

Degtyarev, M., Maziere, A. de, Orr, C., Lin, J., Lee, B.B., Tien, J.Y., Prior, W.W., van Dijk, S., Wu, H., and Gray, D.C., et al. (2008). Akt inhibition promotes autophagy and sensitizes PTEN-null tumors to lysosomotropic agents. The Journal of cell biology *183*, 101-116.

Delamarre, L., Couture, R., Mellman, I., and Trombetta, E.S. (2006). Enhancing immunogenicity by limiting susceptibility to lysosomal proteolysis. The Journal of experimental medicine *203*, 2049-2055.

Delamarre, L., Pack, M., Chang, H., Mellman, I., and Trombetta, E.S. (2005). Differential lysosomal proteolysis in antigen-presenting cells determines antigen fate. Science (New York, N.Y.) *307*, 1630-1634.

Dengjel, J., Schoor, O., Fischer, R., Reich, M., Kraus, M., Muller, M., Kreymborg, K., Altenberend, F., Brandenburg, J., and Kalbacher, H., et al. (2005). Autophagy promotes MHC class II presentation of peptides from intracellular source proteins. Proceedings of the National Academy of Sciences of the United States of America *102*, 7922-7927.

Desjardins, M., and Descoteaux, A. (1997). Inhibition of phagolysosomal biogenesis by the Leishmania lipophosphoglycan. The Journal of experimental medicine *185*, 2061-2068.

Dillon, S., Agrawal, S., Banerjee, K., Letterio, J., Denning, T.L., Oswald-Richter, K., Kasprowicz, D.J., Kellar, K., Pare, J., and van Dyke, T., et al. (2006). Yeast zymosan, a stimulus for TLR2 and dectin-1, induces regulatory antigen-presenting cells and immunological tolerance. The Journal of clinical investigation *116*, 916-928.

Dobrovolskaia, M.A., and Vogel, S.N. (2002). Toll receptors, CD14, and macrophage activation and deactivation by LPS. Microbes and Infection *4*, 903-914.

Donovan, M.J., Tripathi, V., Favila, M.A., Geraci, N.S., Lange, M.C., Ballhorn, W., and McDowell, M.A. (2012). Indoleamine 2,3-dioxygenase (IDO) induced by Leishmania infection of human dendritic cells. Parasite immunology *34*, 464-472.

Du, Z., Kelly, E., Mecklenbrauker, I., Agle, L., Herrero, C., Paik, P., and Ivashkiv, L.B. (2006). Selective Regulation of IL-10 Signaling and Function by Zymosan. The Journal of Immunology *176*, 4785-4792.

Dugas, B., Mossalayi, M.D., Damais, C., and Kolb, J.P. (1995). Nitric oxide production by human monocytes. Evidence for a role of CD23. Immunology today *16*, 574-580.

DUVE, C. de, PRESSMAN, B.C., GIANETTO, R., WATTIAUX, R., and APPELMANS, F. (1955). Tissue fractionation studies. 6. Intracellular distribution patterns of enzymes in rat-liver tissue. The Biochemical journal *60*, 604-617.

DUVE, C. de, and WATTIAUX, R. (1966). Functions of lysosomes. Annual review of physiology *28*, 435-492.

Ehlers, M.R. (2000). CR3. A general purpose adhesion-recognition receptor essential for innate immunity. In The Zinc Industry (Elsevier), pp. 289–294.

Etges, R., Bouvier, J., and Bordier, C. (1986). The major surface protein of Leishmania promastigotes is a protease. The Journal of biological chemistry *261*, 9098-9101.

Fan, Q.-W., Knight, Z.A., Goldenberg, D.D., Yu, W., Mostov, K.E., Stokoe, D., Shokat, K.M., and Weiss, W.A. (2006). A dual PI3 kinase/mTOR inhibitor reveals emergent efficacy in glioma. Cancer cell *9*, 341-349.

Florey, O., Kim, S.E., Sandoval, C.P., Haynes, C.M., and Overholtzer, M. (2011). Autophagy machinery mediates macroendocytic processing and entotic cell death by targeting single membranes. Nature cell biology *13*, 1335-1343.

Frommel, T.O., Button, L.L., Fujikura, Y., and McMaster, W. (1990). The major surface glycoprotein (GP63) is present in both life stages of Leishmania. Molecular and Biochemical Parasitology *38*, 25-32.

Fujii, S.-I., Liu, K., Smith, C., Bonito, A.J., and Steinman, R.M. (2004). The linkage of innate to adaptive immunity via maturing dendritic cells in vivo requires CD40 ligation in addition to antigen presentation and CD80/86 costimulation. The Journal of experimental medicine *199*, 1607-1618.

Fujita, N., Itoh, T., Omori, H., Fukuda, M., Noda, T., and Yoshimori, T. (2008). The Atg16L complex specifies the site of LC3 lipidation for membrane biogenesis in autophagy. Molecular biology of the cell *19*, 2092-2100.

Gaafar, A., KHARAZMI, A., Ismail, A., KEMP, M., Hey, A., Christensen, C.B., Dafalla, M., el Kadaro, A.Y., el Hassan, A.M., and THEANDER, T.G. (1995). Dichotomy of the T cell response to Leishmania antigens in patients suffering from cutaneous leishmaniasis; absence or scarcity of Th1 activity is associated with severe infections. Clinical and experimental immunology *100*, 239-245.

Ganguly, S., Mukhopadhyay, D., Das, N.K., Chaduvula, M., Sadhu, S., Chatterjee, U., Rahman, M., Goswami, R.P., Guha, S.K., and Modak, D., et al. (2010). Enhanced lesional Foxp3 expression and peripheral anergic lymphocytes indicate a role for regulatory T cells in Indian post-kala-azar dermal leishmaniasis. The Journal of investigative dermatology *130*, 1013-1022.

Ganley, I.G., Du Lam, H., Wang, J., Ding, X., Chen, S., and Jiang, X. (2009). ULK1.ATG13.FIP200 complex mediates mTOR signaling and is essential for autophagy. The Journal of biological chemistry *284*, 12297-12305.

Gao, P., Bauvy, C., Souquere, S., Tonelli, G., Liu, L., Zhu, Y., Qiao, Z., Bakula, D., Proikas-Cezanne, T., and Pierron, G., et al. (2010). The Bcl-2 homology domain 3 mimetic gossypol induces both Beclin 1-dependent and Beclin 1-independent cytoprotective autophagy in cancer cells. The Journal of biological chemistry *285*, 25570-25581.

Geng, J., and Klionsky, D.J. (2008). The Atg8 and Atg12 ubiquitin-like conjugation systems in macroautophagy. 'Protein modifications. Beyond the usual suspects' review series. EMBO reports *9*, 859-864.

Gerber, J.S., and Mosser, D.M. (2001). Reversing Lipopolysaccharide Toxicity by Ligating the Macrophage Fc Receptors. The Journal of Immunology *166*, 6861-6868.

Germain, R.N. (1994). MHC-dependent antigen processing and peptide presentation. Providing ligands for T lymphocyte activation. Cell *76*, 287-299.

Ghalib, H.W., Piuvezam, M.R., Skeiky, Y.A., Siddig, M., Hashim, F.A., el-Hassan, A.M., Russo, D.M., and Reed, S.G. (1993). Interleukin 10 production correlates with pathology in human Leishmania donovani infections. The Journal of clinical investigation *92*, 324-329.

Ghalib, H.W., Whittle, J.A., Kubin, M., Hashim, F.A., el-Hassan, A.M., Grabstein, K.H., Trinchieri, G., and Reed, S.G. (1995). IL-12 enhances Th1-type responses in human Leishmania donovani infections. Journal of immunology (Baltimore, Md. : 1950) *154*, 4623-4629.

Giannini, M.S. (1974). Effects of promastigote growth phase, frequency of subculture, and host age on promastigote-initiated infections with Leishmania donovani in the golden hamster. Involvement in immunity and infectious diseases. The Journal of protozoology *21*, 521-527.

Gomez, M.A., Contreras, I., Halle, M., Tremblay, M.L., McMaster, R.W., and Olivier, M. (2009). Leishmania GP63 alters host signaling through cleavage-activated protein tyrosine phosphatases. Science signaling *2*, ra58.

Gomez-Sanchez, R., Pizarro-Estrella, E., Yakhine-Diop, S.M.S., Rodriguez-Arribas, M., Bravo-San Pedro, J.M., Fuentes, J.M., and Gonzalez-Polo, R.A. (2015). Routine Western blot to check autophagic flux. Cautions and recommendations. Analytical biochemistry *477*, 13-20.

Gong, L., Cullinane, M., Treerat, P., Ramm, G., Prescott, M., Adler, B., Boyce, J.D., and Devenish, R.J. (2011). The Burkholderia pseudomallei type III secretion system and BopA are required for evasion of LC3-associated phagocytosis. PloS one *6*, e17852.

Gordon, S., and Martinez, F.O. (2010). Alternative activation of macrophages. Mechanism and functions. Immunity *32*, 593-604.

Gordon, S., and Taylor, P.R. (2005). Monocyte and macrophage heterogeneity. Nature reviews. Immunology *5*, 953-964.

Goto, H., and Lauletta Lindoso, J.A. (2012). Cutaneous and mucocutaneous leishmaniasis. Infectious disease clinics of North America *26*, 293-307.

Greenwood, J., Steinman, L., and Zamvil, S.S. (2006). Statin therapy and autoimmune disease. From protein prenylation to immunomodulation. Nature reviews. Immunology *6*, 358-370.

Grishchuk, Y., Ginet, V., Truttmann, A.C., Clarke, P.G.H., and Puyal, J. (2011). Beclin 1-independent autophagy contributes to apoptosis in cortical neurons. Autophagy *7*, 1115-1131.

Gupta, G., Oghumu, S., and Satoskar, A.R. (2013). Mechanisms of immune evasion in leishmaniasis. Advances in applied microbiology *82*, 155-184.

Gutierrez, M.G., Master, S.S., Singh, S.B., Taylor, G.A., Colombo, M.I., and Deretic, V. (2004). Autophagy is a defense mechanism inhibiting BCG and Mycobacterium tuberculosis survival in infected macrophages. Cell *119*, 753-766.

Hailey, D.W., Rambold, A.S., Satpute-Krishnan, P., Mitra, K., Sougrat, R., Kim, P.K., and Lippincott-Schwartz, J. (2010). Mitochondria supply membranes for autophagosome biogenesis during starvation. Cell *141*, 656-667.

Hailu, A., van Baarle, D., Knol, G.J., Berhe, N., Miedema, F., and Kager, P.A. (2005). T cell subset and cytokine profiles in human visceral leishmaniasis during active and asymptomatic or sub-clinical infection with Leishmania donovani. Clinical immunology (Orlando, Fla.) *117*, 182-191.

Haldar, J.P., Ghose, S., Saha, K.C., and Ghose, A.C. (1983). Cell-mediated immune response in Indian kala-azar and post-kala-azar dermal leishmaniasis. Infection and immunity *42*, 702-707.

Handman, E., and Goding, J.W. (1985). The Leishmania receptor for macrophages is a lipid-containing glycoconjugate. The EMBO journal *4*, 329-336.

Handman, E., and Mitchell, G.F. (1985). Immunization with Leishmania receptor for macrophages protects mice against cutaneous leishmaniasis. Proceedings of the National Academy of Sciences *82*, 5910-5914.

Harris, J., Haro, S.A. de, Master, S.S., Keane, J., Roberts, E.A., Delgado, M., and Deretic, V. (2007). T helper 2 cytokines inhibit autophagic control of intracellular Mycobacterium tuberculosis. Immunity *27*, 505-517.

Heitman, J., Movva, N.R., and Hall, M.N. (1991). Targets for cell cycle arrest by the immunosuppressant rapamycin in yeast. Science (New York, N.Y.) *253*, 905-909.

Hemelaar, J., Lelyveld, V.S., Kessler, B.M., and Ploegh, H.L. (2003). A single protease, Apg4B, is specific for the autophagy-related ubiquitin-like proteins GATE-16, MAP1-LC3, GABARAP, and Apg8L. The Journal of biological chemistry *278*, 51841-51850.

Henault, J., Martinez, J., Riggs, J.M., Tian, J., Mehta, P., Clarke, L., Sasai, M., Latz, E., Brinkmann, M.M., and Iwasaki, A., et al. (2012). Noncanonical autophagy is required for type I interferon secretion in response to DNA-immune complexes. Immunity *37*, 986-997.

HEY, A.S., THEANDER, T.G., HVIID, L., Hazrati, S.M., KEMP, M., and KHARAZMI, A. (1994). The major surface glycoprotein (gp63) from Leishmania major and Leishmania donovani cleaves CD4 molecules on human T cells. Journal of immunology (Baltimore, Md. : 1950) *152*, 4542-4548.

Homer, C.R., Richmond, A.L., Rebert, N.A., Achkar, J.-P., and McDonald, C. (2010). ATG16L1 and NOD2 interact in an autophagy-dependent antibacterial pathway implicated in Crohn's disease pathogenesis. Gastroenterology *139*, 1630-41, 1641.e1-2.

Hooper, K.M., Barlow, P.G., Stevens, C., and Henderson, P. (2017). Inflammatory Bowel Disease Drugs. A Focus on Autophagy. Journal of Crohn's & colitis *11*, 118-127.

Huang, J., Canadien, V., Lam, G.Y., Steinberg, B.E., Dinauer, M.C., Magalhaes, M.A.O., Glogauer, M., Grinstein, S., and Brumell, J.H. (2009). Activation of antibacterial autophagy by NADPH oxidases. Proceedings of the National Academy of Sciences of the United States of America *106*, 6226-6231.

Huang, S., Yang, Z.J., Yu, C., and Sinicrope, F.A. (2011). Inhibition of mTOR kinase by AZD8055 can antagonize chemotherapy-induced cell death through autophagy induction and down-regulation of p62/sequestosome 1. The Journal of biological chemistry *286*, 40002-40012.

Huynh, M.-L.N., Fadok, V.A., and Henson, P.M. (2002). Phosphatidylserine-dependent ingestion of apoptotic cells promotes TGF-beta1 secretion and the resolution of inflammation. The Journal of clinical investigation *109*, 41-50.

Isnard, A., Shio, M.T., and Olivier, M. (2012). Impact of Leishmania metalloprotease GP63 on macrophage signaling. Frontiers in cellular and infection microbiology *2*, 72.

Itakura, E., and Mizushima, N. (2014). Characterization of autophagosome formation site by a hierarchical analysis of mammalian Atg proteins. Autophagy *6*, 764-776.

Jagannath, C., Lindsey, D.R., Dhandayuthapani, S., Xu, Y., Hunter, R.L., JR, and Eissa, N.T. (2009). Autophagy enhances the efficacy of BCG vaccine by increasing peptide presentation in mouse dendritic cells. Nature medicine *15*, 267-276.

Janeway, C.A., and Bottomly, K. (1994). Signals and signs for lymphocyte responses. Cell *76*, 275-285.

Jaramillo, M., Gomez, M.A., Larsson, O., Shio, M.T., Topisirovic, I., Contreras, I., Luxenburg, R., Rosenfeld, A., Colina, R., and McMaster, R.W., et al. (2011). Leishmania repression of host translation through mTOR cleavage is required for parasite survival and infection. Cell host & microbe *9*, 331-341.

Jiang, P., and Mizushima, N. (2014). Autophagy and human diseases. Cell research *24*, 69-79.

Johnson, E.E., Overmeyer, J.H., Gunning, W.T., and Maltese, W.A. (2006). Gene silencing reveals a specific function of hVps34 phosphatidylinositol 3-kinase in late versus early endosomes. Journal of cell science *119*, 1219-1232.

Jones, G.E. (2000). Cellular signaling in macrophage migration and chemotaxis. Journal of leukocyte biology *68*, 593-602.

Joshi, P.B., Sacks, D.L., Modi, G., and McMaster, W.R. (1998). Targeted gene deletion of Leishmania major genes encoding developmental stage-specific leishmanolysin (GP63). Mol Microbiol *27*, 519-530.

Jung, C.H., Jun, C.B., Ro, S.-H., Kim, Y.-M., Otto, N.M., Cao, J., Kundu, M., and Kim, D.-H. (2009). ULK-Atg13-FIP200 complexes mediate mTOR signaling to the autophagy machinery. Molecular biology of the cell *20*, 1992-2003.

Kabeya, Y., Mizushima, N., Ueno, T., Yamamoto, A., Kirisako, T., Noda, T., Kominami, E., Ohsumi, Y., and Yoshimori, T. (2000). LC3, a mammalian homologue of yeast Apg8p, is localized in autophagosome membranes after processing. The EMBO journal *19*, 5720-5728.

Kamphorst, A.O., Guermonprez, P., Dudziak, D., and Nussenzweig, M.C. (2010). Route of antigen uptake differentially impacts presentation by dendritic cells and activated monocytes. Journal of immunology (Baltimore, Md. : 1950) *185*, 3426-3435.

Kane, M.M., and Mosser, D.M. (2000). Leishmania parasites and their ploys to disrupt macrophage activation. Current opinion in hematology *7*, 26-31.

Katara, G.K., Ansari, N.A., Verma, S., Ramesh, V., Salotra, P., and Engwerda, C.R. (2011). Foxp3 and IL-10 Expression Correlates with Parasite Burden in Lesional Tissues of Post Kala Azar Dermal Leishmaniasis (PKDL) Patients. PLoS Negl Trop Dis *5*, e1171.

Kaye, P., and Scott, P. (2011). Leishmaniasis. Complexity at the host-pathogen interface. Nature reviews. Microbiology *9*, 604-615.

KEMP, M., Hansen, M.B., and THEANDER, T.G. (1992). Recognition of Leishmania antigens by T lymphocytes from nonexposed individuals. Infection and immunity *60*, 2246-2251.

KEMP, M., HEY, A.S., Kurtzhals, J.A., Christensen, C.B., Gaafar, A., Mustafa, M.D., Kordofani, A.A., Ismail, A., KHARAZMI, A., and THEANDER, T.G. (1994). Dichotomy of the human T cell response to Leishmania antigens. I. Th1-like response to Leishmania major promastigote antigens in individuals recovered from cutaneous leishmaniasis. Clinical and experimental immunology *96*, 410-415.

KEMP, M., THEANDER, T.G., Handman, E., HEY, A.S., KURTZHALS, J.A.L., HVIID, L., SØRENSEN, A.L., WERE, J.O.B., KOECH, D.K., and KHARAZMI, A. (1991). Activation of Human T Lymphocytes by Leishmania Lipophosphoglycan. Scand J Immunol *33*, 219-224.

Kihara, A., Kabeya, Y., Ohsumi, Y., and Yoshimori, T. (2001). Beclin-phosphatidylinositol 3-kinase complex functions at the trans-Golgi network. EMBO reports *2*, 330-335.

Kim, D.-H., Sarbassov, D.D., Ali, S.M., King, J.E., Latek, R.R., Erdjument-Bromage, H., Tempst, P., and Sabatini, D.M. (2002). mTOR Interacts with Raptor to Form a Nutrient-Sensitive Complex that Signals to the Cell Growth Machinery. Cell *110*, 163-175.

King, D.L., Chang, Y.D., and Turco, S.J. (1987). Cell surface lipophosphoglycan of Leishmania donovani. Molecular and Biochemical Parasitology *24*, 47-53.

Kirkegaard, K., Taylor, M.P., and Jackson, W.T. (2004). Cellular autophagy. Surrender, avoidance and subversion by microorganisms. Nature reviews. Microbiology *2*, 301-314.

Klionsky, D.J., Abdelmohsen, K., Abe, A., Abedin, M.J., Abeliovich, H., Acevedo Arozena, A., Adachi, H., Adams, C.M., Adams, P.D., and Adeli, K., et al. (2016). Guidelines for the use and interpretation of assays for monitoring autophagy (3rd edition). Autophagy *12*, 1-222.

Klionsky, D.J., Cuervo, A.M., and Seglen, P.O. (2014). Methods for Monitoring Autophagy from Yeast to Human. Autophagy *3*, 181-206.

Kobayashi, K.S., and van den Elsen, P.J. (2012). NLRC5. A key regulator of MHC class I-dependent immune responses. Nature reviews. Immunology *12*, 813-820.

Kropf, P., Fuentes, J.M., Fahnrich, E., Arpa, L., Herath, S., Weber, V., Soler, G., Celada, A., Modolell, M., and Muller, I. (2005). Arginase and polyamine synthesis are key factors in the regulation of experimental leishmaniasis in vivo. FASEB journal : official publication of the Federation of American Societies for Experimental Biology *19*, 1000-1002.

Kubach, J., Lutter, P., Bopp, T., Stoll, S., Becker, C., Huter, E., Richter, C., Weingarten, P., Warger, T., and Knop, J., et al. (2007). Human CD4+CD25+ regulatory T cells. Proteome analysis identifies galectin-10 as a novel marker essential for their anergy and suppressive function. Blood *110*, 1550-1558.

Kumar, R., and Engwerda, C. (2014). Vaccines to prevent leishmaniasis. Clinical & translational immunology *3*, e13.

Kundu, M., Lindsten, T., Yang, C.-Y., Wu, J., Zhao, F., Zhang, J., Selak, M.A., Ney, P.A., and Thompson, C.B. (2008). Ulk1 plays a critical role in the autophagic clearance of mitochondria and ribosomes during reticulocyte maturation. Blood *112*, 1493-1502.

Kwan, W.C., McMaster, W.R., Wong, N., and Reiner, N.E. (1992). Inhibition of expression of major histocompatibility complex class II molecules in macrophages infected with Leishmania donovani occurs at the level of gene transcription via a cyclic AMP-independent mechanism. Infection and immunity *60*, 2115-2120.

Kweider, M., Lemesre, J.L., Darcy, F., Kusnierz, J.P., Capron, A., and Santoro, F. (1987). Infectivity of Leishmania braziliensis promastigotes is dependent on the increasing expression of a 65,000-dalton surface antigen. Journal of immunology (Baltimore, Md. : 1950) *138*, 299-305.

Lacey, D.C., Achuthan, A., Fleetwood, A.J., Dinh, H., Roiniotis, J., Scholz, G.M., Chang, M.W., Beckman, S.K., Cook, A.D., and Hamilton, J.A. (2012). Defining GM-

CSF- and macrophage-CSF-dependent macrophage responses by in vitro models. Journal of immunology (Baltimore, Md. : 1950) *188*, 5752-5765.

Lamb, C.A., Yoshimori, T., and Tooze, S.A. (2013). The autophagosome. Origins unknown, biogenesis complex. Nature reviews. Molecular cell biology *14*, 759-774.

Lang, T., Hellio, R., Kaye, P.M., and Antoine, J.C. (1994). Leishmania donovani-infected macrophages. Characterization of the parasitophorous vacuole and potential role of this organelle in antigen presentation. Journal of cell science *107 (Pt 8)*, 2137-2150.

Laskay, T., Mariam, H.G., Berhane, T.Y., Fehniger, T.E., and Kiessling, R. (1991). Immune reactivity to fractionated Leishmania aethiopica antigens during active human infection. Journal of clinical microbiology *29*, 757-763.

Laskay, T., van Zandbergen, G., and Solbach, W. (2003). Neutrophil granulocytes – Trojan horses for Leishmania major and other intracellular microbes? Trends in Microbiology *11*, 210-214.

Lee, E.-J., and Tournier, C. (2014). The requirement of uncoordinated 51-like kinase 1 (ULK1) and ULK2 in the regulation of autophagy. Autophagy *7*, 689-695.

Lee, H.K., Mattei, L.M., Steinberg, B.E., Alberts, P., Lee, Y.H., Chervonsky, A., Mizushima, N., Grinstein, S., and Iwasaki, A. (2010). In vivo requirement for Atg5 in antigen presentation by dendritic cells. Immunity *32*, 227-239.

Lee, Y.-R., Lei, H.-Y., Liu, M.-T., Wang, J.-R., Chen, S.-H., Jiang-Shieh, Y.-F., Lin, Y.-S., Yeh, T.-M., Liu, C.-C., and Liu, H.-S. (2008). Autophagic machinery activated by dengue virus enhances virus replication. Virology *374*, 240-248.

Lennemann, N.J., and Coyne, C.B. (2015). Catch me if you can. The link between autophagy and viruses. PLoS pathogens *11*, e1004685.

Levine, B., Mizushima, N., and Virgin, H.W. (2011). Autophagy in immunity and inflammation. Nature *469*, 323-335.

Li, X., Prescott, M., Adler, B., Boyce, J.D., and Devenish, R.J. (2013). Beclin 1 is required for starvation-enhanced, but not rapamycin-enhanced, LC3-associated phagocytosis of Burkholderia pseudomallei in RAW 264.7 cells. Infection and immunity *81*, 271-277.

Liang, X.H., Jackson, S., Seaman, M., Brown, K., Kempkes, B., Hibshoosh, H., and Levine, B. (1999). Induction of autophagy and inhibition of tumorigenesis by beclin 1. Nature *402*, 672-676.

Lieke, T., Nylen, S., Eidsmo, L., McMaster, W.R., Mohammadi, A.M., Khamesipour, A., Berg, L., and Akuffo, H. (2008). Leishmania surface protein gp63 binds directly to human natural killer cells and inhibits proliferation. Clinical and experimental immunology *153*, 221-230.

Lin, Y.-C., Kuo, H.-C., Wang, J.-S., and Lin, W.-W. (2012). Regulation of inflammatory response by 3-methyladenine involves the coordinative actions on Akt and glycogen synthase kinase 3beta rather than autophagy. Journal of immunology (Baltimore, Md. : 1950) *189*, 4154-4164.

Lindoso, J.A.L., Cunha, M.A., Queiroz, I.T., and Moreira, C.H.V. (2016). Leishmaniasis-HIV coinfection. Current challenges. HIV/AIDS (Auckland, N.Z.) *8*, 147-156.

Linehan, S.A., Martínez-Pomares, L., and Gordon, S. (2000). Macrophage lectins in host defence. Microbes and Infection *2*, 279-288.

Liu, J., Xia, H., Kim, M., Xu, L., Li, Y., Zhang, L., Cai, Y., Norberg, H.V., Zhang, T., and Furuya, T., et al. (2011). Beclin1 controls the levels of p53 by regulating the deubiquitination activity of USP10 and USP13. Cell *147*, 223-234.

Liu, K., Zhao, E., Ilyas, G., Lalazar, G., Lin, Y., Haseeb, M., Tanaka, K.E., and Czaja, M.J. (2015). Impaired macrophage autophagy increases the immune response in obese mice by promoting proinflammatory macrophage polarization. Autophagy *11*, 271-284.

Liu, X., and Chang, K.P. (1992). Extrachromosomal genetic complementation of surface metalloproteinase (gp63)-deficient Leishmania increases their binding to macrophages. Proceedings of the National Academy of Sciences of the United States of America *89*, 4991-4995.

Livak, K.J., and Schmittgen, T.D. (2001). Analysis of relative gene expression data using real-time quantitative PCR and the 2(-Delta Delta C(T)) Method. Methods (San Diego, Calif.) *25*, 402-408.

Locksley, R.M. (2010). Asthma and allergic inflammation. Cell *140*, 777-783.

Lopez-Jaramillo, P., Ruano, C., Rivera, J., Teran, E., Salazar-Irigoyen, R., Esplugues, J.V., and Moncada, S. (1998). Treatment of cutaneous leishmaniasis with nitric-oxide donor. The Lancet *351*, 1176-1177.

Lynch-Day, M.A., Mao, K., Wang, K., Zhao, M., and Klionsky, D.J. (2012). The role of autophagy in Parkinson's disease. Cold Spring Harbor perspectives in medicine *2*, a009357.

Ma, J., Becker, C., Lowell, C.A., and Underhill, D.M. (2012). Dectin-1-triggered recruitment of light chain 3 protein to phagosomes facilitates major histocompatibility complex class II presentation of fungal-derived antigens. The Journal of biological chemistry *287*, 34149-34156.

Macdonald, M.H., Morrison, C.J., and McMaster, W.R. (1995). Analysis of the active site and activation mechanism of the Leishmania surface metalloproteinase GP63. Biochimica et biophysica acta *1253*, 199-207.

MACKANESS, G.B. (1962). Cellular resistance to infection. The Journal of experimental medicine *116*, 381-406.

Mahoney, J.A., Ntolosi, B., DaSilva, R.P., Gordon, S., and McKnight, A.J. (2001). Cloning and characterization of CPVL, a novel serine carboxypeptidase, from human macrophages. Genomics *72*, 243-251.

Makala, L.H.C., Baban, B., Lemos, H., El-Awady, A.R., Chandler, P.R., Hou, D.-Y., Munn, D.H., and Mellor, A.L. (2011). Leishmania major attenuates host immunity by stimulating local indoleamine 2,3-dioxygenase expression. The Journal of infectious diseases *203*, 715-725.

Mansour, M.K., Tam, J.M., Khan, N.S., Seward, M., Davids, P.J., Puranam, S., Sokolovska, A., Sykes, D.B., Dagher, Z., and Becker, C., et al. (2013). Dectin-1 activation controls maturation of beta-1,3-glucan-containing phagosomes. The Journal of biological chemistry *288*, 16043-16054.

Mantovani, A., Sica, A., Sozzani, S., Allavena, P., Vecchi, A., and Locati, M. (2004). The chemokine system in diverse forms of macrophage activation and polarization. Trends in immunology *25*, 677-686.

Marth, T., and Kelsall, B.L. (1997). Regulation of interleukin-12 by complement receptor 3 signaling. The Journal of experimental medicine *185*, 1987-1995.

Martin, C.J., Peters, K.N., and Behar, S.M. (2014). Macrophages clean up. Efferocytosis and microbial control. Current opinion in microbiology *17*, 17-23.

Martinez, F.O., and Gordon, S. (2014). The M1 and M2 paradigm of macrophage activation. Time for reassessment. F1000prime reports *6*, 13.

Martinez, J., Almendinger, J., Oberst, A., Ness, R., Dillon, C.P., Fitzgerald, P., Hengartner, M.O., and Green, D.R. (2011). Microtubule-associated protein 1 light chain 3 alpha (LC3)-associated phagocytosis is required for the efficient clearance of dead cells. Proceedings of the National Academy of Sciences of the United States of America *108*, 17396-17401.

Martinez, J., Malireddi, R.K.S., Lu, Q., Cunha, L.D., Pelletier, S., Gingras, S., Orchard, R., Guan, J.-L., Tan, H., and Peng, J., et al. (2015). Molecular characterization of LC3-associated phagocytosis reveals distinct roles for Rubicon, NOX2 and autophagy proteins. Nature cell biology *17*, 893-906.

Martinez, J., Verbist, K., Wang, R., and Green, D.R. (2013). The relationship between metabolism and the autophagy machinery during the innate immune response. Cell metabolism *17*, 895-900.

Martyniszyn, L., Szulc-Dabrowska, L., Boratynska-Jasinska, A., Struzik, J., Winnicka, A., and Niemialtowski, M. (2013). Crosstalk between autophagy and apoptosis in RAW 264.7 macrophages infected with ectromelia orthopoxvirus. Viral immunology *26*, 322-335.

Mason, J.M., Naidu, M.D., Barcia, M., Porti, D., Chavan, S.S., and Chu, C.C. (2004). IL-4-Induced Gene-1 Is a Leukocyte L-Amino Acid Oxidase with an Unusual Acidic pH Preference and Lysosomal Localization. The Journal of Immunology *173*, 4561-4567.

Mateo, R., Nagamine, C.M., Spagnolo, J., Mendez, E., Rahe, M., Gale, M., JR, Yuan, J., and Kirkegaard, K. (2013). Inhibition of cellular autophagy deranges dengue virion maturation. Journal of virology *87*, 1312-1321.

Matheoud, D., Moradin, N., Bellemare-Pelletier, A., Shio, M.T., Hong, W.J., Olivier, M., Gagnon, E., Desjardins, M., and Descoteaux, A. (2013). Leishmania evades host immunity by inhibiting antigen cross-presentation through direct cleavage of the SNARE VAMP8. Cell host & microbe *14*, 15-25.

Matsuzawa, T., Kim, B.-H., Shenoy, A.R., Kamitani, S., Miyake, M., and MacMicking, J.D. (2012). IFN-gamma elicits macrophage autophagy via the p38 MAPK signaling pathway. Journal of immunology (Baltimore, Md. : 1950) *189*, 813-818.

Matte, C., Casgrain, P.-A., Seguin, O., Moradin, N., Hong, W.J., and Descoteaux, A. (2016). Leishmania major Promastigotes Evade LC3-Associated Phagocytosis through the Action of GP63. PLoS pathogens *12*, e1005690.

McGwire, B.S., and Satoskar, A.R. (2014). Leishmaniasis. Clinical syndromes and treatment. QJM : monthly journal of the Association of Physicians *107*, 7-14.

Medina-Acosta, E., Karess, R.E., Schwartz, H., and Russell, D.G. (1989). The promastigote surface protease (gp63) of Leishmania is expressed but differentially processed and localized in the amastigote stage. Molecular and Biochemical Parasitology *37*, 263-273.

Medzhitov, R., and Janeway, C., JR (2000). Innate immunity. The New England journal of medicine *343*, 338-344.

Mehta, P., Henault, J., Kolbeck, R., and Sanjuan, M.A. (2014). Noncanonical autophagy. One small step for LC3, one giant leap for immunity. Current opinion in immunology *26*, 69-75.

Mendonca, S.C., Russell, D.G., and Coutinho, S.G. (1991). Analysis of the human T cell responsiveness to purified antigens of Leishmania. Lipophosphoglycan (LPG) and glycoprotein 63 (gp 63). Clinical and experimental immunology *83*, 472-478.

Menten, P., Wuyts, A., and van Damme, J. (2002). Macrophage inflammatory protein-1. Cytokine & growth factor reviews *13*, 455-481.

Miller, S., Tavshanjian, B., Oleksy, A., Perisic, O., Houseman, B.T., Shokat, K.M., and Williams, R.L. (2010). Shaping development of autophagy inhibitors with the structure of the lipid kinase Vps34. Science (New York, N.Y.) *327*, 1638-1642.

Mills, C.D., Kincaid, K., Alt, J.M., Heilman, M.J., and Hill, A.M. (2000). M-1/M-2 Macrophages and the Th1/Th2 Paradigm. The Journal of Immunology *164*, 6166-6173.

Mizushima, N. (2003). Mouse Apg16L, a novel WD-repeat protein, targets to the autophagic isolation membrane with the Apg12-Apg5 conjugate. Journal of cell science *116*, 1679-1688.

Mizushima, N., Levine, B., Cuervo, A.M., and Klionsky, D.J. (2008). Autophagy fights disease through cellular self-digestion. Nature *451*, 1069-1075.

Mizushima, N., Noda, T., Yoshimori, T., Tanaka, Y., Ishii, T., George, M.D., Klionsky, D.J., Ohsumi, M., and Ohsumi, Y. (1998a). A protein conjugation system essential for autophagy. Nature *395*, 395-398.

Mizushima, N., Ohsumi, Y., and Yoshimori, T. (2002). Autophagosome Formation in Mammalian Cells. Cell Struct. Funct. *27*, 421-429.

Mizushima, N., Sugita, H., Yoshimori, T., and Ohsumi, Y. (1998b). A new protein conjugation system in human. The counterpart of the yeast Apg12p conjugation system essential for autophagy. The Journal of biological chemistry *273*, 33889-33892.

Mizushima, N., Yoshimori, T., and Levine, B. (2010). Methods in mammalian autophagy research. Cell *140*, 313-326.

Moestrup, S., and Møller, H. (2009). CD163. A regulated hemoglobin scavenger receptor with a role in the anti-inflammatory response. Annals of Medicine *36*, 347-354.

Mortimore, G.E., Hutson, N.J., and Surmacz, C.A. (1983). Quantitative correlation between proteolysis and macro- and microautophagy in mouse hepatocytes during starvation and refeeding. Proceedings of the National Academy of Sciences of the United States of America *80*, 2179-2183.

Mosser, D.M. (2003). The many faces of macrophage activation. Journal of leukocyte biology *73*, 209-212.

Mosser, D.M., and Edelson, P.J. (1984). Activation of the alternative complement pathway by Leishmania promastigotes. Parasite lysis and attachment to macrophages. Journal of immunology (Baltimore, Md. : 1950) *132*, 1501-1505.

Mosser, D.M., and Edelson, P.J. (1985). The mouse macrophage receptor for C3bi (CR3) is a major mechanism in the phagocytosis of Leishmania promastigotes. Journal of immunology (Baltimore, Md. : 1950) *135*, 2785-2789.

Mosser, D.M., and Edelson, P.J. (1987). The third component of complement (C3) is responsible for the intracellular survival of Leishmania major. Nature *327*, 329-331.

Mosser, D.M., and Edwards, J.P. (2008). Exploring the full spectrum of macrophage activation. Nature reviews. Immunology *8*, 958-969.

Mosser, D.M., and Rosenthal, L.A. (1993). Leishmania-macrophage interactions. Multiple receptors, multiple ligands and diverse cellular responses. Seminars in cell biology *4*, 315-322.

Mosser, D.M., Springer, T.A., and Diamond, M.S. (1992). Leishmania promastigotes require opsonic complement to bind to the human leukocyte integrin Mac-1 (CD11b/CD18). The Journal of cell biology *116*, 511-520.

Munn, D.H., Shafizadeh, E., Attwood, J.T., Bondarev, I., Pashine, A., and Mellor, A.L. (1999). Inhibition of T cell proliferation by macrophage tryptophan catabolism. The Journal of experimental medicine *189*, 1363-1372.

Munz, C. (2016a). Autophagy Beyond Intracellular MHC Class II Antigen Presentation. Trends in immunology *37*, 755-763.

Munz, C. (2016b). Autophagy proteins in antigen processing for presentation on MHC molecules. Immunological reviews *272*, 17-27.

Murakami, Y., Hoshi, M., Imamura, Y., Arioka, Y., Yamamoto, Y., and Saito, K. (2013). Remarkable role of indoleamine 2,3-dioxygenase and tryptophan metabolites in infectious diseases. Potential role in macrophage-mediated inflammatory diseases. Mediators of inflammation *2013*, 391984.

Murphy, K., Janeway, C.A., and Mowat, A. (2012). Janeway's immunobiology (London: Garland Science).

Murray, H.W. (1981). Susceptibility of Leishmania to oxygen intermediates and killing by normal macrophages. The Journal of experimental medicine *153*, 1302-1315.

Murray, H.W., Rubin, B.Y., and Rothermel, C.D. (1983). Killing of intracellular Leishmania donovani by lymphokine-stimulated human mononuclear phagocytes. Evidence that interferon-gamma is the activating lymphokine. The Journal of clinical investigation *72*, 1506-1510.

Murray, H.W., Szuro-Sudol, A., Wellner, D., Oca, M.J., Granger, A.M., Libby, D.M., Rothermel, C.D., and Rubin, B.Y. (1989). Role of tryptophan degradation in respiratory burst-independent antimicrobial activity of gamma interferon-stimulated human macrophages. Infection and immunity *57*, 845-849.

Murray, P.J., and Wynn, T.A. (2011). Protective and pathogenic functions of macrophage subsets. Nature reviews. Immunology *11*, 723-737.

Nakatogawa, H., Ichimura, Y., and Ohsumi, Y. (2007). Atg8, a ubiquitin-like protein required for autophagosome formation, mediates membrane tethering and hemifusion. Cell *130*, 165-178.

Nathan, C. (2008). Metchnikoff's Legacy in 2008. Nature immunology *9*, 695-698.

Nathan, C.F., Murray, H.W., Wiebe, M.E., and Rubin, B.Y. (1983). Identification of interferon-gamma as the lymphokine that activates human macrophage oxidative metabolism and antimicrobial activity. The Journal of experimental medicine *158*, 670-689.

Nauseef, W.M. (2008). Biological roles for the NOX family NADPH oxidases. The Journal of biological chemistry *283*, 16961-16965.

Neefjes, J., Jongsma, M.L.M., Paul, P., and Bakke, O. (2011). Towards a systems understanding of MHC class I and MHC class II antigen presentation. Nature reviews. Immunology *11*, 823-836.

Neefjes, J.J., Stollorz, V., Peters, P.J., Geuze, H.J., and Ploegh, H.L. (1990). The biosynthetic pathway of MHC class II but not class I molecules intersects the endocytic route. Cell *61*, 171-183.

Neu, C., Sedlag, A., Bayer, C., Forster, S., Crauwels, P., Niess, J.-H., van Zandbergen, G., Frascaroli, G., and Riedel, C.U. (2013). CD14-dependent monocyte isolation enhances phagocytosis of listeria monocytogenes by proinflammatory, GM-CSF-derived macrophages. PloS one *8*, e66898.

Nielsen, C.H., Galdiers, M.P., Hedegaard, C.J., and Leslie, R.G.Q. (2010). The self-antigen, thyroglobulin, induces antigen-experienced CD4+ T cells from healthy donors to proliferate and promote production of the regulatory cytokine, interleukin-10, by monocytes. Immunology *129*, 291-299.

Nimmerjahn, F., Milosevic, S., Behrends, U., Jaffee, E.M., Pardoll, D.M., Bornkamm, G.W., and Mautner, J. (2003). Major histocompatibility complex class II-restricted presentation of a cytosolic antigen by autophagy. European journal of immunology *33*, 1250-1259.

Nixon, R.A. (2013). The role of autophagy in neurodegenerative disease. Nature medicine *19*, 983-997.

Nobukuni, T., Joaquin, M., Roccio, M., Dann, S.G., Kim, S.Y., Gulati, P., Byfield, M.P., Backer, J.M., Natt, F., and Bos, J.L., et al. (2005). Amino acids mediate mTOR/raptor signaling through activation of class 3 phosphatidylinositol 3OH-kinase. Proceedings of the National Academy of Sciences of the United States of America *102*, 14238-14243.

Noda, T., and Ohsumi, Y. (1998). Tor, a phosphatidylinositol kinase homologue, controls autophagy in yeast. The Journal of biological chemistry *273*, 3963-3966.

Novikoff, A.B. (1959). The proximal tubule cell in experimental hydronephrosis. The Journal of biophysical and biochemical cytology *6*, 136-138.

Novikoff, A.B., BEAUFAY, H., and DUVE, C. de (1956). Electron microscopy of lysosomerich fractions from rat liver. The Journal of biophysical and biochemical cytology *2*, 179-184.

Ohsumi, Y. (2014). Historical landmarks of autophagy research. Cell research *24*, 9-23.

Olivier, M., Atayde, V.D., Isnard, A., Hassani, K., and Shio, M.T. (2012). Leishmania virulence factors. Focus on the metalloprotease GP63. Microbes and Infection *14*, 1377-1389.

O'Neill, A.S.G., van den Berg, T.K., and Mullen, G.E.D. (2013). Sialoadhesin - a macrophage-restricted marker of immunoregulation and inflammation. Immunology *138*, 198-207.

Pan, T., Kondo, S., Le, W., and Jankovic, J. (2008). The role of autophagy-lysosome pathway in neurodegeneration associated with Parkinson's disease. Brain : a journal of neurology *131*, 1969-1978.

Panday, A., Sahoo, M.K., Osorio, D., and Batra, S. (2015). NADPH oxidases. An overview from structure to innate immunity-associated pathologies. Cellular & molecular immunology *12*, 5-23.

Pankiv, S., Clausen, T.H., Lamark, T., Brech, A., Bruun, J.-A., Outzen, H., Overvatn, A., Bjorkoy, G., and Johansen, T. (2007). p62/SQSTM1 binds directly to Atg8/LC3 to facilitate degradation of ubiquitinated protein aggregates by autophagy. The Journal of biological chemistry *282*, 24131-24145.

Park, S., Chapuis, N., Bardet, V., Tamburini, J., Gallay, N., Willems, L., Knight, Z.A., Shokat, K.M., Azar, N., and Viguie, F., et al. (2008). PI-103, a dual inhibitor of Class IA phosphatidylinositide 3-kinase and mTOR, has antileukemic activity in AML. Leukemia *22*, 1698-1706.

Pearson, R.D., Harcus, J.L., Symes, P.H., Romito, R., and Donowitz, G.R. (1982). Failure of the phagocytic oxidative response to protect human monocyte-derived macrophages from infection by Leishmania donovani. Journal of immunology (Baltimore, Md. : 1950) *129*, 1282-1286.

Peters, N.C., Egen, J.G., Secundino, N., Debrabant, A., Kimblin, N., Kamhawi, S., Lawyer, P., Fay, M.P., Germain, R.N., and Sacks, D. (2008). In vivo imaging reveals an essential role for neutrophils in leishmaniasis transmitted by sand flies. Science (New York, N.Y.) *321*, 970-974.

Petiot, A., Ogier-Denis, E., Blommaart, E.F.C., Meijer, A.J., and Codogno, P. (2000). Distinct Classes of Phosphatidylinositol 3'-Kinases Are Involved in Signaling Pathways That Control Macroautophagy in HT-29 Cells. Journal of Biological Chemistry *275*, 992-998.

Pfefferkorn, E.R. (1984). Interferon gamma blocks the growth of Toxoplasma gondii in human fibroblasts by inducing the host cells to degrade tryptophan. Proceedings of the National Academy of Sciences of the United States of America *81*, 908-912.

Pirmez, C., Cooper, C., Paes-Oliveira, M., Schubach, A., Torigian, V.K., and Modlin, R.L. (1990). Immunologic responsiveness in American cutaneous leishmaniasis lesions. Journal of immunology (Baltimore, Md. : 1950) *145*, 3100-3104.

Pirmez, C., Yamamura, M., Uyemura, K., Paes-Oliveira, M., Conceicao-Silva, F., and Modlin, R.L. (1993). Cytokine patterns in the pathogenesis of human leishmaniasis. The Journal of clinical investigation *91*, 1390-1395.

Podinovskaia, M., and Descoteaux, A. (2015). Leishmania and the macrophage. A multifaceted interaction. Future microbiology *10*, 111-129.

Poklepovic, A., and Gewirtz, D.A. (2014). Outcome of early clinical trials of the combination of hydroxychloroquine with chemotherapy in cancer. Autophagy *10*, 1478-1480.

Prina, E., Antoine, J.C., Wiederanders, B., and Kirschke, H. (1990). Localization and activity of various lysosomal proteases in Leishmania amazonensis-infected macrophages. Infection and immunity *58*, 1730-1737.

Privé, C., and Descoteaux, A. (2000). Leishmania donovani promastigotes evade the activation of mitogen-activated protein kinases p38, c-Jun N-terminal kinase, and extracellular signal-regulated kinase-1/2 during infection of naive macrophages. Eur. J. Immunol. *30*, 2235-2244.

Pucadyil, T.J., and Chattopadhyay, A. (2007). Cholesterol. A potential therapeutic target in Leishmania infection? Trends in Parasitology *23*, 49-53.

Puentes, S.M., Sacks, D.L., Da Silva, R.P., and Joiner, K.A. (1988). Complement binding by two developmental stages of Leishmania major promastigotes varying in expression of a surface lipophosphoglycan. The Journal of experimental medicine *167*, 887-902.

Rai, A.K., Thakur, C.P., Singh, A., Seth, T., Srivastava, S.K., Singh, P., and Mitra, D.K. (2012). Regulatory T cells suppress T cell activation at the pathologic site of human visceral leishmaniasis. PloS one *7*, e31551.

Ravikumar, B., Sarkar, S., Davies, J.E., Futter, M., Garcia-Arencibia, M., Green-Thompson, Z.W., Jimenez-Sanchez, M., Korolchuk, V.I., Lichtenberg, M., and Luo, S., et al. (2010). Regulation of mammalian autophagy in physiology and pathophysiology. Physiological reviews *90*, 1383-1435.

Reiner, N.E., Ng, W., Ma, T., and McMaster, W.R. (1988). Kinetics of gamma interferon binding and induction of major histocompatibility complex class II mRNA in Leishmania-infected macrophages. Proceedings of the National Academy of Sciences of the United States of America *85*, 4330-4334.

Ribeiro-de-Jesus, A., Almeida, R.P., Lessa, H., Bacellar, O., and Carvalho, E.M. (1998). Cytokine profile and pathology in human leishmaniasis. Braz J Med Biol Res *31*, 143-148.

Riganti, C., Gazzano, E., Polimeni, M., Costamagna, C., Bosia, A., and Ghigo, D. (2004). Diphenyleneiodonium inhibits the cell redox metabolism and induces oxidative stress. The Journal of biological chemistry *279*, 47726-47731.

Rioux, J.A., Lanotte, G., Serres, E., Pratlong, F., Bastien, P., and Perieres, J. (1990). Taxonomy of Leishmania. Use of isoenzymes. Suggestions for a new classification. Annales de parasitologie humaine et comparee *65*, 111-125.

Rioux, J.D., Xavier, R.J., Taylor, K.D., Silverberg, M.S., Goyette, P., Huett, A., Green, T., Kuballa, P., Barmada, M.M., and Datta, L.W., et al. (2007). Genome-wide association study identifies new susceptibility loci for Crohn disease and implicates autophagy in disease pathogenesis. Nature genetics *39*, 596-604.

Rizvi, F.S., Ouaissi, M.A., Marty, B., Santoro, F., and Capron, A. (1988). The major surface protein of Leishmania promastigotes is a fibronectin-like molecule. European journal of immunology *18*, 473-476.

Roche, P.A., and Furuta, K. (2015). The ins and outs of MHC class II-mediated antigen processing and presentation. Nature reviews. Immunology *15*, 203-216.

Rodriguez, N.E., Gaur, U., and Wilson, M.E. (2006). Role of caveolae in Leishmania chagasi phagocytosis and intracellular survival in macrophages. Cellular microbiology *8*, 1106-1120.

Roggo, L., Bernard, V., Kovacs, A.L., Rose, A.M., Savoy, F., Zetka, M., Wymann, M.P., and Muller, F. (2002). Membrane transport in Caenorhabditis elegans. An essential role for VPS34 at the nuclear membrane. The EMBO journal *21*, 1673-1683.

Romao, S., Gasser, N., Becker, A.C., Guhl, B., Bajagic, M., Vanoaica, D., Ziegler, U., Roesler, J., Dengjel, J., and Reichenbach, J., et al. (2013). Autophagy proteins stabilize pathogen-containing phagosomes for prolonged MHC II antigen processing. The Journal of cell biology *203*, 757-766.

Rosenthal, L.A., Sutterwala, F.S., Kehrli, M.E., and Mosser, D.M. (1996). Leishmania major-human macrophage interactions. Cooperation between Mac-1 (CD11b/CD18) and complement receptor type 1 (CD35) in promastigote adhesion. Infection and immunity *64*, 2206-2215.

Rossjohn, J., Gras, S., Miles, J.J., Turner, S.J., Godfrey, D.I., and McCluskey, J. (2015). T cell antigen receptor recognition of antigen-presenting molecules. Annual review of immunology *33*, 169-200.

Rubinsztein, D.C., Codogno, P., and Levine, B. (2012). Autophagy modulation as a potential therapeutic target for diverse diseases. Nature reviews. Drug discovery *11*, 709-730.

Russell, D.G., and Alexander, J. (1988). Effective immunization against cutaneous leishmaniasis with defined membrane antigens reconstituted into liposomes. Journal of immunology (Baltimore, Md. : 1950) *140*, 1274-1279.

Russell, D.G., and Wright, S.D. (1988). Complement receptor type 3 (CR3) binds to an Arg-Gly-Asp-containing region of the major surface glycoprotein, gp63, of Leishmania promastigotes. The Journal of experimental medicine *168*, 279-292.

Russell, D.G., Xu, S., and Chakraborty, P. (1992). Intracellular trafficking and the parasitophorous vacuole of Leishmania mexicana-infected macrophages. Journal of cell science *103 (Pt 4)*, 1193-1210.

Sacks, D.L., and Perkins, P.V. (1984). Identification of an infective stage of Leishmania promastigotes. Science (New York, N.Y.) *223*, 1417-1419.

Sagona, A.P., Nezis, I.P., Pedersen, N.M., Liestol, K., Poulton, J., Rusten, T.E., Skotheim, R.I., Raiborg, C., and Stenmark, H. (2010). PtdIns(3)P controls cytokinesis through KIF13A-mediated recruitment of FYVE-CENT to the midbody. Nature cell biology *12*, 362-371.

Salem, M., Nielsen, O.H., Nys, K., Yazdanyar, S., and Seidelin, J.B. (2015). Impact of T300A Variant of ATG16L1 on Antibacterial Response, Risk of Culture Positive Infections, and Clinical Course of Crohn's Disease. Clinical and translational gastroenterology *6*, e122.

Samson, E. (1981). Xenophagy. British dental journal *150*, 136.

Sanjuan, M.A., Dillon, C.P., Tait, S.W.G., Moshiach, S., Dorsey, F., Connell, S., Komatsu, M., Tanaka, K., Cleveland, J.L., and Withoff, S., et al. (2007). Toll-like receptor signalling in macrophages links the autophagy pathway to phagocytosis. Nature *450*, 1253-1257.

Sato, M., Sano, H., Iwaki, D., Kudo, K., Konishi, M., Takahashi, H., Takahashi, T., Imaizumi, H., Asai, Y., and Kuroki, Y. (2003). Direct Binding of Toll-Like Receptor 2 to Zymosan, and Zymosan-Induced NF- B Activation and TNF- Secretion Are Down-Regulated by Lung Collectin Surfactant Protein A. The Journal of Immunology *171*, 417-425.

Savina, A., Jancic, C., Hugues, S., Guermonprez, P., Vargas, P., Moura, I.C., Lennon-Dumenil, A.-M., Seabra, M.C., Raposo, G., and Amigorena, S. (2006). NOX2 controls phagosomal pH to regulate antigen processing during crosspresentation by dendritic cells. Cell *126*, 205-218.

Scherz-Shouval, R., and Elazar, Z. (2011). Regulation of autophagy by ROS. Physiology and pathology. Trends in biochemical sciences *36*, 30-38.

Schlagenhauf, E., Etges, R., and Metcalf, P. (1998). The crystal structure of the Leishmania major surface proteinase leishmanolysin (gp63). Structure *6*, 1035-1046.

Schmid, D., and Munz, C. (2007). Innate and adaptive immunity through autophagy. Immunity *27*, 11-21.

Schneider, P., Rosat, J.P., Bouvier, J., Louis, J., and Bordier, C. (1992). Leishmania major. Differential regulation of the surface metalloprotease in amastigote and promastigote stages. Experimental parasitology *75*, 196-206.

Seglen, P.O., and Gordon, P.B. (1982). 3-Methyladenine. Specific inhibitor of autophagic/lysosomal protein degradation in isolated rat hepatocytes. Proceedings of the National Academy of Sciences of the United States of America *79*, 1889-1892.

Sharif, T., Martell, E., Dai, C., Kennedy, B.E., Murphy, P., Clements, D.R., Kim, Y., Lee, P.W.K., and Gujar, S.A. (2017). Autophagic homeostasis is required for the pluripotency of cancer stem cells. Autophagy *13*, 264-284.

Sharma, U., and Singh, S. (2009). Immunobiology of leishmaniasis. When is a library not a library? Indian journal of experimental biology *47*, 412-423.

Shimizu, T., Numata, T., and Okada, Y. (2004). A role of reactive oxygen species in apoptotic activation of volume-sensitive Cl(-) channel. Proceedings of the National Academy of Sciences of the United States of America *101*, 6770-6773.

Shintani, T., Yamazaki, F., Katoh, T., Umekawa, M., Matahira, Y., Hori, S., Kakizuka, A., Totani, K., Yamamoto, K., and Ashida, H. (2010). Glucosamine induces autophagy via an mTOR-independent pathway. Biochemical and biophysical research communications *391*, 1775-1779.

Shoji-Kawata, S., Sumpter, R., Leveno, M., Campbell, G.R., Zou, Z., Kinch, L., Wilkins, A.D., Sun, Q., Pallauf, K., and MacDuff, D., et al. (2013). Identification of a candidate therapeutic autophagy-inducing peptide. Nature *494*, 201-206.

Singh, A.K., Pandey, R.K., Shaha, C., and Madhubala, R. (2016). MicroRNA expression profiling of Leishmania donovani-infected host cells uncovers the regulatory role of MIR30A-3p in host autophagy. Autophagy *12*, 1817-1831.

Sini, P., James, D., Chresta, C., and Guichard, S. (2010). Simultaneous inhibition of mTORC1 and mTORC2 by mTOR kinase inhibitor AZD8055 induces autophagy and cell death in cancer cells. Autophagy *6*, 553-554.

Smith, D.M., Patel, S., Raffoul, F., Haller, E., Mills, G.B., and Nanjundan, M. (2010). Arsenic trioxide induces a beclin-1-independent autophagic pathway via modulation of SnoN/SkiL expression in ovarian carcinoma cells. Cell death and differentiation *17*, 1867-1881.

Souza Leao, S. de, Lang, T., Prina, E., Hellio, R., and Antoine, J.C. (1995). Intracellular Leishmania amazonensis amastigotes internalize and degrade MHC class II molecules of their host cells. Journal of cell science *108 (Pt 10)*, 3219-3231.

Spath, G.F., Garraway, L.A., Turco, S.J., and Beverley, S.M. (2003). The role(s) of lipophosphoglycan (LPG) in the establishment of Leishmania major infections in mammalian hosts. Proceedings of the National Academy of Sciences of the United States of America *100*, 9536-9541.

Srivastava, S., Shankar, P., Mishra, J., and Singh, S. (2016). Possibilities and challenges for developing a successful vaccine for leishmaniasis. Parasites & vectors *9*, 277.

Stebut, E. von (2015). Leishmaniasis. Journal der Deutschen Dermatologischen Gesellschaft = Journal of the German Society of Dermatology : JDDG *13*, 191-200; quiz 201.

Stein, M., Keshav, S., Harris, N., and Gordon, S. (1992). Interleukin 4 potently enhances murine macrophage mannose receptor activity. A marker of alternative immunologic macrophage activation. The Journal of experimental medicine *176*, 287-292.

Sturgill-Koszycki, S., Schlesinger, P.H., Chakraborty, P., Haddix, P.L., Collins, H.L., Fok, A.K., Allen, R.D., Gluck, S.L., Heuser, J., and Russell, D.G. (1994). Lack of acidification in Mycobacterium phagosomes produced by exclusion of the vesicular proton-ATPase. Science (New York, N.Y.) *263*, 678-681.

Sun, L., Youn, H.-D., Loh, C., Stolow, M., He, W., and Liu, J.O. (1998). Cabin 1, A Negative Regulator for Calcineurin Signaling in T Lymphocytes. Immunity *8*, 703-711.

Takeshige, K., Baba, M., Tsuboi, S., Noda, T., and Ohsumi, Y. (1992). Autophagy in yeast demonstrated with proteinase-deficient mutants and conditions for its induction. The Journal of cell biology *119*, 301-311.

Tanida, I., Sou, Y.-s., Ezaki, J., Minematsu-Ikeguchi, N., Ueno, T., and Kominami, E. (2004a). HsAtg4B/HsApg4B/autophagin-1 cleaves the carboxyl termini of three human Atg8 homologues and delipidates microtubule-associated protein light chain 3- and GABAA receptor-associated protein-phospholipid conjugates. The Journal of biological chemistry *279*, 36268-36276.

Tanida, I., Ueno, T., and Kominami, E. (2004b). LC3 conjugation system in mammalian autophagy. The international journal of biochemistry & cell biology *36*, 2503-2518.

Thiakaki, M., Kolli, B., Chang, K.-P., and Soteriadou, K. (2006). Down-regulation of gp63 level in Leishmania amazonensis promastigotes reduces their infectivity in BALB/c mice. Microbes and Infection *8*, 1455-1463.

Tian, S., Lin, J., Jun Zhou, J., Wang, X., Li, Y., Ren, X., Yu, W., Zhong, W., Xiao, J., and Sheng, F., et al. (2010). Beclin 1-independent autophagy induced by a Bcl-XL/Bcl-2 targeting compound, Z18. Autophagy *6*, 1032-1041.

Tolosa, E., Li, W., Yasuda, Y., Wienhold, W., Denzin, L.K., Lautwein, A., Driessen, C., Schnorrer, P., Weber, E., and Stevanovic, S., et al. (2003). Cathepsin V is involved in the degradation of invariant chain in human thymus and is overexpressed in myasthenia gravis. The Journal of clinical investigation *112*, 517-526.

Tsukada, M., and Ohsumi, Y. (1993). Isolation and characterization of autophagy-defective mutants of Saccharomyces cerevisiae. FEBS letters *333*, 169-174.

Ueno, N., and Wilson, M.E. (2012). Receptor-mediated phagocytosis of Leishmania. Implications for intracellular survival. Trends in Parasitology *28*, 335-344.

van den Berg, T.K., Breve, J.J., Damoiseaux, J.G., Dopp, E.A., Kelm, S., Crocker, P.R., Dijkstra, C.D., and Kraal, G. (1992). Sialoadhesin on macrophages. Its identification as a lymphocyte adhesion molecule. The Journal of experimental medicine *176*, 647-655.

van Kasteren, S.I., and Overkleeft, H.S. (2014). Endo-lysosomal proteases in antigen presentation. Current opinion in chemical biology *23*, 8-15.

van Zandbergen, G., Bollinger, A., Wenzel, A., Kamhawi, S., Voll, R., Klinger, M., Muller, A., Holscher, C., Herrmann, M., and Sacks, D., et al. (2006). Leishmania disease development depends on the presence of apoptotic promastigotes in the virulent inoculum. Proceedings of the National Academy of Sciences of the United States of America *103*, 13837-13842.

van Zandbergen, G., Hermann, N., Laufs, H., Solbach, W., and Laskay, T. (2002). Leishmania Promastigotes Release a Granulocyte Chemotactic Factor and Induce Interleukin-8 Release but Inhibit Gamma Interferon-Inducible Protein 10 Production by Neutrophil Granulocytes. Infection and immunity *70*, 4177-4184.

van Zandbergen, G., Solbach, W., and Laskay, T. (2007). Apoptosis driven infection. Autoimmunity *40*, 349-352.

Vanderheijden, N., Delputte, P.L., Favoreel, H.W., Vandekerckhove, J., van Damme, J., van Woensel, P.A., and Nauwynck, H.J. (2003). Involvement of Sialoadhesin in Entry of Porcine Reproductive and Respiratory Syndrome Virus into Porcine Alveolar Macrophages. Journal of virology *77*, 8207-8215.

Verreck, F.A.W., Boer, T. de, Langenberg, D.M.L., Hoeve, M.A., Kramer, M., Vaisberg, E., Kastelein, R., Kolk, A., Waal-Malefyt, R. de, and Ottenhoff, T.H.M. (2004). Human IL-23-producing type 1 macrophages promote but IL-10-producing type 2 macrophages subvert immunity to (myco)bacteria. Proceedings of the National Academy of Sciences of the United States of America *101*, 4560-4565.

Verreck, F.A.W., Boer, T. de, Langenberg, D.M.L., van der Zanden, L., and Ottenhoff, T.H.M. (2006). Phenotypic and functional profiling of human proinflammatory type-1 and anti-inflammatory type-2 macrophages in response to microbial antigens and IFN-gamma- and CD40L-mediated costimulation. Journal of leukocyte biology *79*, 285-293.

Vinet, A.F., Fukuda, M., Turco, S.J., and Descoteaux, A. (2009). The Leishmania donovani lipophosphoglycan excludes the vesicular proton-ATPase from phagosomes by impairing the recruitment of synaptotagmin V. PLoS pathogens *5*, e1000628.

Vinod, V., Padmakrishnan, C.J., Vijayan, B., and Gopala, S. (2014). 'How can I halt thee?' The puzzles involved in autophagic inhibition. Pharmacological research *82*, 1-8.

Voll, R.E., Herrmann, M., Roth, E.A., Stach, C., Kalden, J.R., and Girkontaite, I. (1997). Immunosuppressive effects of apoptotic cells. Nature *390*, 350-351.

Vouldoukis, I., Riveros-Moreno, V., Dugas, B., Ouaaz, F., Becherel, P., Debre, P., Moncada, S., and Mossalayi, M.D. (1995). The killing of Leishmania major by human macrophages is mediated by nitric oxide induced after ligation of the Fc epsilon RII/CD23 surface antigen. Proceedings of the National Academy of Sciences of the United States of America *92*, 7804-7808.

Wang, Y., Weiss, L.M., and Orlofsky, A. (2009). Host cell autophagy is induced by Toxoplasma gondii and contributes to parasite growth. The Journal of biological chemistry *284*, 1694-1701.

Warburg, A., and Schlein, Y. (1986). The effect of post-bloodmeal nutrition of Phlebotomus papatasi on the transmission of Leishmania major. The American journal of tropical medicine and hygiene *35*, 926-930.

Watanabe, Y., and Tanaka, M. (2011). p62/SQSTM1 in autophagic clearance of a non-ubiquitylated substrate. Journal of cell science *124*, 2692-2701.

White, E. (2012). Deconvoluting the context-dependent role for autophagy in cancer. Nature reviews. Cancer *12*, 401-410.

Wilson, M.E., Jeronimo, S.M.B., and Pearson, R.D. (2005). Immunopathogenesis of infection with the visceralizing Leishmania species. Microbial pathogenesis *38*, 147-160.

Wilson, M.E., and Pearson, R.D. (1988). Roles of CR3 and mannose receptors in the attachment and ingestion of Leishmania donovani by human mononuclear phagocytes. Infection and immunity *56*, 363-369.

Winberg, M.E., Holm, A., Sarndahl, E., Vinet, A.F., Descoteaux, A., Magnusson, K.-E., Rasmusson, B., and Lerm, M. (2009). Leishmania donovani lipophosphoglycan inhibits phagosomal maturation via action on membrane rafts. Microbes and Infection *11*, 215-222.

Workman, P., and van Montfort, R.L.M. (2010). Unveiling the secrets of the ancestral PI3 kinase Vps34. Cancer cell *17*, 421-423.

Wright, S.D., and Silverstein, S.C. (1983). Receptors for C3b and C3bi promote phagocytosis but not the release of toxic oxygen from human phagocytes. The Journal of experimental medicine *158*, 2016-2023.

Wu, Y.-T., Tan, H.-L., Shui, G., Bauvy, C., Huang, Q., Wenk, M.R., Ong, C.-N., Codogno, P., and Shen, H.-M. (2010). Dual role of 3-methyladenine in modulation of autophagy via different temporal patterns of inhibition on class I and III phosphoinositide 3-kinase. The Journal of biological chemistry *285*, 10850-10861.

Xing, C., Zhu, B., Liu, H., Yao, H., and Zhang, L. (2008). Class I phosphatidylinositol 3-kinase inhibitor LY294002 activates autophagy and induces apoptosis through p53 pathway in gastric cancer cell line SGC7901. Acta Biochim Biophys Sinica *40*, 194-201.

Xu, W., Roos, A., Schlagwein, N., Woltman, A.M., Daha, M.R., and van Kooten, C. (2006). IL-10-producing macrophages preferentially clear early apoptotic cells. Blood *107*, 4930-4937.

Xu, W., Zhao, X., Daha, M.R., and van Kooten, C. (2013). Reversible differentiation of pro- and anti-inflammatory macrophages. Molecular immunology *53*, 179-186.

Yamamoto, A., Tagawa, Y., Yoshimori, T., Moriyama, Y., Masaki, R., and Tashiro, Y. (1998). Bafilomycin A1 prevents maturation of autophagic vacuoles by inhibiting fusion between autophagosomes and lysosomes in rat hepatoma cell line, H-4-II-E cells. Cell Struct. Funct. *23*, 33-42.

Yang, C.-S., Lee, J.-S., Rodgers, M., Min, C.-K., Lee, J.-Y., Kim, H.J., Lee, K.-H., Kim, C.-J., Oh, B., and Zandi, E., et al. (2012). Autophagy protein Rubicon mediates phagocytic NADPH oxidase activation in response to microbial infection or TLR stimulation. Cell host & microbe *11*, 264-276.

Yang, Z., and Klionsky, D.J. (2010). Eaten alive. A history of macroautophagy. Nature cell biology *12*, 814-822.

Yao, C., Donelson, J.E., and Wilson, M.E. (2003). The major surface protease (MSP or GP63) of Leishmania sp. Biosynthesis, regulation of expression, and function. Molecular and Biochemical Parasitology *132*, 1-16.

Yem, A.W., and Parmely, M.J. (1981). Modulation of Ia-like antigen expression and antigen-presenting activity of human monocytes by endotoxin and zymosan A. Journal of immunology (Baltimore, Md. : 1950) *127*, 2245-2251.

Yiallouros, I., Kappelhoff, R., Schilling, O., Wegmann, F., Helms, M.W., Auge, A., Brachtendorf, G., Berkhoff, E.G., Beermann, B., and Hinz, H.-J., et al. (2002). Activation Mechanism of Pro-astacin. Role of the Pro-peptide, Tryptic and Autoproteolytic Cleavage and Importance of Precise Amino-terminal Processing. Journal of Molecular Biology *324*, 237-246.

Yoshimori, T., Yamamoto, A., Moriyama, Y., Futai, M., and Tashiro, Y. (1991). Bafilomycin A1, a specific inhibitor of vacuolar-type H(+)-ATPase, inhibits acidification and protein degradation in lysosomes of cultured cells. The Journal of biological chemistry *266*, 17707-17712.

Young, A.R.J., Chan, E.Y.W., Hu, X.W., Kochl, R., Crawshaw, S.G., High, S., Hailey, D.W., Lippincott-Schwartz, J., and Tooze, S.A. (2006). Starvation and ULK1-dependent cycling of mammalian Atg9 between the TGN and endosomes. Journal of cell science *119*, 3888-3900.

Yuk, J.-M., Shin, D.-M., Lee, H.-M., Yang, C.-S., Jin, H.S., Kim, K.-K., Lee, Z.-W., Lee, S.-H., Kim, J.-M., and Jo, E.-K. (2009). Vitamin D3 induces autophagy in human monocytes/macrophages via cathelicidin. Cell host & microbe *6*, 231-243.

Zilberstein, D., and Shapira, M. (1994). The role of pH and temperature in the development of Leishmania parasites. Annual Review of Microbiology *48*, 449-470.

6 Acronyms and Abbreviations

°C	Degree Celsius
µl	Microliter
µM	Micromolar
µm	Micrometer
3-MA	3-Methyladenine
AF	Aggregation factor
APC	Antigen presenting cell
APS	Ammoniumpersulfat
ATG	Autophagy related
BCG	Bacille Calmette-Guérin
BMDM	Bone marrow derived macrophages
BSA	Bovine serum albumin
C3	Complement component 3
CD	Cluster of differentiation
cDNA	Complementary DNA
CFSE	5(6)-Carboxyfluorescein diacetate N-succinimidyl ester
CL	Cutaneous leishmaniasis
CLIP	Class-II associated invariant chain peptide
CLR	C-type lectin receptors
cm	Centimeter
CR	Complement receptor
CT	Cycle threshold
DIC	Differential interference contrast
DMSO	Dimethylsulfoxid
DNA	Deoxyribonucleic acid
dNTP	Deoxy-nucleotide tri-phosphate
DPI	Diphenyleneiodonium
DTT	Dithiothreitol
ECL	Enhanced chemiluminescence
EDTA	Ethylenediaminetetraacetic acid
ELISA	Enzyme-linked Immunosorbent Assay
EtOH	Ethanol
FACS	Fluorescence activated cell sorting
FCS	Fetal Calf Serum
FIP200	Focal adhesion kinase-interacting protein of 200 kDa

FnR	Fibronectin receptor
FSC	Forward scatter
fwd	Forward
g	Gramm
g	Gravitational force
GAPDH	Glycerinaldehyd-3-phosphat-Dehydrogenase
GFP	Green fluorescent protein
GM-CSF	Granulocyte macrophage colony-stimulating factor
GP	Glycoprotein
GP63	Glycoprotein of 63 kDa
h	Hour/s
HCl	Hydrochloric acid
HEPES	4-(2-hydroxyethyl)-1-piperazineethanesulfonic acid
HIV	Human immunodeficiency virus
HLA-DM	Human leukocyte antigen DM
hMDM	Human monocyte derived macrophage
hMDM-1 (M1)	Pro-inflammatory human monocyte derived macrophage
hMDM-2 (M2)	Anti-inflammatory human monocyte derived macrophage
HRP	Horseradish peroxidase
IC	Immune complex
iC3b	Inactive complement component 3b
IDO1	Indoleamine 2,3-dioxygenase 1
IF	Immunofluorescence
IFN-α	Interferon α
IFN-γ	Interferon γ
Ig	Immunoglobulin
Ii	Invariant chain
IL	Interleukin
KD	Knockdown
kDa	Kilo Dalton
CPVL	Carboxypeptidase, vitellogenic like
KO	Knockout
L.	*Leishmania*
LAMP	Lysosomal-associated membrane protein
LAP	LC3-associated phagocytosis
LC3	Microtubule-associated protein 1A/1B-light chain 3
LC3-I	Cytosolic form of LC3
LC3-II	Lipidated, membrane bound form of LC3

LCF	*Leishmania* chemotactic factor
Lm	*Leishmania major*
log. phase	Logarithmic phase
LPG	Lipophosphoglycan
LPS	Lipopolysaccharide
mA	Milliampere
MACS	Magnetic activated cell sorting
MCL	Mucocutaneous leishmaniasis
M-CSF	Macrophage colony-stimulating factor
MEF	Mouse embryonic fibroblasts
MF	Macrophage
MFI	Mean fluorescence intensity
MHC	Major histocompatibility complex
MIIC	MHC class II compartments
min	Minute/s
MIP-1β	Macrophage inflammatory protein-1β
ml	Milliliter
mM	Millimolar
mm	Millimeter
MOI	Multiplicity of infection
MR	Mannose receptor
mRNA	Messenger Ribonucleic Acid
mTOR	mammalian target of Rapamycin
NaCl	Sodium chloride
NADPH	Nicotinamide adenine dinucleotide phosphate
NaN_3	Sodium azide
NaOH	Sodium hydroxide
ng	Nanogramm
NK	Natural killer
NLR	Nucleotide-binding oligomerization domain-like receptors
NO	Nitric oxide
NOD	Non-obese diabetic
NOX2	NADPH oxidase isoform 2
NT	Non target
OVA	Ovalbumin
p.i.	Post infection
PAGE	Polyacrylamide Gel Electrophoresis
PAMP	Pathogen-associated molecular pattern

PBLs	Peripheral Blood Lymphocytes
PBMCs	Peripheral Blood Mononuclear Cells
PBS	Phosphate buffered saline
PE	Phosphatidylethanolamine
PFA	Paraformaldehyde
pg	Picogramm
PI3K	Phosphatidylinositol 3 kinase
PI3P	Phosphatidylinositol-3-phosphate
PKC	Protein kinase C
PKDL	Post kala-azar dermal leishmaniasis
PMN	Polymorphonuclear neutrophil granulocytes
PS	Phosphatidylserine
qRT-PCR	Quantitative Real-Time Polymerase Chain Reaction
rev	Reverse
RIG-I	Retinoic acid inducible gene I
RNA	Ribonucleic Acid
ROS	Reactive oxygen species
RT	Room temperature (22°C)
Rubicon	Run domain Beclin-1-interacting and cysteine-rich domain-containing protein
SD	Seidmann
SD	Standard deviation
SDS	Sodium Dodecyl Sulfate
sec	Second/s
siRNA	Small interfering RNA
SNARE	Soluble N-ethylmaleimide-sensitive-factor attachment receptor
Spautin-1	Specific autophagy inhibitor 1
SSC	Side scatter
stat. phase	Stationary phase
Tat	Twin-Arginine Translocation
TCR	T cell receptor
TEMED	N, N, N´,N´-tetramethylethylenediamine
TGF	Transforming growth factor
Th	T-helper
TIM4	T cell immunoglobulin domain and mucin domain protein-4
TLM	Translocation motif
TLR	Toll-like receptor
TNF-α	Tumor necrosis factor α

Tris	Tris(hydroxylmethyl)-aminomethan
TT	Tetanus Toxoid
TUNEL	Terminal deoxynucleotidyl transferase (TdT)-mediated dUTP nick end labeling
ULK-1	Unc-51 like autophagy activating kinase 1
UVRAG	Ultra violet radiation resistance-associated gene
V	Volt
v/v	Volume per volume
VAMP8	Vesicle-associated membrane protein 8
V-ATPase	Vacuolar-type H^+- *Adenosine triphosphat*ase
VL	Visceral leishmaniasis
Vps34	Phosphatidylinositol 3-kinase catalytic subunit type 3
w/v	Weight per volume
WB	Western Blot
WHO	World health organization
WT	Wildtype
x	Times

7 Figure list

8 Table list

9 Declaration of authorship

I hereby certify that I have written the present dissertation with the topic:

Canonical and non-canonical autophagy modulation in human primary macrophages and its effect on the adaptive immune system

independently, using no other aids then those I have cited. I have clearly mentioned the source of the passages that are taken word for word or paraphrased from other works.

The presented thesis has not been submitted in this or any other form to another faculty or examination institution.

Eidesstattliche Versicherung

Hiermit versichere ich, dass ich die vorgelegte Dissertation mit dem Titel

Canonical and non-canonical autophagy modulation in human primary macrophages and its effect on the adaptive immune system

selbstständig verfasst habe und keine anderen als die angegebenen Quellen und Hilfsmittel verwendet habe. Die Stellen der Dissertation, die anderen Werken und Veröffentlichungen dem Wortlaut oder dem Sinn nach entnommen wurden, sind durch Quellenangaben gekennzeichnet.

Diese Dissertation wurde in der jetzigen oder in ähnlicher Form noch an keiner anderen Hochschule eingereicht und hat noch keinen sonstigen Prüfungszwecken gedient.

Langen, 07.04.2017

Rebecca Bohn

10 Acknowledgements

12 Curriculum Vitae